Three-dimensional Analysis of Palatal Morphology in the Unaffected Relatives of Individuals with Non-syndromic Orofacial Clefting

by

Ahmed Mamdouh Mahmoud El Sergani

Bachelor of Oral and Dental Medicine, Misr International University, 2012

Membership in Oral & Maxillofacial Surgery, Royal College of Surgeons of Edinburgh, 2017

Diplomate, Arab Board of Oral & Maxillofacial Surgery, 2019

Submitted to the Graduate Faculty of the

School of Dental Medicine in partial fulfillment

of the requirements for the degree of

Doctor of Philosophy

University of Pittsburgh

2020

UNIVERSITY OF PITTSBURGH

SCHOOL OF DENTAL MEDICINE

This thesis was presented

by

Ahmed Mamdouh Mahmoud El Sergani

It was defended on

May 21, 2020

and approved by

Mary L. Marazita, PhD, Professor

Katherine Neiswanger, PhD, Research Associate Professor

John R. Shaffer, PhD, Assistant Professor

Thesis Advisor: Seth M. Weinberg, PhD, Associate Professor

Three-dimensional Analysis of Palatal Morphology in the Unaffected Relatives of Individuals with Non-syndromic Orofacial Clefting

Ahmed M. El Sergani, BDS, PhD, MOMS RCSEd, Dipl. AB(OMS)

University of Pittsburgh, 2020

Subclinical endophenotypes in biological relatives of individuals with non-syndromic orofacial clefts have been the subject of extensive investigation. The rationale for studying these endophenotypes is that they may assist in the identification of genetic risk factors being passed down within families. Cleft endophenotypes include characteristic craniofacial morphological patterns that have been identified in the midface region (e.g. increased midface retrusion). Since the secondary palate is an integral part of the nasomaxillary complex, we hypothesized that palate shape could be an important endophenotypic risk marker. We therefore analyzed 3D palatal morphology using landmark-based morphometric approaches (geometric morphometrics and EDMA). To accomplish this, physical dental impressions were obtained, scanned as 3D surface models, and landmarked with seven points. Our cohort (N=935) included 141 unaffected biological parents of individuals with non-syndromic orofacial clefting and 794 demographically matched controls from three ancestral groups. We first analyzed normal palatal morphological patterns in controls and found an association between a higher palatal vault and deficient sagittal and/or transverse dimensions. These findings agree with previous reports from 2D cephalometry. We also found sex and ancestry differences in palate shape among controls ($p \leq .0148$). By sex, males had wider transverse and shorter sagittal dimensions with higher posterior vaults than females, who had higher anterior vaults. By ancestry, Africans had overall highest vaults while Asians had the shallowest. Europeans had longer sagittal and narrower transverse dimensions with

higher anterior vaults than other ancestries. We also analyzed those sex- and ancestry-specific patterns in the unaffected cleft parent population and found that ancestry-specific differences were less distinct between fathers, and sex-specific differences were less distinct between mothers and fathers. Comparing the unaffected parents to controls, differences in palate shape were limited to females ($p \leq .0093$). Furthermore, some of these shape differences were ancestry specific. In comparison to controls, European mothers had narrower transverse and longer sagittal dimensions with higher anterior vaults, while Asian mothers had wider transverse dimensions and retruded anterior palates. Although preliminary, our findings may pave the way for advanced and more sophisticated genetic and morphometric analyses that would aid in dissecting the genetic etiology of orofacial clefting.

Table of Contents

List of Tables

List of Figures

Preface

There are not enough words to describe my gratitude to the people who helped me realize this dream. I would like to thank my committee members – Seth Weinberg, Mary Marazita, Katherine Neiswanger and John Shaffer – for their guidance and mentorship. I would also like to thank the CCDG family for their never-ending support throughout the process. Especially, I would like to thank Joel Anderton, Linda Carr, Jill Ciciarelli, Stephanie Brandebura, Kathy O'Connor, MyoungKeun Lee, Jim Gallagher and Lance Kennelty whom each made significant contributions to my journey.

This project was possible through the generous support of the National Institute of Health: National Institute for Dental & Craniofacial Research grant R01-DE016148 (PIs: Mary Marazita & Seth Weinberg) and the Graduate Student Researcher scholarship through the University of Pittsburgh School of Dental Medicine.

Finally, I could have never done it without my loving family, the greatest blessing of all. I would like to express my gratitude and appreciation to the three first ladies of my life; my mother Hanaa, my wife Rana and my daughter Hana. They have been the backbone through it all and to them I am ever indebted. To my late father Mamdouh El Sergani, who first sparked my curiosity interest in pursuing science, I would like to say that even though you are not here with us today to witness this dream come to life, I know you are at peace.

1.0 Significance, Background and Rationale

1.1 Introduction

Clefting of the orofacial region is a congenital anomaly affecting the structures in/or around the face and oral cavity. Individuals present with one of three major forms of orofacial clefting: clefts involving the lip (CL), clefts involving the secondary palate only (CPO), and clefts involving both the lip and the palate (CLP) simultaneously. At the epidemiolocal level, CL and CLP are often combined as cleft lip with or without cleft palate (CL/P) (Mossey, Little, Munger, Dixon, & Shaw, 2009). This condition is the most common congenital birth defect affecting the craniofacial region in humans (Leslie & Marazita, 2013). Orofacial clefting can have incidences as high as 1 in 500 live births according to geographic region and socioeconomic status (Murray et al., 1997; M. M. Tolarová & Cervenka, 1998).

Treatment for orofacial clefting is very costly, lengthy and challenging as it requires a multidisciplinary team comprised of surgeons, dentists, speech and language therapists, psychiatrists, feeding therapists and ENTs, with the average lifetime medical cost of treatment for one affected individual totaling about $100,000 ("Center for Disease Control and Prevention: Facts about Cleft Lip and Cleft Palate," ; Leslie & Marazita, 2013; Waitzman, Romano, & Scheffler, 1994; Wehby & Cassell, 2010). The mean and median healthcare costs for children ≤10 years of age with an orofacial cleft are eight times higher than those for children of the same age without an orofacial cleft, in part because the affected children require additional surgical procedures as they get older (Agbenorku, 2013). Affected individuals and their parents often suffer psychological burdens requiring extensive management that starts before birth for the parents and continues for

the child as he/she matures. There are additional comorbidities as well, with studies showing an association between clefts and increased incidences of certain types of cancers (Bille et al., 2005).

Orofacial clefting can occur either in isolation, that is, as a sole congenital anomaly affecting the individual, thus termed non-syndromic (NS), or as part of myriad other anomalies affecting the individual, hence being part of a syndrome and termed syndromic. Isolated or non-syndromic orofacial clefts (NSCL/P) comprise about 70% of all cases of CL/P and 50% of CPO (Stanier & Moore, 2004).

Despite extensive research, the etiology of orofacial clefting is still poorly understood, with evidence pointing towards it being multifactorial, being affected by both genetic and environmental factors (Leslie & Marazita, 2013). Various genetic loci have been identified for overt syndromic and non-syndromic orofacial clefting (Indencleef et al., 2018; Leslie & Marazita, 2013).

Several subclinical phenotypes have been identified in the relatives of affected individuals (Leslie & Marazita, 2013). These subclinical phenotypes include morphometric differences of the craniofacial complex, dental anomalies, brain structural differences, dermatoglyphic and lip prints, orbicularis oris muscle defects, bifid uvulae, submucous cleft palate, velopharyngeal insufficiency as well as olfactory deficits (Leslie & Marazita, 2013; May, Sanchez, Deleyiannis, Marazita, & Weinberg, 2015; Neiswanger et al., 2009; Neiswanger et al., 2007; Nopoulos, Richman, Murray, & Canady, 2002; Rogers et al., 2008; Vieira, McHenry, Daack-Hirsch, Murray, & Marazita, 2008; S. M. Weinberg et al., 2009; S. M. Weinberg et al., 2008; S. M. Weinberg et al., 2013). Morphological differences in the craniofacial complex pointed towards a deficiency at the nasal and upper lip region. Since the palate is part of the nasomaxillary morphological continuum, it is

only reasonable to assess palatal morphology that may provide in-depth three-dimensional insight about the craniofacial morphology in a selected population.

1.2 Classification of the Overt Cleft Phenotype

Clefts may occur at different sites within the craniofacial region. The current conceptualization of the commonly used classifications today stems from that proposed by Kernahan & Stark, which included clefts of the alveolar process into the cleft lip spectrum (Kernahan & Stark, 1958). Based on that, Dr. Paul Tessier, a French surgeon who is considered the father of craniofacial surgery, developed a classification system for facial clefts (Figure 1) (Tessier, 1976). According to Tessier's classification, clefts occur in axes around three landmarks, namely the oral cavity, nose, and orbit. The numbers on the lower end (0-7) represent the facial clefts while those on the higher end (8-14) represent cranial extensions and 30 representing those that occur through the mandible. In addition, clefts can occur through soft tissue with or without skeletal involvement. Interestingly, Tessier developed this classification before the advent of advanced imaging and visualization techniques, which proved the classification system valid, establishing it as a communication tool among craniofacial surgeons.

Orofacial clefting (OC), which is the more common entity that affects the craniofacial region, has been described through several different classifications. This is due to the differing disciplines of surgery, genetic counselling and research, with surgeons requiring anatomical classifications while genetic counsellors and researchers requiring more embryology-based classifications (Watkins, Meyer, Strauss, & Aylsworth, 2014). Based on that, embryologically, OC affects the lips with or without the palate (CL/P) or the palate only. Studies on animal models as

well as epidemiological analyses in humans showed an increased degree of distinction etiologically and pathogenetically between CL/P and CPO (Juriloff & Harris, 2008; Mossey et al., 2009; Murray, 2002; Watkins et al., 2014). Therefore, this brings the local anatomical grouping of OC to CL/P and CPO (Figure 2) (Mossey et al., 2009).

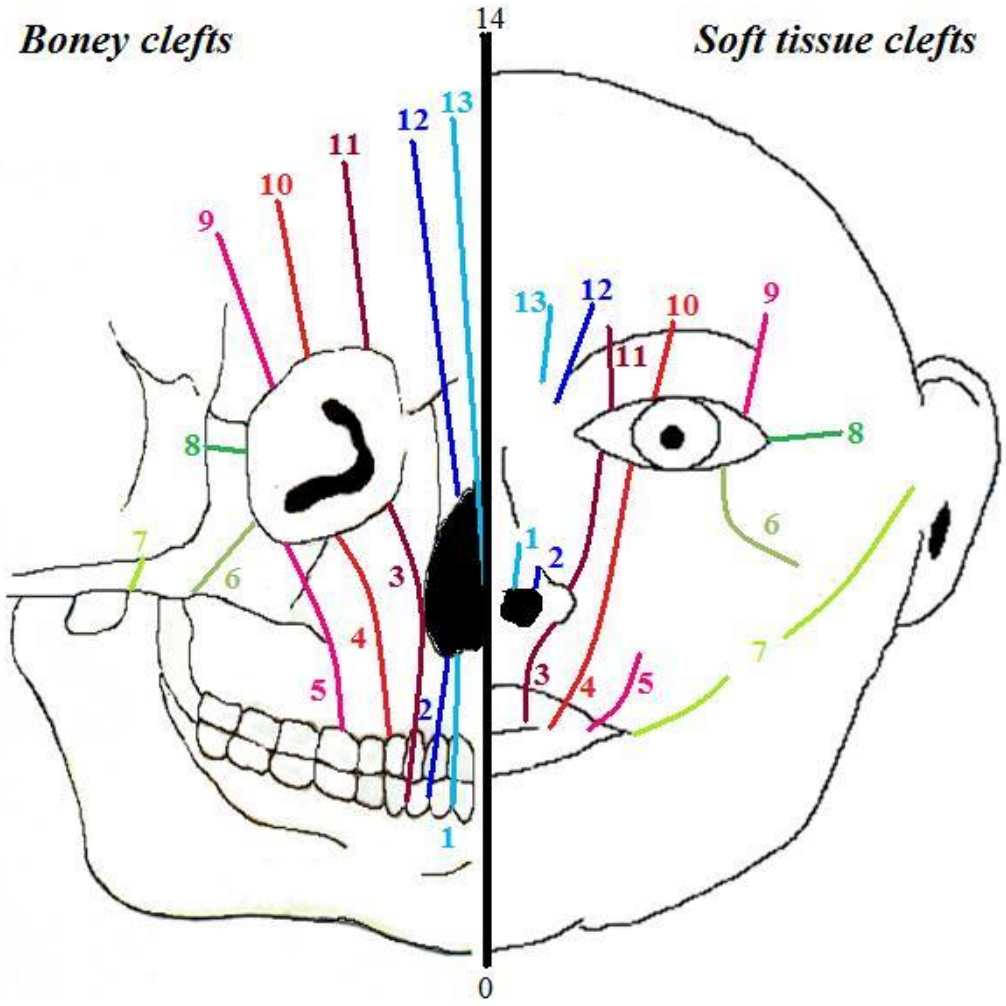

Figure 1 Tessier classification for craniofacial clefts.

Right = Path of various clefts on the face. Left = Location of the clefts on the facial skeleton.

https://en.wikipedia.org/wiki/File:Picture_Tessier_classification.jpg#filelinks

However, the classification of OC into CL/P or CPO stands valid with most but not all cases. There are syndromes affecting the craniofacial region, namely Van der Woude and popliteal pterygium syndromes that have been shown to present as either CL/P or CPO along with the presence of lip pits despite a shared genetic component of the etiology (Kondo et al., 2002).

Beyond classifications based on local anatomical structures involved, OC has also been classified based on its association with and occurrence among other conditions as part of a syndrome. Those occurring with other syndromes are described as syndromic, while others solely occurring in isolation as the only condition affecting the craniofacial complex are described as non-syndromic (NS) or isolated (Watkins et al., 2014). Hundreds of syndromes have been identified where OC is a primary feature and most of which have a known genetic cause including single-gene Mendelian genetic patterns of inheritance (Leslie & Marazita, 2013). Table 1 summarizes some of the known syndromes presenting with OC and their associated genetic loci.

Table 1 Selected CL/P syndromes with known genetic cause.

CL = Cleft lip. CP = Cleft palate. CL/P = Cleft lip with or without cleft palate (Leslie & Marazita, 2013).

Syndrome	Cleft Type	Gene	Reference
Ankyloblepharon-ectodermal dysplasia-clefting	CL/P	*TP63*	(McGrath et al., 2001)
Apert	CP	*FGFR2*	(Wilkie et al., 1995)
Bamforth-Lazarus	CP	*FOXE1*	(Bamforth, Hughes, Lazarus, Weaver, & Harper, 1989)
Bartsocas-Papas	CL/P	*RIPK4*	(Kalay et al., 2012; Mitchell et al., 2012)
Branchio-oculo-facial	CL/P	*TFAP2A*	(Milunsky et al., 2008)
Campomelic dysplasia	CP	*SOX9*	(Foster et al., 1994; Wagner et al., 1994)
CHARGE	CP	*CHD7*	(Vissers et al., 2004)
CLP ectodermal dysplasia	CL/P	*PVRL1*	(Suzuki et al., 2000)
Cornelia de Lange	CP	*NIPBL*	(Krantz et al., 2004; Tonkin, Wang, Lisgo, Bamshad, & Strachan, 2004)
Crouzon	CP	*FGFR2*	(Reardon et al., 1994)
DiGeorge	CP	*TBX1*	(Packham & Brook, 2003)
Ectrodactyly-ectodermal dysplasia-clefting	CL/P	*TP63*	(Celli et al., 1999)

Syndrome	Cleft Type	Gene	Reference
Familial gastric cancer and CLP	CL/P	*CDH1*	(Frebourg et al., 2006)
Gorlin	CL/P	*PTCH1*	(Hahn et al., 1996; Johnson et al., 1996)
Holoprosencephaly	CL/P	*GLI2*	(Roessler et al., 2003)
Holoprosencephaly	CL/P	*SHH*	(Roessler et al., 1996)
Holoprosencephaly	CL/P	*SIX3*	(Wallis et al., 1999)
Holoprosencephaly	CL/P	*TGIF*	(Gripp et al., 2000)
Isolated cleft palate	CP	*SATB2*	(FitzPatrick et al., 2003)
Kabuki	CL/P	*MLL2* *KDM6A*	(Lederer et al., 2012; S. B. Ng, Bigham, et al., 2010)
Kallmann	CL/P	*FGFR1*	(Dodé et al., 2003)
Lethal and Escobar multiple pterygium	CP	*CHRNG*	(Morgan et al., 2006)
Loeys-Dietz	CP	*TGFBR1*, *TGFBR2*	(Loeys et al., 2005)
Miller	CP	*DHODH*	(S. B. Ng, Buckingham, et al., 2010)
Occulofaciocardiodental	CP	*BCOR*	(D. Ng et al., 2004)
Opitz G/BBB	CL/P	*MID1*	(Quaderi et al., 1997)
Oro-facial-digital	CL/P	*GLI3*	(Johnston et al., 2010)
Oro-facial-digital type 1	CL/P	*OFD1*	(Ferrante et al., 2001)

Syndrome	Cleft Type	Gene	Reference
Otopalatodigital types 1 and 2	CP	*FLNA*	(Robertson et al., 2003)
Pierre Robin	CP	*SOX9*	(Benko et al., 2009)
Popliteal pterygium	CL/P	*IRF6*	(Kondo et al., 2002)
Saethre-Chotzen	CP	*TWIST1*	(el Ghouzzi et al., 1997; Howard et al., 1997)
Stickler type 1	CP	*COL2A1*	(Snead & Yates, 1999)
Stickler type 2	CP	*COL11A1, COL11A2*	(Snead & Yates, 1999)
Tetra-amelia with CLP	CL/P	*WNT3*	(Niemann et al., 2004)
Tooth agenesis with or without cleft	CL/P	*MSX1*	(van den Boogaard, Dorland, Beemer, & van Amstel, 2000)
Treacher Collins	CP	*TCOF1*	(Group, 1996)
Van der Woude	CL/P	*IRF6*	(Kondo et al., 2002)
X-linked cleft palate and ankyloglossia	CP	*TBX22*	(Braybrook et al., 2001)
Siderius X-linked mental retardation	CL/P	*PHF8*	(Laumonnier et al., 2005)

1.3 Epidemiology

1.3.1 Measure of Occurrence of Orofacial Clefting

It is difficult to measure occurrence of OC (a birth defect) since they occur during the first 9 weeks of gestation, a period during which many women are not aware of conception and many pregnancies are lost unnoticed. Therefore, birth prevalence is an agreed-upon measure of occurrence of birth defects, used in birth defects research, in which prevalence is quantified as a ratio of live births (Mason, Kirby, Sever, & Langlois, 2005). Therefore, prevalence of OC is a ratio of cases per live births.

Worldwide, the estimate of birth prevalence of CL/P is about 1:700 live births (Murray, 2002). This birth prevalence varies considerably by ancestry, having East-to-West and North-to-South gradients. That is, they are highest in those of Asian or Amerindian descent at about 1:500 live births and lowest in those of African descent at about 1:2500 live births with those of Caucasian descent having an intermediate birth prevalence of 1:1000 live births (Dixon, Marazita, Beaty, & Murray, 2011; Leslie & Marazita, 2013; Mossey et al., 2009). Studies that have distinguished between cleft lip only (CL) and cleft lip with cleft palate (CLP) have reported that CLP is twice as common as CL (Jensen, Kreiborg, Dahl, & Fogh-Andersen, 1988; Leslie & Marazita, 2013).

1.3.2 Gender Patterns and Laterality

With regards to gender, non-syndromic CL/P is twice as common in males while CPO occurs as twice as common in females (Leslie & Marazita, 2013; Mossey et al., 2009). CL/P can

occur bilaterally on both sides of the lip or unilaterally on one side only. CL/P occurs unilaterally ~80% of the time with significant laterality (Hallgrímsson, Donnabháin, Blom, Lozada, & Willmore, 2005; Paulozzi & Lary, 1999; S. Weinberg, 2007). There is a strong preponderance of unilateral CL/P affecting the left side in two thirds of the cases (Shapira, Lubit, Kuftinec, & Borell, 1999; M. Tolarová, 1987; S. Weinberg, 2007).

1.4 Embryology

1.4.1 Normal Development of the Craniofacial Complex

Development of the craniofacial complex requires an intricate and finely choreographed growth and morphogenesis of multiple embryological prominences, namely the frontonasal prominence, paired nasal, paired maxillary and paired mandibular prominences that converge to form the forehead, nose, upper jaws and lower jaws (Hooper et al., 2017; Mossey et al., 2009). This process occurs during the first 10 weeks of gestation (Figure 2) (S. Weinberg, 2007; Wilderman, VanOudenhove, Kron, Noonan, & Cotney, 2018). These prominences originate as mesenchymal bulges encased in an overlying layer of ectoderm and surround the primitive stomodeum (Hooper et al., 2017). Neural crest cells then delaminate from the neural tube and migrate through mesenchymal tissue and contribute to the development of craniofacial region. By the 4^{th} week of gestation, they contribute in the formation of the aforementioned prominences around the primitive oral cavity (Mossey et al., 2009). By the end of the 4^{th} week intrauterine, the formation of the nasal placodes as ectodermal thickening divides the lower portion of the frontonasal prominence into paired medial and lateral nasal prominences (Mossey et al., 2009).

As mentioned, the facial mesenchyme, derived from both mesoderm and neural crest cells, gives rise to bone, cartilage, connective tissue and muscles of the face while the cranial ectoderm gives rise to the epidermis as well as the mucous linings of both the oral and nasal cavities (Hooper et al., 2017). The ectoderm also provides critical components for the sensory organs, exocrine glands and teeth via placodal intermediates (Hooper et al., 2017; Singh & Groves, 2016). Despite the bulk of the embryonic facial prominences being comprised by mesenchyme, essential patterning information is conveyed by the surrounding tissues including the ectoderm, endoderm and the neural tube (Adameyko & Fried, 2016; Chai & Maxson, 2006; Hooper et al., 2017; Singh & Groves, 2016). A complex interplay occurs between the facial ectoderm and mesenchyme whereby the ectoderm provides both permissive and inductive signals for normal development of the underlying mesenchyme while the mesenchyme also provides critical signaling input to the ectoderm in order to regulate growth, maintain competence and diversify derivatives (Hooper et al., 2017). Several growth factors are involved in this signaling cross talk. These include Fibroblast Growth Factors (Fgfs), Bone Morphogenetic proteins (BMPs), Wnts, Hedgehogs (Hhs), Platelet Derived Growth Factors (PDGFs), Retinoic Acid (RA), and endothelin (Hooper et al., 2017). Therefore, it is a highly complex process depending on intricate spatial and temporal orchestration among different embryonic facial prominences and also the ectoderm and mesenchyme layers of those embryonic structures. Thus, any manipulation of those structures that leads to the disruption of this orchestration whether genetic or surgical manipulation or teratogenic insults will lead to major congenital anomalies such as OC and craniosynostosis (Hooper et al., 2017; Wilderman et al., 2018).

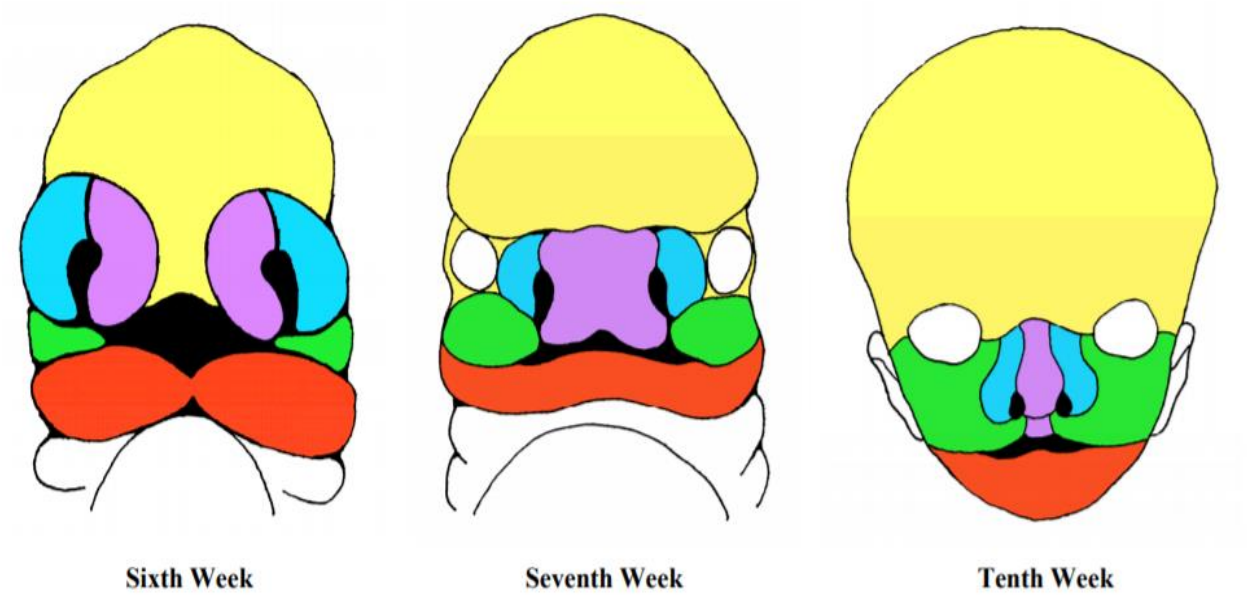

Figure 2 Craniofacial morphogenesis from the 6th to 10th week.

The embryonic facial prominences are color-coded to show their contribution to definitive facial structures.

Yellow = Frontonasal prominence. Purple = Medial nasal prominence. Blue = Lateral nasal prominence,

Green = Maxillary prominence and Orange = Mandibular prominence.

Used with permission from Weinberg - personal communication.

1.4.2 Developmental Pathogenesis of Orofacial Clefting

By the end of the 6th week of embryogenesis, the paired medial nasal processes fuse with each other as well as with the maxillary processes on either side leading to the formation of the upper lip and primary palate. During this phase, the cell division rate at the lateral nasal processes peaks resulting in increased susceptibility to teratogenic insults that might compromise growth and lead to a failure of this closure mechanism (Mossey et al., 2009).

On the other hand, the development of the secondary palate occurs during the 6th week of intrauterine life through the outgrowth of paired palatal shelves from the maxillary processes.

These shelves initially grow vertically downwards on either side of the developing tongue. During the 7th week of embryogenesis, these palatal shelves rise to a horizontal position above the tongue and come into contact with each other and fuse through the medial edge epithelium forming a midline epithelial seam. This midline epithelial seam subsequently degenerates and mesenchymal continuity across the palate is achieved. This mesenchyme then gives rise to bony and muscular structures corresponding to the hard and soft palate respectively (Mossey et al., 2009).

In addition to fusion at the midline, the palatal shelves comprising the secondary palate also fuse with the primary palate and the nasal septum. All of the fusion processes are completed by the 10th week of embryogenesis leading to the separation between oral and nasal cavities allowing for mastication and respiration to occur simultaneously (Mossey et al., 2009). Therefore, failure of fusion during any of the above-mentioned processes leads to the development of clefting at that particular location of loss of fusion.

1.5 Etiology

NSCL/P has been established as a genetically complex disorder with multifactorial etiology. This means that it is caused by the interaction of multiple genetic and environmental risk factors (Leslie & Marazita, 2013). This complexity has added difficulty to the identification of a sharply outlined etiology or pathophysiological process as well as the identification of at-risk individuals and families.

1.5.1 Environmental Risk Factors

Environmental factors, especially regarding maternal exposure to teratogens and nutritional status during pregnancy have been reported in multiple studies (Leslie & Marazita, 2013). Maternal exposure to cigarette smoking has been consistently associated with an increased risk of orofacial clefting in the fetus, with a population-attributable risk estimate of as high as 20% and an odds ratio of CL/P of ~1.3 (Little, Cardy, & Munger, 2004; Rahimov, Jugessur, & Murray, 2012; Shi, Wehby, & Murray, 2008). Alcohol has also been established as a teratogen (West & Blake, 2005). Some association has been reported with variants of the alcohol dehydrogenase gene *ADHC1*, especially with the combination of *ADHC1* variants with heavy maternal alcohol consumption (Boyles et al., 2010; Jugessur et al., 2009). However, evidence for the role of alcohol is inconsistent and may be confounded by the presence of other risk factors, namely smoking, nutritional status or stress that may be associated with alcohol consumption to some extent (Leslie & Marazita, 2013; Murray, 2002).

Nutritional status during pregnancy has also been of concern to the development of orofacial clefting, especially from observational and interventional studies using folate supplementation as a preventive measure (Wehby & Murray, 2010). However, evidence of folate use has not been consistently replicated among studies (Wehby & Murray, 2010; Wilcox et al., 2007). Maternal exposure to other teratogens and environmental pathogens including valproic acid, retinoic acid and phenytoin have also been implicated in the increased risk of orofacial clefting (Abbott, 2010).

1.5.2 Genetic Risk Factors

The identification of genes contributing to orofacial clefting has been the subject of decades of research employing multiple approaches for genetic studies (Leslie & Marazita, 2013). While orofacial clefting shows strong familial aggregation, they do not follow Mendel's laws of inheritance, even in multiplex families that have two or more affected individuals (Beaty, Marazita, & Leslie, 2016). Those approaches include linkage analyses and association studies, namely candidate gene approaches, genomic rearrangements and copy number variants, genome-wide association studies (GWAS) and more recently, genomic sequencing studies (Beaty et al., 2016; Leslie & Marazita, 2013).

Linkage analysis is performed in large multiplex families and is based on the co-segregation of a genetic marker or hypothetical genetic locus (or loci) involved in a phenotype between affected vs. unaffected family members. While being a powerful approach in mapping individual genes for traits following clear Mendelian patterns in multiplex families, it is less effective in mapping genes contributing to complex traits such as orofacial clefting (Beaty et al., 2016; Leslie & Marazita, 2013).

On the other hand, other approaches of genetic association studies are suitable for larger-scale mapping of genes associated with complex traits in a case-control setting of the study population. The candidate gene approach, for example, is similar to linkage analysis in that it is based on *a priori* determination of the genes to be tested, but for frequency among cases and controls. Beginning in the early 21st century, and with the advent of the Human Genome Project, GWAS became feasible as genotyping technology improved to allow millions of single nucleotide polymorphism (SNP) markers to be typed efficiently on large samples (Beaty et al., 2016). GWAS are designed as hypothesis-free approaches to map out genetic loci associated with a particular

phenotype and have become popular due to their unbiased approach for detecting candidate genes or loci associated with complex traits such as NSCL/P (Leslie & Marazita, 2013). Table 2 shows a list of lead SNPs at different genes/loci attaining genome-wide significance (Indencleef et al., 2018).

Table 2 Overview of lead SNPs from a literature survey (Indencleef et al., 2018).

Region	Lead SNP	Location (bp)	*p*-value	Population	Method	References
1p22	rs560426	94553438	5.01E-12	Asian + European	GWAS	Beaty et al., 2010
			3.14E-12	Asian + European	Meta-analysis	Ludwig et al., 2012
	rs481931	94570016	1.06E-12	Chinese	Meta-analysis	Yu et al., 2017
	rs4147803	94582293	7.97E-12	Chinese	Meta-analysis	Yu et al., 2017
	rs66515264	94558110	4.14E-17	Multi-ethnic	Meta-analysis	Leslie et al., 2017
1p36	rs742071	18979874	7.02E-09	Asian + European	Meta-analysis	Ludwig et al., 2012
	rs4920524	18978372	3.72E-09	Multi-ethnic	Meta-analysis	Leslie et al., 2016
	rs9439713	18972776	6.02E-13	Multi-ethnic	Meta-analysis	Leslie et al., 2017

1q32	rs861020	209977111	3.24E-12	Asian + European	Meta-analysis	Ludwig et al., 2012
			1.3E-14	Chinese	Meta-analysis	Yu et al., 2017
	rs2235371	209964080	8.69E-22	Chinese	Meta-analysis	Sun et al., 2015
	rs1044516	209959614	6.57E-13	Chinese	Meta-analysis	Sun et al., 2015
	rs596731	209993801	3.77E-10	Chinese	Meta-analysis	Sun et al., 2015
	rs742214	209960925	1.62E-19	Chinese	Meta-analysis	Sun et al., 2015
	rs2064163	210048819	8.6E-19	Chinese	Meta-analysis	Yu et al., 2017
	rs642961	209989270	2.76E-15	Chinese	Meta-analysis	Yu et al., 2017
	rs9430019	210050794	1.68E-12	Chinese	Meta-analysis	Yu et al., 2017
2p21(*THADA*)	rs7590268	43540125	1.25E-08	Asian + European	Meta-analysis	Ludwig et al., 2012
2p21(*PKDCC*)	rs6740960	42181679	5.71E-13	Multi-ethnic	Meta-analysis	Ludwig et al., 2017

2p24.2	rs7552	16733928	4.22E-08	Multi-ethnic	Meta-analysis	Leslie et al., 2016
			5.83E-22	Chinese	Meta-analysis	Yu et al., 2017
	rs7566780	16729357	4.28E-09	Multi-ethnic	Meta-analysis	Leslie et al., 2017
	rs10172734	16733054	2.89E-20	Chinese	Meta-analysis	Yu et al., 2017
2p25.1	rs287980	9971366	1.94E-08	Chinese	Meta-analysis	Yu et al., 2017
3p11.1	rs7632427	89534377	3.9E-08	Asian + European	Meta-analysis	Ludwig et al., 2012
3q28	rs76479869	189553372	1.16E-08	Multi-ethnic	Meta-analysis	Leslie et al., 2017
3q29	rs338217	2979676	9.70E-10	European	Mega-analysis	Mostowska et al., 2018
4p16.2	rs34246903	4794195	4.45E-08	Chinese	Meta-analysis	Yu et al., 2017
	rs1907989	4818925	1.58E-08	Chinese	Meta-analysis	Yu et al., 2017
4q28.1	rs908822	124906257	4.33E-08	Chinese	Meta-analysis	Yu et al., 2017

5p12	rs10462065	44068846	1.12E-08	Chinese	Meta-analysis	Yu et al., 2017
6p24.3	rs9381107	9469238	2.72E-09	Chinese	Meta-analysis	Yu et al., 2017
8p11.23	rs13317	38269514	3.96E-08	Chinese	Meta-analysis	Yu et al., 2017
8q21	rs12543318	88868340	1.9E-08	Asian + European	Meta-analysis	Ludwig et al., 2012
			8.8E-12	Chinese	Meta-analysis	Yu et al., 2017
			8.75E-12	Multi-ethnic	Meta-analysis	Leslie et al., 2017
	rs1034832	88918331	1.35E-10	Chinese	Meta-analysis	Yu et al., 2017
8q22.1	rs957448	95541302	9.6E-13	Chinese	Meta-analysis	Yu et al., 2017
	rs12681366	95401265	2.35E-10	Chinese	Meta-analysis	Yu et al., 2017
8q24	rs987525	129946154	1.11E-16	Asian + European	GWAS	Beaty et al., 2010
			3.41E-10	Central European	GWAS	Birnbaum et al., 2009

			9.18E-10	European	GWAS	Grant et al., 2009
			Not reported	European	GWAS	Mangold et al., 2010
			5.12E-35	Asian + European	Meta-analysis	Ludwig et al., 2012
	rs7845615	129888794	1.03E-10	Chinese	Meta-analysis	Yu et al., 2017
	rs7017252	129950844	8.47E-16	Chinese	Meta-analysis	Yu et al., 2017
	rs55658222	129976136	8.3E-44	Multi-ethnic	Meta-analysis	Leslie et al., 2017
9q22.2	rs7871395	92209587	6.06E-09	Chinese	Meta-analysis	Yu et al., 2017
9q22.32	rs10512248	98259703	5.1E-10	Chinese	Meta-analysis	Yu et al., 2017
10q25	rs7078160	118827560	1.07E-07	Asian + European	GWAS	Beaty et al., 2010
			1.92E-08	European	GWAS	Mangold et al., 2010
			3.96E-11	Asian + European	Meta-analysis	Ludwig et al., 2012

			3.09E-10	Chinese	Meta-analysis	Sun et al., 2015
	rs6585429	118893231	7.14E-13	Chinese	Meta-analysis	Yu et al., 2017
12q13.13	rs3741442	53346750	3.72E-12	Chinese	Meta-analysis	Yu et al., 2017
12q13.2	rs705704	56435412	1.29E-09	Chinese	Meta-analysis	Yu et al., 2017
12q21.1	rs2304269	72080272	1.32E-12	Chinese	Meta-analysis	Yu et al., 2017
	rs7967428	72089040	3.08E-12	Chinese	Meta-analysis	Yu et al., 2017
13q31.1	rs9545308	80639405	2E-09	Chinese	Meta-analysis	Yu et al., 2017
	rs8001641	80692811	2.62E-10	Asian + European	Meta-analysis	Ludwig et al., 2012
	rs11841646	80679302	3.62E-10	Multi-ethnic	Meta-analysis	Leslie et al., 2017
14q22.1	rs7148069	51839645	1.69E-08	Chinese	Meta-analysis	Yu et al., 2017
	rs4901118	51856109	6.94E-10	Multi-ethnic	Meta-analysis	Ludwig et al., 2017

14q32.13	rs1243573	95379583	8.61E-10	Chinese	Meta-analysis	Yu et al., 2017
15q13	rs1258763	33050423	8.13E-14	European	Meta-Analysis	Ludwig et al., 2016
15q22.2	rs1873147	63312632	2.81E-08	European	Meta-analysis	Ludwig et al., 2012
15q24	rs28689146	75005575	6.61E-09	Multi-ethnic	Meta-analysis	Ludwig et al., 2017
	rs11072494	74889163	2.4E-08	Multi-ethnic	Meta-analysis	Leslie et al., 2017
16p13.3	rs8049367	3980445	8.98E-12	Chinese	Meta-analysis	Sun et al., 2015
	rs2283487	3969886	1.27E-10	Chinese	Meta-analysis	Yu et al., 2017
	rs17136624	3996282	3.82E-10	Chinese	Meta-analysis	Yu et al., 2017
17p13.1	rs9788972	8919630	7.05E-09	Asian + European	GWAS	Beaty et al., 2010
	rs4791774	8930220: 8930232	5.05E-19	Chinese	Meta-analysis	Sun et al., 2015
	rs11273201	8930225	7.84E-12	Multi-ethnic	Meta-analysis	Leslie et al., 2016

	rs7406226	8914693	1.46E-08	Central/ South American	Meta-analysis	Leslie et al., 2016
	rs2872615	8929845	8.81E-12	Chinese	GWAS	Yu et al., 2017
	rs1880646	8929845	1.69E-11	Chinese	GWAS	Yu et al., 2017
	rs12944377	8947708	8.23E-21	Multi-ethnic	Meta-analysis	Leslie et al., 2017
17q21.32	rs4968247	44988703	8.7E-10	Chinese	GWAS	Yu et al., 2017
	rs1838105	45008935	1.31E-11	Chinese	GWAS	Yu et al., 2017
17q22	rs227731	54773238	1.07E-08	European	GWAS	Mangold et al., 2010
			1.87E-09	Asian + European	Meta-analysis	Ludwig et al., 2012
			8.83E-09	Chinese	Meta-analysis	Yu et al., 2017
			1.77E-09	Multi-ethnic	Meta-analysis	Leslie et al., 2017
17q23.2	rs1588366	61076428	1.41E-08	European	Meta-analysis	Leslie et al., 2016

19p13.3	rs3746101	2050823	2.44E-08	European	Meta-analysis	Ludwig et al., 2017
19q12	rs73039428	33521150	2.92E-08	Multi-ethnic	Meta-analysis	Leslie et al., 2016
20q12	rs13041247	39269074	1.44E-11	Asian + European	GWAS	Beaty et al., 2010
			6.17E-09	Asian + European	Meta-analysis	Ludwig et al., 2012
	rs6129653	39275603	8.57E-12	Chinese	Meta-analysis	Yu et al., 2017
	rs6072081	39261054	1.87E-12	Multi-ethnic	Meta-analysis	Leslie et al., 2017

1.6 Craniofacial Morphology as a Risk Factor

1.6.1 Expanding the Orofacial Cleft Phenotype

In order to probe deeper into etiology of orofacial clefting, several subclinical phenotypes have been identified in relatives of affected individuals (Leslie & Marazita, 2013). These subclinical phenotypes include morphometric differences of the craniofacial complex, dental anomalies, brain structural differences, dermatoglyphic and lip prints, orbicularis oris muscle defects, bifid uvulae, submucous cleft palate, velopharyngeal insufficiency as well as olfactory deficits (Leslie & Marazita, 2013; May et al., 2015; Neiswanger et al., 2009; Neiswanger et al., 2007; Nopoulos et al., 2002; Rogers et al., 2008; Vieira et al., 2008; S. M. Weinberg et al., 2009; S. M. Weinberg et al., 2008; S. M. Weinberg et al., 2013). The rationale behind this approach is that these subclinical phenotypes may represent an incomplete expression of the more overt cleft phenotype, reflecting the presence of underlying genetic risk factors being passed down within families.

For decades, studies have attempted to establish a link between craniofacial morphology and orofacial cleft predisposition (S. M. Weinberg et al., 2009). These studies have included two-dimensional cephalometry as well as three-dimensional stereophotogrammetry of the face. There has been success in identifying subtle subclinical facial differences in the first-degree biological relatives of affected individuals with NSCL/P, especially parents. (McIntyre & Mossey, 2002, 2004; S. M. Weinberg et al., 2009; S. M. Weinberg et al., 2008).

Studies on lateral and postero-anterior (PA) cephalometric radiographs have investigated the bony facial structure of biological parents of affected individuals with NSCL/P. Despite the heterogeneity and methodological inconsistency of these studies, they have all identified

distinctive facial characteristics that discriminate these parents from controls with no family history of clefting (McIntyre & Mossey, 2002, 2003). Some of the major findings from these two-dimensional analyses include decreased transverse maxillary width, increased palatal length, increased upper incisor proclination, decreased upper anterior facial height in comparison to lower facial height, and other combinations indicating a more concave facial profile.

Studies based on non-invasive methods such as stereophotogrammetry have provided additional insights into the relationship between craniofacial shape and orofacial clefting risk. The utilization of two-dimensional data provides only rudimentary information and presents with a lack of standardization of variables that summarize craniofacial form (S. M. Weinberg et al., 2008). Studies using landmark-based statistical shape analysis on the 3D facial images of unaffected relatives have pointed to a deficiency at the nasomaxillary complex region (S. M. Weinberg et al., 2009; S. M. Weinberg et al., 2008). Beyond landmark-based methods, studies utilizing dense-surface mapping approaches further confirmed the findings of the presence of midface retrusion in those unaffected relatives (Roosenboom et al., 2017; Roosenboom et al., 2015). Recently, a data-driven facial segmentation approach has been developed to map the genetic variation of facial development (Claes et al., 2018). This approach resulted in 63 facial segments that are hierarchically clustered based on a generalized Procrustes superimposition of thousands of quasi-landmarks. This segmentation was tested against a set of orofacial clefting candidate genes, which resulted in significant associations between six NSCL/P candidate genes with variations in the nasomaxillary complex, with findings pointing towards a deficiency in the nasomaxillary complex region with the minor allele variants, in agreement with the aforementioned morphometric studies (Indencleef et al., 2018). Specifically, these findings point towards a facial endophenotype of these relatives that shows retrusion of the midfacial region and decreased philtrum width.

1.6.2 Altered Palatal Shape as an Orofacial Cleft Risk Factor

Individuals with CL/P often display significant midface/maxillary hypoplasia (Figure 3), often identified as a class III malocclusion (Sant'Anna, Cury-Saramago, Lau, Polley, & Figueroa, 2013). The development of this maxillary hypoplasia has been attributed to growth restriction from scars resulting from primary surgical correction of the cleft defect (Ganoo & Sjöström, 2019; Sakoda et al., 2017). However, questions remain whether surgical correction is worsening a deformity in a genetically predisposed individual (see below) or is the primary driver of the deformity. As early as the 19th century, professor of surgery William Rose, wrote in his book entitled "*On Hare Lip and Cleft Palate*": "An examination of the parents' mouths should always be made when possible, and very commonly it will be found that one or both possess a short upper lip, and a high arched narrow palate" (Rose, 1891). Multiple studies in the mid-20th century investigated for the presence of discrete morphological changes in the nasal cavity and/or palate through a series of radiographs. They did report some degree of increased frequency in occult but observable defects in the family members (Fukuhara & Saito, 1962, 1963; Niswander, 1968; S. Weinberg, 2007). A similar study investigated palatal morphology from dental casts, yielding observable, yet not statistically significant, higher arched and narrower palates (Mills, Niswander, Mazaheri, & Brunelle, 1968).

The morphological differences noted in both 2D and 3D facial studies suggest the presence of an altered palatal shape. For example, a combination of increased S-N-ANS angle on cephalometry in the presence of decreased upper anterior facial height, decreased facial height ratio and a concave facial profile may indicate a more superiorly situated anterior cranial base, which may be linked to a higher vaulted palate. Furthermore, a retrusive midfacial region with decreased philtrum width may reflect a retrusive and constricted maxilla. Multiple syndromes that

affect the craniofacial region are associated with orofacial clefting. Some of these syndromes are associated with midface hypoplasia and a narrow V-shaped maxillary arch, examples of those are Apert and Crouzon syndromes (Buchanan, Xue, & Hollier, 2014). An individual affected with one of these syndromes on the mild end of the spectrum may not present with clefting but will still have a narrow V-shaped maxillary arch.

Direct investigation of the palate as an orofacial clefting risk phenotype has been limited to a few simple dimensions using 2D cephalometric radiographs. These provide only rudimentary information about the nature of the morphological differences. No study to date has systematically and directly investigated 3D quantitative palatal shape in this context. To address this deficit, this study carries out a three-dimensional analysis of palatal morphology in the unaffected relatives of affected individuals with NS orofacial clefting. An anticipated outcome of this study will be an improved understanding of the phenotypic characteristics of the chosen study subjects with regards to their overall palatal morphology and dimensional distinctions.

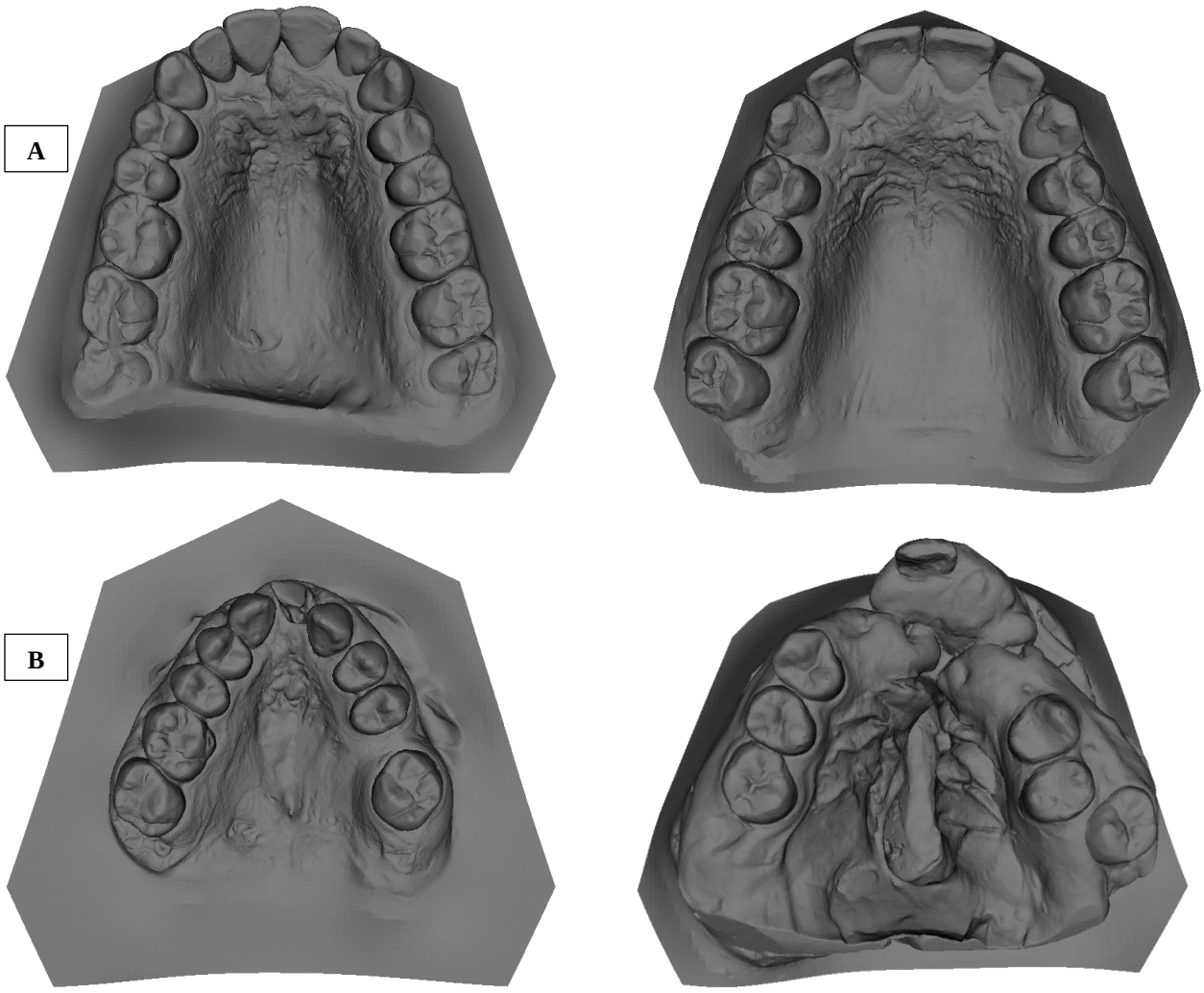

Figure 3 Adult dental casts from normal and affected individuals.

A = Normal unaffected individuals (Top). B = Individuals with BCLP (Bottom).

1.7 The Potential Significance of this Research

Firstly, this study attempts to map out and quantify patterns of palatal morphology among normal adult males and females from three ancestral groups, namely European, African, and Asian populations. This approach captures and characterizes patterns of morphological changes across those different ancestral groups as well as detects and quantifies patterns of sexual dimorphism pertaining palatal shape and form. In addition, this study also carries out the same approach to investigate the same morphological patterns with regards to unaffected biological relatives of individuals with NSCL/P. This will map out patterns of morphological changes that would occur among those relatives signifying a genetic risk being passed down in families. This data can later be tested via different genetic association study approaches to map out and identify genetic loci contributing to normal palatal development as well as those associated with increased risk of development of NSCL/P.

In addition to exploring genetic etiology of NSCL/P, this approach will also have an impact on clinical care for individuals with NSCL/P. This will take shape in identifying morphological patterns of shape change that are due to the biologic predisposition of the affected individual, thereby aiding treatment planning, and also as a means of objective assessment of clinical outcome. The correction of maxillary hypoplasia in non-CL/P individuals with a class III malocclusion involves a combination of orthopedic and orthodontic treatment, which is often carried out at or before adolescence (~10-13yrs). However, the maxillary hypoplasia in CL/P patients can be severe enough to necessitate orthognathic surgery. Currently, there are no means of assessing which individuals will respond well to orthopedic/orthodontic treatment, and who will need more extensive surgical procedures, or when these treatments should be carried out (Austin, Mattick, & Waterhouse, 2015). Therefore, efforts should be made try to detect the onset of and characterize

deformity as early as possible and act upon it accordingly through less invasive, non-surgical orthopedic interventions, thereby reducing the need for and/or invasiveness of surgery later on.

1.8 The Present Study: Hypotheses and Goals

This study aims at characterizing patterns of normal palatal morphology as well as in the unaffected biological relatives of individuals with NSCL/P through the utilization of three-dimensional surface scanning and landmark-based statistical analysis of shape. The general hypotheses of this study are that there will be differences in palatal morphology between unaffected biological relatives of individuals with NSCL/P and age/sex/ancestry-matched controls. Furthermore, those differences will have sex-specific as well as ancestry-specific patterns describing the nature of those differences.

2.0 Methodology

2.1 Study Sample

2.1.1 The Pittsburgh Orofacial Cleft Study (POFC)

The POFC (PIs: Marazita & Weinberg) is a project based in the Center for Craniofacial and Dental Genetics at the University of Pittsburgh School of Dental Medicine. It is dedicated to understanding the causes of orofacial clefting by investigating genetic contributions with an emphasis on subclinical phenotypic predictors. The project recruits individuals with a history of non-syndromic orofacial clefting and their families as well as unaffected controls from multiple US and international sites in order to represent as much ethnic diversity as possible. US sites include Pittsburgh and Lancaster cities as well the state of Puerto Rico. International sites include Colombia, Philippines, and Nigeria. Data are collected on study participants including 3D images of the face through stereophotogrammetry, maxillary and mandibular dental casts that are surface scanned into three-dimensional digitized 3D models, dermatoglyphic and lip prints, ultrasound scans of the orbicularis oris muscle and intraoral videos of the velopharyngeal mechanism of the soft palate. Demographic data such as age, gender and ethnicity are available. In addition, past dental history, family, and social history as well as maternal exposures that may predispose to any congenital malformation are available. All subjects provided written consent and the data collection protocols outlined below have been approved by the Internal Review Board of the University of Pittsburgh.

2.1.2 Subject Inclusion

Included subjects were unaffected biological parents of individuals with NSCL/P and normal controls with no family history of clefting. The unaffected controls were matched to the study group based on age, gender, and ethnicity. Thus, all subjects are adults aged 18 years or older. Three ancestral groups were included, namely European, African, and Asian.

Exclusion criteria included missing canine or first permanent molar teeth, presence of Torus Palatinus, prior dimension-altering orthodontic or surgical treatment, prior palatal trauma causing palatal fractures, any surgical procedures involving the palatal region or dental casts with artifact hindering the ability to place landmarks in their correct position. In addition, the Latino admixed ancestry was excluded due to inadequate sample size in the male control subgroup.

Data were collected from 2625 subjects. However, after applying inclusion and exclusion criteria, the breakdown of included sample sizes is provided in Table 3. (Total N = 935)

Table 3 Sample size after applying exclusion criteria.

M = Males. F = Females. C = Sexes combined.

	Unaffected CL/P Parents (N = 141)			**Controls (N = 794)**		
Population	**M**	**F**	**C**	**M**	**F**	**C**
European	18	26	44	157	272	429
Asian	18	36	54	42	28	70
African	13	30	43	157	138	295
Combined	49	92	**141**	356	438	**794**

The control sample comprised a total of 794 subjects, with a mean age of 35.4 (±14.6), ranging from 18 to 80 years of age. The unaffected biological parent sample comprised a total of 141 subjects, with mean age of 35.1 (±9.1), ranging from 18.4 to 72.4. The two-tailed p-value for a two-sample t-test comparing means of ages between the two groups yielded no significant differences ($p = 0.7$).

2.2 Data Acquisition and Phenotype Capture

Maxillary dental impressions were obtained by standard techniques using a hydrocolloid material that is later poured into a plaster cast. The casts are later digitized by three-dimensional scanning using 3Shape scanning devices (both laser scanning and direct intraoral scanner), both of which have been validated for dimensional accuracy. This method has enough dimensional accuracy as direct intraoral scanning with regards to the study regions of interest (tooth-related regions) within the maxillary arch (Deferm et al., 2018). Casts are then processed digitally to be cleaned and boxed using 3Shape Ortho Analyzer software in order to obtain the final standard dental cast 3D mesh that can be used for study purposes.

2.2.1 Landmarking, Analysis and Visualization Software

A combination of software was used for landmarking, analysis and visualization of data for this study. Landmarking of the processed meshes was performed using 3dMD Vultus software. Geometric morphometric (GM) analysis was performed using MorphoJ. Visualization of the results was performed using MorphoJ, SlicerMorph package of 3D Slicer as well as the packages

geomorph and Morpho in R. A synthetic mesh was constructed by warping into mean shape that would later be used to visualize morphological differences (Figure 4). Euclidean Distance Matrix Analysis (EDMA) was performed using winEDMA software.

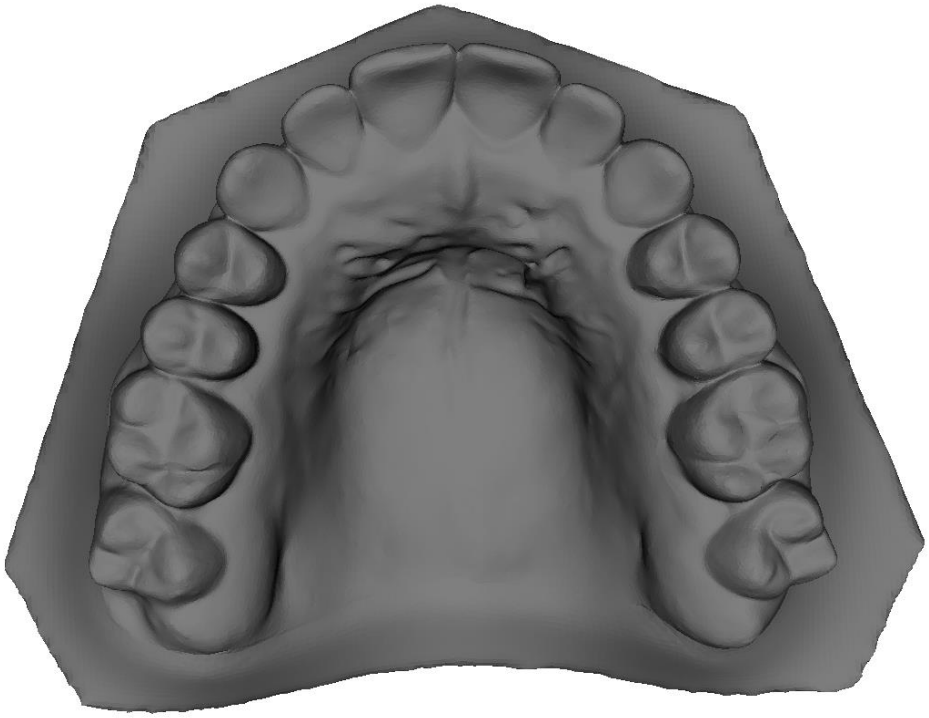

Figure 4 Synthetic mesh representing the mean shape.

Synthetic mesh created by warping a mesh into the mean shape using thin-plate spline method.

2.2.2 Dental Cast Landmarking

Three-dimensional coordinate data from seven landmarks were collected using 3dMD Vultus software that are then exported as numerical coordinates in the X, Y and Z dimensions in Euclidean space as numerical values in each dimension (Figure 5). Those seven landmarks are comprised of two paired bilateral landmarks and three midline landmarks (Figure 6).

Bilateral Landmarks are located at the deepest point of the gingival crevice or the cemento-enamel junction on the palatal surface of the canines and first permanent molars. These teeth were chosen due to their high positional stability within the dental arch in comparison to other teeth. They are seldom prone to migratory or full-bodily movement. The canine tooth being considered the "Cornerstone of the Mouth" is one of the longest-rooted teeth in the oral cavity and is one of the last teeth to be extracted or lost. They also separate anterior incisor teeth from posterior premolars and serve as a turning point in the course of the dental arch, thus giving a good indication of anterior arch width. Landmarks at the canine teeth were termed "Right Canine" or (CR) and "Left Canine" or (CL). First permanent molars are also very stable teeth that are, in fact, used for orthodontic anchorage. They have three roots that are embedded in the basal bone of the maxilla. In individuals with an erupted first permanent molar, at the first permanent molar region, the dental arch will have reached its maximum transverse width. Also, at the first molar region, the palatal vault will have reached its maximum height. Landmarks at the first permanent molar teeth were termed "Right Molar" or (6R) and "Left Molar" or (6L).

Midline landmarks are located in the midline at three regions. The first being at the tip of the incisive papilla, which is a soft tissue structure present in every oral cavity at the most anterior region of the palate in between the crowns of the maxillary central incisors. This landmark is termed "Incisive Papilla" or (IP). The remaining two landmarks are at the midline in between the aforementioned bilateral tooth-related landmarks. The midline landmark at the canine region are termed "Midline at Canine" or (CM), while the one at the molar region is termed "Midline at Molar" or (MM). Figure 6 shows a sample of a landmarked dental cast.

	X	Y	Z
IP	0.004193	-0.08634	0.379394
CR	-0.26194	-0.06508	0.177213
CL	0.26492	-0.07092	0.174893
6R	-0.3806	-0.05239	-0.25519
6L	0.376706	-0.0581	-0.25855
CM	8.81E-05	0.087193	0.128803
MM	-0.00337	0.245643	-0.34656

Figure 5 A landmark coordinate data file in the X, Y and Z planes.

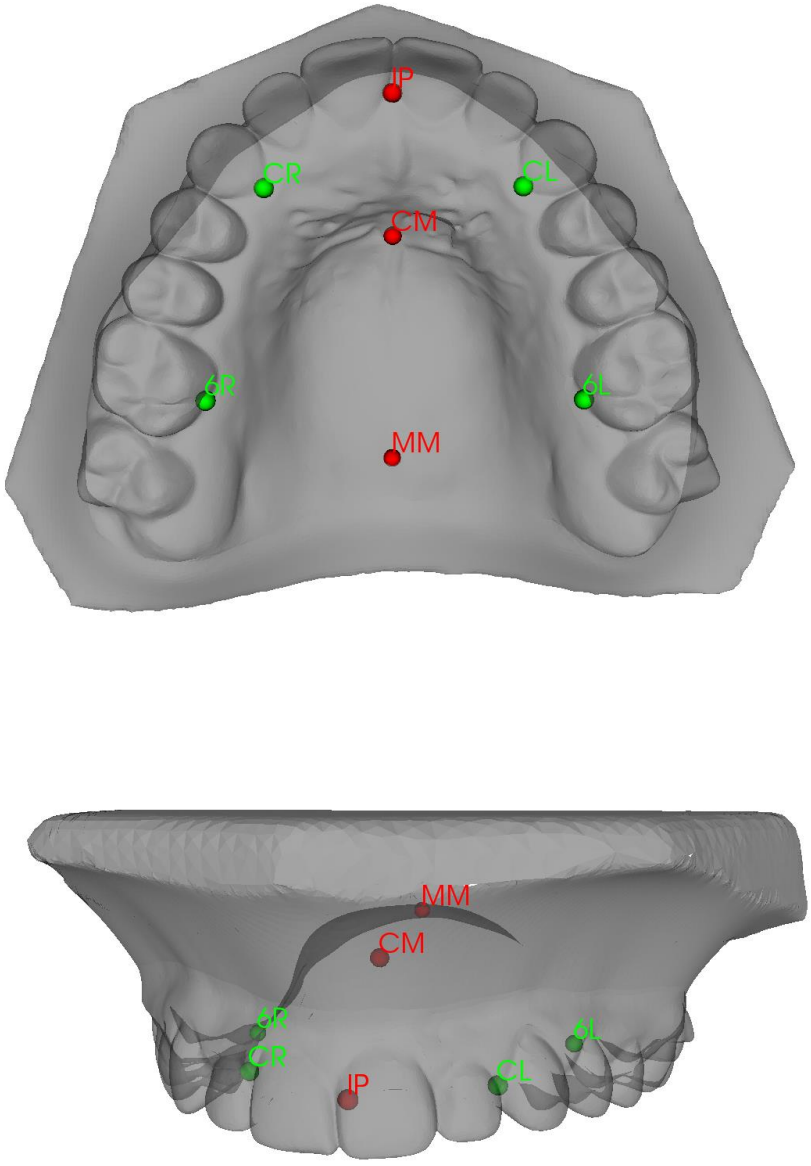

Figure 6 Landmarks on a 3D mesh of a maxillary dental cast.

Red = Midline Landmarks. Green = Bilateral Landmarks.

During landmarking, the observer was blinded to age, sex, family type, parent/control status and ancestry. The only information available to the observer was the coded series of anonymized individual identifiers of study participants, which coded for the recruitment site through the first two letters followed by a 5-digit number as follows:

- Lancaster: LC00000
- Pittsburgh: FC00000
- Nigeria: NG00000
- Philippines: PH00000
- Puerto Rico: PR00000
- Columbia: CO00000

2.2.3 Assessment of Landmarking Error

Landmark data was collected by one observer. Prior to data collection, landmarking was performed twice by the same observer on a set of 30 dental casts to evaluate intra-observer error. Each landmarking session was separated by at least 24 hours, and error in the x, y and z dimensions for each landmark was evaluated by calculating intraclass correlation coefficients. The resulting intraclass correlations ranged from 0.871 to 0.999, indicating low error. Table 4 presents intraclass correlation coefficients for the numerical value of coordinates in all three planes of Euclidean space.

Table 4 Assessment of Landmarking Error.

ICC = Intraclass correlation coefficient. SM = Single Measures. AM = Average Measures. CI = Confidence Interval.

Landmarks	**Plane**	**ICC** (SM)	**95% CI** (SM)	**ICC** (AM)	**95% CI** (AM)
Incisive Papilla (IP)	X	0.997	(0.995, 0.999)	0.999	(0.997, 0.999)
	Y	0.994	(0.988, 0.997)	0.997	(0.994, 0.999)
	Z	0.963	(0.923, 0.982)	0.981	(0.960, 0.991)
Right Canine (CR)	X	0.983	(0.958, 0.992)	0.991	(0.979, 0.996)
	Y	0.997	(0.993, 0.998)	0.998	(0.997, 0.999)
	Z	0.998	(0.995, 0.999)	0.999	(0.997, 0.999)
Left Canine (CL)	X	0.997	(0.993, 0.998)	0.998	(0.997, 0.999)
	Y	0.995	(0.990, 0.998)	0.998	(0.995, 0.999)
	Z	0.997	(0.994, 0.999)	0.999	(0.997, 0.999)
Right Molar (6R)	X	0.995	(0.990, 0.998)	0.998	(0.995, 0.999)
	Y	0.994	(0.987, 0.997)	0.997	(0.994, 0.999)
	Z	0.997	(0.993, 0.998)	0.998	(0.996, 0.999)
Left Molar (6L)	X	0.995	(0.990, 0.998)	0.998	(0.995, 0.999)
	Y	0.996	(0.991, 0.998)	0.998	(0.995, 0.999)
	Z	0.996	(0.990, 0.998)	0.998	(0.995, 0.999)
Midline at Canine (CM)	X	0.992	(0.978, 0.997)	0.996	(0.989, 0.998)
	Y	0.871	(0.622, 0.948)	0.931	(0.767, 0.973)
	Z	0.944	(0.816, 0.978)	0.971	(0.899, 0.989)
Midline at Molar (MM)	X	0.972	(0.933, 0.987)	0.986	(0.965, 0.994)
	Y	0.999	(0.997, 0.999)	0.999	(0.999, 1.000)
	Z	0.951	(0.776, 0.983)	0.975	(0.874, 0.991)

2.2.4 Types of Landmarks

Landmarks are points that have a numerical value mathematically (i.e. defined by coordinates in two or three dimensions in Euclidean space) that are assumed to be homologous, meaning they have an anatomical correspondence in a set of forms under comparison (Bookstein, 1991; Palci & Lee, 2019; Zelditch, Swiderski, & Sheets, 2012). Landmarks fall into three main categories, namely Type I, Type II and Type III (Bookstein, 1991).

Type I landmarks are points where anatomical correspondence among different individuals is dictated by histological evidence (juxtaposition of two or more tissues). This includes the meeting of two or more bones, or foramina for nerves and blood vessels (Palci & Lee, 2019). Type II landmarks are those dictated by geometry, such as the tip of a process or the deepest point on a bony notch. The type of geometry guiding the placement of Type II landmarks is usually self-evident, and are occurring along the margins of structural elements that can be homologized in their entirety (Palci & Lee, 2019).

On the other hand, Type III landmarks are also dictated by geometry, but where correspondence is more loosely supported. Examples include intersection of inter-landmark segments, points furthest from inter-landmark segments or those involving perpendiculars (Palci & Lee, 2019). In such cases, the geometry becomes less self-evident and requires an extra step involving a subjective choice of the observer in order for it to be placed. This step involves a geometric construction that permits the identification of landmarks, such as drawing an imaginary line joining landmarks to find its midpoint (Palci & Lee, 2019).

The definitions and categorizations of landmarks, however, are not mutually exclusive, as the same landmark can be categorized as two types (Palci & Lee, 2019). In the present study, five landmarks are located at juxtapositions of two tissues while also being at the deepest point on the

cervical line on the palatal aspects of teeth (bilateral landmarks) or the tip of the incisive papilla. Those five landmarks satisfy the definitions to be categorized as both Type I and Type II landmarks.

In contrast, the midline landmarks that are located at the deepest (highest) aspect of the palatal vault at the canine and molar regions are considered Type III landmarks. This might explain their relatively lower, albeit still reliable, intraclass correlation coefficients.

2.2.5 Generalized Least Squares Procrustes Superimposition

The generalized least squares Procrustes superimposition (GPS) is the most commonly used and the most favorable method of superimposition, mostly due to the fact that the resulting superimposition retains a series of properties that make it suitable for further statistical testing (Palci & Lee, 2019; Zelditch et al., 2012).

Procrustes superimposition relies on the translation, rotation, and scaling, all are mathematical processes that do not affect shape. It is based on Procrustes distances as the criterion used to minimize differences in configurations (Zelditch et al., 2012). Procrustes distance is the summed squared Euclidean distances between corresponding (homologous) landmarks across different shapes. Zelditch et al. summarized the steps of GPS as follows:

1. Center each configuration of landmarks at the origin by subtracting the coordinates of its centroid from the corresponding coordinates of each landmark. This translates each centroid to the origin. (A configuration is the set of landmarks representing each specimen.)
2. Scale the landmark configurations to unit centroid size by dividing each coordinate of each landmark by the centroid size of that configuration.

3. Choose one configuration to be the reference, then rotate the other configuration to minimize the summed squared distances between homologous landmarks (Procrustes distances).

When there are more than two configurations, which is the case for the present study, the first configuration is used as the reference. Following this, the average shape is calculated, and all are brought to optimum alignment with this average shape acting as a new reference. The average shape is then re-calculated, and the configurations re-aligned until the newest reference is the same as the previous, at which point the iterations stop. The final reference shape is the one that minimizes the average distances of configurations from that reference (Zelditch et al., 2012). Figure 7 shows the plot of Procrustes distances of individual subject configurations in incremental order. Figure 8 shows a visualization of landmark variances among the study cohort after GPS.

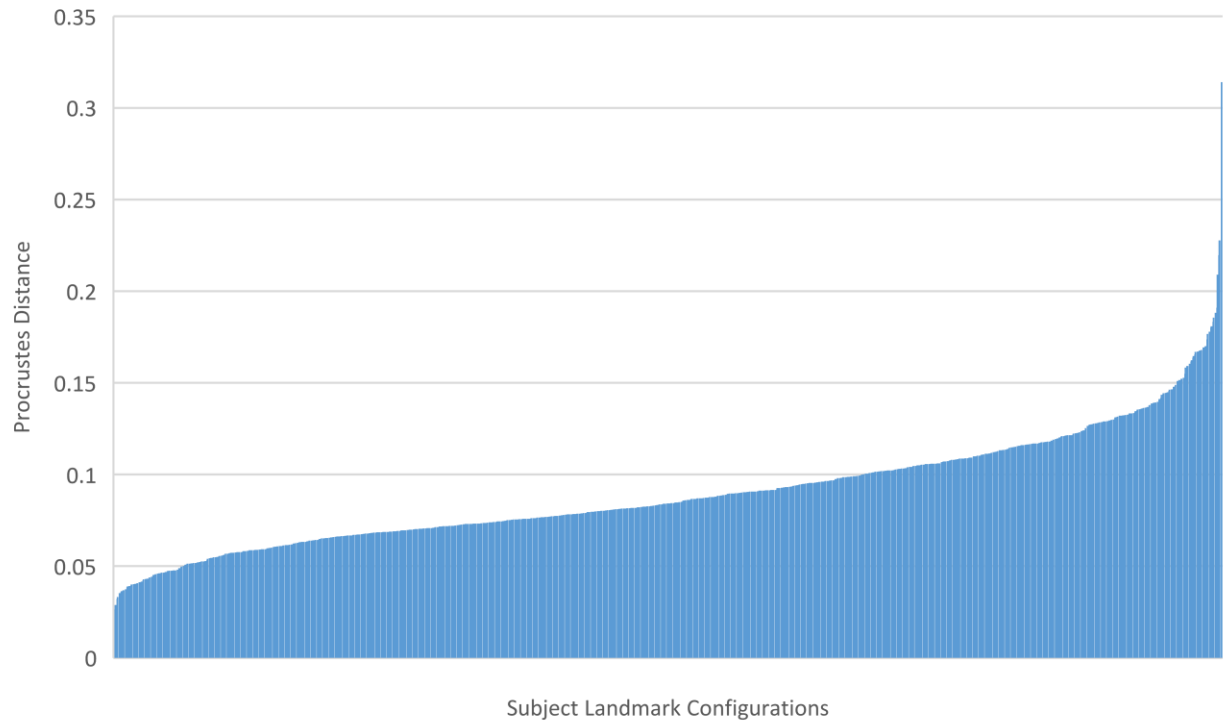

Figure 7 Bar plot of individual subjects (N=935) against their Procrustes distances.

Sudden non-gradual changes in Procrustes distances would suggest possible misplaced landmarks.

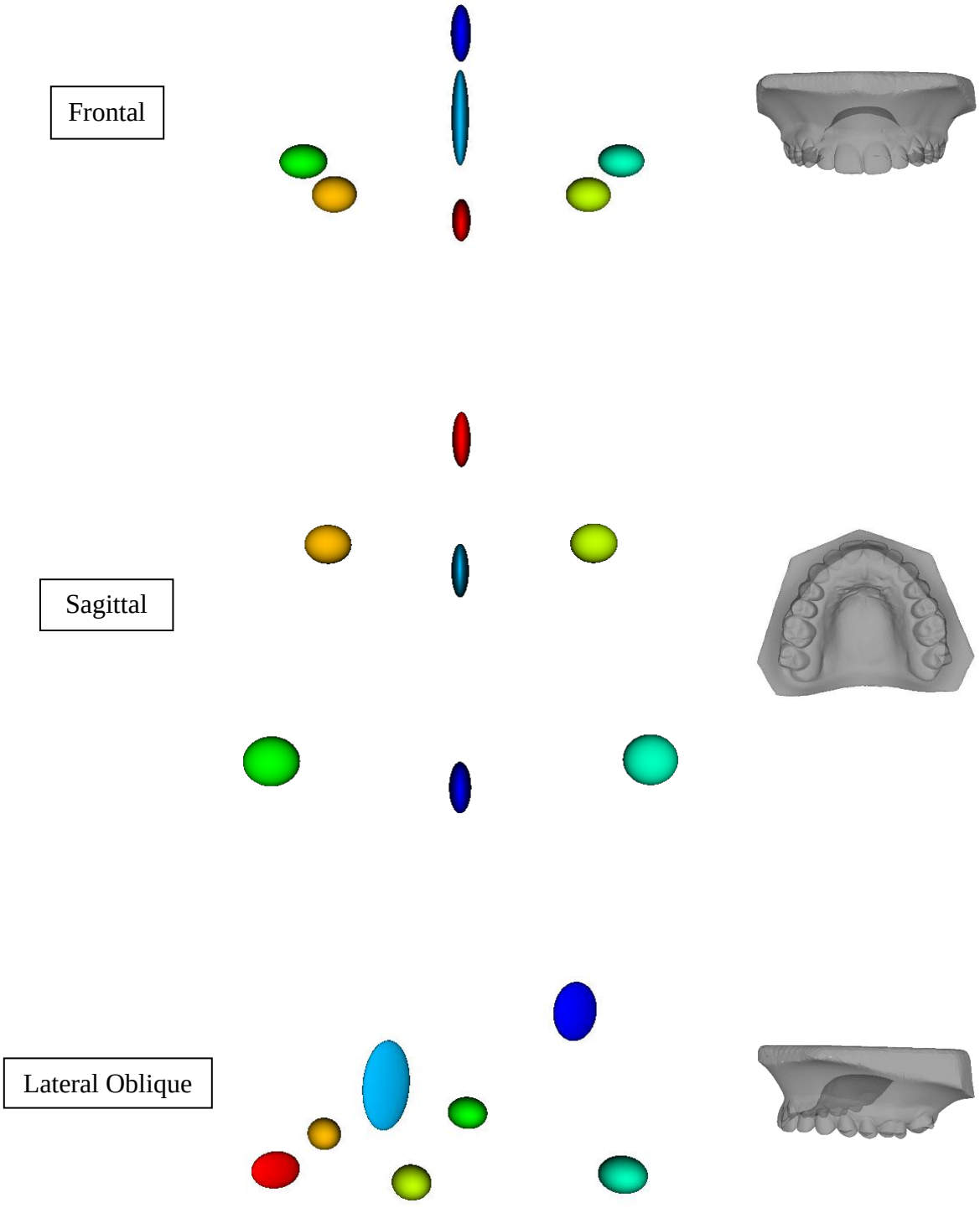

Figure 8 Landmark variances with their respective cast orientations.

Red = IP. Orange = CR. Yellow = CL. Green = 6R. Turqoise = 6L. Light Blue = CM. Dark Blue = MM.

Very large individual variances would suggest possible misplaced landmarks.

2.2.6 Cross Validation of Software

GPS was performed using two software, namely MorphoJ and the geomorph package in R. Alignment was done while enforcing symmetry, meaning the pairing of bilateral landmarks yielding a symmetric component of shape to be analyzed. Principal component scores for the first principal components of both software are plotted in Figure 9. Linear regression yielded a correlation coefficient of 0.999, R-Squared value of 0.999 with a standard error of 0.001.

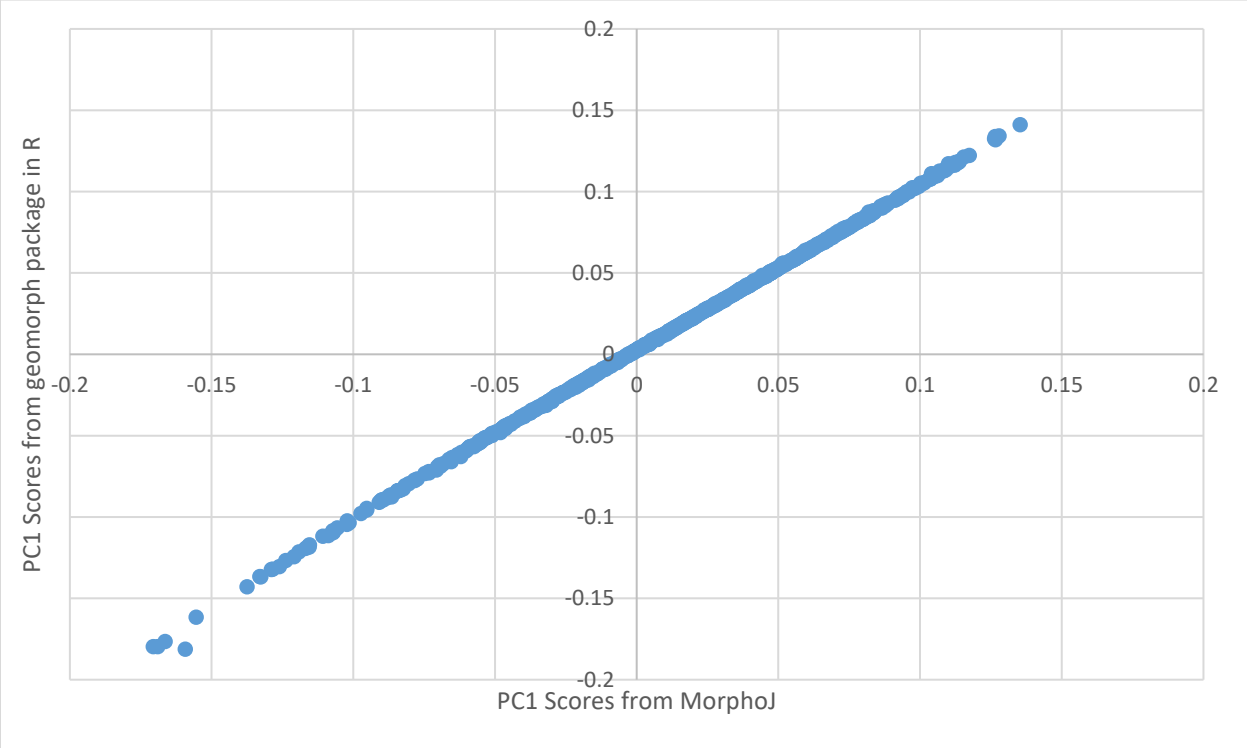

Figure 9 Plot of the first principal component scores from two morphometrics software.

X-axis = MorphoJ. Y-axis = R package geomorph.

2.2.7 Allometry

Allometry is defined as the size-related changes in morphological traits (Klingenberg, 2016). Albeit a lot of controversy over including the effect of centroid size on shape in analyses, for the purpose of the current study, it is only reasonable to keep the allometric component included in our analyses. In addition, while there was a positive correlation, the centroid size in our sample only contributed to 2.29% of variation in shape. Figure 10 shows the plot of the regression of the centroid size against the symmetric shape component in our sample. In our sample, males on average had larger centroid sizes than females. With regards to ancestral groups, Africans on average had the largest centroid sizes followed by Asians with Europeans having the smallest centroid sizes. It was also shown that age had minimal effects on centroid size and the overall variation in shape, contributing to only 0.99% of variation in shape (Figures 11 and 12). No difference in centroid size was detected by parent/control status.

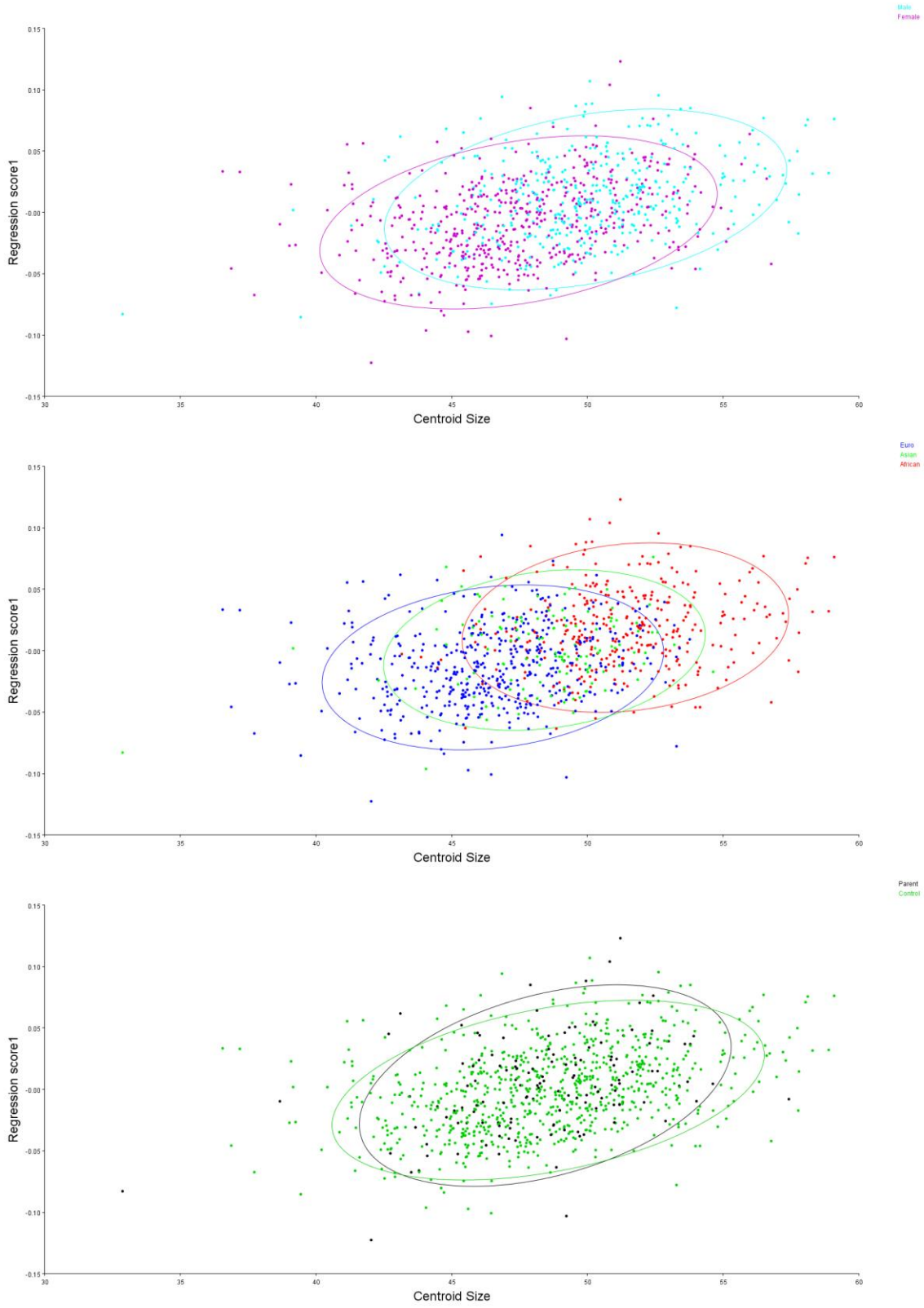

Figure 10 Plot of Allometry.

Colors: Top = By Sex, Middle = By Ancestry, Bottom = By Individual Type.

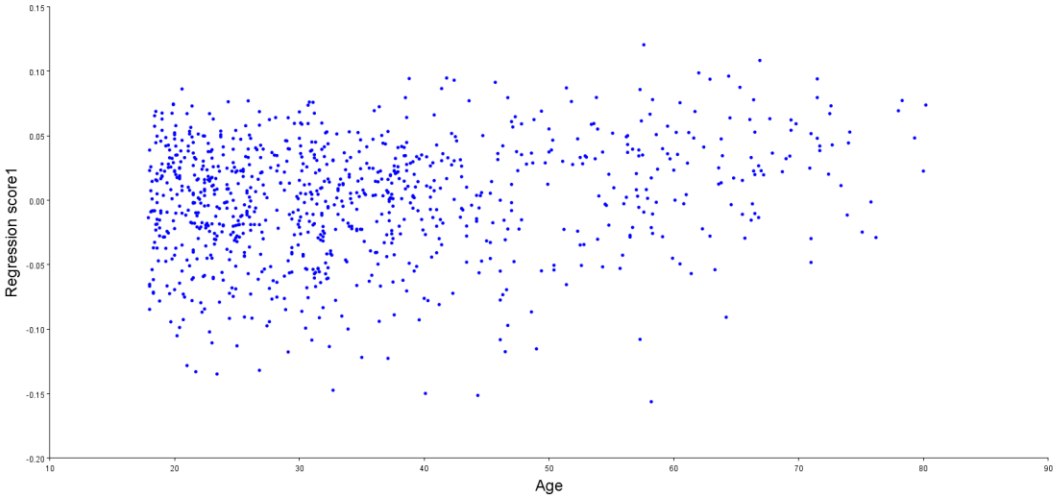

Figure 11 Plot of Age and Variation in Shape.

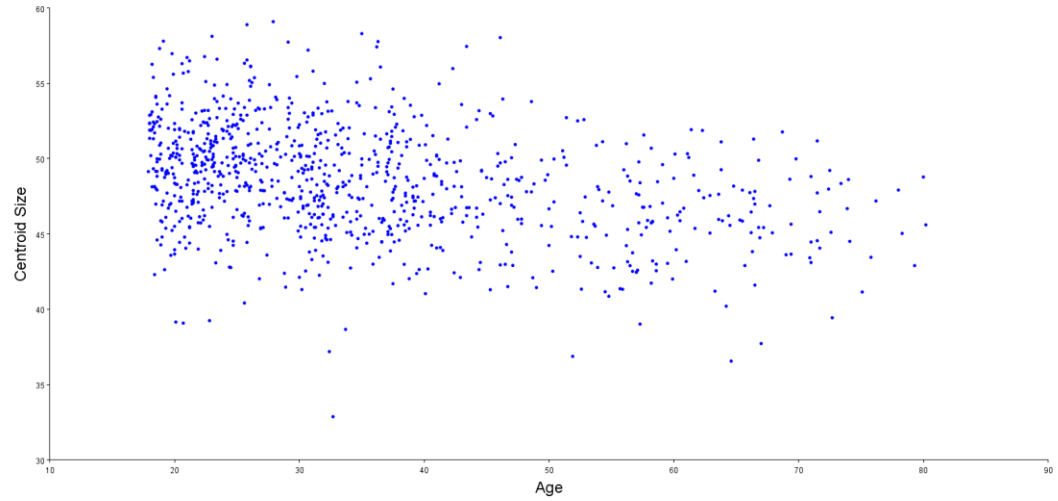

Figure 12 Plot of Age and Centroid Size.

2.3 Statistical Analysis of Shape: Geometric Morphometrics

2.3.1 Ordination Methods

Ordination methods, namely Principal Component analysis (PCA) and Canonical Variates Analysis (CVA) are used to describe shape variation and diversity in a sample. Both analyses produce a new set of variables that are linear combinations of the original variables. They also provide individual scores on those variables, which are then plotted and used to inspect patterns visually. These scores order the individuals along the new variables, hence the term "ordination methods". PCA is used to simplify description of variation among individuals, while CVA is used to simplify descriptions between different groups (Zelditch et al., 2012).

2.3.1.1 Principal Component Analysis

Geometric shape variables are neither biologically nor statistically independent. Because morphometric variables are expected to be correlated as they describe features of an organism that are functionally, developmentally, or genetically linked, they present with patterns of variation and covariation that are complex and difficult to interpret. PCA simplifies those patterns and facilitates interpretation by introducing new independent variables that are linear combinations of the original variables. This simplifies the presentation of findings and may aid future research efforts in identifying causal factors underlying those covariances.

A PCA yields a list of principle components (PC) with their corresponding eigenvalues in decreasing order of variance explained by each principal component. If PCs are to be statistically analyzed, only those that contribute to higher than 5% of variance individually and/or 90% of

variance cumulatively are of meaningful interest (Zelditch et al., 2012). Regarding our data, the first five PCs contributed, in general, to higher than 90% of variance explained.

For the present study, PCA will be used to detect, characterize, and quantify the contribution of patterns of morphological variation among individuals in the overall sample. Those patterns are each independently represented by a principal component along with the corresponding contribution to total variance.

2.3.1.2 Canonical Variates Analysis

CVA serves to facilitate identification of the differences between groups that are determined *a priori*. In a similar manner to PCA, CVA constructs a new coordinate system (the canonical variates) that determines scores for each individual on those axes. Those canonical variates (CV) are also linear combinations of the original variables. While PCA is used to describe differences among individuals, CVA is used to describe differences among group means. However, CVA utilizes patterns of within-group variation to scale the axes of the new coordinate system. Therefore, the distances in canonical variate space are not equal to the distances in the original coordinate system. These distances provide directionality to the discrimination between groups. Thus, CV1 is the direction in which groups are most effectively discriminated (Zelditch et al., 2012). It is those distances that can later be utilized in multivariate statistics for hypothesis testing. A discriminant function Analysis is a two-group CVA.

As mentioned, the distances in CV space between group means are statistically tested. Two types of distances are analyzed. The first is the Procrustes distance mentioned above, which is the summed squared distances between corresponding landmarks. The second is the Mahalanobis distance, which is the squared distance between two means divided by the pooled sample variance-covariance matrix, thereby adjusting for correlations among variables (Zelditch et al., 2012).

For the present study, CVA will be used to detect and characterize patterns of morphological variation among groups that are specified *a priori* by comparing group means as well as represent the possible presence of differing within-group variations. In addition, CVA will also yield Procrustes and Mahalanobis distances that represent the differences between groups. Those differences will then be tested later for statistical significance using permutation tests.

2.3.2 Permutation Tests

Permutation testing is a resampling approach in which the observed data themselves are used as a basis in order to approximate an unknown statistical distribution through random resampling. Unlike bootstrap tests, permutation tests perform resampling without replacement. In order to test hypotheses that the means of two groups are equal, the differences between the means of the two groups are calculated (which are the distances for morphometric analyses). Then the groups are merged together into one large group, then a series of paired permutations are drawn with each pair containing two permutations sets, each set of equal sample sizes (N) to the original groups but with elements randomly drawn without replacement from the merged set. The difference between the means of the paired permutation tests is then calculated and the process is repeated for $N_{Permutation}$ sets. We are performing 10000 permutations for the current study. The proportion of times in which the difference in means of the paired permutation sets exceeds that of the means of the original data is considered as the probability that the observed value could have resulted from a random splitting of a single underlying distribution, or in other words, the p-value.

For the present study, permutation tests will be used to test for statistical significance of differences among groups represented by Procrustes and Mahalanobis distances yielded by CVA.

2.3.3 Bonferroni Correction

The baseline p-value to infer statistical significance from our tests is set at 0.05. However, there are multiple contrasts being tested within each aim of this study. Therefore, we adjusted for multiple testing within each aim by dividing the baseline p-value by the number of contrasts in that aim. Therefore, the corrected alpha levels are p=0.01 for Aim I, p=0.01 for Aim II and p=0.0083 for Aim III.

2.3.4 The Pinocchio Effect

The generalized least squares Procrustes superimposition (GPS) disfavors large local changes in shape brought about by any particular landmarks in favor of smaller shifts across all landmarks as a whole. This leads to the generation of what is called the Pinocchio effect, that is, when there are relatively isolated landmarks causing significant local changes in shape, the changes are distributed over all other landmarks during the alignment procedure (Palci & Lee, 2019). This leads to the creation of a mean shape (and Procrustes distances) with the resultant analyses that would detect a variation in shape but might fail to detect the localized nature of this shape variation (if there was any) due to it being masked by the Pinocchio effect. Figure 13 depicts an example of the Pinocchio effect arising due to GPS alignment of two shapes as opposed to using a different type of alignment, the resistance fit theta-rho analysis (RFTRA) which is less prone to the Pinocchio effect and aligns the two shapes without creating an artificial displacement of non-displaced points.

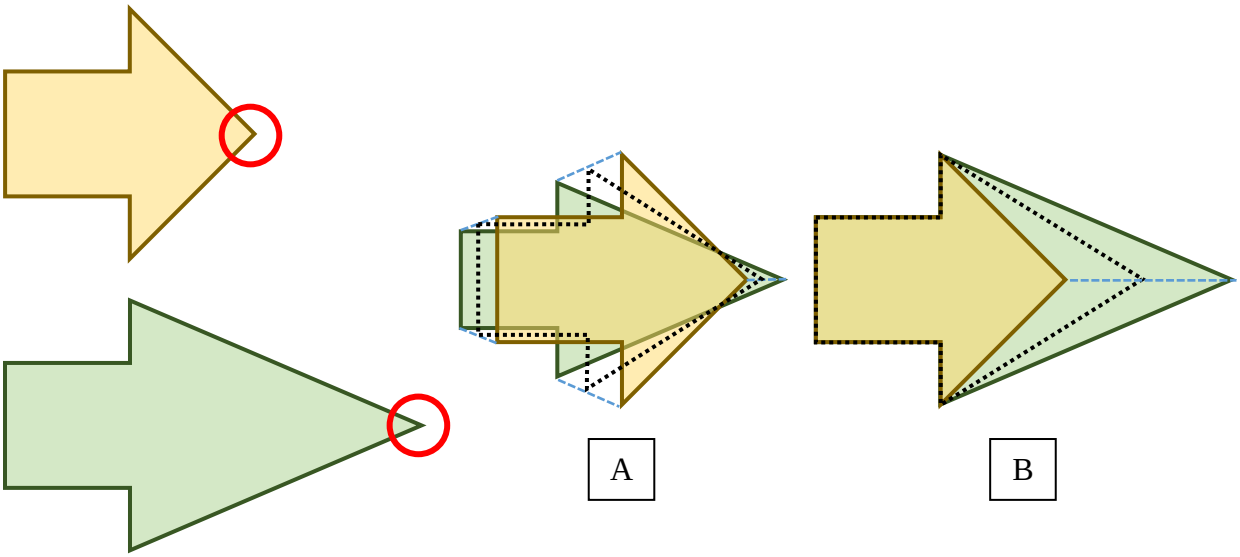

Figure 13 The Pinocchio Effect.

The difference between shapes is due to a localized displacement at one landmark (circled in red).

A = GPS alignment. B = RFTRA alignment. Dotted lines = Mean shape.

2.4 Statistical Analysis of Shape: Euclidean Distance Matrix Analysis

The shape of an object is all of the geometric features of that object with the exception of size, position and orientation, while the form of an object is the shape combined with the log-transformed centroid size (Klingenberg, 2016). Euclidean Distance Matrix Analysis (EDMA) is an approach in morphometrics based on the principle of form invariance, that is, the form of an object remains invariant under any rotation, translation or reflection of this object (Richtsmeier, DeLeon, & Lele, 2002; S. Weinberg, 2007). The form of an object in EDMA is the complete set of linear distances between all landmarks. For an object with K landmarks, there will be K(K – 1)/2 linear distances. This means that EDMA for this study will be based on the statistical analysis of 21 linear distances from 7 landmarks. Due to the presence of the Pinocchio effect, EDMA will complement the findings of significant differences in shape by assisting in the discovery of

localized regions were shape is different, if there were any. Therefore, EDMA will act as a screening and quality control measure rather than a means to test hypotheses.

In EDMA, coordinate data is used to construct a matrix of numerical values, that is the form matrix (FM) for each individual using the set of landmarks and thus, a mean FM for each group can be calculated. The difference between the mean FM for each group is then used to create a form difference matrix (FDM). The form matrix can also be scaled to unit centroid size to obtain a shape matrix (SM) and a corresponding shape difference matrix (SDM).

Statistics in EDMA are based on the utilization of bootstrap resampling to conduct t-tests to compare means. The bootstrap resampling method is similar to the permutation tests mentioned above, but with replacement. Therefore, bootstrap resampling is able to provide confidence intervals. The first component of EDMA is to compare mean SM for each group and the corresponding SDM. The second component is to compare means of every possible linear distance between landmarks and obtain confidence intervals. Based on the recommendations of Lele and Richtsmeier, the p-value is based on an alpha level of 0.1 instead of 0.05, with recommendations to aim for 90% confidence intervals instead of 95%, as the tails of the estimated distribution tend to be less precisely estimated than the middle portion of the distribution, with a 95% confidence interval becoming more unstable than 90% or 80% confidence intervals (Lele & Richtsmeier, 2001; S. Weinberg, 2007).

Finally, for the present study, EDMA will only be performed when statistically significant differences in shape have been detected in group comparisons using CVA and permutation tests. This will aid in detecting possible localized regions contributing to morphological differences between the groups being compared.

2.5 Specific Aims and Study Design

The overall study design for this project is divided into three aims representing three phases of the study. The overall hypothesis for this study is that palatal morphology will differ between biological parents of individuals with NSCL/P and demographically matched controls, and these differences might show sex- and ancestry-specific patterns of shape change.

2.5.1 Aim 1 Characterize normal palatal morphology: The effect of sex and ancestry.

This is a descriptive portion of the study aimed at characterizing patterns of normal variation of palatal shape as well as differences in shape brought about by sex and ancestry. This aim comprises five contrasts. The p-value for statistical significance for this aim is set to 0.01.

- General Contrast 1: Compare all controls (ancestries combined) by sex.
- General Contrast 2: Compare all controls (sexes combined) by ancestry.
- Stratified Contrast 1: Compare all male controls by ancestry.
- Stratified Contrast 2: Compare all female controls by ancestry.
- Stratified Contrast 3: Compare male controls vs. female controls within each ancestry.

2.5.2 Aim 2 Characterize palatal morphology in unaffected parents: The effect of sex and ancestry.

This is a descriptive portion of the study aimed at characterizing patterns of variation of palatal shape as well as differences in shape brought about by sex and ancestry but within the

biological parents of unaffected individuals with NSCL/P. This aim comprises five contrasts. The p-value for statistical significance for this aim is set to 0.01.

- General Contrast 1: Compare all parents (ancestries combined) by sex.
- General Contrast 2: Compare all parents (sexes combined) by ancestry.
- Stratified Contrast 1: Compare all fathers by ancestry.
- Stratified Contrast 2: Compare all mothers by ancestry.
- Stratified Contrast 3: Compare fathers vs. mothers within each ancestry.

2.5.3 Aim 3 Examine the effects of sex and ancestry on parent-control differences in palatal morphology.

This aim targets the comparison between parents and controls as well as the influences of sex and ancestry on the shape differences between parents and controls. A preliminary t-test comparing means of inter-canine Euclidean distances pointed towards a significant decrease ($p=0.0008$) in males and a borderline significant increase ($p=0.049$) in females, thereby suggesting a sex-specific pattern of difference. This aim comprises six contrasts. The p-value for statistical significance for this aim is set to 0.0083.

- General Contrast: Compare all study subjects (sexes and ancestries combined) by parent/control status.
- Stratified Contrast 1: Compare all fathers vs. all male controls (ancestries combined).
- Stratified Contrast 2: Compare all mothers vs. all female controls (ancestries combined).
- Stratified Contrast 3: Compare all parents vs. all controls (sexes combined) by ancestry.
- Stratified Contrast 4: Compare fathers vs. male controls within each ancestry.

- Stratified Contrast 5: Compare mothers vs. female controls within each ancestry.

3.0 Results

3.1 Principal Component Analysis

3.1.1 Control Sample

PCA yielded a total of eight principal components with the first five principal components explaining cumulatively 92.53% of the total variance (Table 5).

There was a pattern of separation of sexes along the third PC where males had higher posterior palatal vaults and a shorter anteroposterior (AP) dimension (Figure 14). There was a pattern of separation of the African from Asian ancestries along the first PC where Africans had higher palatal vaults and shorter AP dimension than Asians. There was also a pattern of separation of the European from African ancestries along the third and fourth PC axes where Europeans had higher anterior palatal vaults and a longer AP dimension than Africans (Figure 15).

The first principal component (PC) describes a pattern of variation in palatal vault height coupled with AP dimension whereby a higher palatal vault is coupled with a shorter AP dimension. The second PC coupled a higher palatal vault with a shorter mediolateral (ML) dimension. The third PC described a higher palatal vault occurring more posteriorly coupled with a shorter AP dimension. The fourth PC showed a pattern of increased palatal vault height occurring more anteriorly (Figure 16).

Table 5 PCA of the control sample.

PC	Eigenvalues	% Variance	Cumulative %
1	0.002679	34.386	34.386
2	0.001874	24.052	58.438
3	0.001409	18.086	76.524
4	0.000752	9.651	86.174
5	0.000495	6.359	92.533
6	0.00032	4.111	96.644
7	0.00021	2.697	99.342
8	5.13E-05	0.658	100

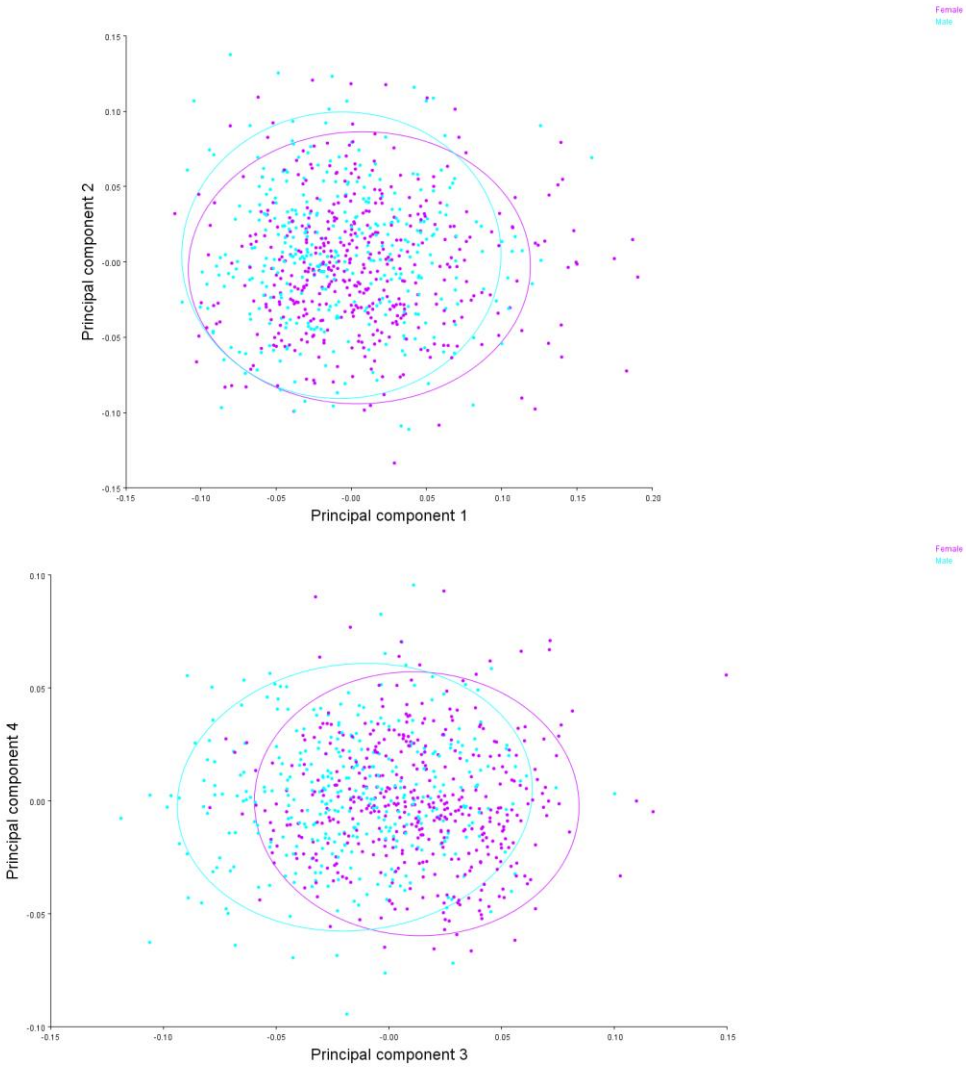

Figure 14 PCA of the control sample by sex.

Confidence ellipses represent 90% frequency.

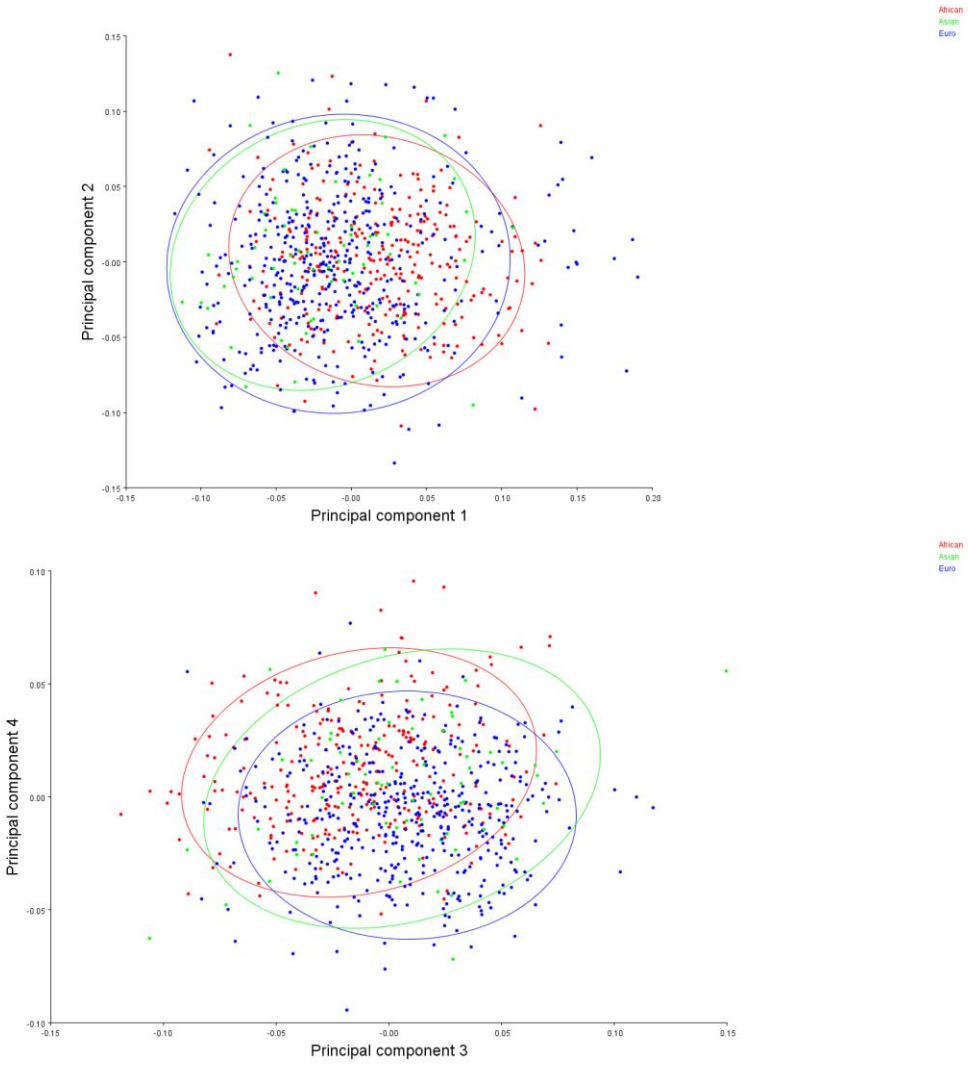

Figure 15 PCA of the control sample by ancestry.

Confidence ellipses represent 90% frequency.

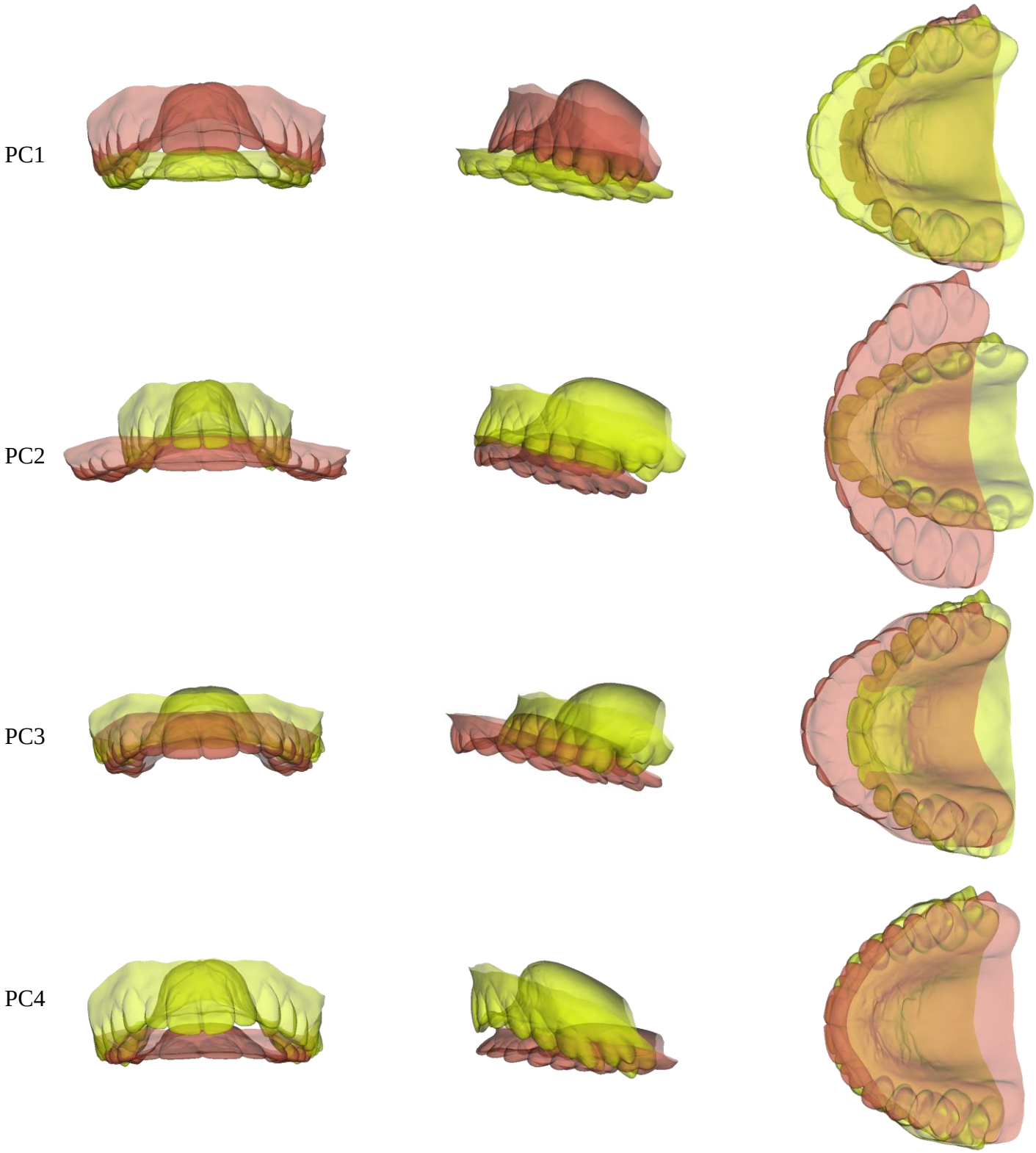

Figure 16 Principal component effects in the control sample.

Red = Positive. Yellow = Negative.

3.1.2 Parent Sample

The parent sample yielded a series of 8 principal components with the first five principal components (PC) explaining 91.75% of the total variance cumulatively (Table 6).

There was a pattern of separation of the African ancestry from the other two ancestries along the second PC where Africans had a higher palatal vault with shorter anteroposterior (AP) dimension and a wider mediolateral (ML) dimension. There was also a pattern of separation of European ancestry from the other two ancestries along the fourth PC where Europeans had a higher anterior palatal vault (Figure 18).

The first PC showed a pattern of shape difference related to the height of the palatal vault but with less effect on AP or ML dimensions of the palate than that found in controls. The second PC showed a pattern whereby increased palatal vault height was coupled with a shorter AP and wider ML dimensions. The third PC showed a coupling of increased palatal vault height with a decreased ML dimension. The fourth PC again showed a pattern related to vault height but with the increased vault height occurring more anteriorly than posteriorly (Figure 19).

Table 6 PCA of the parent sample.

PC	Eigenvalues	% Variance	Cumulative %
1	0.00299	34.586	34.586
2	0.001923	22.251	56.837
3	0.001575	18.215	75.052
4	0.000806	9.33	84.382
5	0.000637	7.372	91.753
6	0.000508	5.875	97.628
7	0.000159	1.834	99.462
8	4.65E-05	0.538	100

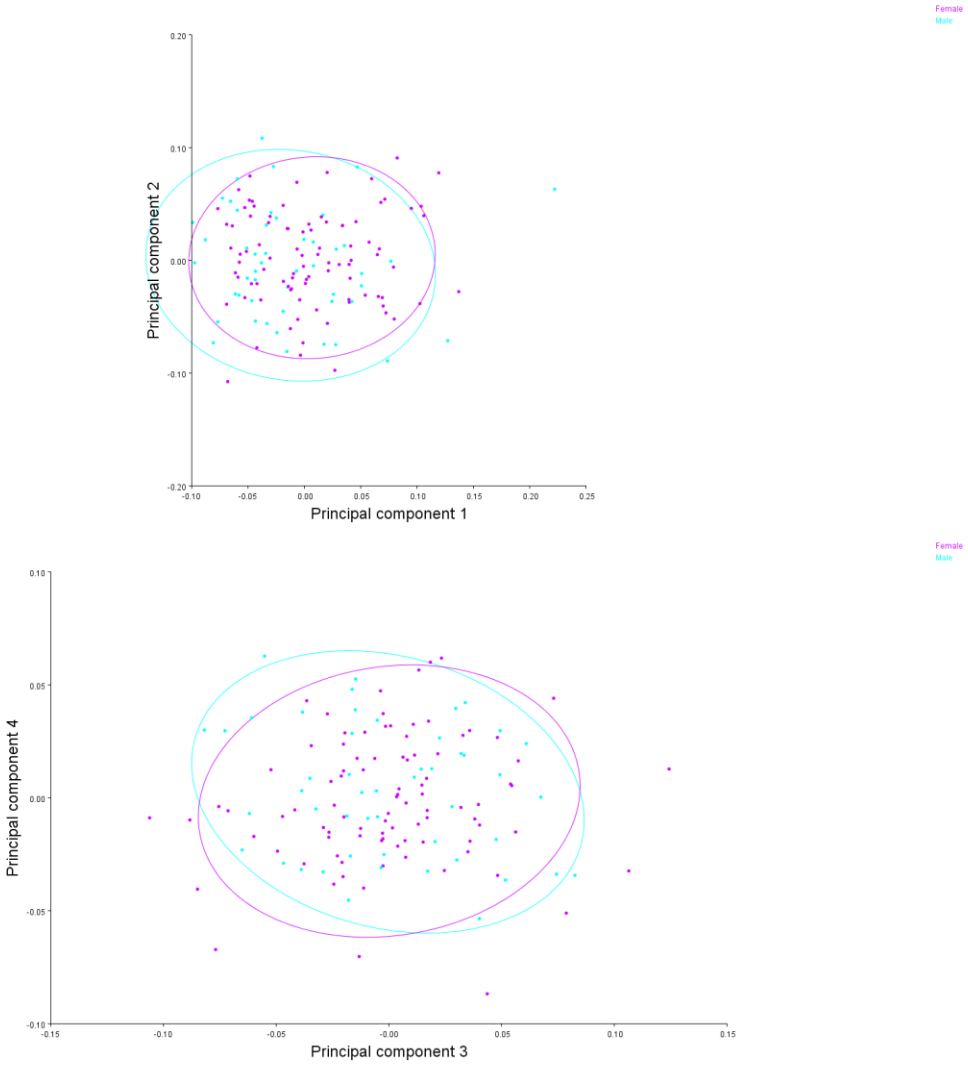

Figure 17 PCA of the parent sample by sex.

Confidence ellipses represent 90% frequency.

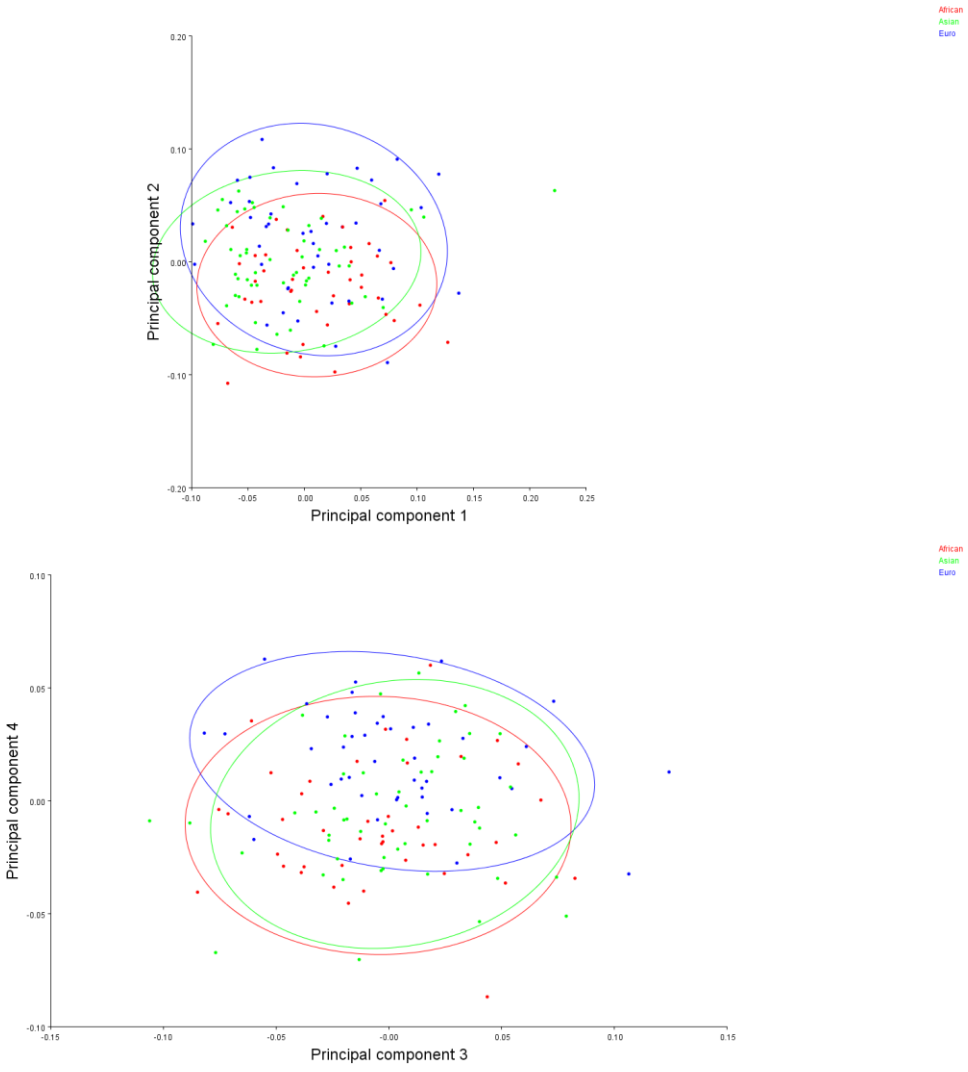

Figure 18 PCA of the parent sample by ancestry.

Confidence ellipses represent 90% frequency.

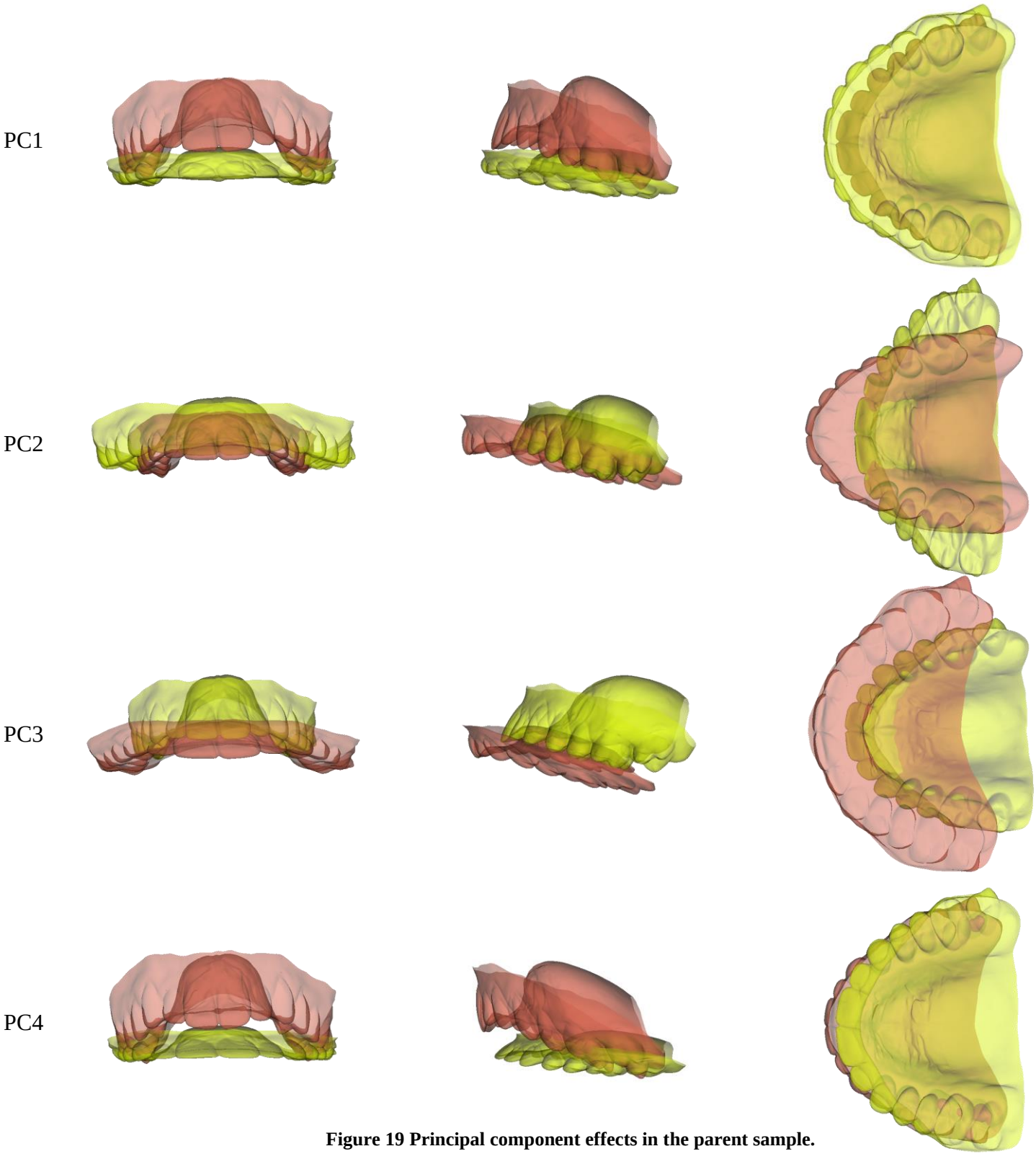

Figure 19 Principal component effects in the parent sample.

Red = Positive. Yellow = Negative.

3.1.3 Combined Sample (Parents and Controls)

PCA of the combined sample yielded 8 principal components with the first five principal components explaining 92.18% of the total variance cumulatively (Table7).

There was a pattern of separation of sexes along the third PC where females had higher palatal vaults and shorter anteroposterior (AP) dimension (Figure 21). There was a pattern of separation of the African from Asian ancestries along the first PC where Africans had higher palatal vaults and shorter AP dimension than Asians. There was also a pattern of separation of the European from African ancestries along the third and fourth PC axes where Europeans had a higher anterior palatal vault and a longer AP dimension than Africans (Figure 21). No patterns of separation were noted by parent/control status along any of the PC axes (Figure 22).

Patterns of variation in the combined sample were very similar to the control sample. The first principal component (PC) showed a pattern related to the palatal vault height coupled with the AP dimension whereby increased vault height was coupled with shorter AP dimension. The second PC showed a pattern where a higher palatal vault was coupled with a narrower mediolateral (ML) dimension and a longer AP dimension. The third PC showed a pattern where the increase in palatal vault height was more posteriorly and coupled with a shorter AP dimension. The fourth PC again was related to the palatal vault height where the increased vault height was occurring more anteriorly (Figure 23).

Table 7 PCA of the combined sample (parents and controls).

PC	Eigenvalues	% Variance	Cumulative %
1	0.002693	34.003	34.003
2	0.001853	23.402	57.406
3	0.00147	18.555	75.961
4	0.000768	9.701	85.662
5	0.000516	6.517	92.179
6	0.000361	4.562	96.741
7	0.000207	2.613	99.354
8	5.12E-05	0.646	100

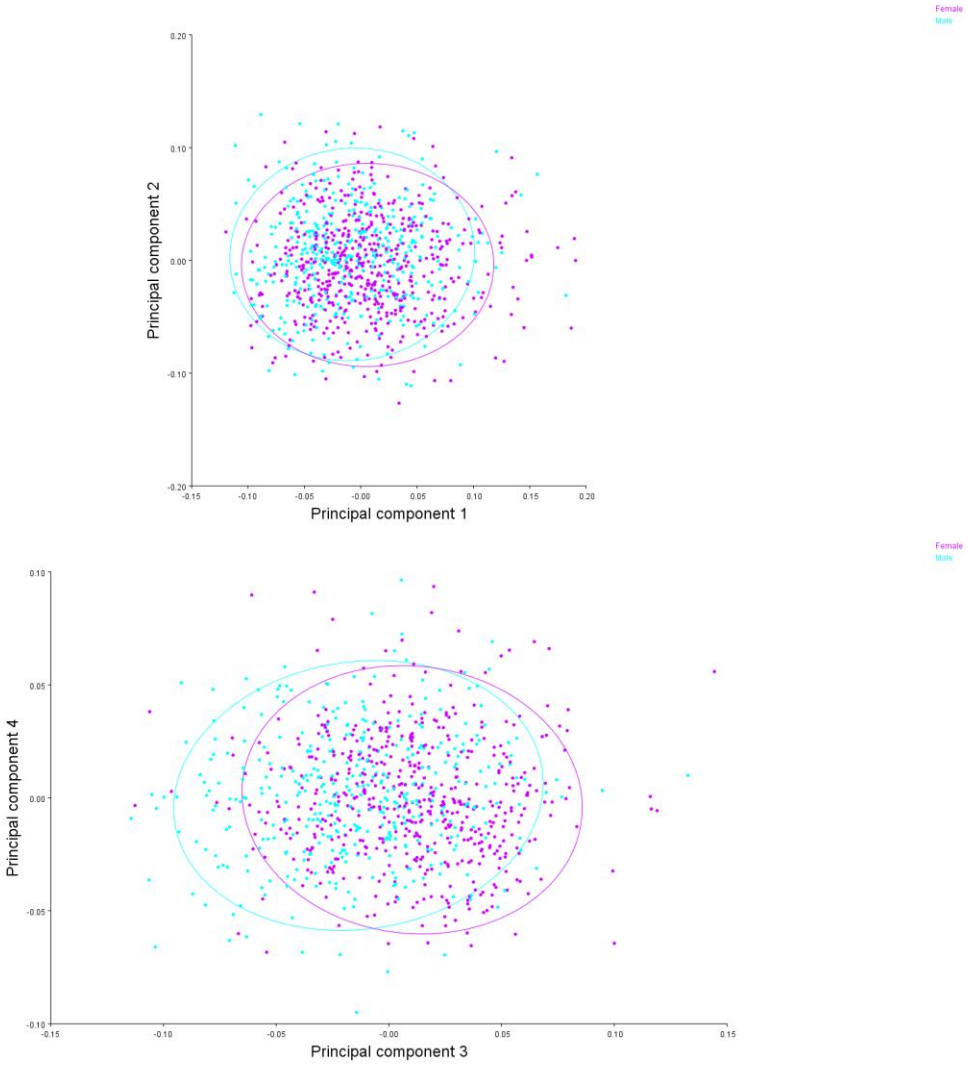

Figure 20 PCA of the combined sample by sex.

Confidence ellipses represent 90% frequency.

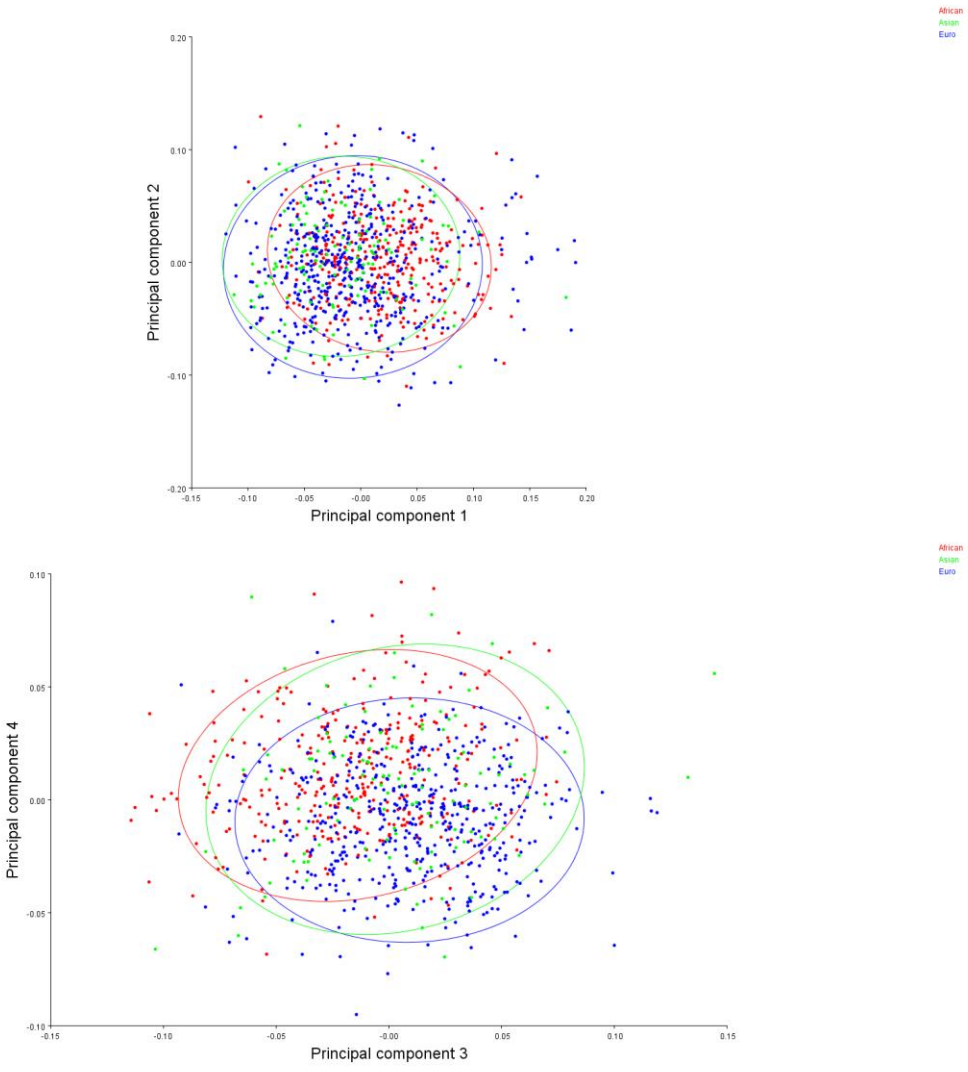

Figure 21 PCA of the combined sample by ancestry.

Confidence ellipses represent 90% frequency.

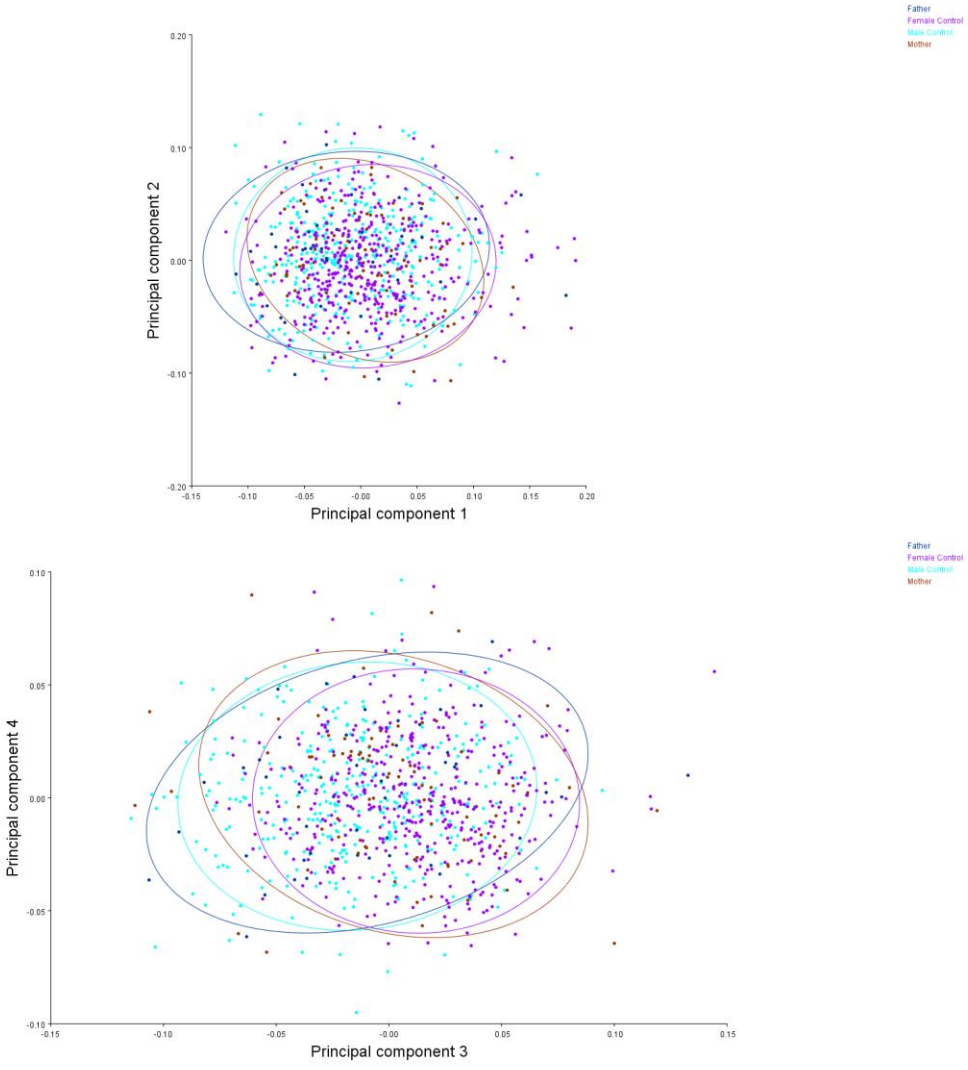

Figure 22 PCA of the combined sample by parent/control status.

Confidence ellipses represent 90% frequency.

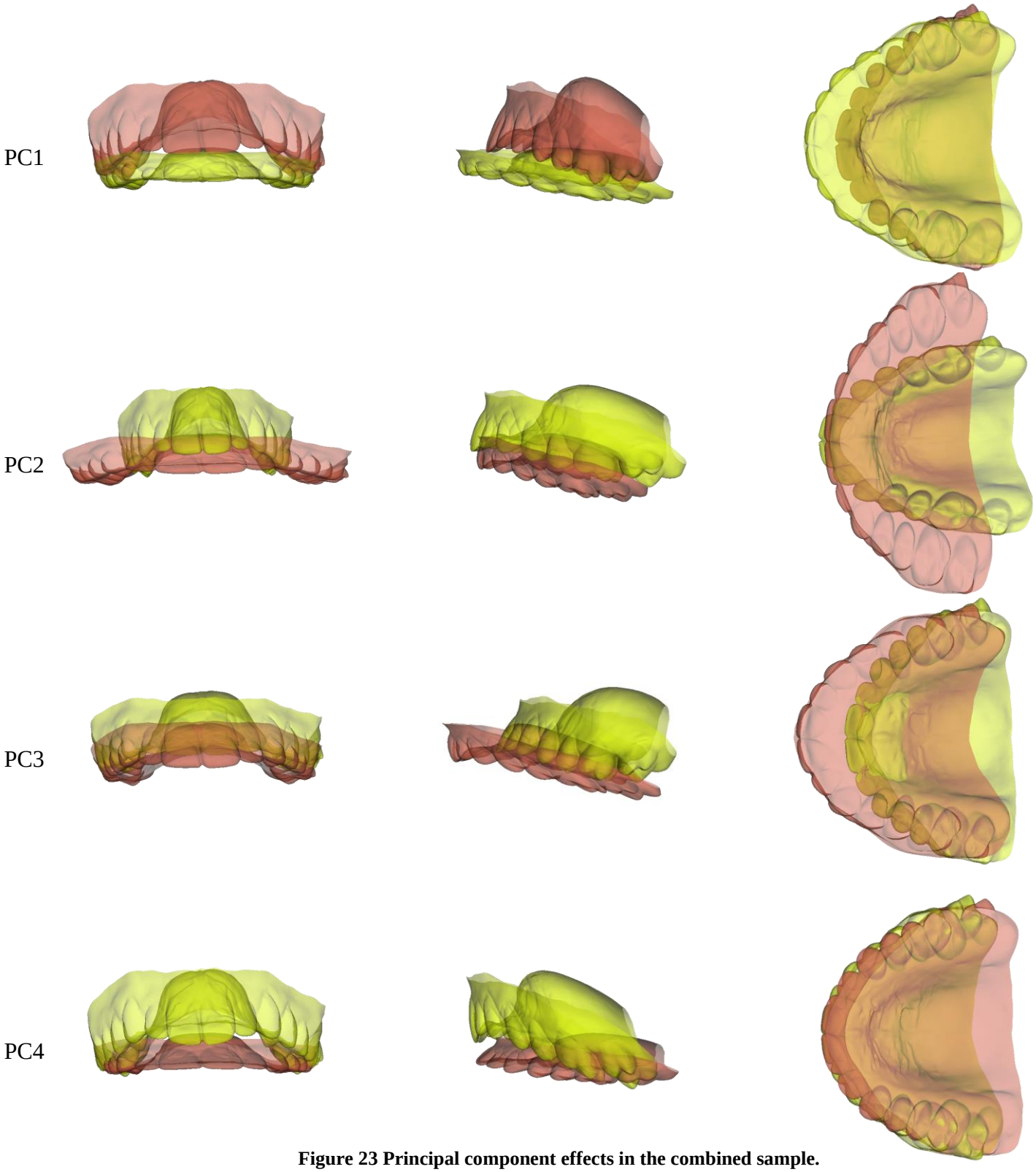

Figure 23 Principal component effects in the combined sample.

Red = Positive. Yellow = Negative.

3.2 Patterns of Morphological Differences among Groups

3.2.1 Aim 1: Patterns of sex and ancestry in the control population

3.2.1.1 Report of findings

By sex, males had a wider ML dimension while females had a longer AP dimension. Males had higher posterior palatal vaults while females had higher anterior palatal vaults ($p \leq .0006$) (Figures 24-26, 42-46) (Tables 8, 18-20).

By ancestry, Africans had the highest palatal vaults while Asians had the shallowest palatal vaults ($p < .0001$). The point of maximum palatal vault was located more anteriorly in Europeans in comparison to other ancestries ($p < .0001$). Africans also had the widest jaws in the ML dimension while Europeans had the most constricted jaws ($p < .0001$) (Figures 27-41) (Tables 9-17). The degree distinction was less between Asian and European males, achieving only baseline significance ($p = .0148$) (Table 14).

The alpha level for this aim was set as follows:

[b] Baseline Significance Level $p < .05$

* Corrected Significance Level $p < .01$

3.2.1.2 General Contrast 1: Comparison by sex (ancestries combined)

In controls, males had shorter AP and wider ML dimensions than females. Males had higher posterior palatal vault while females had higher anterior palatal vault.

- Canonical Variate Analysis: (Figures 24 & 25)

Eigenvalue	% Variance	Cumulative %
0.292459	100	100

Procrustes distance (p-value) = 0.0323 (<.0001)*

Mahalanobis distance (p-value) = 1.0860 (<.0001)*

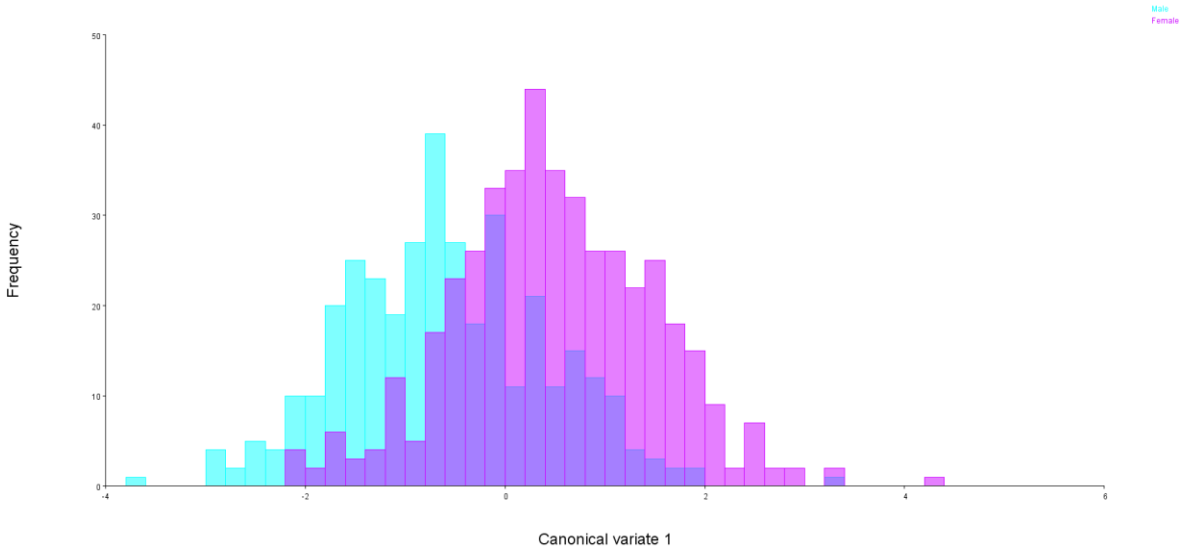

Figure 24 CVA of sexes in controls (ancestries combined).

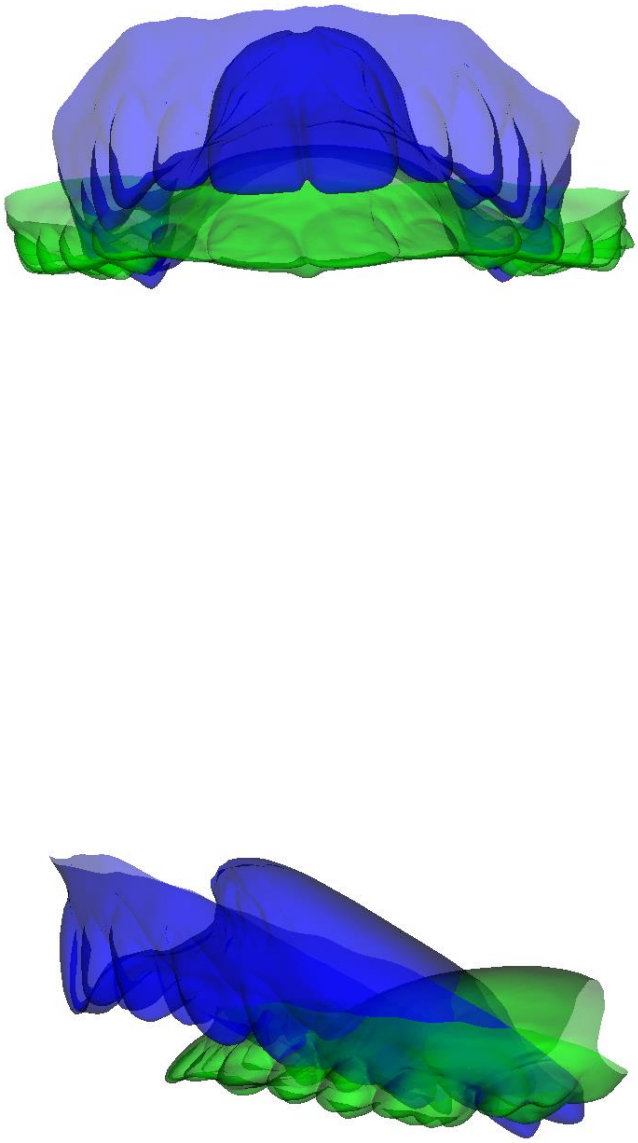

Figure 25 Canonical variate effects of sex in controls (ancestries combined).

Green = Negative (Male). Blue = Positive (Female). Scale factor = 10

Table 8 Euclidean Distance Matrix Analysis: Male vs. female control (ancestries combined). (Figure26)

	Distance		Difference	90% Confidence Interval	
1	Lmk1	Lmk6	-0.031	-0.039	-0.023
2	Lmk2	Lmk6	-0.025	-0.03	-0.019
3	Lmk3	Lmk6	-0.025	-0.031	-0.019
4	Lmk1	Lmk4	-0.009	-0.014	-0.004
5	Lmk1	Lmk5	-0.009	-0.014	-0.004
6	Lmk2	Lmk4	-0.008	-0.013	-0.004
7	Lmk3	Lmk5	-0.008	-0.013	-0.004
8	Lmk4	Lmk6	-0.007	-0.013	-0.001
9	Lmk5	Lmk6	-0.007	-0.013	-0.001
10	Lmk1	Lmk2	-0.004	-0.01	0.001
11	Lmk1	Lmk3	-0.004	-0.009	0
12	Lmk2	Lmk3	0	-0.004	0.004
13	Lmk3	Lmk4	0.008	0.003	0.013
14	Lmk2	Lmk5	0.008	0.003	0.013
15	Lmk1	Lmk7	0.016	0.009	0.022
16	Lmk3	Lmk7	0.02	0.015	0.025
17	Lmk2	Lmk7	0.02	0.015	0.025
18	Lmk6	Lmk7	0.034	0.027	0.041
19	Lmk4	Lmk7	0.037	0.03	0.043
20	Lmk5	Lmk7	0.037	0.03	0.043
21	Lmk4	Lmk5	0.039	0.033	0.045

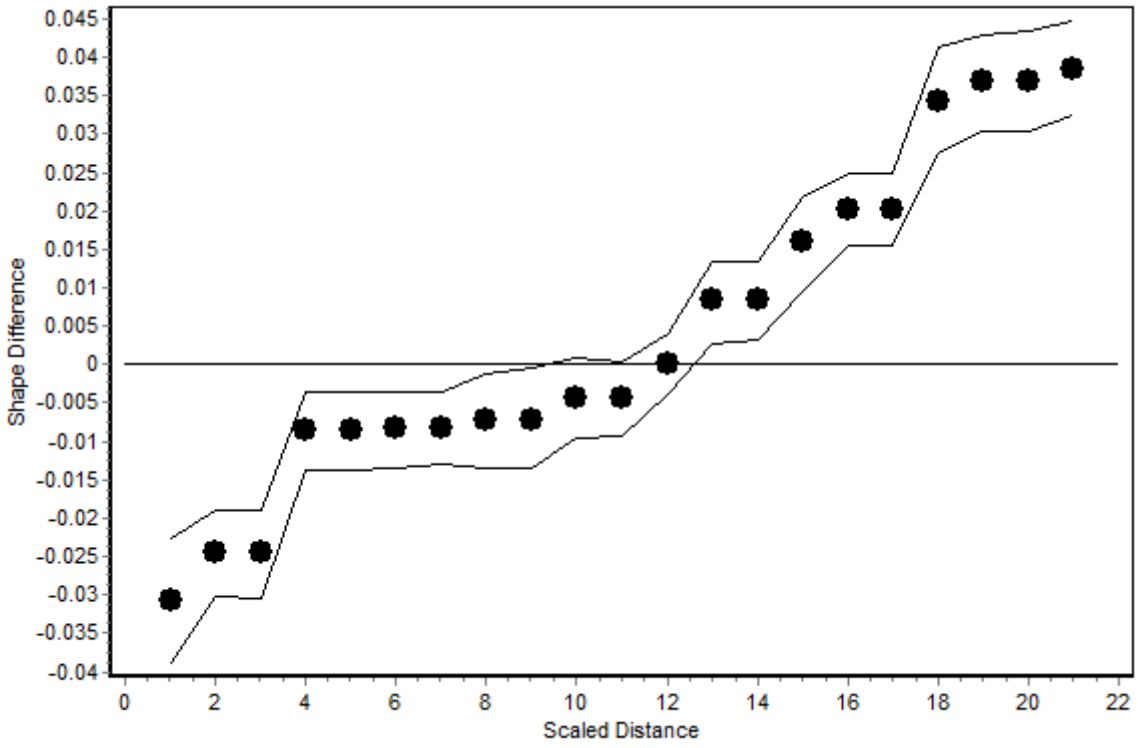

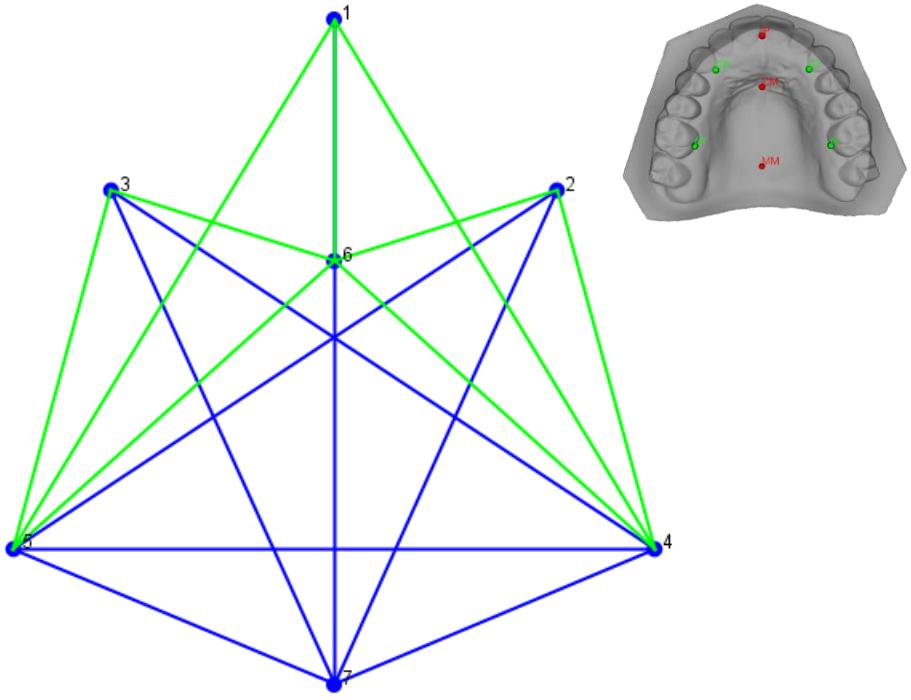

Figure 26 EDMA: Male vs. female control (ancestries combined).

Distances = Green: Male < Female, Blue: Male > Female.

3.2.1.3 General Contrast 2: Comparison by ancestry (sexes combined)

In controls, Africans had highest overall palatal vaults and widest palates. Asians had overall shallowest palatal vaults while Europeans had the narrowest palates. The point of maximal vault height was located more anteriorly in Europeans.

- Canonical Variates Analysis: (Figures 27 &28)

	Eigenvalues	% Variance	Cumulative %
CV1	0.482768	93.694	93.694
CV2	0.032494	6.306	100

Procrustes distance (p-value):

	African	Asian
Asian	0.0422 (<.0001)*	
Euro	0.0404 (<.0001)*	0.0203 (0.0121)[b]

Mahalanobis distance (p-value):

	African	Asian
Asian	1.2039 (<.0001)*	
Euro	1.4751 (<.0001)*	0.7806 (0.0001)*

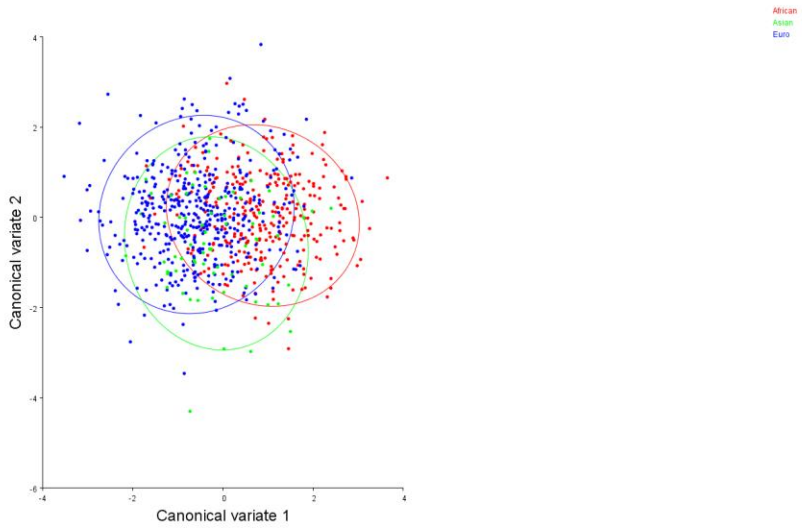

Figure 27 CVA of controls by ancestry (sexes combined).

Confidence ellipses represent 90% frequency.

CV1

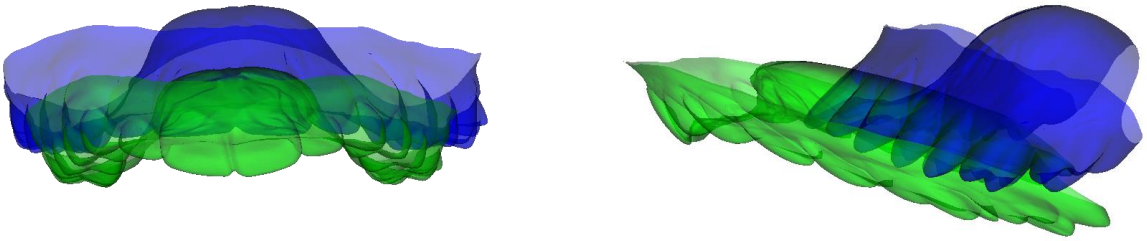

CV2

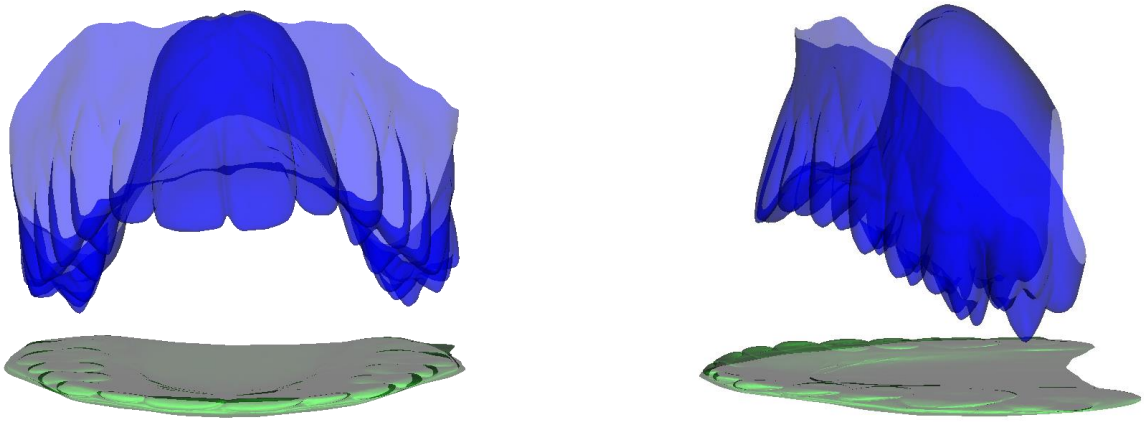

Figure 28 Canonical variate effects of ancestry in controls (sexes combined).

Green = Negative. Blue = Positive. Scale factor = 10.

CV1: Separation of Europeans (Green) from Africans (Blue).

CV2: Separation of Asian (Green) from the other ancestries (Blue).

Table 9 Euclidean Distance Matrix Analysis: Asian vs. African control (sexes combined). (Figure 29)

	Distance		Difference	90% Confidence Interval	
1	Lmk1	Lmk6	-0.044	-0.061	-0.027
2	Lmk2	Lmk6	-0.032	-0.041	-0.022
3	Lmk3	Lmk6	-0.032	-0.042	-0.022
4	Lmk5	Lmk7	-0.03	-0.041	-0.018
5	Lmk4	Lmk7	-0.03	-0.041	-0.02
6	Lmk1	Lmk2	-0.013	-0.021	-0.004
7	Lmk1	Lmk3	-0.013	-0.022	-0.004
8	Lmk2	Lmk3	-0.007	-0.014	0.001
9	Lmk4	Lmk5	-0.005	-0.018	0.007
10	Lmk2	Lmk7	-0.003	-0.014	0.006
11	Lmk3	Lmk7	-0.003	-0.013	0.006
12	Lmk1	Lmk7	-0.001	-0.014	0.012
13	Lmk2	Lmk5	0.024	0.013	0.035
14	Lmk3	Lmk4	0.024	0.013	0.035
15	Lmk1	Lmk4	0.028	0.018	0.039
16	Lmk1	Lmk5	0.028	0.018	0.039
17	Lmk5	Lmk6	0.036	0.024	0.049
18	Lmk4	Lmk6	0.036	0.023	0.049
19	Lmk6	Lmk7	0.043	0.025	0.06
20	Lmk2	Lmk4	0.05	0.04	0.061
21	Lmk3	Lmk5	0.05	0.039	0.061

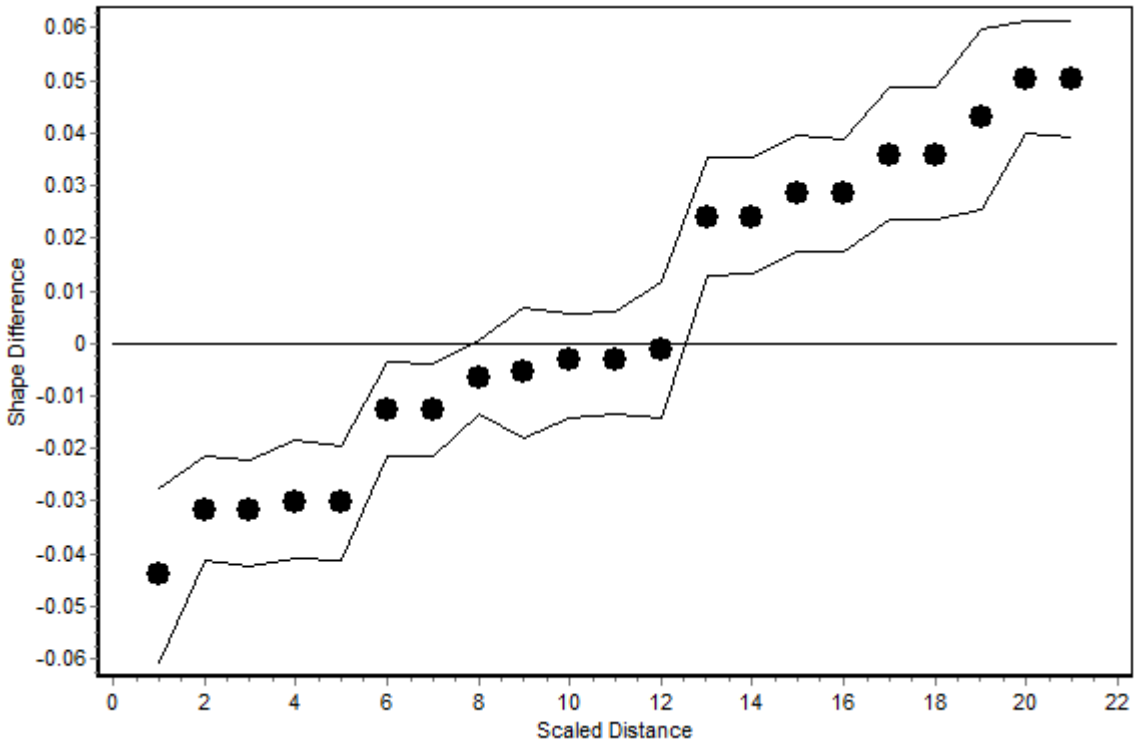

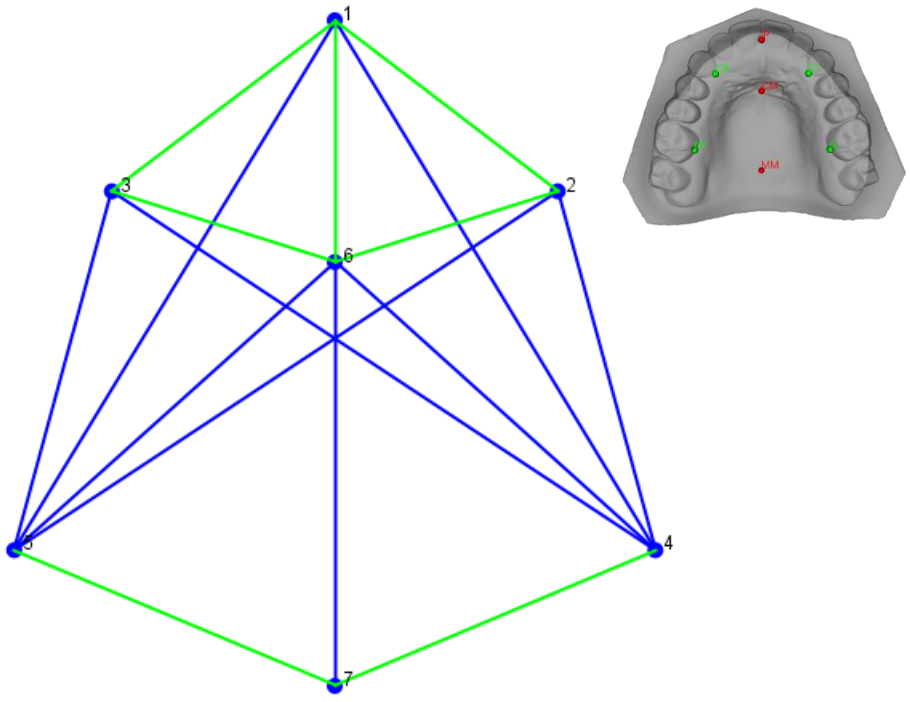

Figure 29 EDMA: Asian vs. African control (sexes combined).

Distances = Green: Asian < African, Blue: Asian > African.

Table 10 Euclidean Distance Matrix Analysis: Euro vs. African control (sexes combined). (Figure 30)

	Distance		Difference	90% Confidence Interval	
1	Lmk1	Lmk6	-0.03	-0.04	-0.02
2	Lmk2	Lmk6	-0.029	-0.035	-0.022
3	Lmk3	Lmk6	-0.029	-0.035	-0.023
4	Lmk3	Lmk7	-0.02	-0.025	-0.015
5	Lmk2	Lmk7	-0.02	-0.026	-0.015
6	Lmk2	Lmk3	-0.02	-0.023	-0.016
7	Lmk5	Lmk7	-0.019	-0.026	-0.012
8	Lmk4	Lmk7	-0.019	-0.026	-0.013
9	Lmk4	Lmk5	-0.013	-0.019	-0.007
10	Lmk1	Lmk3	-0.011	-0.016	-0.006
11	Lmk1	Lmk2	-0.011	-0.016	-0.006
12	Lmk1	Lmk7	-0.007	-0.014	0.001
13	Lmk3	Lmk4	0.012	0.006	0.018
14	Lmk2	Lmk5	0.012	0.007	0.019
15	Lmk6	Lmk7	0.028	0.02	0.037
16	Lmk1	Lmk5	0.032	0.026	0.038
17	Lmk1	Lmk4	0.032	0.025	0.038
18	Lmk2	Lmk4	0.046	0.04	0.051
19	Lmk3	Lmk5	0.046	0.041	0.051
20	Lmk4	Lmk6	0.047	0.04	0.054
21	Lmk5	Lmk6	0.047	0.04	0.054

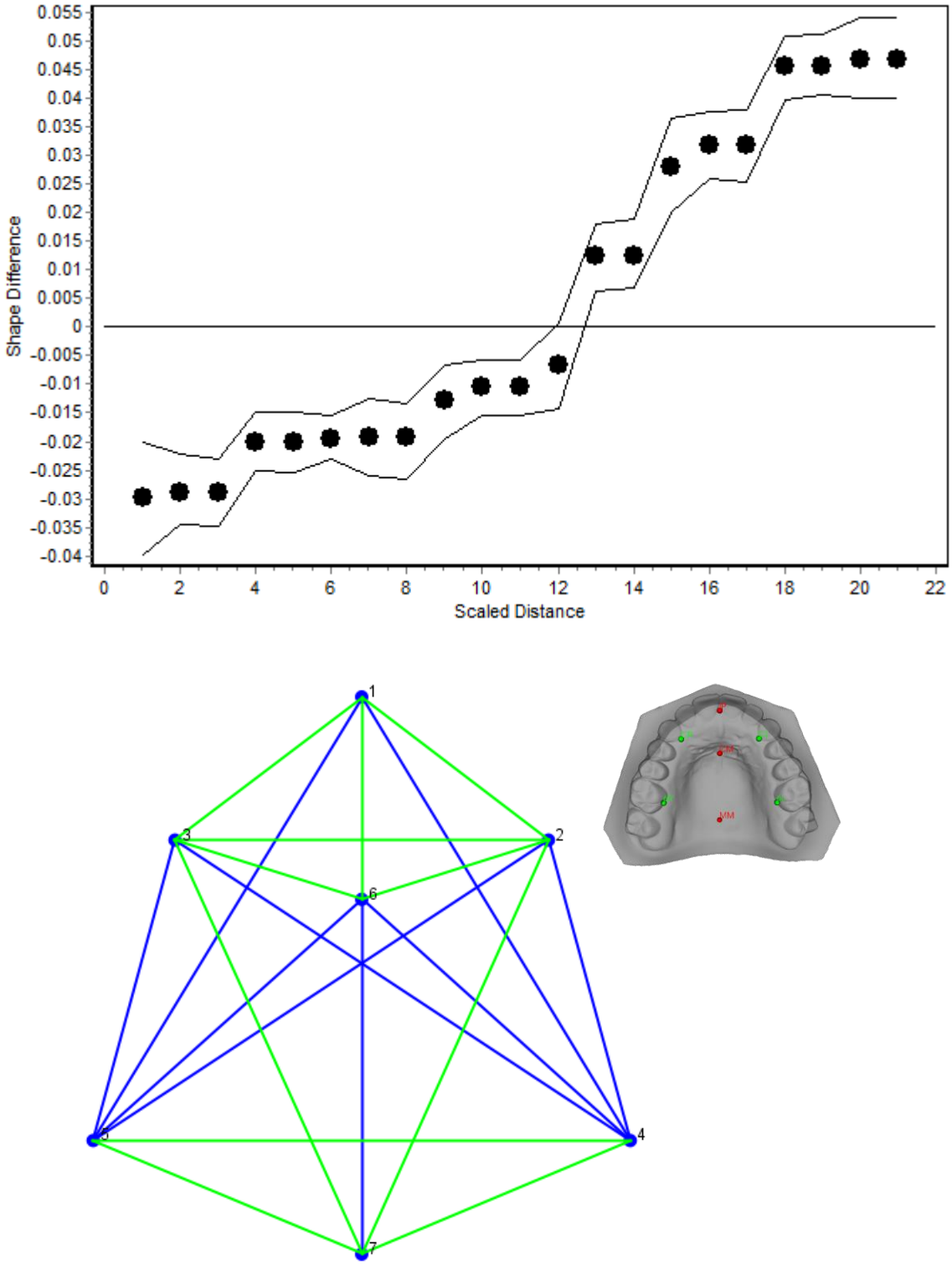

Figure 30 EDMA: Euro vs. African control (sexes combined).

Distances = Green: Euro < African, Blue: Euro > African.

Table 11 Euclidean Distance Matrix Analysis: Euro vs. Asian control (sexes combined). (Figure 31)

	Distance		Difference	90% Confidence Interval	
1	Lmk3	Lmk7	-0.017	-0.025	-0.007
2	Lmk2	Lmk7	-0.017	-0.025	-0.007
3	Lmk6	Lmk7	-0.015	-0.029	-0.001
4	Lmk2	Lmk3	-0.013	-0.02	-0.005
5	Lmk3	Lmk4	-0.012	-0.022	-0.002
6	Lmk2	Lmk5	-0.012	-0.022	-0.001
7	Lmk4	Lmk5	-0.008	-0.021	0.005
8	Lmk1	Lmk7	-0.005	-0.017	0.007
9	Lmk3	Lmk5	-0.005	-0.014	0.005
10	Lmk2	Lmk4	-0.005	-0.014	0.006
11	Lmk1	Lmk3	0.002	-0.007	0.011
12	Lmk1	Lmk2	0.002	-0.007	0.012
13	Lmk2	Lmk6	0.003	-0.009	0.014
14	Lmk3	Lmk6	0.003	-0.009	0.014
15	Lmk1	Lmk5	0.003	-0.007	0.013
16	Lmk1	Lmk4	0.003	-0.007	0.013
17	Lmk5	Lmk7	0.011	-0.002	0.023
18	Lmk4	Lmk7	0.011	-0.002	0.022
19	Lmk4	Lmk6	0.011	-0.001	0.023
20	Lmk5	Lmk6	0.011	-0.001	0.023
21	Lmk1	Lmk6	0.014	0	0.029

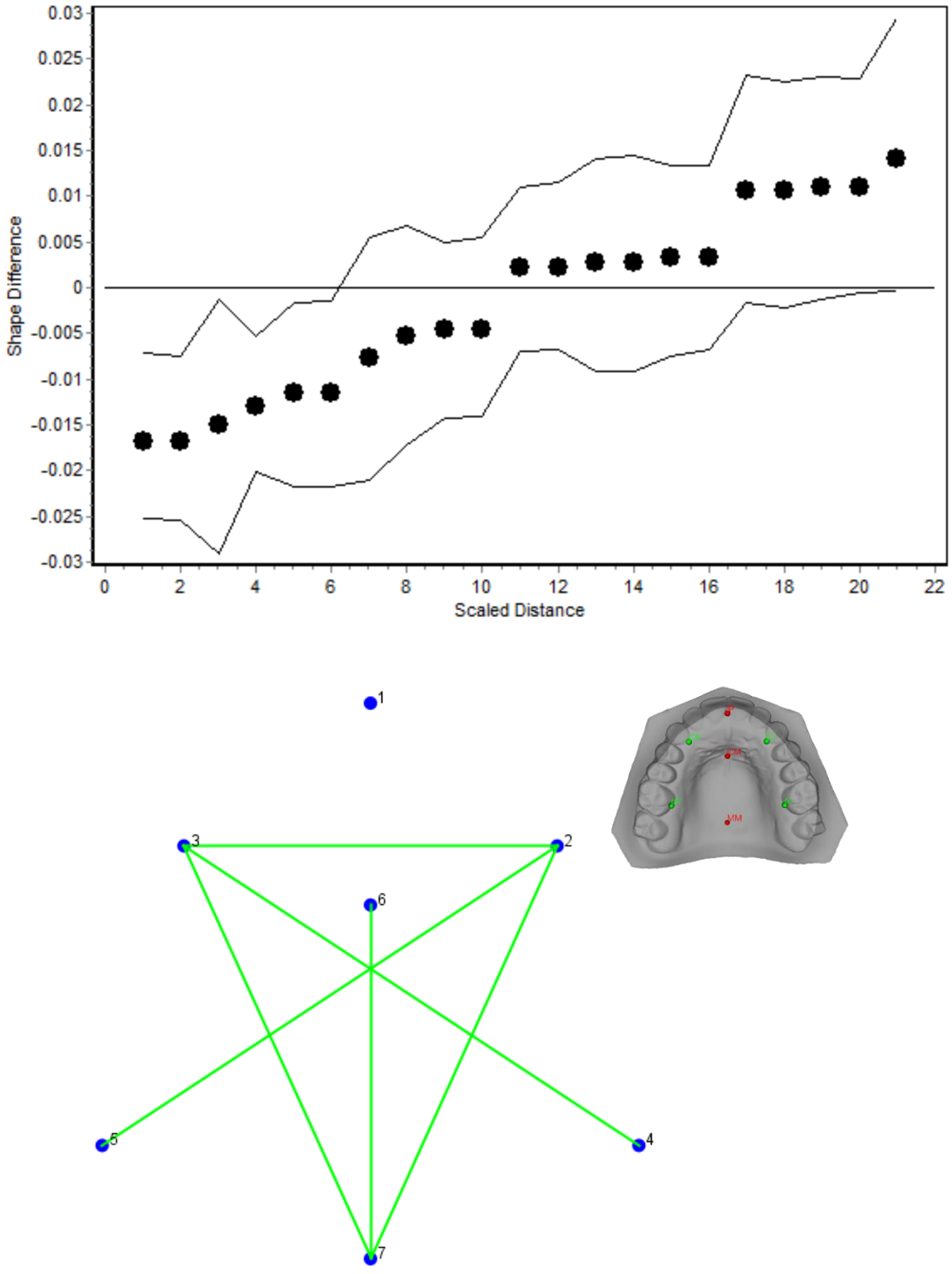

Figure 31 EDMA: Euro vs. Asian controls (sexes combined).

Distances = Green: Euro < Asian.

3.2.1.4 Stratified Contrast 1: Comparison of male controls by ancestry

In male controls, Africans had highest overall palatal vaults and widest palates. Asians had overall shallowest palatal vaults while Europeans had the narrowest palates. The point of maximal vault height was located more anteriorly in Europeans.

- Canonical Variates Analysis: (Figures 32 & 33)

	Eigenvalues	% Variance	Cumulative %
CV1	0.706504	95.602	95.602
CV2	0.032504	4.398	100

Procrustes distance (p-value):

	African	Asian
Asian	0.0478 (<.0001)*	
Euro	0.0491 (<.0001)*	0.0189 (0.1453)

Mahalanobis distance (p-value):

	African	Asian
Asian	1.375 (<.0001)*	
Euro	1.763 (<.0001)*	0.7583 (0.0148)[b]

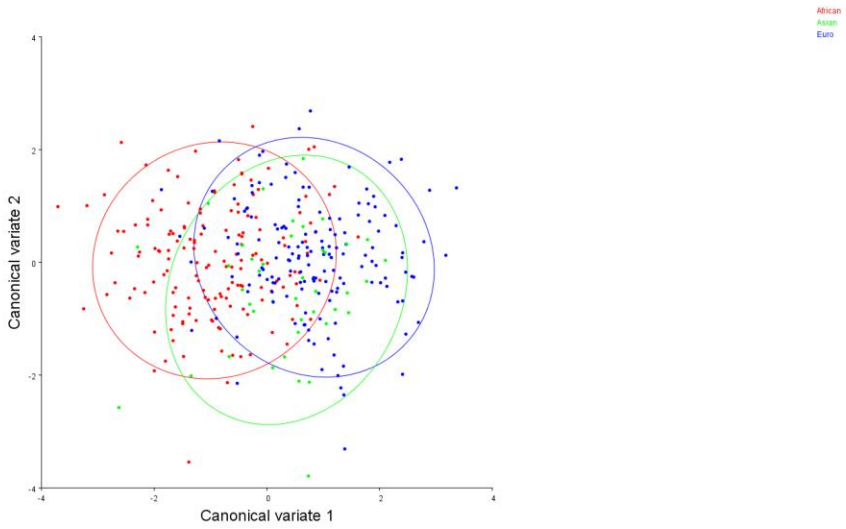

Figure 32 CVA of male controls by ancestry.

Confidence ellipses represent 90% frequency.

CV1

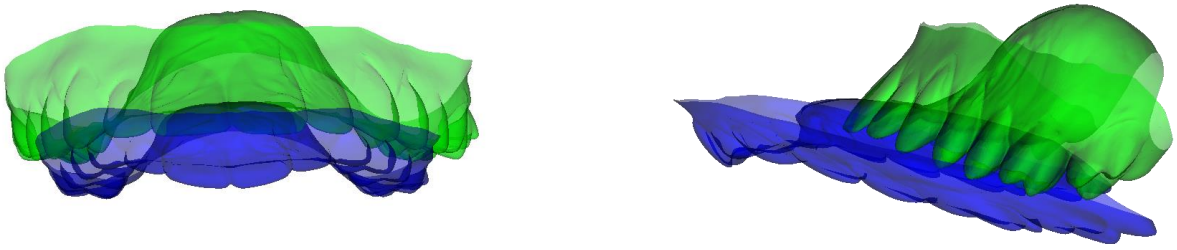

CV2

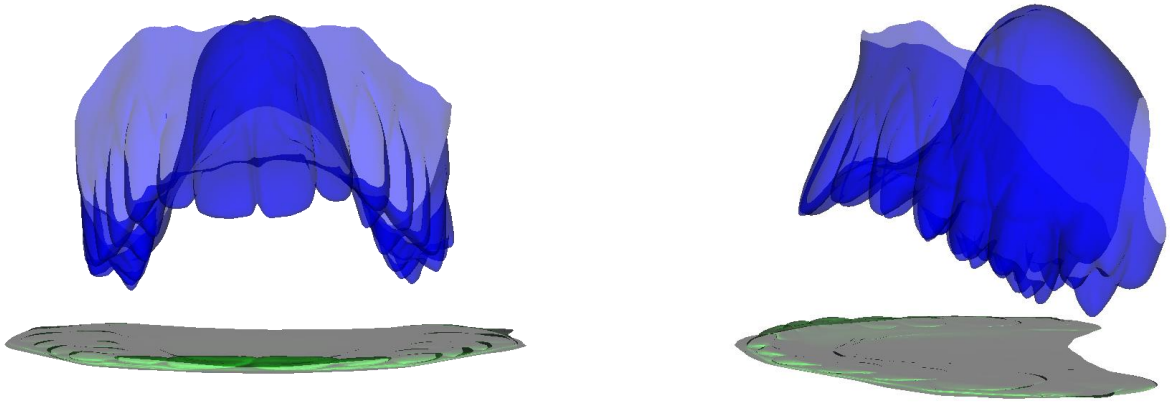

Figure 33 Canonical variate effects of ancestry in male controls.

Green = Negative. Blue = Positive. Scale factor = 10.

CV1: Separation of Africans (Green) from Europeans (Blue).

CV2: Separation of Asians (Green) from the other ancestries (Blue).

Table 12 Euclidean Distance Matrix Analysis: Asian vs. African male control. (Figure 34)

	Distance		Difference	90% Confidence Interval	
1	Lmk1	Lmk6	-0.058	-0.079	-0.036
2	Lmk3	Lmk6	-0.037	-0.049	-0.025
3	Lmk2	Lmk6	-0.037	-0.048	-0.025
4	Lmk4	Lmk7	-0.029	-0.044	-0.013
5	Lmk5	Lmk7	-0.029	-0.045	-0.013
6	Lmk1	Lmk3	-0.016	-0.028	-0.003
7	Lmk1	Lmk2	-0.016	-0.028	-0.003
8	Lmk2	Lmk3	-0.009	-0.019	0.001
9	Lmk1	Lmk7	-0.008	-0.025	0.011
10	Lmk3	Lmk7	-0.007	-0.021	0.007
11	Lmk2	Lmk7	-0.007	-0.022	0.007
12	Lmk4	Lmk5	0.004	-0.013	0.02
13	Lmk3	Lmk4	0.03	0.015	0.044
14	Lmk2	Lmk5	0.03	0.014	0.044
15	Lmk1	Lmk4	0.032	0.018	0.047
16	Lmk1	Lmk5	0.032	0.017	0.047
17	Lmk4	Lmk6	0.047	0.031	0.063
18	Lmk5	Lmk6	0.047	0.03	0.064
19	Lmk6	Lmk7	0.05	0.029	0.072
20	Lmk2	Lmk4	0.057	0.042	0.072
21	Lmk3	Lmk5	0.057	0.042	0.073

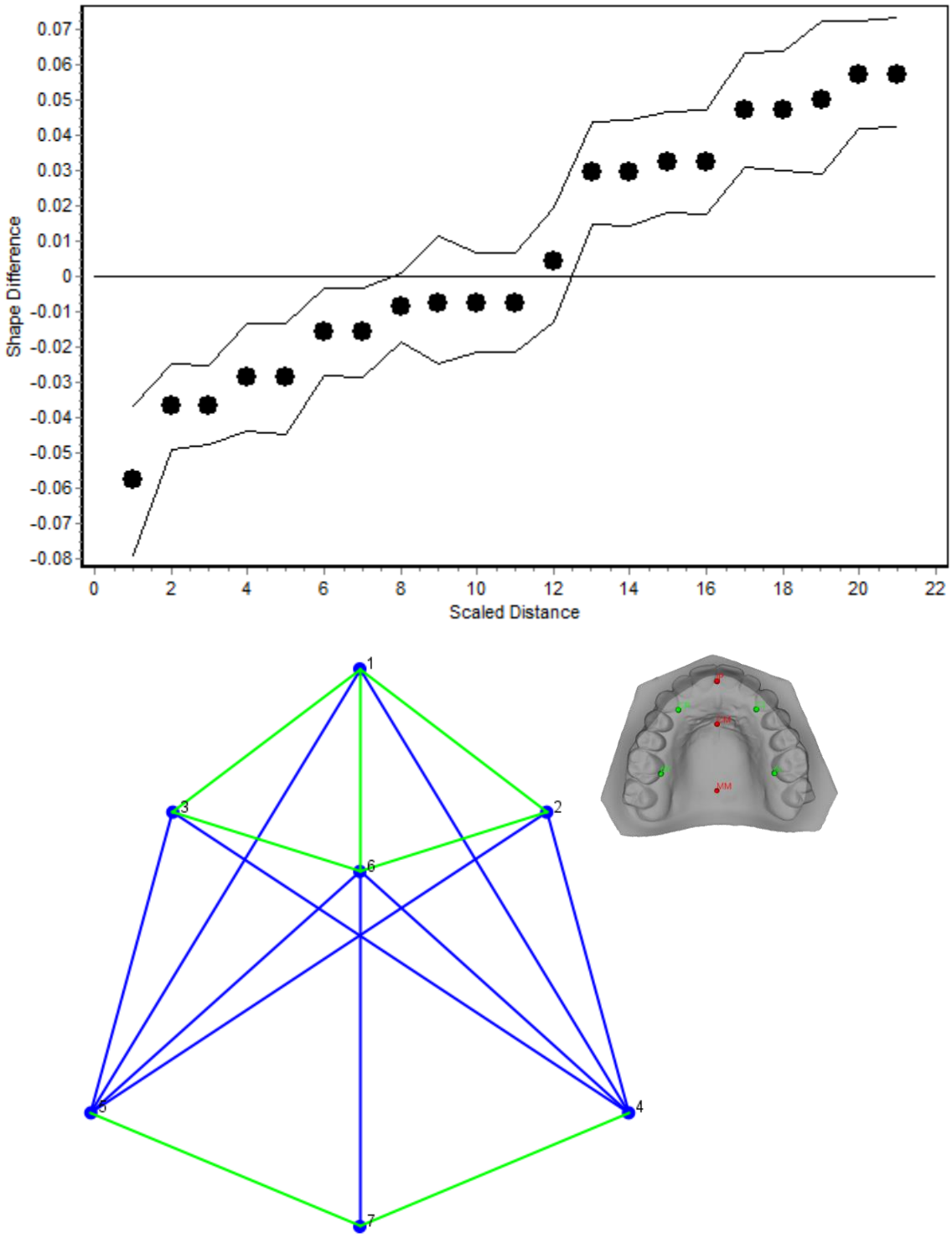

Figure 34 EDMA: Asian vs. African male control.

Distances = Green: Asian < African, Blue: Asian > African.

Table 13 Euclidean Distance Matrix Analysis: Euro vs. African male control. (Figure 35)

	Distance		Difference	90% Confidence Interval	
1	Lmk2	Lmk6	-0.043	-0.049	-0.037
2	Lmk3	Lmk6	-0.043	-0.049	-0.036
3	Lmk1	Lmk6	-0.037	-0.052	-0.023
4	Lmk2	Lmk3	-0.03	-0.035	-0.025
5	Lmk5	Lmk7	-0.022	-0.03	-0.013
6	Lmk4	Lmk7	-0.022	-0.031	-0.015
7	Lmk1	Lmk3	-0.014	-0.021	-0.007
8	Lmk1	Lmk2	-0.014	-0.021	-0.007
9	Lmk3	Lmk7	-0.014	-0.022	-0.005
10	Lmk2	Lmk7	-0.014	-0.024	-0.004
11	Lmk4	Lmk5	-0.013	-0.022	-0.005
12	Lmk1	Lmk7	0.008	-0.005	0.02
13	Lmk3	Lmk4	0.014	0.005	0.024
14	Lmk2	Lmk5	0.014	0.004	0.023
15	Lmk1	Lmk5	0.042	0.033	0.05
16	Lmk1	Lmk4	0.042	0.033	0.051
17	Lmk6	Lmk7	0.047	0.032	0.06
18	Lmk5	Lmk6	0.05	0.039	0.06
19	Lmk4	Lmk6	0.05	0.04	0.06
20	Lmk2	Lmk4	0.058	0.05	0.067
21	Lmk3	Lmk5	0.058	0.05	0.067

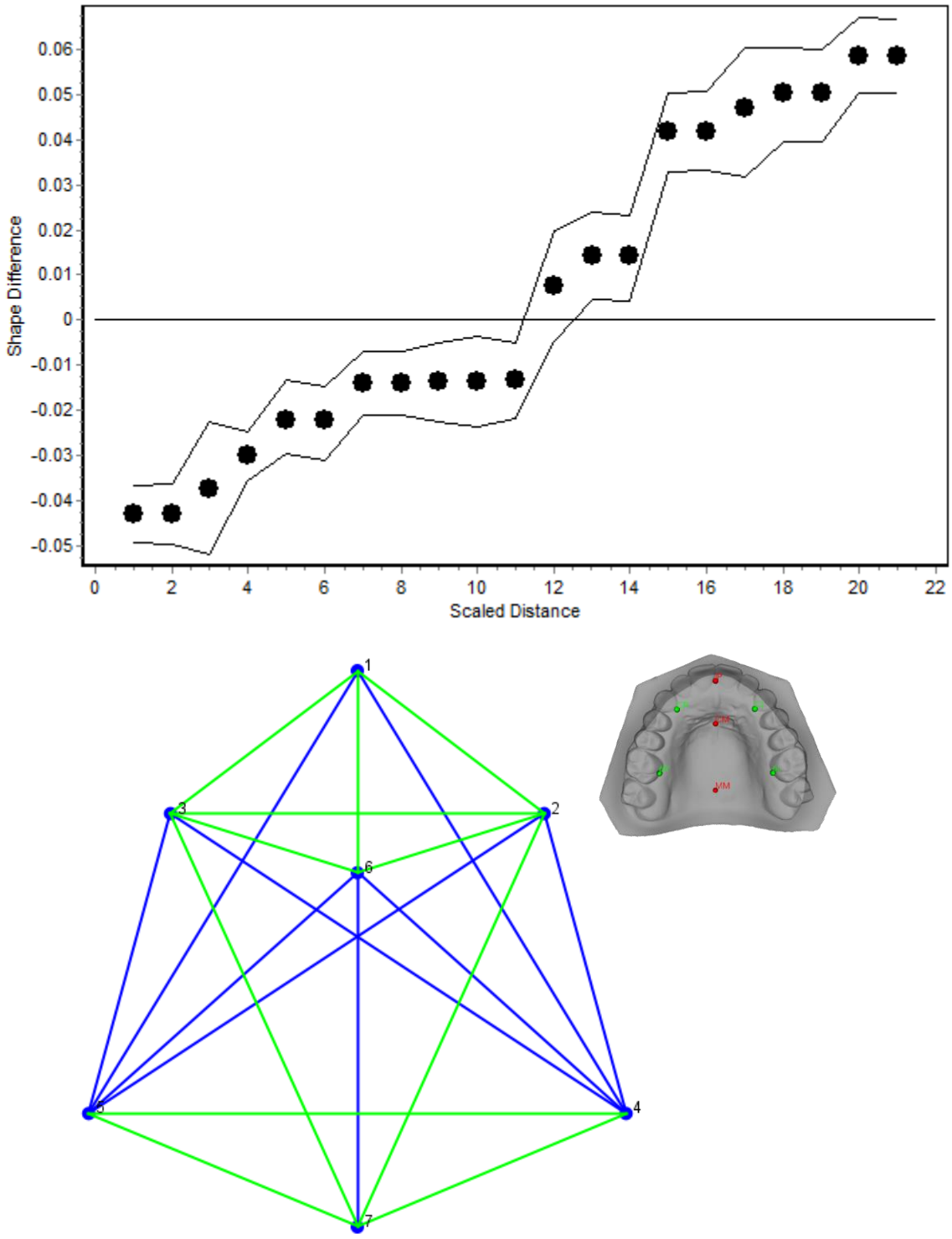

Figure 35 EDMA: Euro vs. African male control.

Distances = Green: Euro < African, Blue: Euro > African.

Table 14 Euclidean Distance Matrix Analysis: Euro vs. Asian male control. (Figure 36)

	Distance		Difference	90% Confidence Interval	
1	Lmk2	Lmk3	-0.021	-0.031	-0.011
2	Lmk4	Lmk5	-0.017	-0.035	0
3	Lmk2	Lmk5	-0.015	-0.028	-0.002
4	Lmk3	Lmk4	-0.015	-0.028	-0.001
5	Lmk3	Lmk7	-0.006	-0.019	0.006
6	Lmk2	Lmk7	-0.006	-0.019	0.007
7	Lmk2	Lmk6	-0.006	-0.018	0.006
8	Lmk3	Lmk6	-0.006	-0.018	0.006
9	Lmk6	Lmk7	-0.003	-0.021	0.014
10	Lmk3	Lmk5	0.001	-0.012	0.015
11	Lmk2	Lmk4	0.001	-0.011	0.014
12	Lmk1	Lmk3	0.002	-0.01	0.013
13	Lmk1	Lmk2	0.002	-0.011	0.014
14	Lmk5	Lmk6	0.003	-0.012	0.018
15	Lmk4	Lmk6	0.003	-0.012	0.019
16	Lmk5	Lmk7	0.006	-0.011	0.022
17	Lmk4	Lmk7	0.006	-0.011	0.023
18	Lmk1	Lmk5	0.009	-0.004	0.022
19	Lmk1	Lmk4	0.009	-0.003	0.022
20	Lmk1	Lmk7	0.015	-0.002	0.031
21	Lmk1	Lmk6	0.02	0.002	0.037

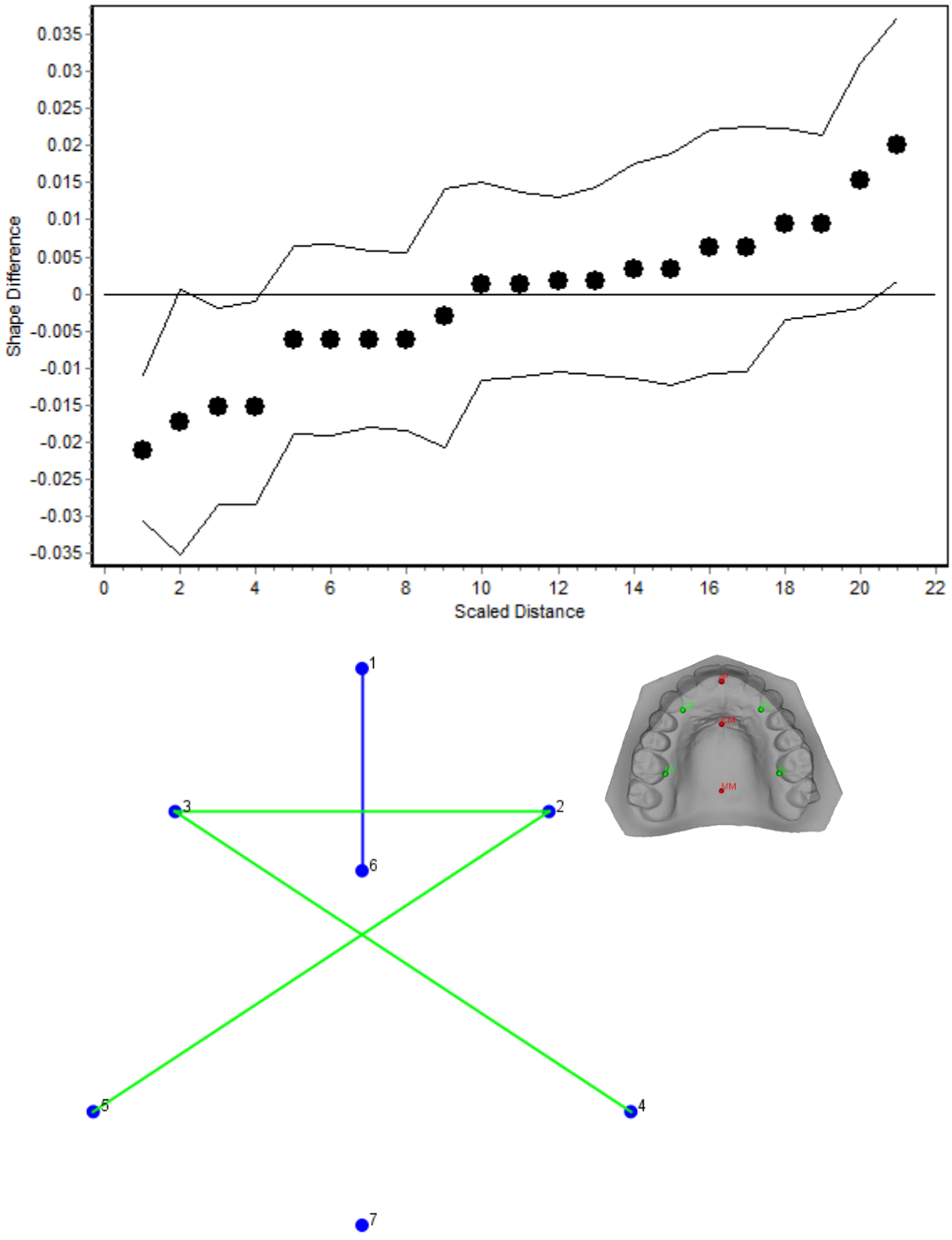

Figure 36 EDMA: Euro vs. Asian male control.

Distances = Green: Euro < Asian, Blue: Euro > Asian.

3.2.1.5 Stratified Contrast 2: Comparison of female controls by ancestry

In female controls, Africans had highest overall palatal vaults and widest palates. Asians had overall shallowest palatal vaults while Europeans had the narrowest palates. The point of maximal vault height was located more anteriorly in Europeans.

- Canonical Variates Analysis: (Figures 37 & 38)

	Eigenvalues	% Variance	Cumulative %
CV1	0.353347	86.025	86.025
CV2	0.057404	13.975	100

Procrustes distance (p-value):

	African	Asian
Asian	0.0376 (0.0003)*	
Euro	0.0335 (<.0001)*	0.0257 (0.0719)

Mahalanobis distance (p-value):

	African	Asian
Asian	1.239 (<.0001)*	
Euro	1.2945 (<.0001)*	1.1127 (0.0003)*

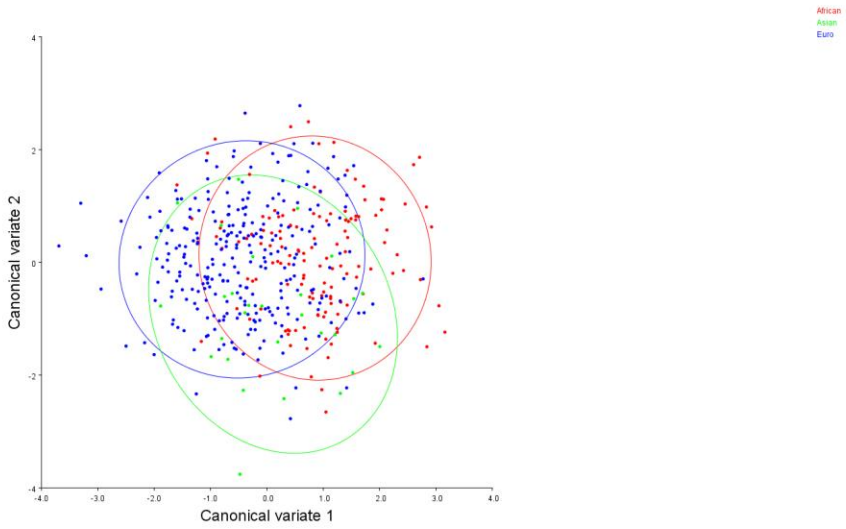

Figure 37 CVA of female controls by ancestry.

Confidence ellipses represent 90% frequency.

CV1

CV2

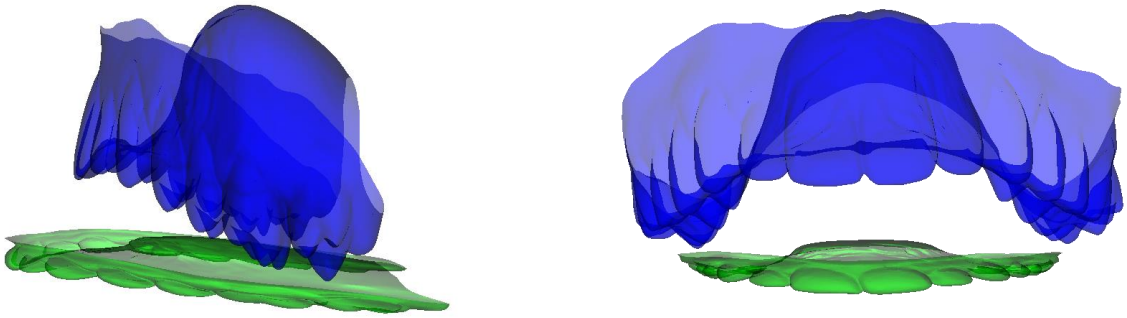

Figure 38 Canonical variate effects of ancesty in female controls.

Green = Negative. Blue = Positive. Scale factor = 10.

CV1: Separation of Africans (Blue) from Europeans (Green).

CV2: Separation of Asians (Green) from the other ancestries (Blue).

Table 15 Euclidean Distance Matrix Analysis: Asian vs. African female control. (Figure 39)

	Distance		Difference	90% Confidence Interval	
1	Lmk5	Lmk7	-0.039	-0.055	-0.024
2	Lmk4	Lmk7	-0.039	-0.055	-0.026
3	Lmk4	Lmk5	-0.025	-0.039	-0.011
4	Lmk3	Lmk6	-0.02	-0.034	-0.006
5	Lmk2	Lmk6	-0.02	-0.034	-0.006
6	Lmk1	Lmk6	-0.017	-0.036	0.004
7	Lmk1	Lmk3	-0.008	-0.02	0.003
8	Lmk1	Lmk2	-0.008	-0.019	0.002
9	Lmk2	Lmk3	-0.005	-0.014	0.004
10	Lmk3	Lmk7	0	-0.012	0.011
11	Lmk2	Lmk7	0	-0.012	0.011
12	Lmk1	Lmk7	0.007	-0.006	0.021
13	Lmk3	Lmk4	0.014	0.003	0.025
14	Lmk2	Lmk5	0.014	0.004	0.025
15	Lmk5	Lmk6	0.02	0.006	0.035
16	Lmk4	Lmk6	0.02	0.006	0.034
17	Lmk1	Lmk5	0.025	0.012	0.038
18	Lmk1	Lmk4	0.025	0.013	0.036
19	Lmk6	Lmk7	0.028	0.007	0.048
20	Lmk3	Lmk5	0.043	0.032	0.054
21	Lmk2	Lmk4	0.043	0.032	0.053

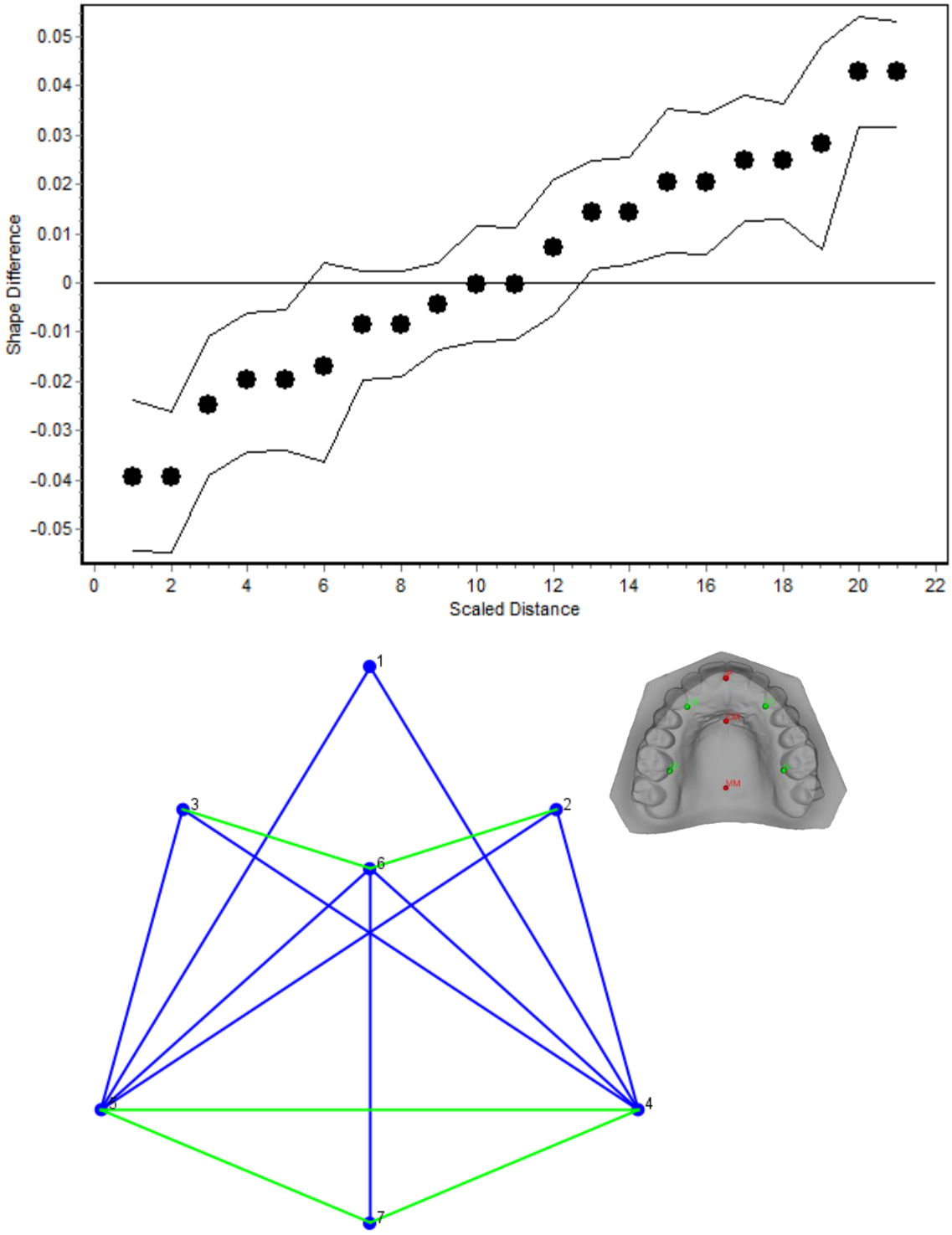

Figure 39 EDMA: Asian vs. African female control.

Distances = Green: Asian < African, Blue: Asian > African.

Table 16 Euclidean Distance Matrix Analysis: Euro vs. African female control. (Figure 40)

	Distance		Difference	90% Confidence Interval	
1	Lmk1	Lmk6	-0.032	-0.043	-0.022
2	Lmk2	Lmk6	-0.025	-0.032	-0.019
3	Lmk3	Lmk6	-0.025	-0.032	-0.018
4	Lmk3	Lmk7	-0.02	-0.024	-0.015
5	Lmk2	Lmk7	-0.02	-0.024	-0.015
6	Lmk1	Lmk7	-0.013	-0.021	-0.006
7	Lmk2	Lmk3	-0.012	-0.016	-0.007
8	Lmk1	Lmk3	-0.009	-0.015	-0.003
9	Lmk1	Lmk2	-0.009	-0.015	-0.003
10	Lmk5	Lmk7	-0.007	-0.014	0
11	Lmk4	Lmk7	-0.007	-0.014	0
12	Lmk4	Lmk5	-0.002	-0.01	0.005
13	Lmk3	Lmk4	0.013	0.007	0.02
14	Lmk2	Lmk5	0.013	0.007	0.019
15	Lmk1	Lmk5	0.022	0.016	0.028
16	Lmk1	Lmk4	0.022	0.016	0.028
17	Lmk6	Lmk7	0.023	0.015	0.032
18	Lmk3	Lmk5	0.034	0.028	0.039
19	Lmk2	Lmk4	0.034	0.028	0.04
20	Lmk5	Lmk6	0.043	0.036	0.051
21	Lmk4	Lmk6	0.043	0.035	0.051

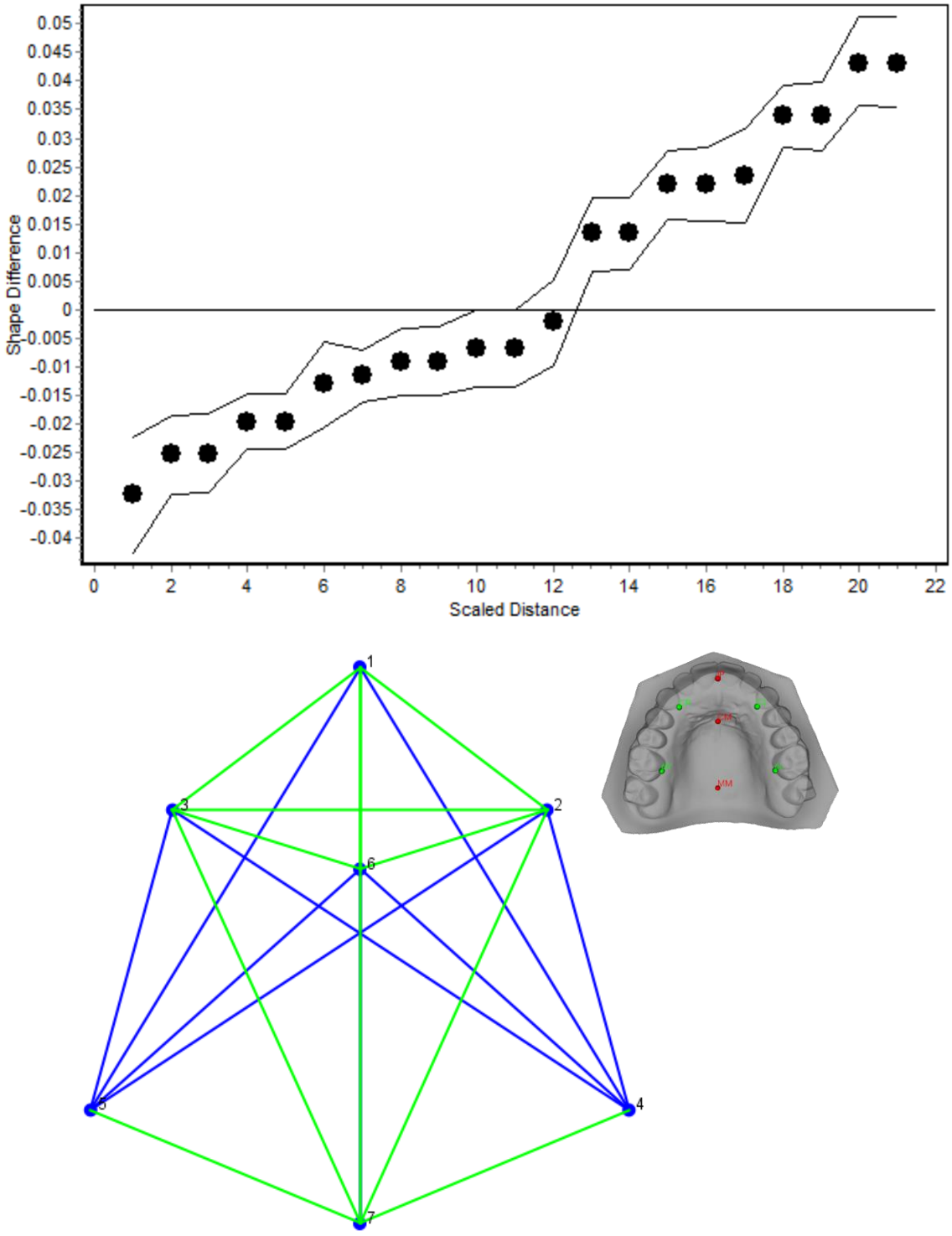

Figure 40 EDMA: Euro vs. African female control.

Distances = Green: Euro < African, Blue: Euro > African.

Table 17 Euclidean Distance Matrix Analysis: Euro vs. Asian female control. (Figure 41)

	Distance		Difference	90% Confidence Interval	
1	Lmk1	Lmk7	-0.02	-0.035	-0.006
2	Lmk2	Lmk7	-0.02	-0.033	-0.007
3	Lmk3	Lmk7	-0.02	-0.032	-0.007
4	Lmk1	Lmk6	-0.015	-0.037	0.004
5	Lmk3	Lmk5	-0.009	-0.02	0.002
6	Lmk2	Lmk4	-0.009	-0.021	0.003
7	Lmk2	Lmk3	-0.007	-0.017	0.002
8	Lmk2	Lmk6	-0.006	-0.021	0.01
9	Lmk3	Lmk6	-0.006	-0.022	0.009
10	Lmk6	Lmk7	-0.005	-0.027	0.017
11	Lmk1	Lmk5	-0.003	-0.016	0.01
12	Lmk1	Lmk4	-0.003	-0.016	0.01
13	Lmk3	Lmk4	-0.001	-0.013	0.011
14	Lmk2	Lmk5	-0.001	-0.013	0.012
15	Lmk1	Lmk2	-0.001	-0.013	0.011
16	Lmk1	Lmk3	-0.001	-0.013	0.011
17	Lmk4	Lmk5	0.023	0.007	0.039
18	Lmk5	Lmk6	0.023	0.008	0.039
19	Lmk4	Lmk6	0.023	0.008	0.038
20	Lmk5	Lmk7	0.032	0.015	0.05
21	Lmk4	Lmk7	0.032	0.016	0.049

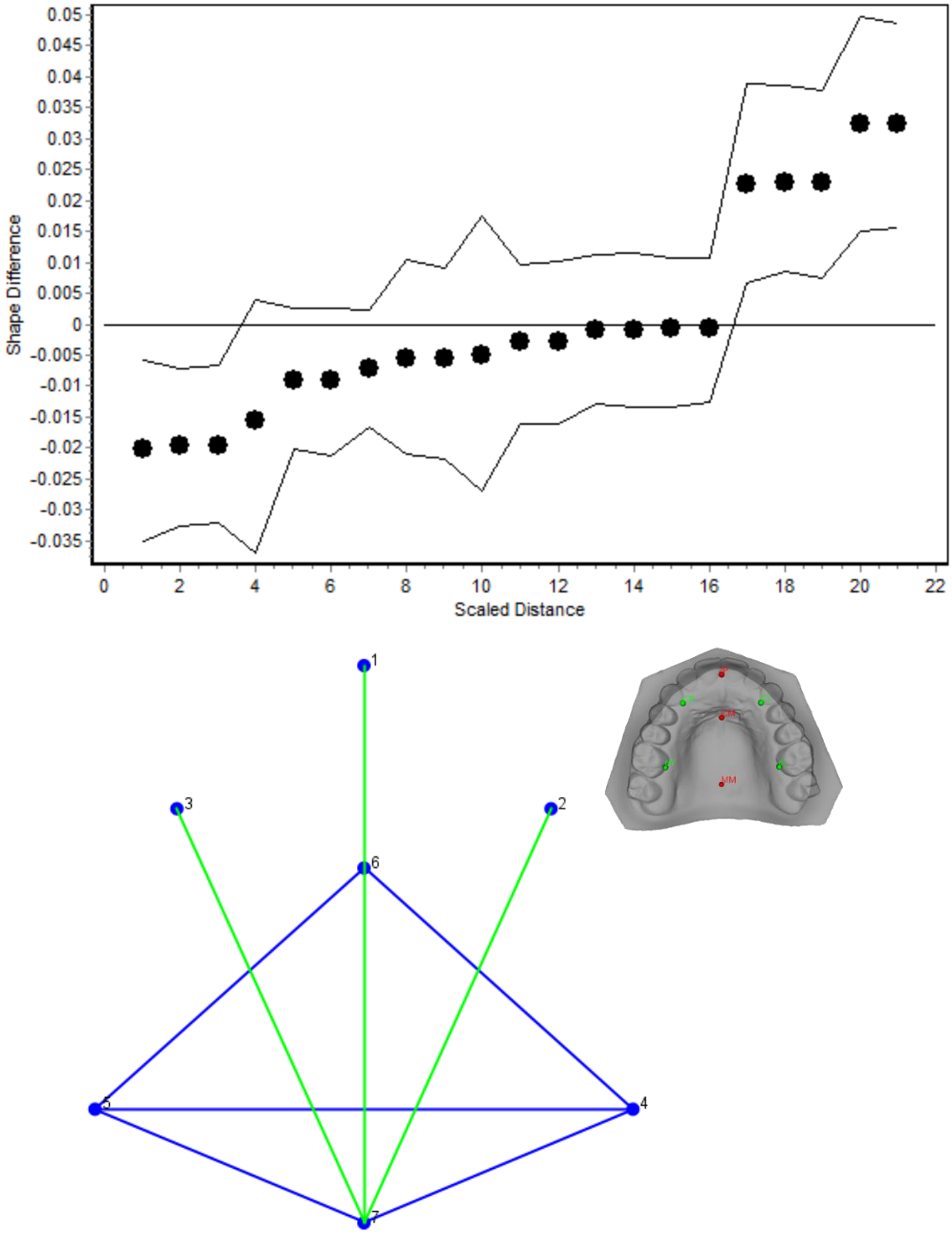

Figure 41 EDMA: Euro vs. Asian female control.

Distances: Green: Euro < Asian, Blue: Euro > Asian.

3.2.1.6 Stratified Contrast 3: Comparison of sexes within ancestries

Within each ancestry, male controls had shorter AP and wider ML dimensions than female controls. Males had higher posterior palatal vault while females had higher anterior palatal vault.

- Canonical Variates Analysis: (Figures 42 & 43)

Race	Eigenvalue	% Variance	Cumulative %
Asian	0.342609	100	100
African	0.373978	100	100
Euro	0.304461	100	100

Race	Procrustes distance (p-value)	Mahalanobis distance (p-value)
Asian	0.0466 (0.0005)*	1.1776 (0.0006)*
African	0.0326 (<.0001)*	1.2215 (<.0001)*
Euro	0.0324 (<.0001)*	1.1428 (<.0001)*

Asian

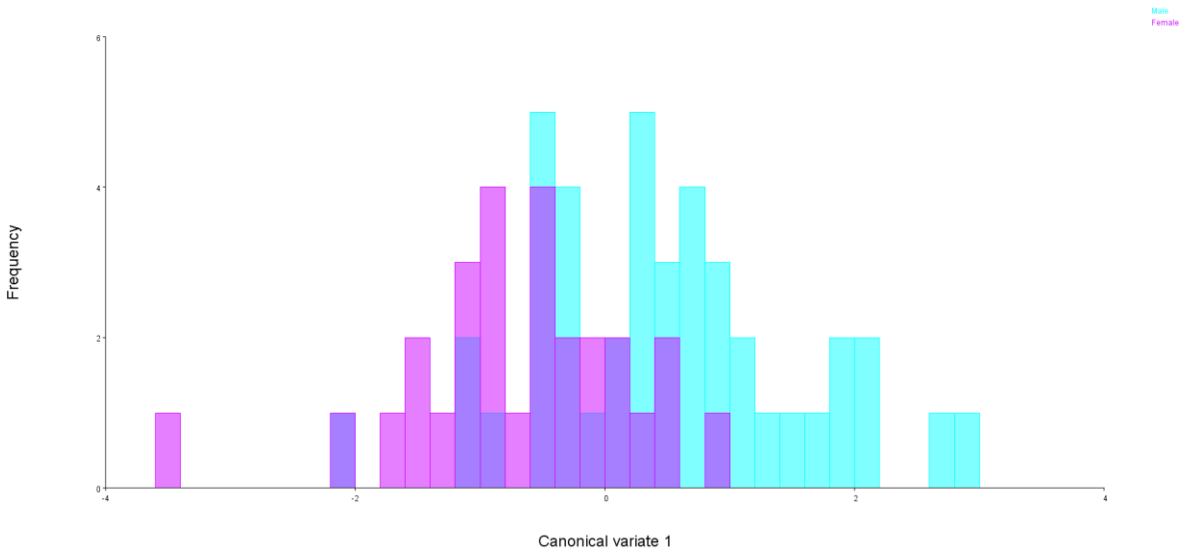

African

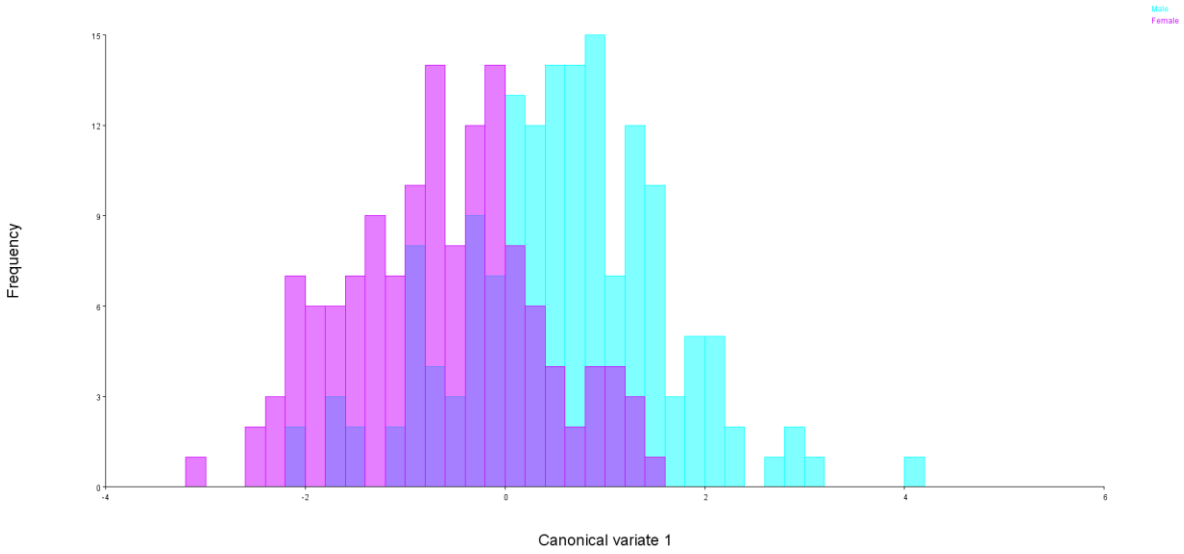

Euro

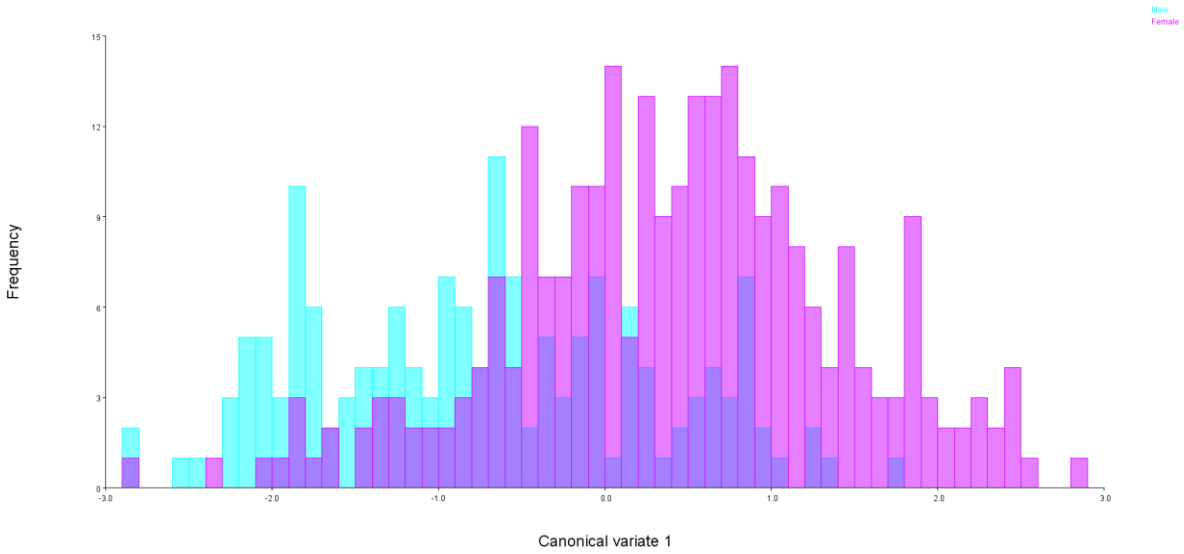

Figure 42 CVA of sexes in controls within ancestries.

Asian

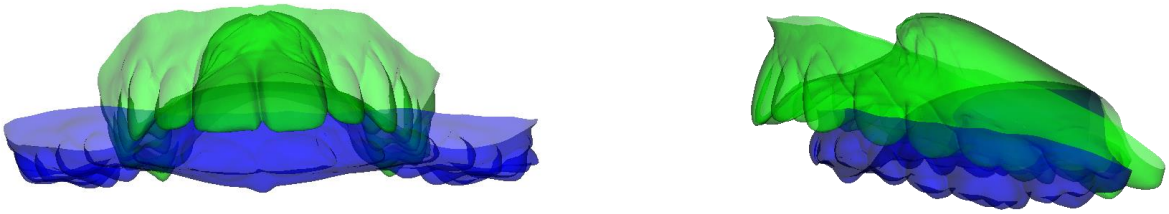

African

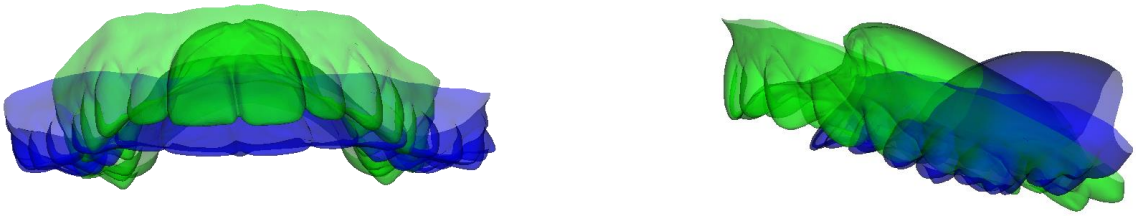

Euro

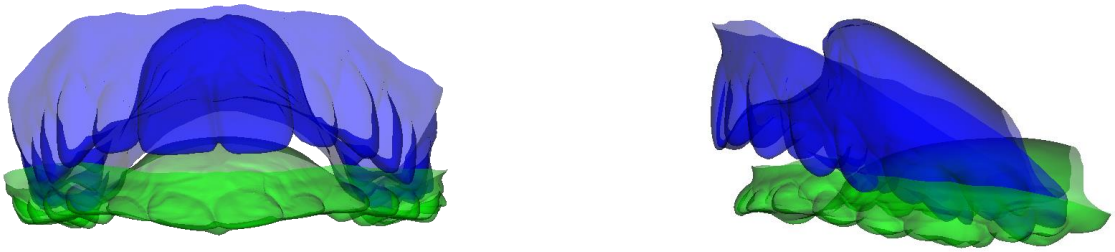

Figure 43 Canonical variate effects of sex within ancestries in controls.

Green = Negative. Blue = Positive. Scale factor = 10.

Asian & African: Blue = Male, Green = Female. Euro: Green = Male, Blue = Female.

Table 18 Euclidean Distance Matrix Analysis: Asian male vs. female control. (Figure 44)

	Distance		Difference	90% Confidence Interval	
1	Lmk1	Lmk6	-0.069	-0.086	-0.05
2	Lmk2	Lmk6	-0.035	-0.05	-0.021
3	Lmk3	Lmk6	-0.035	-0.05	-0.02
4	Lmk1	Lmk3	-0.01	-0.019	-0.001
5	Lmk1	Lmk2	-0.01	-0.018	-0.001
6	Lmk1	Lmk7	-0.009	-0.02	0.003
7	Lmk1	Lmk4	-0.008	-0.02	0.004
8	Lmk1	Lmk5	-0.008	-0.02	0.005
9	Lmk2	Lmk4	-0.003	-0.013	0.007
10	Lmk3	Lmk5	-0.003	-0.013	0.008
11	Lmk2	Lmk3	0.002	-0.005	0.01
12	Lmk2	Lmk7	0.008	-0.003	0.018
13	Lmk3	Lmk7	0.008	-0.003	0.018
14	Lmk4	Lmk6	0.02	0.006	0.034
15	Lmk5	Lmk6	0.02	0.007	0.035
16	Lmk3	Lmk4	0.023	0.013	0.034
17	Lmk2	Lmk5	0.023	0.012	0.034
18	Lmk6	Lmk7	0.045	0.028	0.06
19	Lmk5	Lmk7	0.054	0.035	0.074
20	Lmk4	Lmk7	0.054	0.033	0.074
21	Lmk4	Lmk5	0.07	0.058	0.082

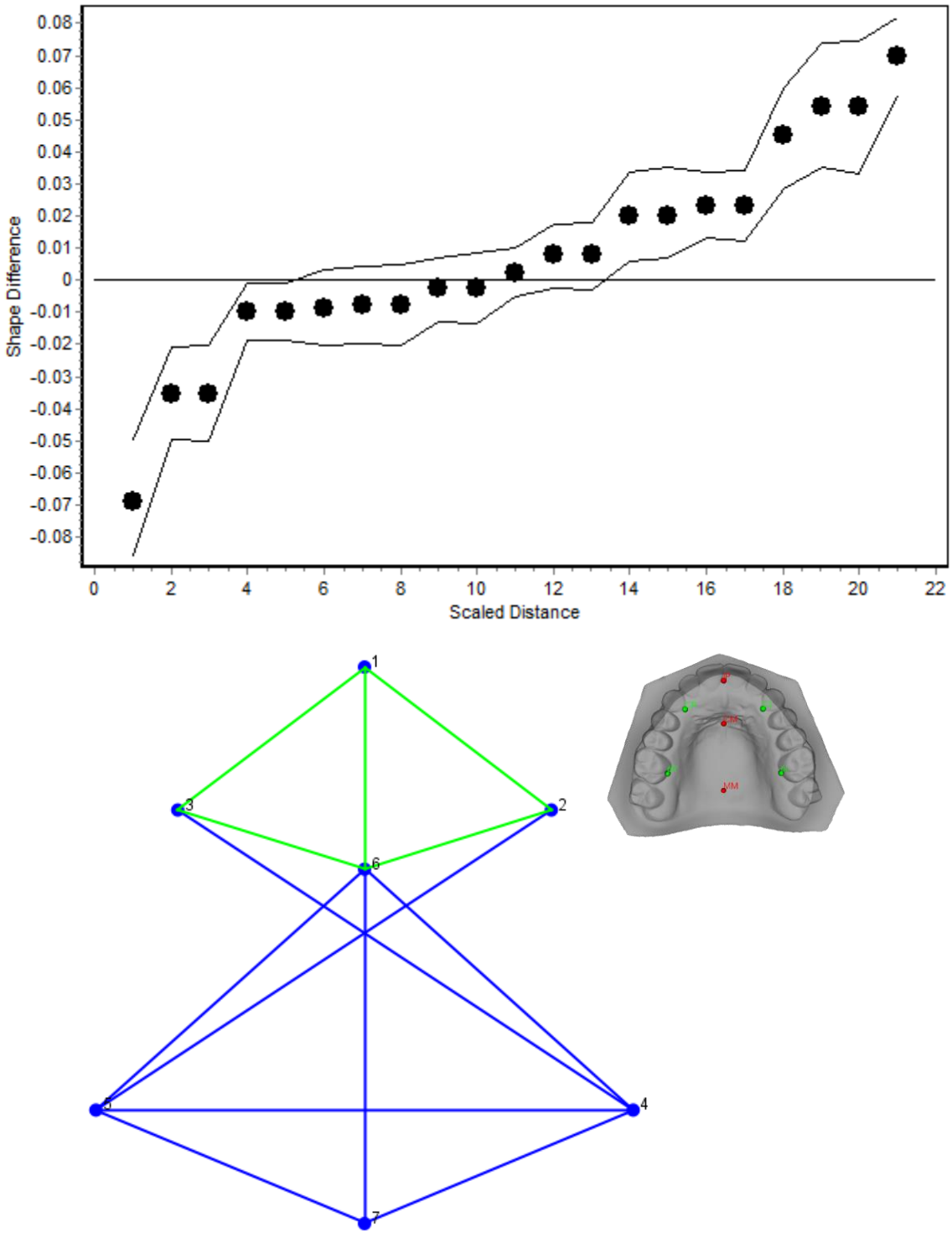

Figure 44 EDMA: Male vs. female Asian control.

Distances = Green: Male < Female, Blue: Male > Female.

Table 19 Euclidean Distance Matrix Analysis: African male vs. female control. (Figure 45)

	Distance		Difference	90% Confidence Interval	
1	Lmk1	Lmk6	-0.028	-0.044	-0.013
2	Lmk3	Lmk6	-0.018	-0.025	-0.012
3	Lmk2	Lmk6	-0.018	-0.026	-0.011
4	Lmk3	Lmk5	-0.017	-0.026	-0.008
5	Lmk2	Lmk4	-0.017	-0.025	-0.008
6	Lmk1	Lmk5	-0.015	-0.025	-0.007
7	Lmk1	Lmk4	-0.015	-0.024	-0.006
8	Lmk5	Lmk6	-0.007	-0.018	0.004
9	Lmk4	Lmk6	-0.007	-0.017	0.004
10	Lmk1	Lmk3	-0.002	-0.009	0.003
11	Lmk1	Lmk2	-0.002	-0.009	0.004
12	Lmk1	Lmk7	0.006	-0.005	0.018
13	Lmk2	Lmk3	0.007	0.002	0.011
14	Lmk2	Lmk5	0.008	-0.001	0.017
15	Lmk3	Lmk4	0.008	-0.001	0.017
16	Lmk3	Lmk7	0.015	0.007	0.023
17	Lmk2	Lmk7	0.015	0.007	0.023
18	Lmk6	Lmk7	0.024	0.011	0.037
19	Lmk4	Lmk5	0.041	0.033	0.048
20	Lmk5	Lmk7	0.043	0.034	0.053
21	Lmk4	Lmk7	0.043	0.034	0.052

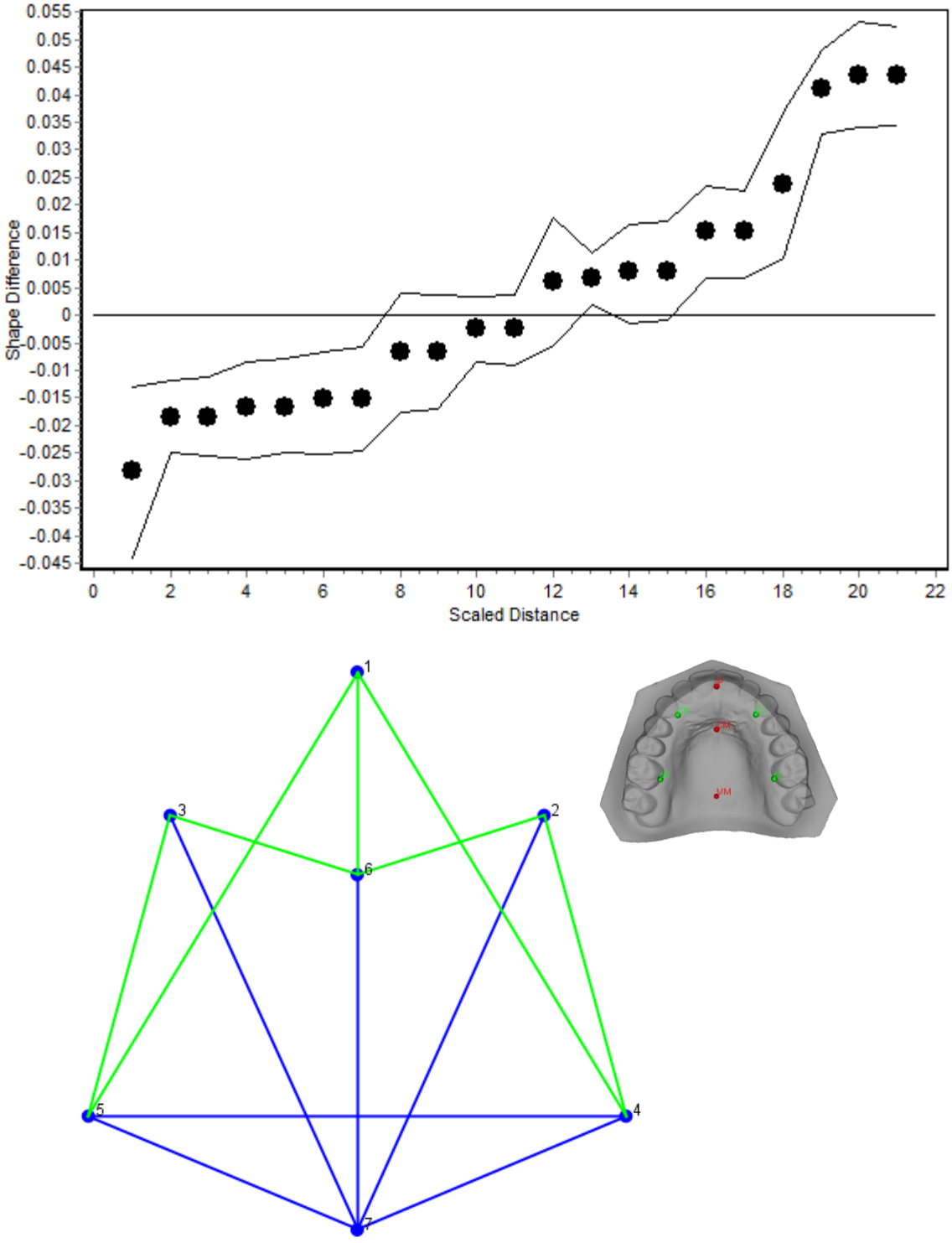

Figure 45 EDMA: Male vs. female African control.

Distances = Green: Male < Female, Blue: Male > Female.

Table 20 Euclidean Distance Matrix Analysis: Euro male vs. female control. (Figure 46)

	Distance		Difference	90% Confidence Interval	
1	Lmk3	Lmk6	-0.036	-0.043	-0.029
2	Lmk2	Lmk6	-0.036	-0.043	-0.029
3	Lmk1	Lmk6	-0.033	-0.042	-0.025
4	Lmk2	Lmk3	-0.011	-0.016	-0.007
5	Lmk1	Lmk3	-0.007	-0.012	-0.002
6	Lmk1	Lmk2	-0.007	-0.012	-0.002
7	Lmk4	Lmk6	0	-0.006	0.008
8	Lmk5	Lmk6	0	-0.006	0.007
9	Lmk1	Lmk5	0.005	-0.002	0.011
10	Lmk1	Lmk4	0.005	-0.002	0.01
11	Lmk2	Lmk4	0.008	0.003	0.012
12	Lmk3	Lmk5	0.008	0.003	0.012
13	Lmk2	Lmk5	0.009	0.003	0.014
14	Lmk3	Lmk4	0.009	0.003	0.015
15	Lmk3	Lmk7	0.021	0.016	0.026
16	Lmk2	Lmk7	0.021	0.016	0.026
17	Lmk1	Lmk7	0.027	0.02	0.034
18	Lmk5	Lmk7	0.028	0.02	0.037
19	Lmk4	Lmk7	0.028	0.02	0.036
20	Lmk4	Lmk5	0.03	0.023	0.036
21	Lmk6	Lmk7	0.047	0.04	0.054

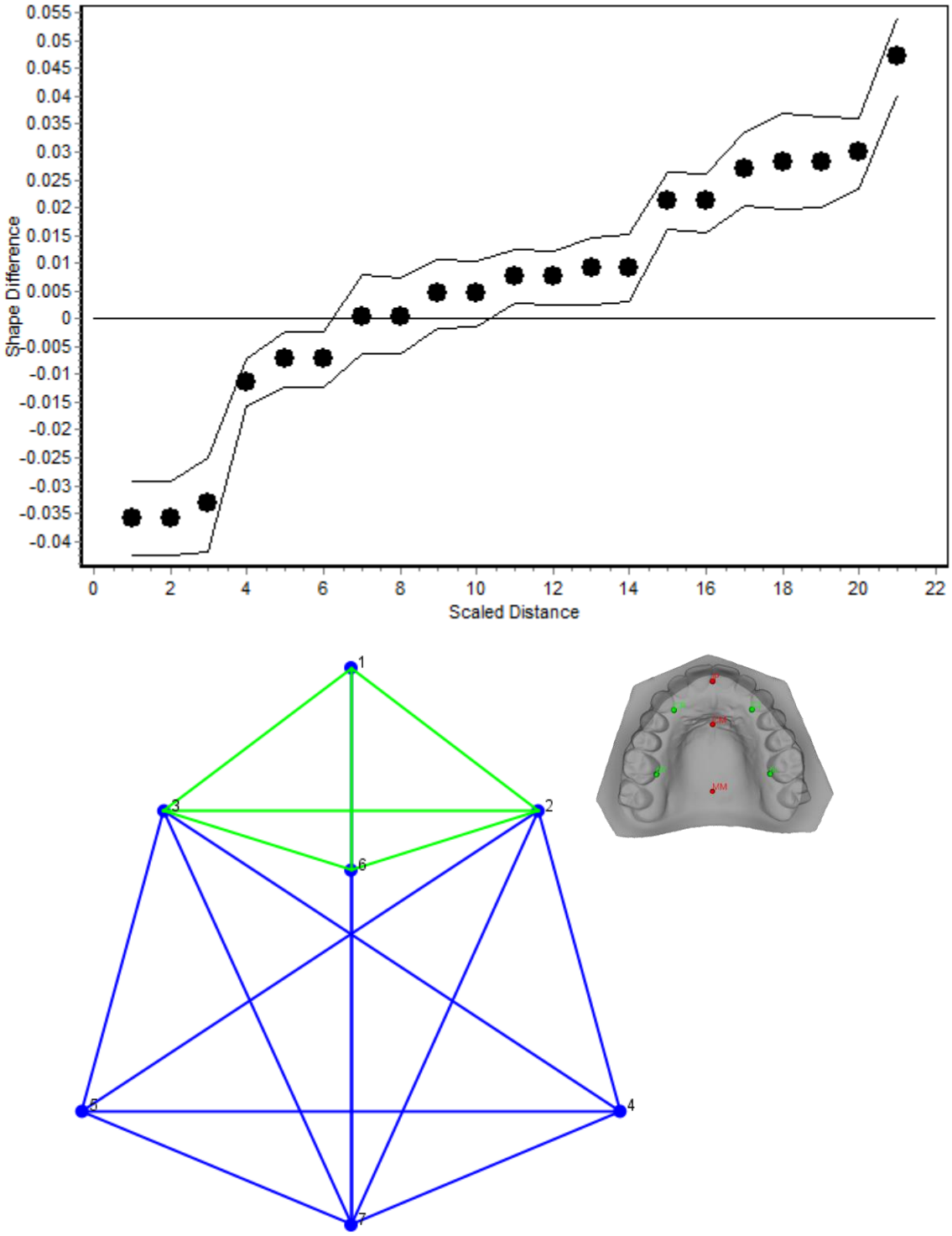

Figure 46 EDMA: Male vs. female Euro control.

Distances = Green: Male < Female, Blue: Male > Female.

3.2.2 Aim 2: Patterns of sex and ancestry in the parent population

3.2.2.1 Report of findings:

By sex, males again generally had higher posterior palatal vaults in comparison to females who had higher anterior palatal vaults. Males also in general had wider ML dimension than females, but no difference was detected in the AP dimension between sexes ($p \leq .0017$) (Figures 47-49) (Tables 21, 30, 31). No difference in shape was found when comparing African fathers to mothers ($p = .4379$).

By ancestry, Africans again in general had highest palatal vaults overall in comparison to other ancestries ($p \leq .0001$). Europeans in general had more constricted jaws with a longer AP dimension ($p \leq .0016$) (Figures 47, 48, 50-63) (Tables 22-29). No difference was detected between African and Asian fathers ($p = .602$) and the differences between European and Asian fathers were less distinct that in the control population, achieving only baseline significance level ($p = .017$) (Table 26). Within females, European mothers had higher anterior palatal vaults while Asian mothers had higher posterior palatal vaults ($p < .0001$) (Figures 60-63) (Tables 27-29).

The alpha level for this aim was set as follows:

[b] Baseline Significance Level $p < .05$

* Corrected Significance Level $p < .01$

3.2.2.2 General Contrast 1: Comparison by sex (ancestries combined)

In parents, fathers had higher posterior palatal vaults and wider posterior palates. Mothers had higher anterior palatal vaults.

- Canonical Variate Analysis: (Figures 47 & 48)

Eigenvalue	% Variance	Cumulative %
0.300481	100	100

Procrustes distance (p-value) = 0.0282 (0.0164)[b]

Mahalanobis distance (p-value) = 1.1430 (<.0001)*

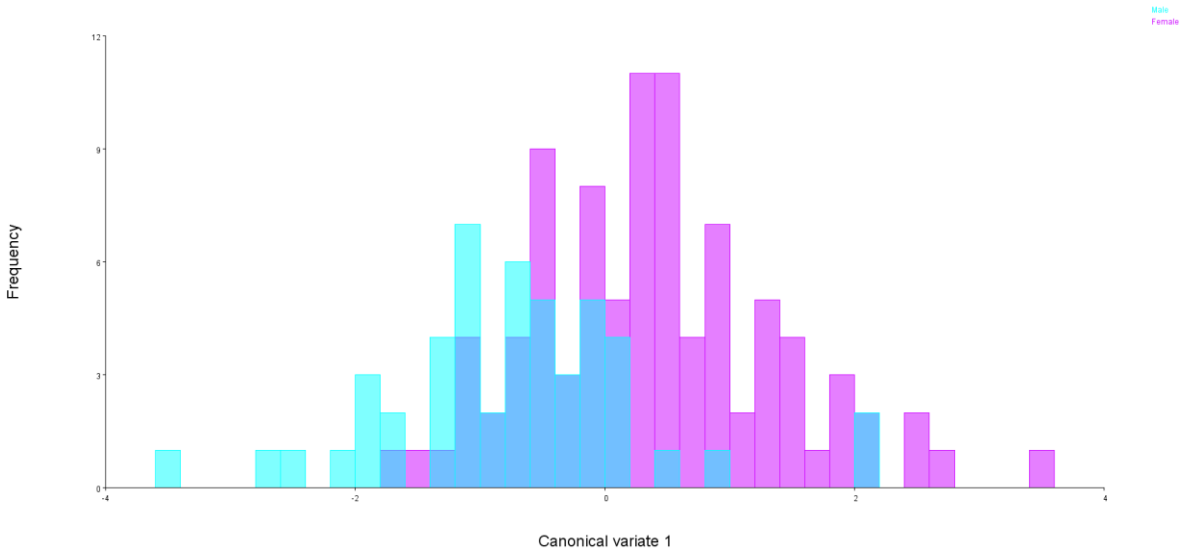

Figure 47 CVA of sexes in parents (ancestries combined).

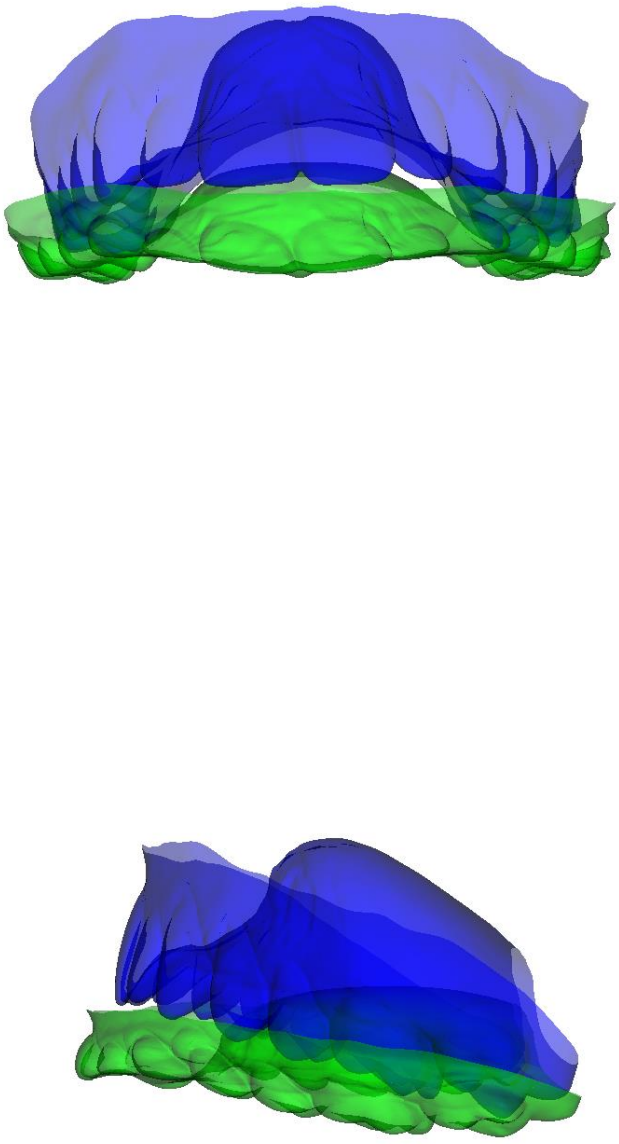

Figure 48 Canonical variate effect of sex in parents (ancestries combined).

Green = Negative (Male). Blue = Positive (Female). Scale factor = 10

Table 21 Euclidean Distance Matrix Analysis: Male vs. female parent. (Figure 49)

	Distance		Difference	90% Confidence Interval	
1	Lmk2	Lmk6	-0.034	-0.051	-0.018
2	Lmk3	Lmk6	-0.034	-0.05	-0.017
3	Lmk1	Lmk6	-0.031	-0.064	0.002
4	Lmk2	Lmk3	-0.007	-0.018	0.003
5	Lmk2	Lmk4	-0.005	-0.024	0.013
6	Lmk3	Lmk5	-0.005	-0.023	0.015
7	Lmk3	Lmk7	-0.001	-0.012	0.009
8	Lmk2	Lmk7	-0.001	-0.012	0.009
9	Lmk3	Lmk4	0.002	-0.017	0.021
10	Lmk2	Lmk5	0.002	-0.017	0.02
11	Lmk4	Lmk6	0.01	-0.016	0.033
12	Lmk5	Lmk6	0.01	-0.013	0.033
13	Lmk1	Lmk3	0.01	-0.005	0.025
14	Lmk1	Lmk2	0.01	-0.004	0.024
15	Lmk1	Lmk4	0.017	0	0.034
16	Lmk1	Lmk5	0.017	-0.002	0.036
17	Lmk4	Lmk7	0.018	0.002	0.035
18	Lmk5	Lmk7	0.018	0.002	0.034
19	Lmk1	Lmk7	0.022	0.001	0.043
20	Lmk4	Lmk5	0.023	0.007	0.039
21	Lmk6	Lmk7	0.042	0.02	0.063

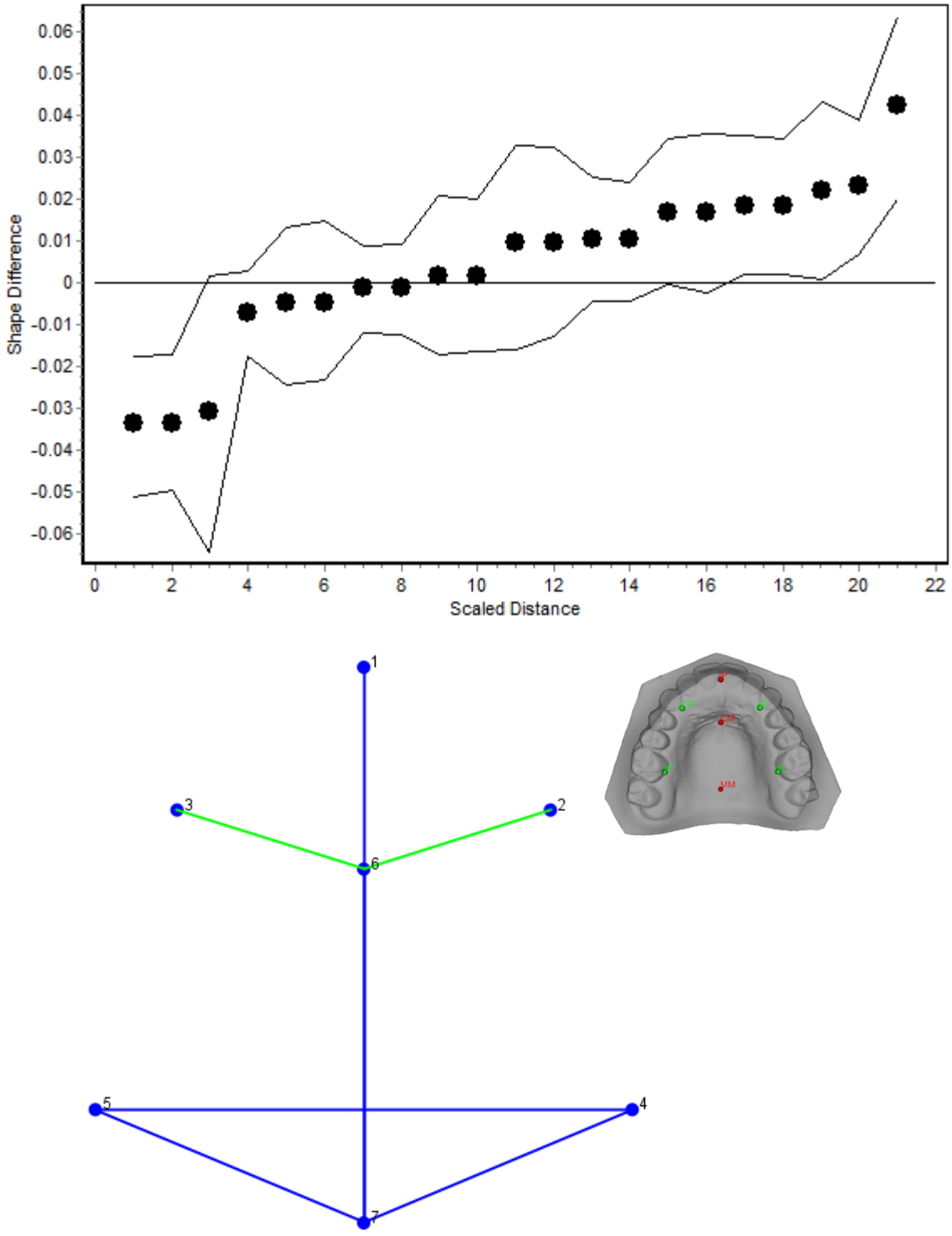

Figure 49 EDMA: Male vs. female parent (ancestries combined).

Distances = Green: Male < Female, Blue: Male > Female.

3.2.2.3 General Contrast 2: Comparison by ancestry (sexes combined)

In parents, Africans again had overall highest palatal vaults while Asians had overall shallowest. Europeans had the narrowest palatal vaults and an anteriorly located maximal vault height.

- Canonical Variates Analysis: (Figures 50 & 51)

	Eigenvalues	% Variance	Cumulative %
CV1	0.569286	75.785	75.785
CV2	0.181896	24.215	100

Procrustes distance (p-value):

	African	Asian
Asian	0.0369 (0.0028)*	
Euro	0.0511 (<.0001)*	0.0421 (0.0002)*

Mahalanobis distance (p-value):

	African	Asian
Asian	1.0656 (0.0001)*	
Euro	1.8183 (<.0001)*	1.5522 (<.0001)*

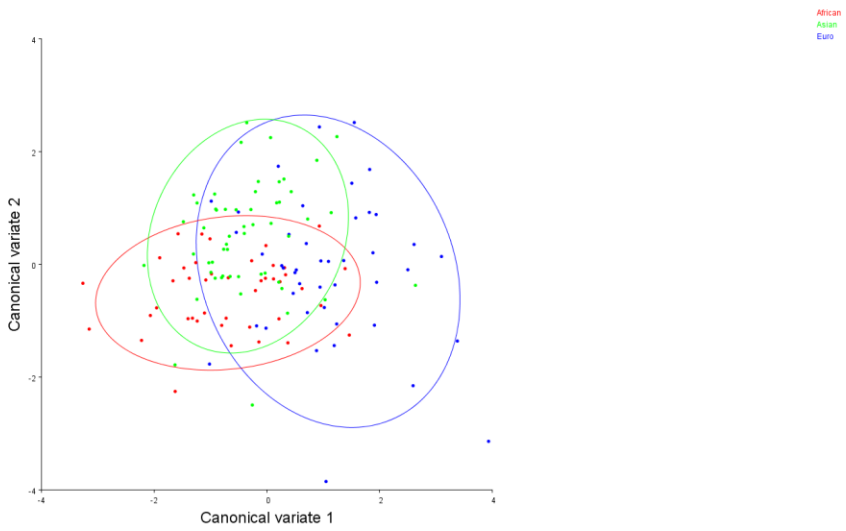

Figure 50 CVA of ancestry in parents (sexes combined).

Confidence ellipses represent 90% frequency.

CV1

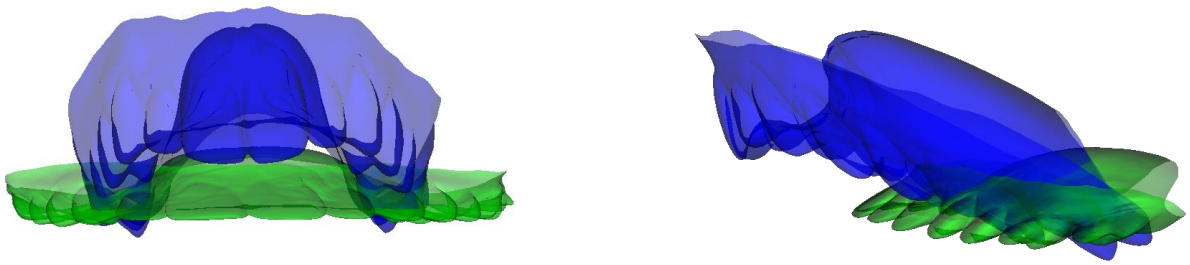

CV2

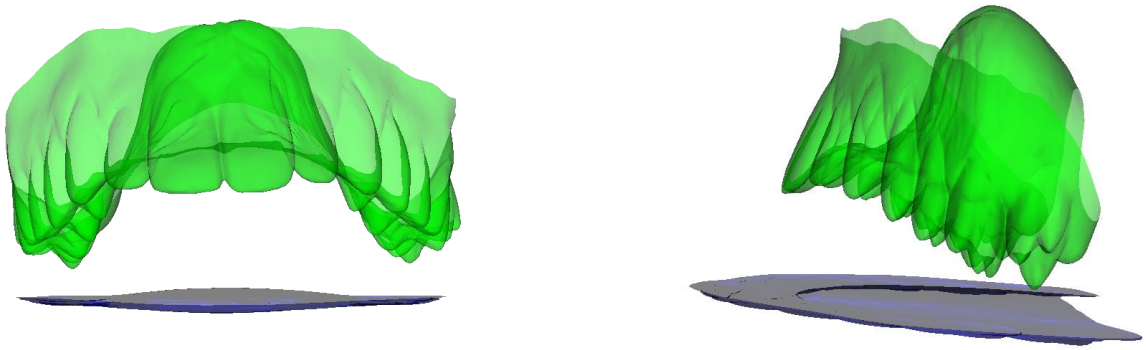

Figure 51 Canonical variate effects of ancestry in parents (sexes combined).

Green = Negative. Blue = Positive. Scale factor = 10

CV1: Separation of Europeans (Blue) from the other ancestries (green).

CV2: Separation of Africans (Green) from Asians (Blue).

Table 22 Euclidean Distance Matrix Analysis: Asian vs. African parent (sexes combined). (Figure 52)

	Distance		Difference	90% Confidence Interval	
1	Lmk1	Lmk6	-0.066	-0.105	-0.03
2	Lmk5	Lmk7	-0.025	-0.044	-0.005
3	Lmk4	Lmk7	-0.025	-0.045	-0.006
4	Lmk3	Lmk6	-0.024	-0.042	-0.007
5	Lmk2	Lmk6	-0.024	-0.04	-0.007
6	Lmk1	Lmk2	-0.011	-0.026	0.003
7	Lmk1	Lmk3	-0.011	-0.026	0.004
8	Lmk4	Lmk5	-0.009	-0.027	0.007
9	Lmk2	Lmk3	-0.003	-0.015	0.008
10	Lmk1	Lmk7	-0.001	-0.025	0.023
11	Lmk3	Lmk7	0.014	0	0.029
12	Lmk2	Lmk7	0.014	-0.001	0.029
13	Lmk2	Lmk5	0.018	0	0.039
14	Lmk3	Lmk4	0.018	-0.002	0.038
15	Lmk1	Lmk5	0.019	-0.001	0.038
16	Lmk1	Lmk4	0.019	0	0.039
17	Lmk5	Lmk6	0.033	0.005	0.057
18	Lmk4	Lmk6	0.033	0.005	0.059
19	Lmk3	Lmk5	0.04	0.021	0.059
20	Lmk2	Lmk4	0.04	0.02	0.061
21	Lmk6	Lmk7	0.061	0.038	0.085

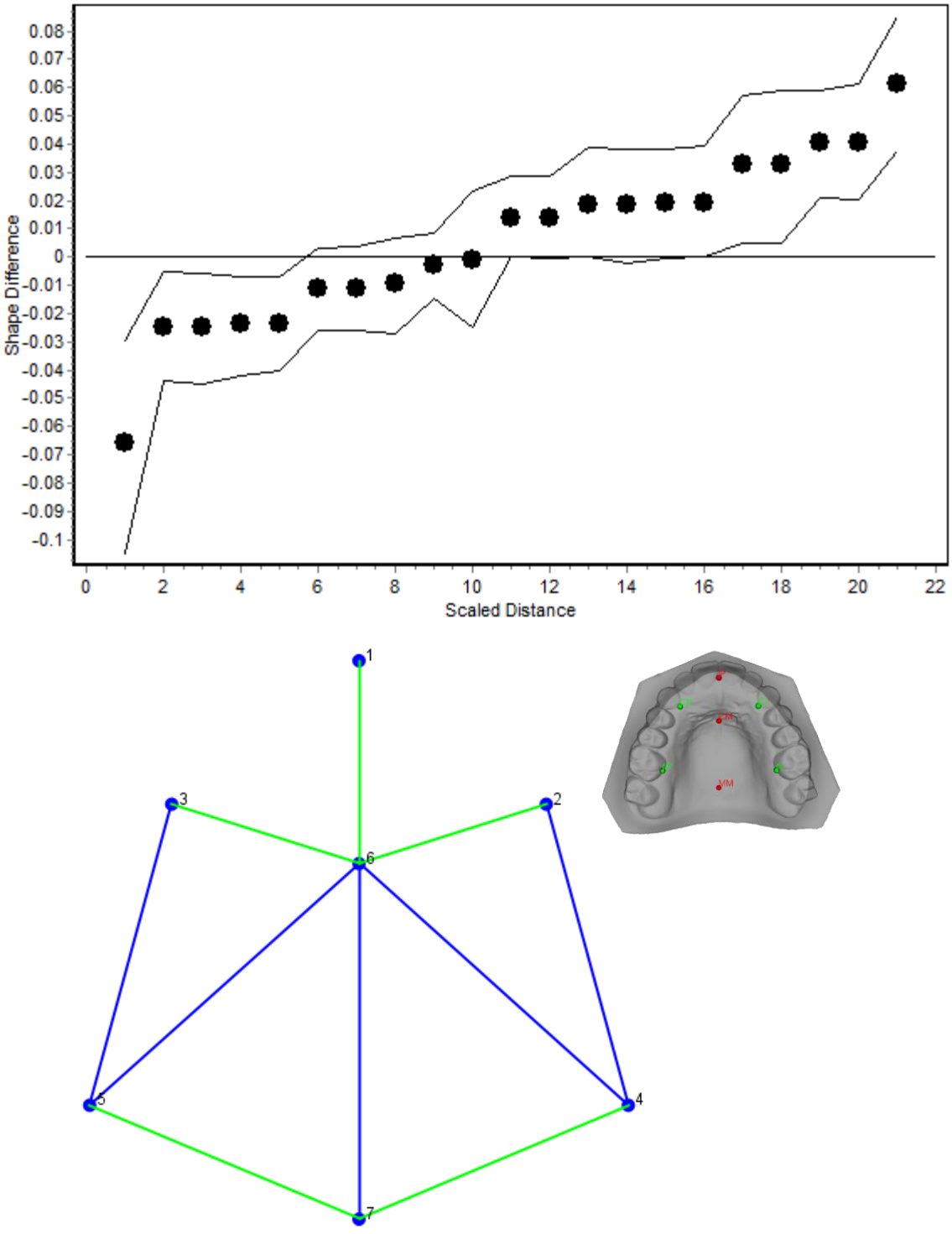

Figure 52 EDMA: Asian vs. African parent (sexes combined).

Distances = Green: Asian < African, Blue: Asian > African.

Table 23 Euclidean Distance Matrix Analysis: Euro vs. African parent (sexes combined). (Figure 53)

	Distance		Difference	90% Confidence Interval	
1	Lmk4	Lmk5	-0.061	-0.075	-0.045
2	Lmk5	Lmk7	-0.034	-0.055	-0.016
3	Lmk4	Lmk7	-0.034	-0.054	-0.015
4	Lmk2	Lmk3	-0.028	-0.037	-0.018
5	Lmk3	Lmk7	-0.02	-0.037	-0.004
6	Lmk2	Lmk7	-0.02	-0.038	-0.005
7	Lmk3	Lmk6	-0.016	-0.03	-0.002
8	Lmk2	Lmk6	-0.016	-0.029	-0.002
9	Lmk1	Lmk6	-0.011	-0.048	0.022
10	Lmk1	Lmk3	-0.009	-0.021	0.003
11	Lmk1	Lmk2	-0.009	-0.022	0.003
12	Lmk1	Lmk7	-0.005	-0.03	0.018
13	Lmk2	Lmk5	-0.003	-0.022	0.016
14	Lmk3	Lmk4	-0.003	-0.02	0.015
15	Lmk6	Lmk7	0.014	-0.016	0.042
16	Lmk1	Lmk5	0.038	0.02	0.058
17	Lmk1	Lmk4	0.038	0.019	0.058
18	Lmk5	Lmk6	0.046	0.021	0.07
19	Lmk4	Lmk6	0.046	0.024	0.068
20	Lmk2	Lmk4	0.053	0.035	0.071
21	Lmk3	Lmk5	0.053	0.036	0.072

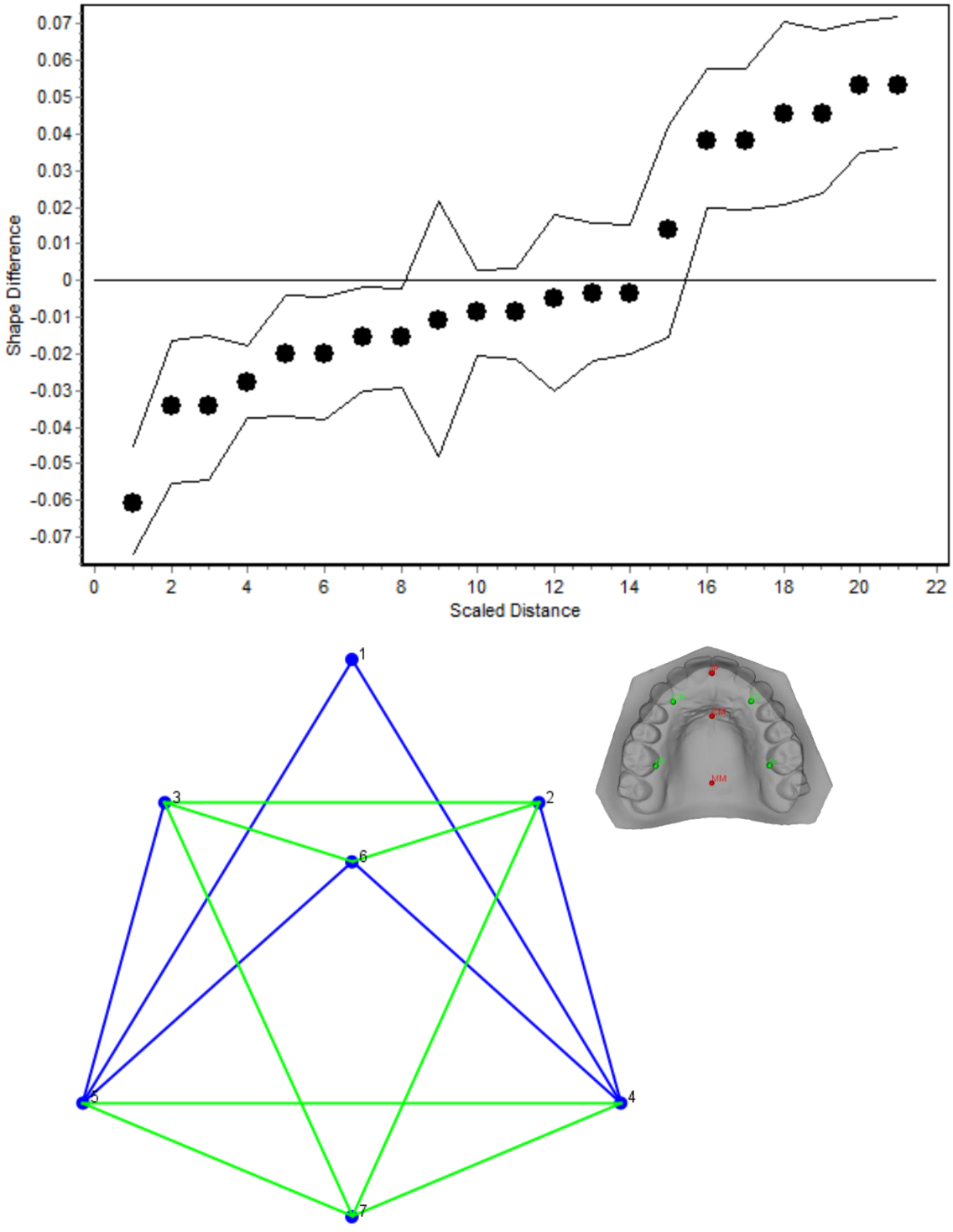

Figure 53 EDMA: Euro vs. African parent (sexes combined).

Distances = Green: Euro < African, Blue: Euro > African.

Table 24 Euclidean Distance Matrix Analysis: Euro vs. Asian parent (sexes combined). (Figure 54)

	Distance		Difference	90% Confidence Interval	
1	Lmk4	Lmk5	-0.051	-0.062	-0.042
2	Lmk6	Lmk7	-0.047	-0.06	-0.033
3	Lmk3	Lmk7	-0.034	-0.044	-0.024
4	Lmk2	Lmk7	-0.034	-0.045	-0.025
5	Lmk2	Lmk3	-0.025	-0.031	-0.02
6	Lmk3	Lmk4	-0.022	-0.033	-0.012
7	Lmk2	Lmk5	-0.022	-0.033	-0.012
8	Lmk4	Lmk7	-0.01	-0.023	0.004
9	Lmk5	Lmk7	-0.01	-0.022	0.003
10	Lmk1	Lmk7	-0.004	-0.015	0.01
11	Lmk1	Lmk3	0.002	-0.006	0.012
12	Lmk1	Lmk2	0.002	-0.006	0.011
13	Lmk2	Lmk6	0.008	-0.002	0.018
14	Lmk3	Lmk6	0.008	-0.004	0.02
15	Lmk4	Lmk6	0.013	0	0.023
16	Lmk5	Lmk6	0.013	0	0.023
17	Lmk2	Lmk4	0.013	0.004	0.021
18	Lmk3	Lmk5	0.013	0.003	0.021
19	Lmk1	Lmk4	0.019	0.011	0.027
20	Lmk1	Lmk5	0.019	0.01	0.028
21	Lmk1	Lmk6	0.055	0.04	0.071

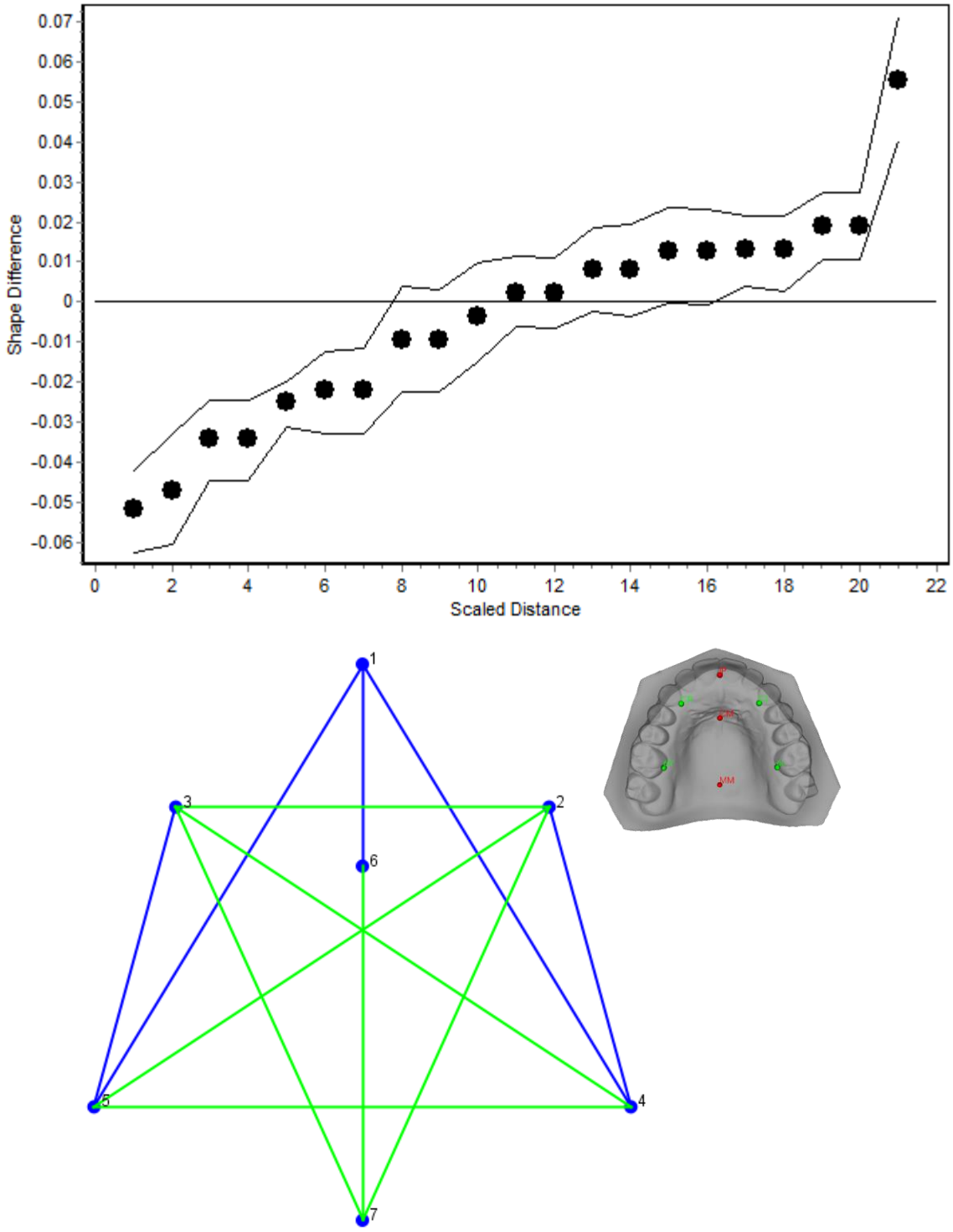

Figure 54 EDMA: Euro vs. Asian parent (sexes combined).

Distances = Green: Euro < Asian, Blue: Euro > Asian.

3.2.2.4 Stratified Contrast 1: Comparison of fathers by ancestry

In fathers, no shape differences were detected when comparing Asians to Africans. Europeans had the narrowest palates in comparison to the other ancestries. Europeans also had higher anterior palates when compared to Africans.

- Canonical Variates Analysis: (Figures 55 & 56)

	Eigenvalues	% Variance	Cumulative %
CV1	0.616951	86.144	86.144
CV2	0.099231	13.856	100

Procrustes distance (p-value):

	African	Asian
Asian	0.0281 (0.6912)	
Euro	0.0509 (0.0662)	0.0357 (0.3319)

Mahalanobis distance (p-value):

	African	Asian
Asian	0.9283 (0.6024)	
Euro	1.8516 (0.0016)*	1.3726 (0.0170)[b]

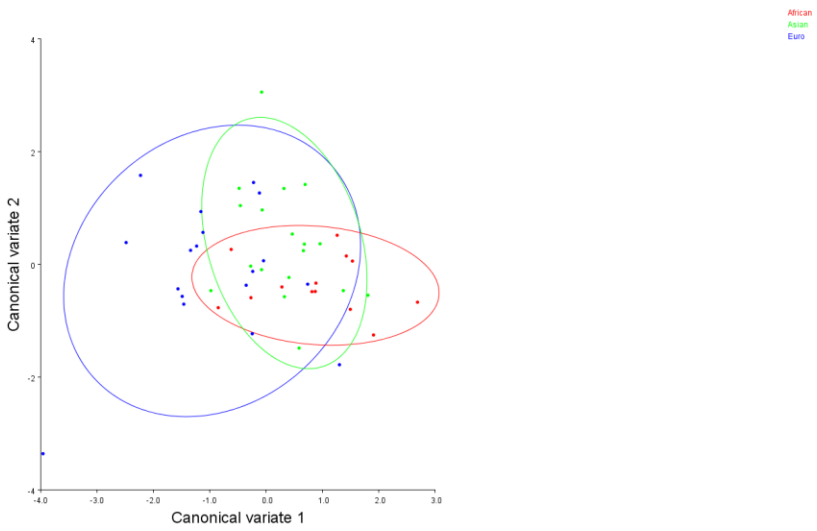

Figure 55 CVA of fathers by ancestry.

Confidence ellipses represent 90% frequency.

CV1

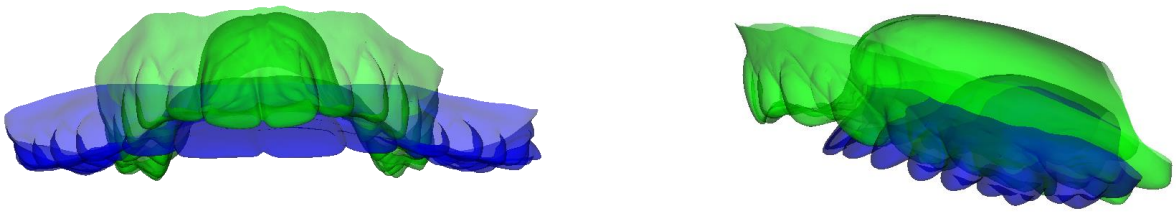

CV2

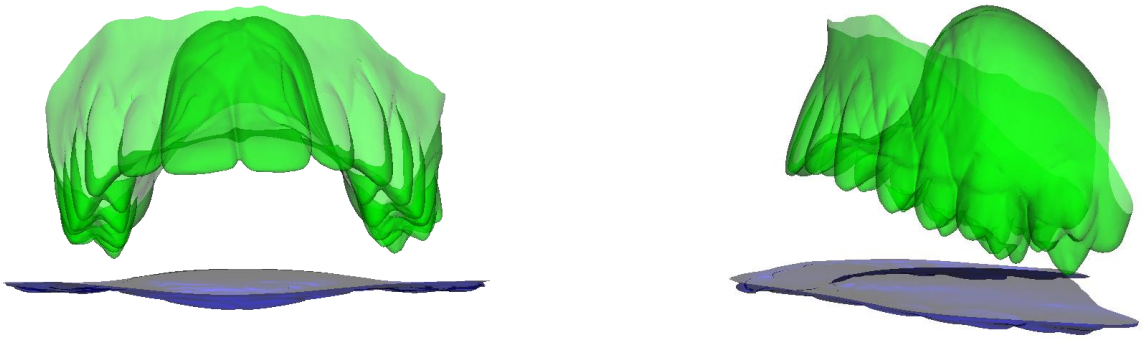

Figure 56 Canonical variate effects of ancestry in fathers.

Green = Negative. Blue = Positive. Scale factor = 10.

CV1: Separation of Europeans (Green) from the other ancestries.

Table 25 Euclidean Distance Matrix Analysis: Euro vs. African father. (Figure 57)

	Distance		Difference	90% Confidence Interval	
1	Lmk1	Lmk6	-0.048	-0.104	0.003
2	Lmk4	Lmk5	-0.047	-0.071	-0.024
3	Lmk2	Lmk6	-0.038	-0.058	-0.018
4	Lmk3	Lmk6	-0.038	-0.06	-0.017
5	Lmk2	Lmk3	-0.037	-0.054	-0.022
6	Lmk1	Lmk2	-0.03	-0.054	-0.008
7	Lmk1	Lmk3	-0.03	-0.053	-0.007
8	Lmk4	Lmk7	-0.003	-0.031	0.027
9	Lmk5	Lmk7	-0.003	-0.032	0.028
10	Lmk3	Lmk4	0.003	-0.027	0.032
11	Lmk2	Lmk5	0.003	-0.029	0.034
12	Lmk1	Lmk7	0.022	-0.016	0.059
13	Lmk1	Lmk4	0.025	-0.012	0.057
14	Lmk1	Lmk5	0.025	-0.006	0.055
15	Lmk2	Lmk7	0.03	-0.005	0.066
16	Lmk3	Lmk7	0.03	-0.005	0.067
17	Lmk4	Lmk6	0.034	0	0.065
18	Lmk5	Lmk6	0.034	0	0.068
19	Lmk2	Lmk4	0.065	0.034	0.095
20	Lmk3	Lmk5	0.065	0.034	0.097
21	Lmk6	Lmk7	0.066	0.011	0.123

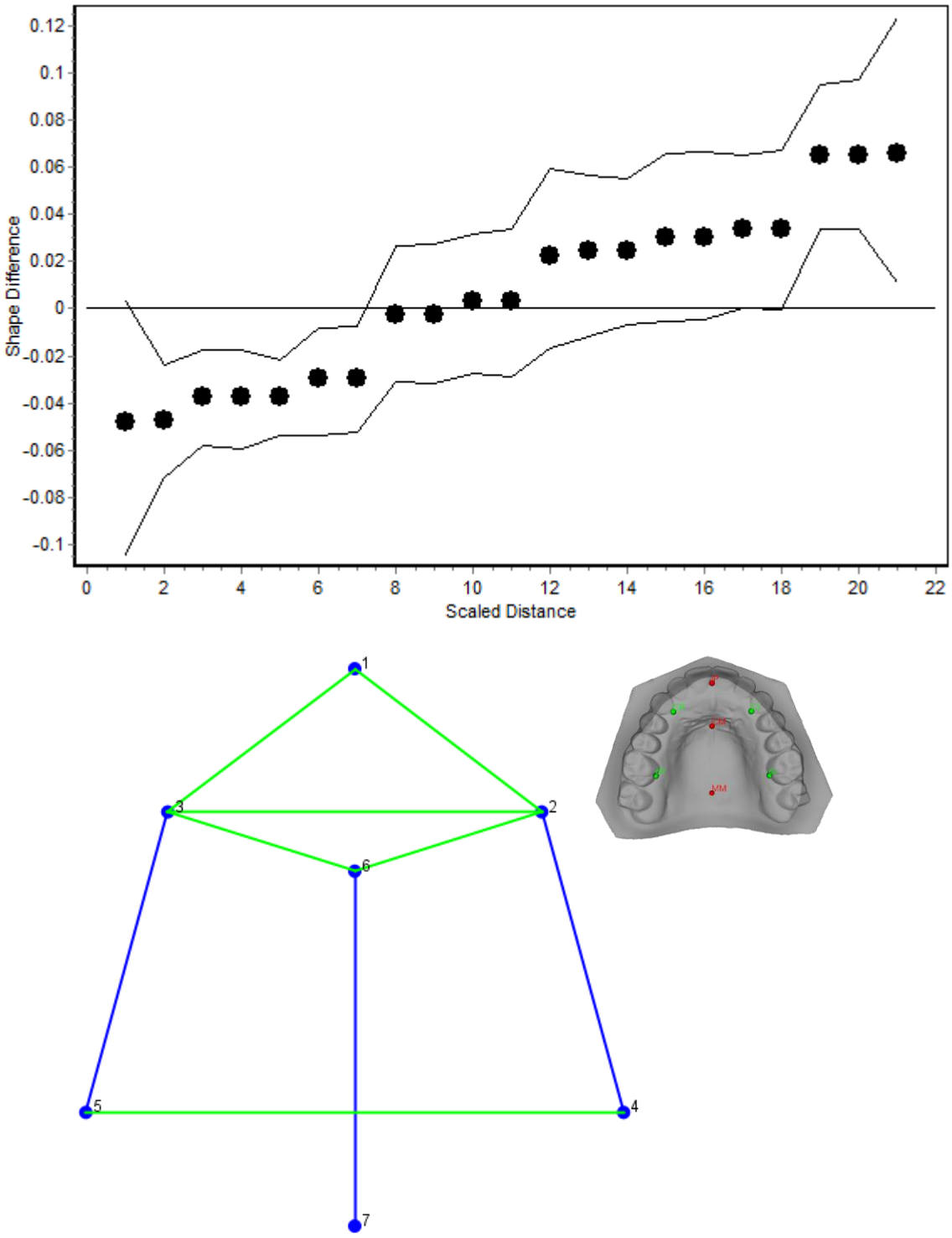

Figure 57 EDMA: Euro vs. African father.

Distances = Green: Euro < African, Blue: Euro > African.

Table 26 Euclidean Distance Matrix Analysis: Euro vs. Asian father. (Figure 58)

	Distance		Difference	90% Confidence Interval	
1	Lmk4	Lmk5	-0.057	-0.084	-0.025
2	Lmk1	Lmk2	-0.033	-0.065	-0.004
3	Lmk1	Lmk3	-0.033	-0.065	-0.005
4	Lmk6	Lmk7	-0.022	-0.077	0.036
5	Lmk4	Lmk6	-0.016	-0.072	0.034
6	Lmk5	Lmk6	-0.016	-0.063	0.037
7	Lmk2	Lmk3	-0.014	-0.036	0.011
8	Lmk2	Lmk6	-0.009	-0.052	0.034
9	Lmk3	Lmk6	-0.009	-0.054	0.024
10	Lmk1	Lmk4	-0.004	-0.044	0.031
11	Lmk1	Lmk5	-0.004	-0.038	0.04
12	Lmk3	Lmk4	0.002	-0.051	0.048
13	Lmk2	Lmk5	0.002	-0.046	0.06
14	Lmk4	Lmk7	0.002	-0.032	0.044
15	Lmk5	Lmk7	0.002	-0.031	0.047
16	Lmk1	Lmk7	0.018	-0.036	0.07
17	Lmk2	Lmk7	0.022	-0.001	0.051
18	Lmk3	Lmk7	0.022	-0.011	0.052
19	Lmk1	Lmk6	0.043	-0.041	0.12
20	Lmk2	Lmk4	0.047	-0.012	0.089
21	Lmk3	Lmk5	0.047	0	0.106

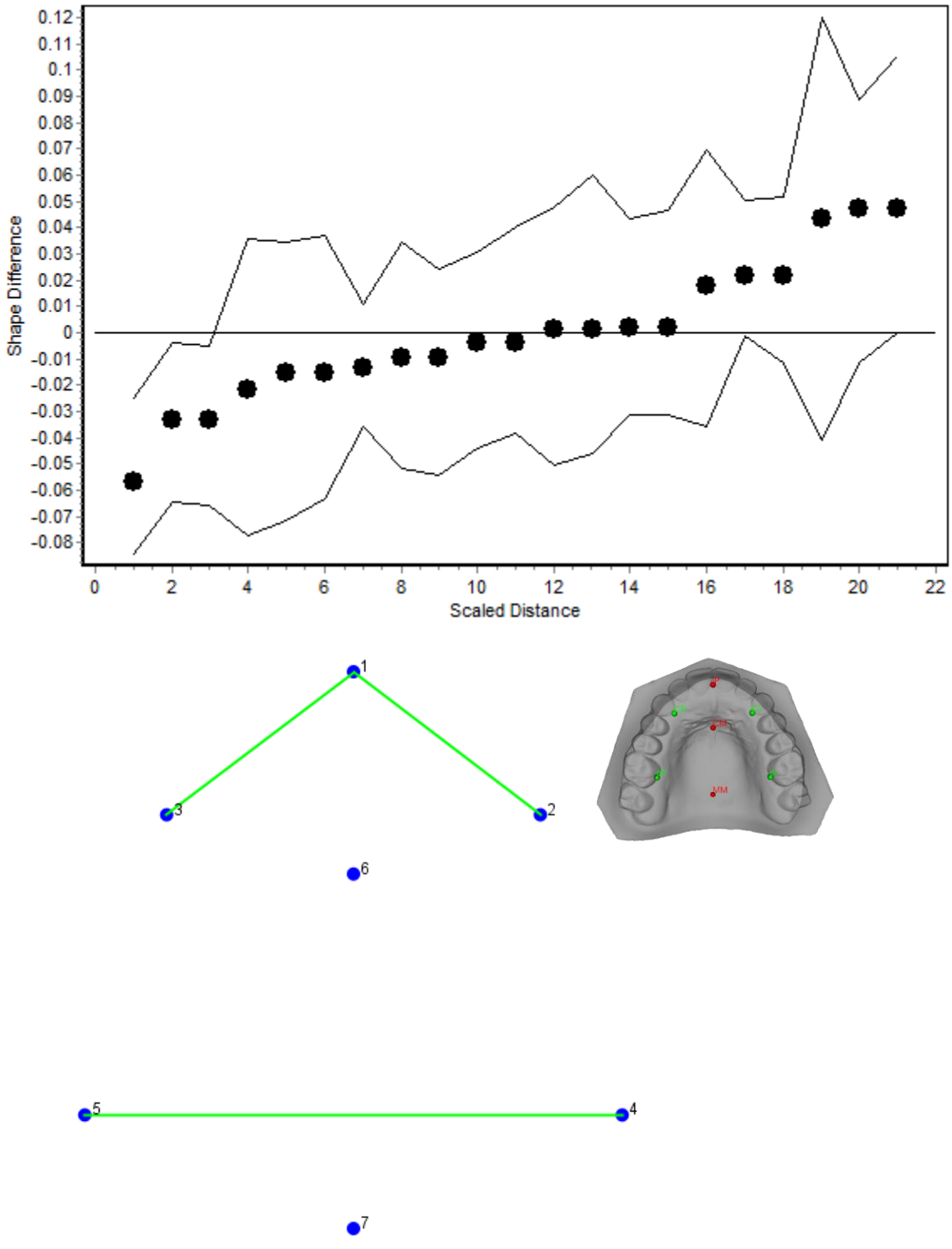

Figure 58 EDMA: Euro vs. Asian father.

Distances = Green: Euro < Asian.

3.2.2.5 Stratified Contrast 2: Comparison of mothers by ancestry

In mothers, Europeans had the narrowest palates while Asians had over shallowest palatal vaults. Africans had overall highest palatal vaults and wider palates. The point of maximum vault height was located more anteriorly in Europeans.

- Canonical Variates Analysis: (Figures 59 & 60)

	Eigenvalues	% Variance	Cumulative %
CV1	0.744843	64.596	64.596
CV2	0.408242	35.404	100

Procrustes distance (p-value):

	African	Asian
Asian	0.0435 (0.0004)*	
Euro	0.0628 (<.0001)*	0.0593 (<.0001)*

Mahalanobis distance (p-value):

	African	Asian
Asian	1.5133 (<.0001)*	
Euro	2.1289 (<.0001)*	1.9152 (<.0001)*

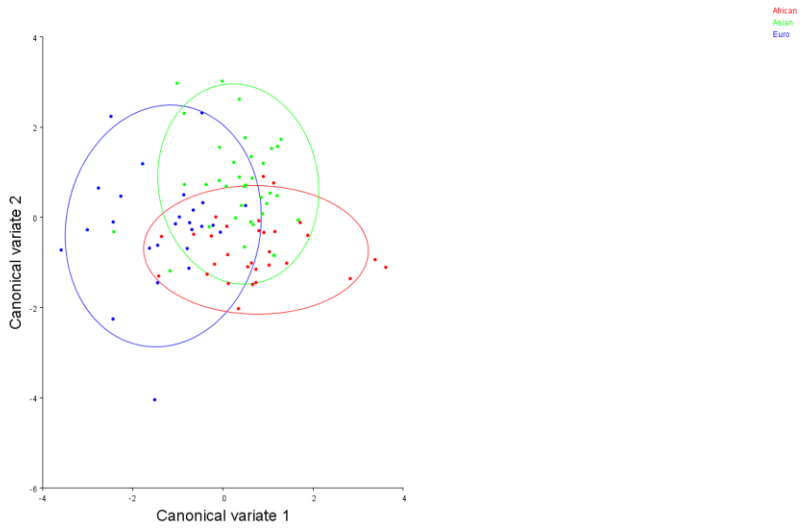

Figure 59 CVA of mothers by ancestry.

Confidence ellipses represent 90% frequency.

CV1

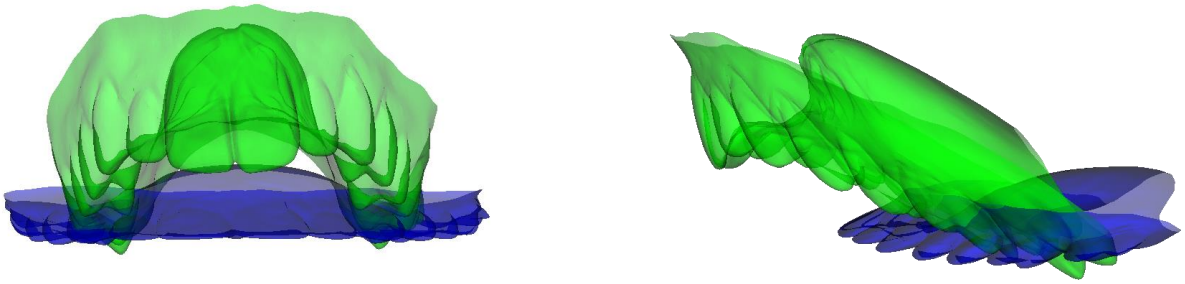

CV2

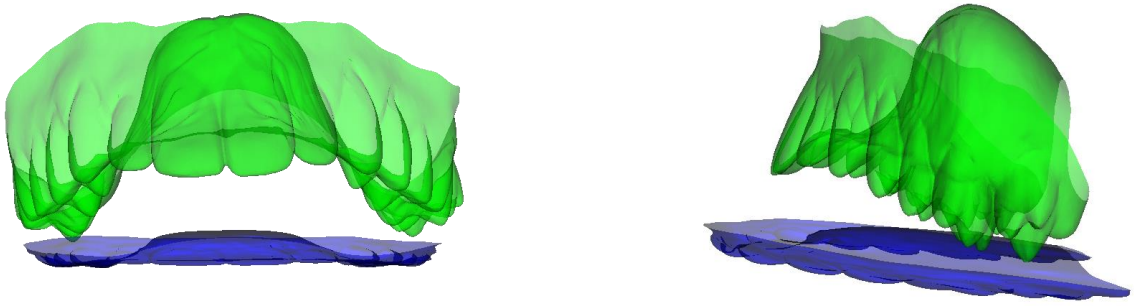

Figure 60 Canonical variate effects of ancestry in mothers.

Green = Negative. Blue = Positive. Scale factor = 10.

CV1: Separation of Europeans (Green) from the other ancestries (Blue).

CV2: Separation of Africans (Green) from Asians (Blue).

Table 27 Euclidean Distance Matrix Analysis: Asian vs. African mother. (Figure 61)

	Distance		Difference	90% Confidence Interval	
1	Lmk1	Lmk6	-0.06	-0.093	-0.022
2	Lmk5	Lmk7	-0.037	-0.058	-0.015
3	Lmk4	Lmk7	-0.037	-0.057	-0.017
4	Lmk4	Lmk5	-0.021	-0.039	-0.002
5	Lmk3	Lmk6	-0.018	-0.034	-0.003
6	Lmk2	Lmk6	-0.018	-0.034	-0.002
7	Lmk1	Lmk3	-0.015	-0.028	-0.003
8	Lmk1	Lmk2	-0.015	-0.027	-0.003
9	Lmk1	Lmk7	-0.006	-0.032	0.021
10	Lmk2	Lmk3	0.006	-0.008	0.019
11	Lmk1	Lmk5	0.015	-0.01	0.037
12	Lmk1	Lmk4	0.015	-0.009	0.039
13	Lmk3	Lmk7	0.017	-0.001	0.037
14	Lmk2	Lmk7	0.017	-0.002	0.037
15	Lmk2	Lmk5	0.023	-0.002	0.044
16	Lmk3	Lmk4	0.023	-0.001	0.045
17	Lmk5	Lmk6	0.03	0.003	0.056
18	Lmk4	Lmk6	0.03	0.002	0.056
19	Lmk2	Lmk4	0.048	0.024	0.068
20	Lmk3	Lmk5	0.048	0.025	0.066
21	Lmk6	Lmk7	0.055	0.028	0.079

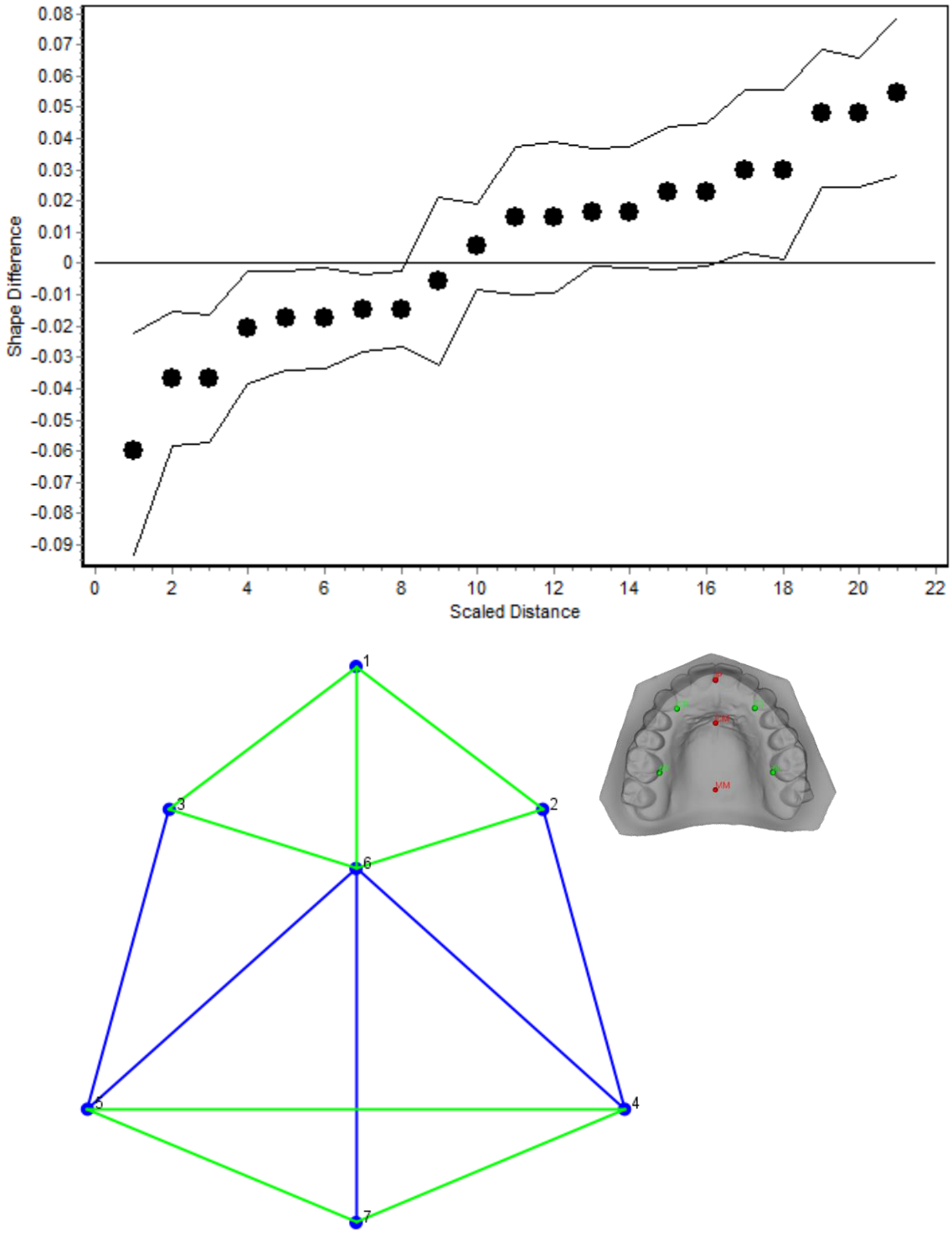

Figure 61 EDMA: Asian vs. African mother.

Distances = Green: Asian < African, Blue: Asian > African.

Table 28 Euclidean Distance Matrix Analysis: Euro vs. African mother. (Figure 62)

	Distance		Difference	90% Confidence Interval	
1	Lmk4	Lmk5	-0.071	-0.089	-0.053
2	Lmk5	Lmk7	-0.054	-0.079	-0.03
3	Lmk4	Lmk7	-0.054	-0.077	-0.032
4	Lmk2	Lmk7	-0.05	-0.067	-0.033
5	Lmk3	Lmk7	-0.05	-0.067	-0.033
6	Lmk1	Lmk7	-0.023	-0.052	0.005
7	Lmk2	Lmk3	-0.023	-0.039	-0.011
8	Lmk6	Lmk7	-0.022	-0.054	0.014
9	Lmk2	Lmk5	-0.009	-0.036	0.014
10	Lmk3	Lmk4	-0.009	-0.031	0.014
11	Lmk1	Lmk3	0.002	-0.011	0.015
12	Lmk1	Lmk2	0.002	-0.013	0.017
13	Lmk3	Lmk6	0.003	-0.014	0.02
14	Lmk2	Lmk6	0.003	-0.013	0.026
15	Lmk1	Lmk6	0.019	-0.026	0.063
16	Lmk1	Lmk5	0.044	0.02	0.064
17	Lmk1	Lmk4	0.044	0.019	0.067
18	Lmk2	Lmk4	0.047	0.025	0.067
19	Lmk3	Lmk5	0.047	0.027	0.064
20	Lmk5	Lmk6	0.052	0.022	0.088
21	Lmk4	Lmk6	0.052	0.02	0.084

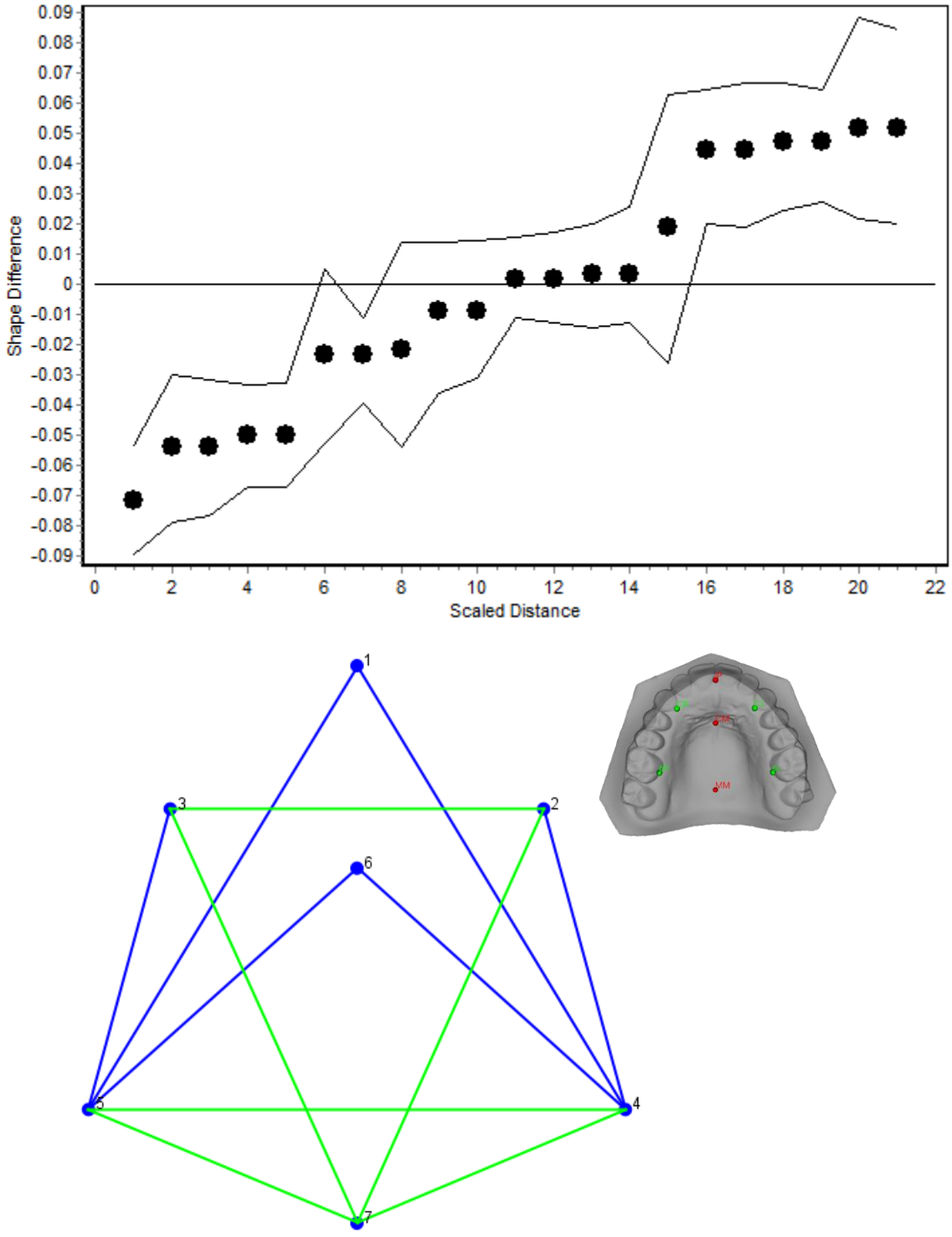

Figure 62 EDMA: Euro vs. African mother.

Distances = Green: Euro < African, Blue: Euro > African.

Table 29 Euclidean Distance Matrix Analysis: Euro vs. Asian mother. (Figure 63)

	Distance		Difference	90% Confidence Interval	
1	Lmk6	Lmk7	-0.076	-0.086	-0.067
2	Lmk3	Lmk7	-0.067	-0.072	-0.06
3	Lmk2	Lmk7	-0.067	-0.075	-0.06
4	Lmk4	Lmk5	-0.051	-0.061	-0.038
5	Lmk3	Lmk4	-0.032	-0.041	-0.023
6	Lmk2	Lmk5	-0.032	-0.041	-0.023
7	Lmk2	Lmk3	-0.029	-0.034	-0.023
8	Lmk1	Lmk7	-0.018	-0.028	-0.008
9	Lmk5	Lmk7	-0.017	-0.026	-0.009
10	Lmk4	Lmk7	-0.017	-0.027	-0.006
11	Lmk3	Lmk5	-0.001	-0.008	0.007
12	Lmk2	Lmk4	-0.001	-0.009	0.007
13	Lmk1	Lmk3	0.017	0.009	0.024
14	Lmk1	Lmk2	0.017	0.007	0.024
15	Lmk3	Lmk6	0.021	0.012	0.032
16	Lmk2	Lmk6	0.021	0.011	0.031
17	Lmk5	Lmk6	0.022	0.013	0.033
18	Lmk4	Lmk6	0.022	0.011	0.032
19	Lmk1	Lmk5	0.03	0.021	0.039
20	Lmk1	Lmk4	0.03	0.021	0.039
21	Lmk1	Lmk6	0.079	0.066	0.093

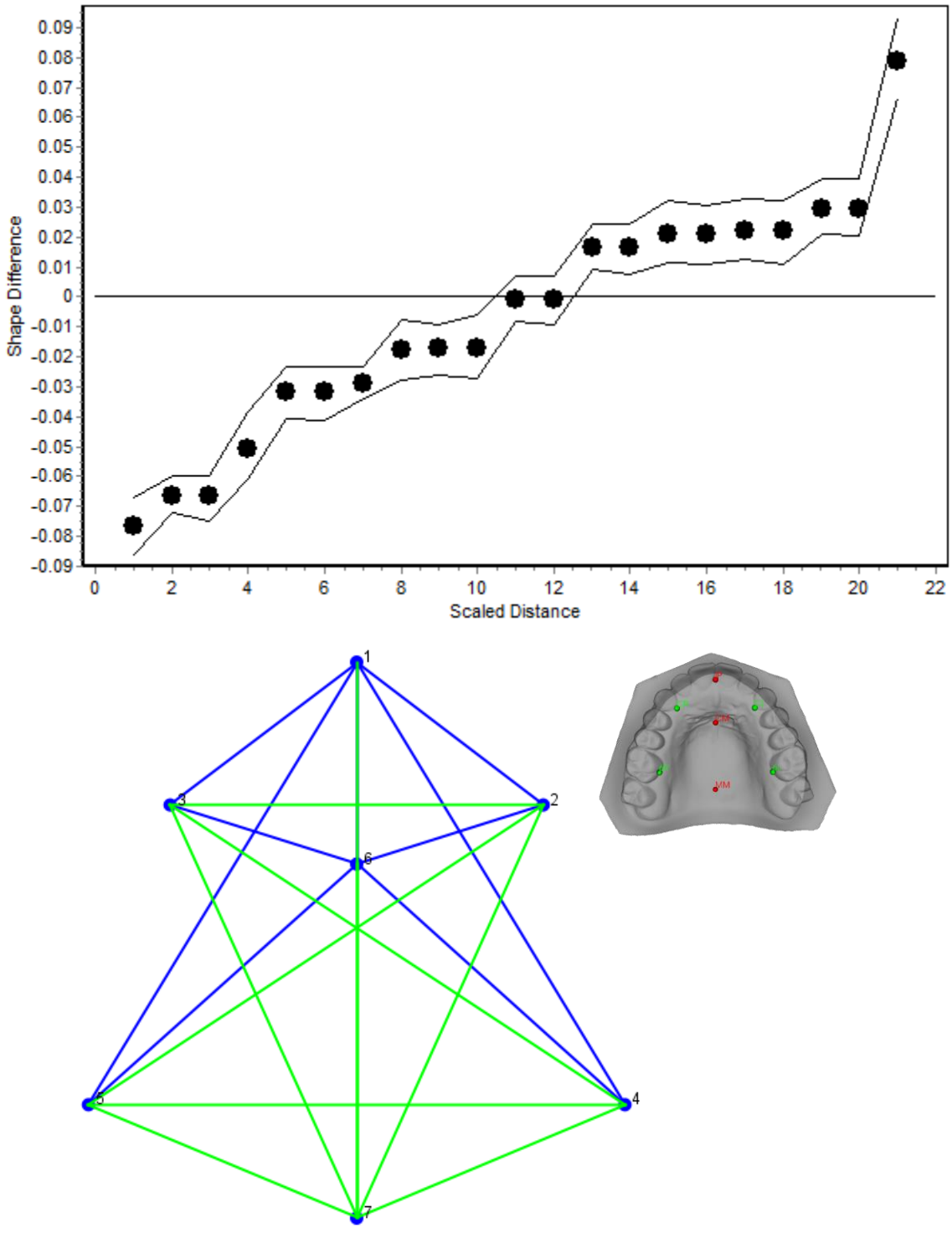

Figure 63 EDMA: Euro vs. Asian mother.

Distances = Green: Euro < Asian, Blue: Euro > Asian.

3.2.2.6 Stratified Contrast 3: Comparison of sexes within ancestries

Within ancestries, father vs. mother differences were only detected among Asians and Europeans, but not Africans. In Asians and Europeans, fathers had wider ML dimensions than mothers. In Europeans, fathers had higher posterior palatal vaults while mothers had higher anterior palatal vaults.

- Canonical Variates Analysis: (Figures 64 & 65)

Race	Eigenvalue	% Variance	Cumulative %
Asian	0.442164	100	100
African	0.197218	100	100
Euro	0.911781	100	100

Race	Procrustes distance (p-value)	Mahalanobis distance (p-value)
Asian	0.0331 (0.1516)	1.3842 (0.0017)*
African	0.0202 (0.7645)	0.9442 (0.4379)
Euro	0.0592 (0.0021)*	1.8975 (<.0001)*

Asian

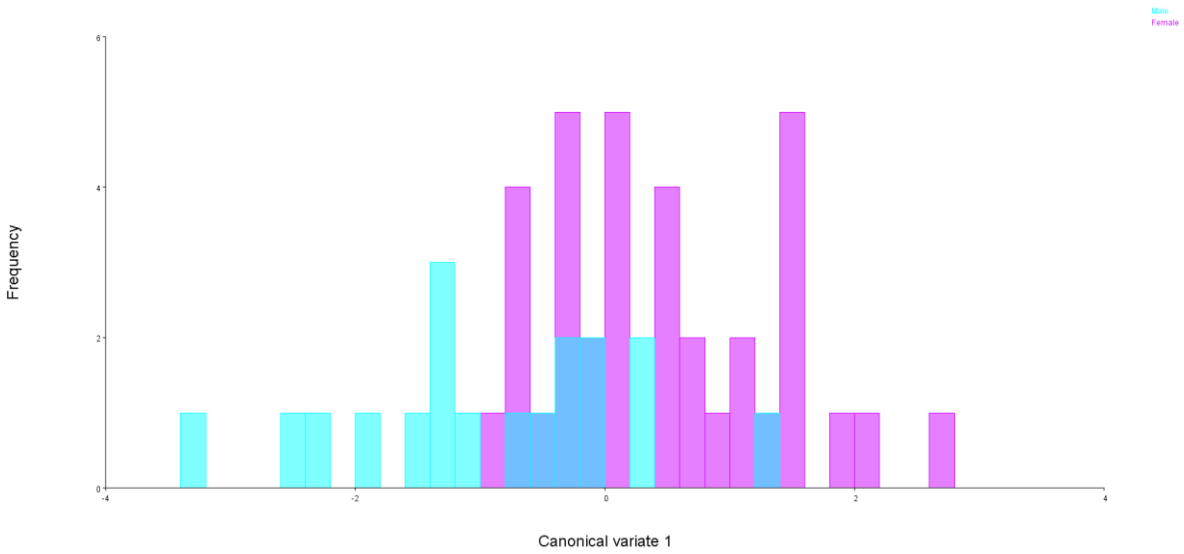

African

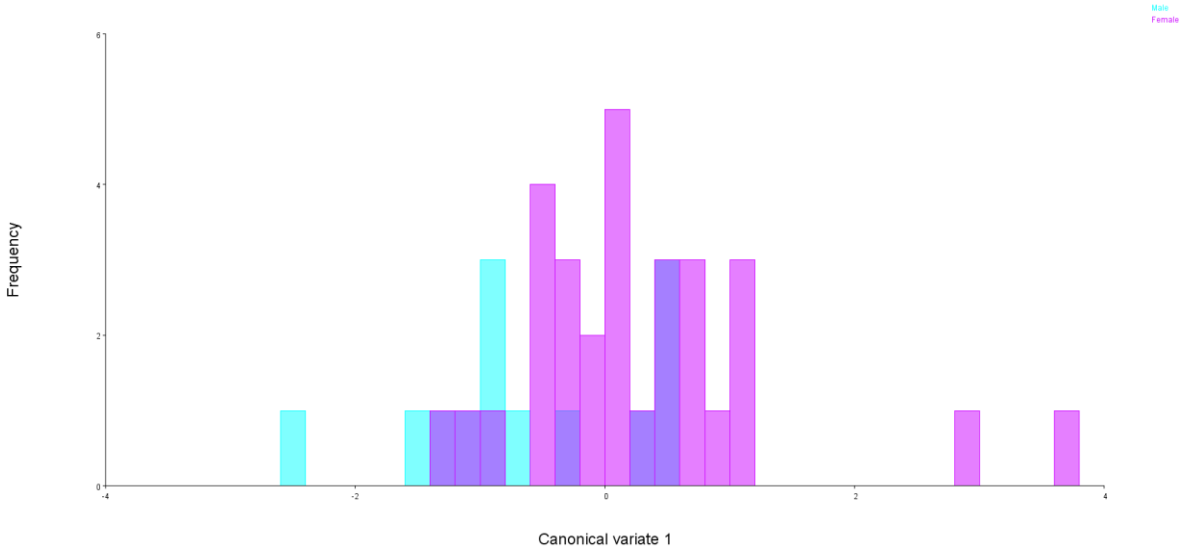

Euro

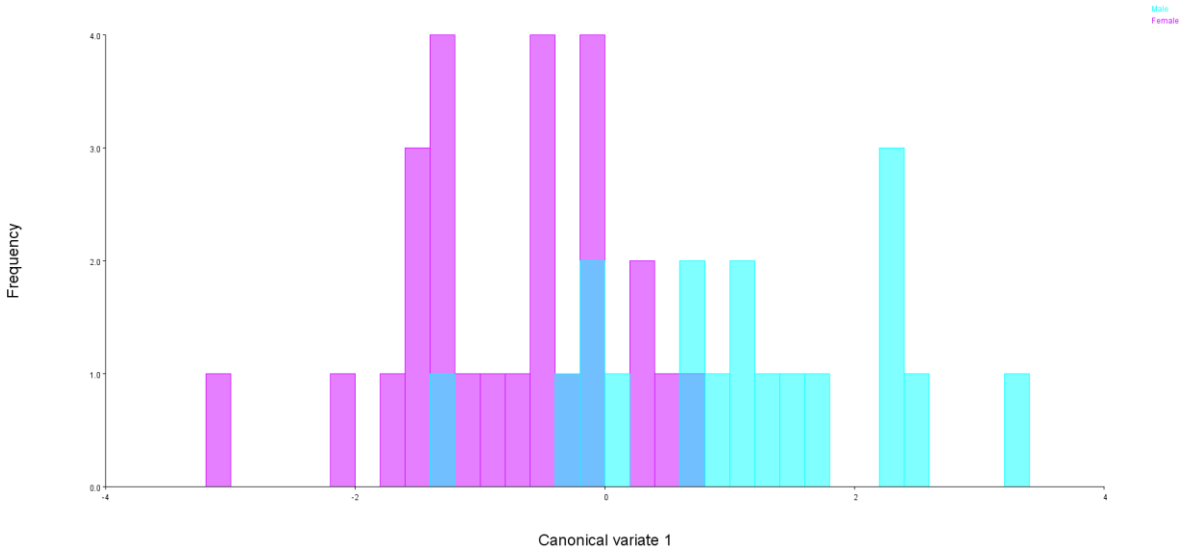

Figure 64 CVA of sexes in parents within ancestries.

Asian

Euro

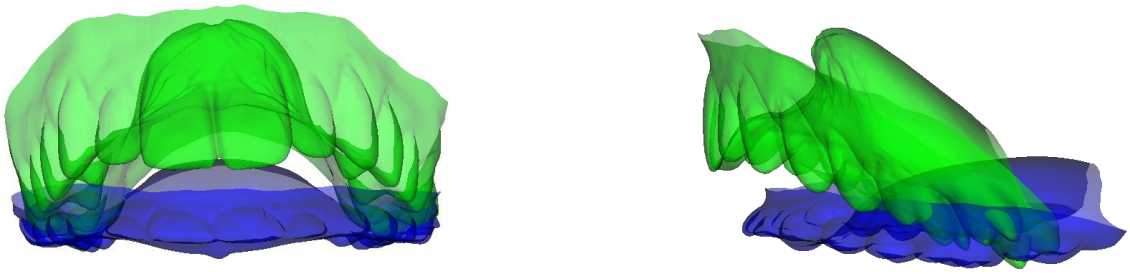

Figure 65 Canonical variate effects of sex within ancestries in parents.

Green = Negative. Blue = Positive. Scale factor = 10.

Asian: Green = Males, Blue = Females.

Euro: Blue = Males, Green = Females.

Table 30 Euclidean Distance Matrix Analysis: Asian male vs. female parent. (Figure 66)

	Distance		Difference	90% Confidence Interval	
1	Lmk3	Lmk5	-0.037	-0.078	0.015
2	Lmk2	Lmk4	-0.037	-0.09	0.013
3	Lmk1	Lmk6	-0.036	-0.107	0.021
4	Lmk3	Lmk7	-0.032	-0.055	-0.01
5	Lmk2	Lmk7	-0.032	-0.059	-0.007
6	Lmk3	Lmk6	-0.023	-0.071	0.019
7	Lmk2	Lmk6	-0.023	-0.059	0.036
8	Lmk2	Lmk3	-0.019	-0.04	0.006
9	Lmk3	Lmk4	-0.018	-0.07	0.023
10	Lmk2	Lmk5	-0.018	-0.055	0.037
11	Lmk1	Lmk7	0.013	-0.054	0.055
12	Lmk5	Lmk7	0.021	-0.028	0.06
13	Lmk4	Lmk7	0.021	-0.025	0.073
14	Lmk5	Lmk6	0.029	-0.016	0.08
15	Lmk4	Lmk6	0.029	-0.013	0.088
16	Lmk1	Lmk5	0.03	0.001	0.067
17	Lmk1	Lmk4	0.03	-0.014	0.064
18	Lmk1	Lmk2	0.037	0.001	0.075
19	Lmk1	Lmk3	0.037	0.003	0.076
20	Lmk4	Lmk5	0.038	0.006	0.077
21	Lmk6	Lmk7	0.039	0.005	0.089

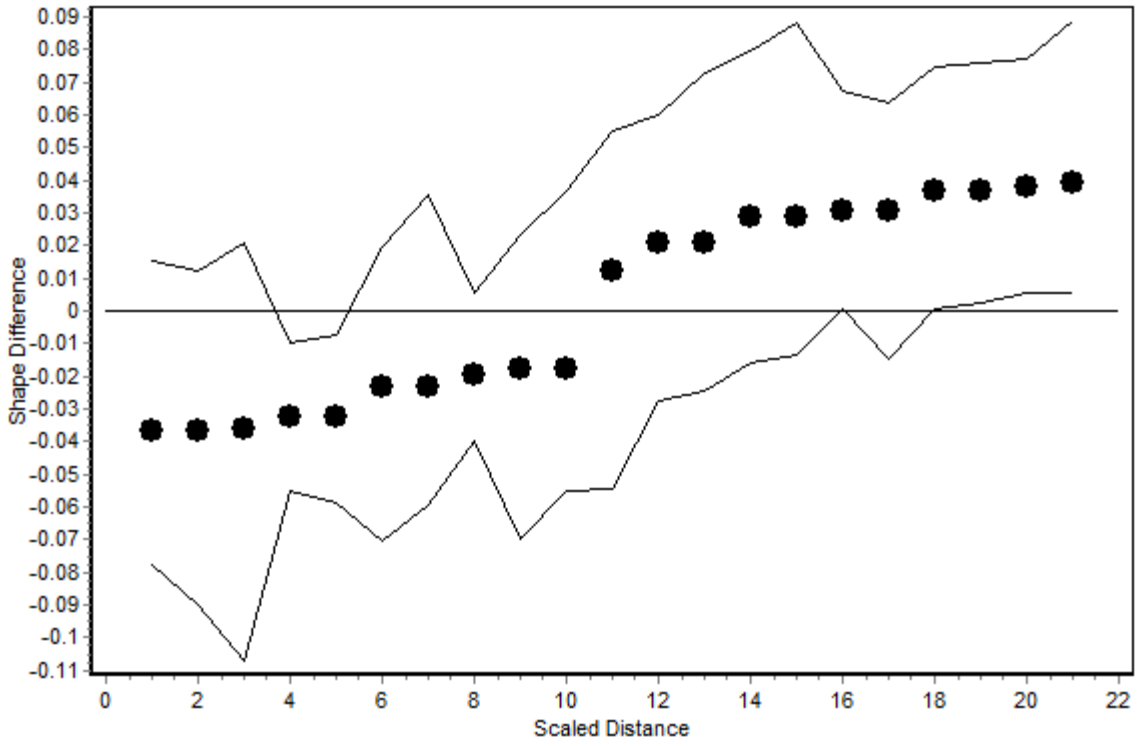

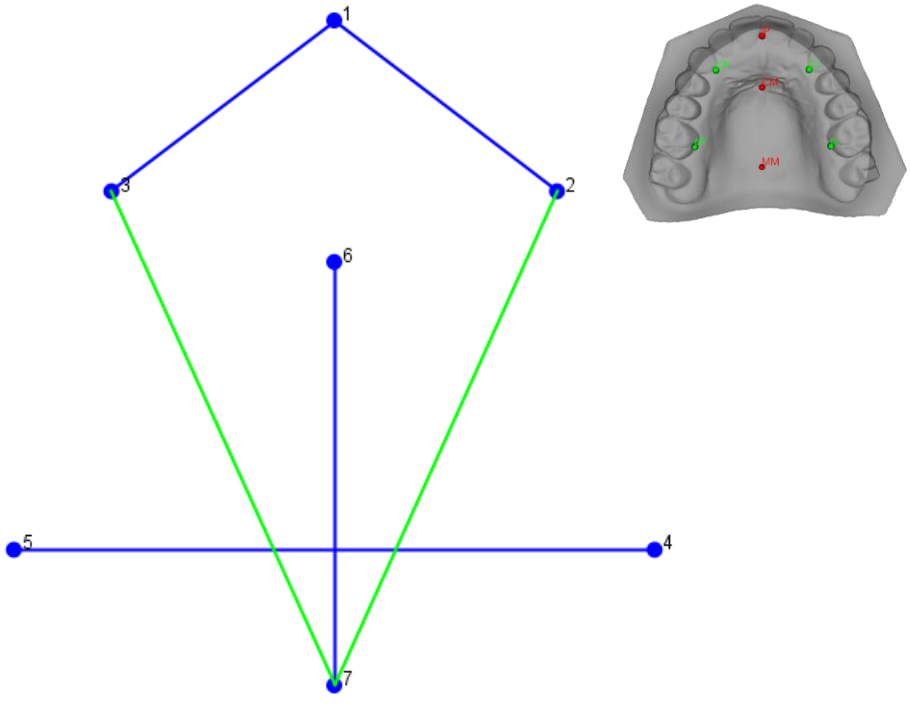

Figure 66 EDMA: Male vs. female Asian parent.

Distances = Green: Male < Female, Blue: Male > Female.

Table 31 Euclidean Distance Matrix Analysis: Euro male vs. female parent. (Figure 67)

	Distance		Difference	90% Confidence Interval	
1	Lmk1	Lmk6	-0.071	-0.093	-0.051
2	Lmk2	Lmk6	-0.054	-0.069	-0.037
3	Lmk3	Lmk6	-0.054	-0.072	-0.037
4	Lmk1	Lmk2	-0.013	-0.026	-0.002
5	Lmk1	Lmk3	-0.013	-0.025	-0.006
6	Lmk4	Lmk6	-0.009	-0.029	0.009
7	Lmk5	Lmk6	-0.009	-0.024	0.01
8	Lmk2	Lmk3	-0.004	-0.014	0.008
9	Lmk1	Lmk4	-0.003	-0.018	0.012
10	Lmk1	Lmk5	-0.003	-0.021	0.018
11	Lmk3	Lmk5	0.011	-0.002	0.027
12	Lmk2	Lmk4	0.011	-0.002	0.026
13	Lmk3	Lmk4	0.015	0.001	0.033
14	Lmk2	Lmk5	0.015	0.002	0.032
15	Lmk4	Lmk5	0.031	0.014	0.058
16	Lmk4	Lmk7	0.04	0.013	0.073
17	Lmk5	Lmk7	0.04	0.012	0.064
18	Lmk1	Lmk7	0.048	0.031	0.065
19	Lmk3	Lmk7	0.056	0.041	0.072
20	Lmk2	Lmk7	0.056	0.043	0.075
21	Lmk6	Lmk7	0.094	0.078	0.111

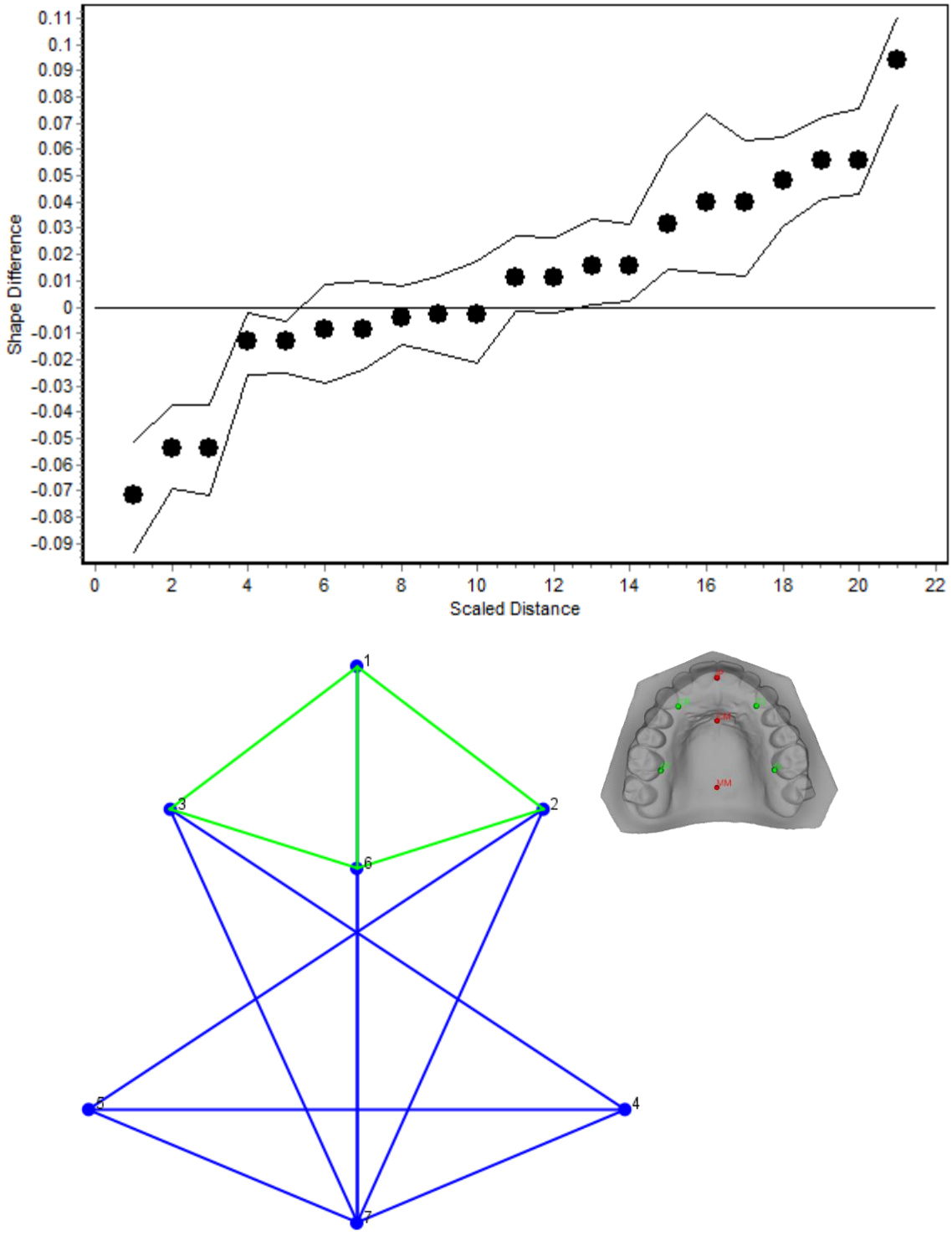

Figure 67 EDMA: Male vs. female Euro parent.

Distances = Green: Male < Female, Blue: Male > Female.

3.2.3 Aim 3: Effects of sex and ancestry on parent-control differences

3.2.3.1 Report of findings:

Parent-control differences in palate shape were only found among females when comparing mothers to female controls achieving baseline significance level or below ($p \leq .0093$) (Figures 73, 74, 81-84) (Tables 33, 36-38) but not among males ($p \geq .24$).

In addition, two patterns of ancestry-specific mother-control differences were detected. Asian mothers tended to have a wider ML dimension with a shorter AP dimension that was due to localized retrusion at the anterior palate ($p = .0005$). European mothers tended to have a more constricted palate with a narrower ML dimension and a higher anterior palatal vault ($p < .0001$). While less distinct (crossing only the baseline significance threshold), the differences between African mothers and controls followed the pattern shown in the Asian ancestry ($p = .0093$) (Figures 81-84) (Tables 36-38).

The alpha level for this aim was set as follows:

[b] Baseline Significance Level $p < .05$

* Corrected Significance Level $p < .0083$

3.2.3.2 General Contrast: Comparison by parent/control status (sexes and ancestries combined)

In the combined sample, parents had overall wider palates and shallower anterior palatal vault.

- Canonical Variate Analysis: (Figures 68 & 69)

Eigenvalues	% Variance	Cumulative %
0.017946	100	100

Procrustes distance (p-value) = 0.0085 (0.3459)

Mahalanobis distance (p-value) = 0.3739 (0.0322)[b]

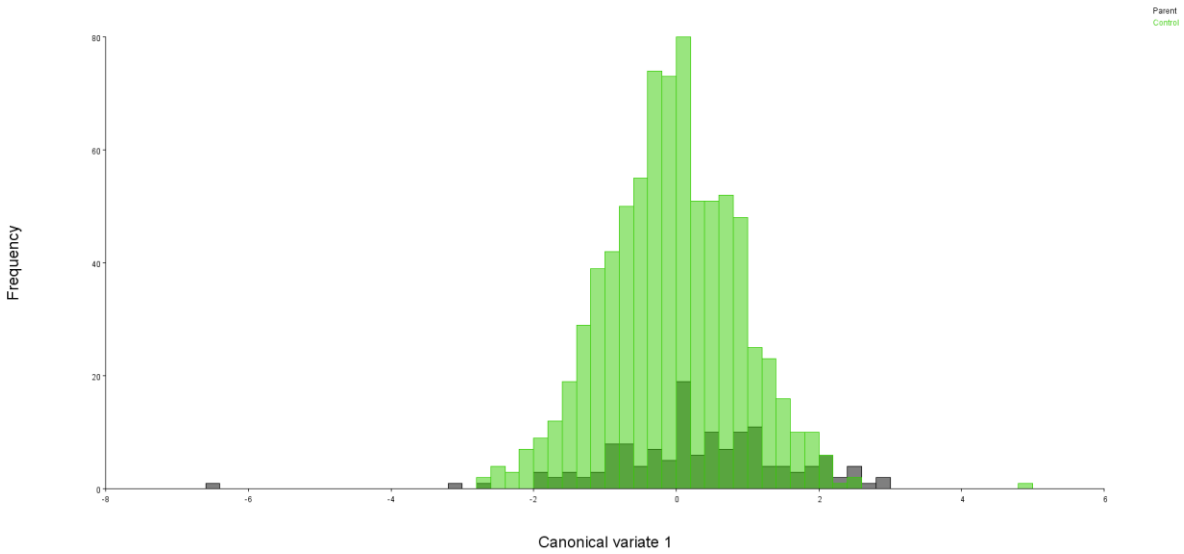

Figure 68 CVA of individual status (sexes and ancestries combined).

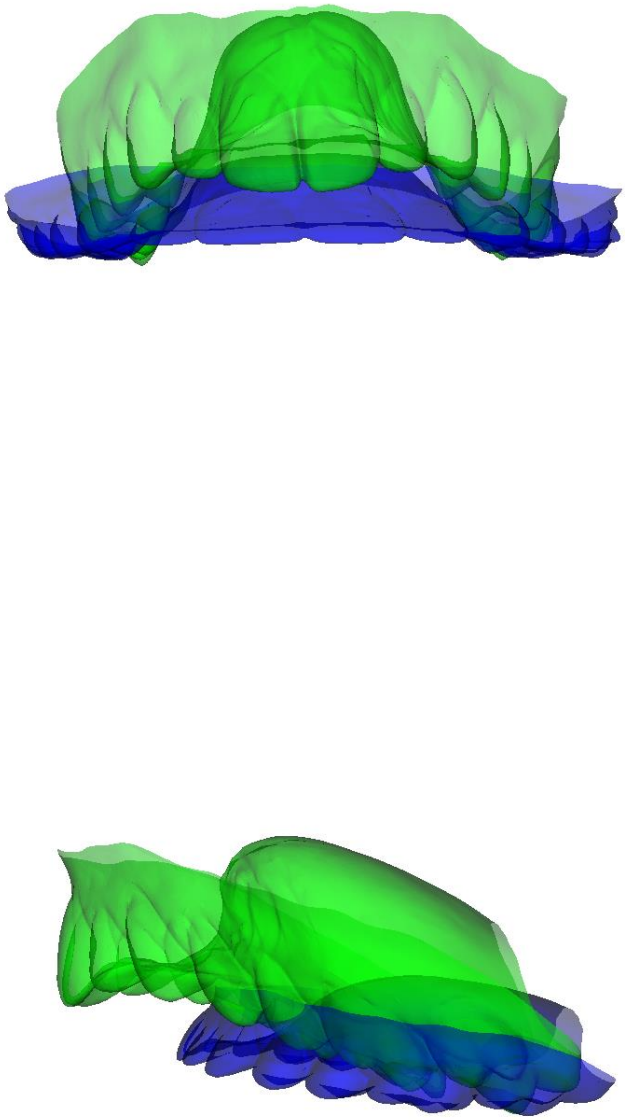

Figure 69 Canonical variate effects of individual status (sexes and ancestries combined).

Green = Negative (Control). Blue = Positive (Parent). Scale factor = 10.

Table 32 Euclidean Distance Matrix Analysis: Parent vs. control (sexes and ancestries combined). (Figure 70)

	Distance		Difference	90% Confidence Interval	
1	Lmk1	Lmk6	-0.016	-0.032	-0.001
2	Lmk1	Lmk5	-0.008	-0.016	0
3	Lmk1	Lmk4	-0.008	-0.016	0.001
4	Lmk1	Lmk7	-0.007	-0.017	0.002
5	Lmk1	Lmk3	-0.003	-0.01	0.004
6	Lmk1	Lmk2	-0.003	-0.01	0.004
7	Lmk5	Lmk7	0	-0.008	0.008
8	Lmk4	Lmk7	0	-0.008	0.008
9	Lmk5	Lmk6	0	-0.011	0.01
10	Lmk4	Lmk6	0	-0.011	0.012
11	Lmk3	Lmk5	0	-0.008	0.008
12	Lmk2	Lmk4	0	-0.008	0.007
13	Lmk3	Lmk6	0.004	-0.005	0.012
14	Lmk2	Lmk6	0.004	-0.005	0.012
15	Lmk4	Lmk5	0.005	-0.004	0.014
16	Lmk3	Lmk4	0.006	-0.002	0.014
17	Lmk2	Lmk5	0.006	-0.002	0.014
18	Lmk6	Lmk7	0.008	-0.003	0.018
19	Lmk3	Lmk7	0.008	0.002	0.014
20	Lmk2	Lmk7	0.008	0.003	0.015
21	Lmk2	Lmk3	0.01	0.005	0.015

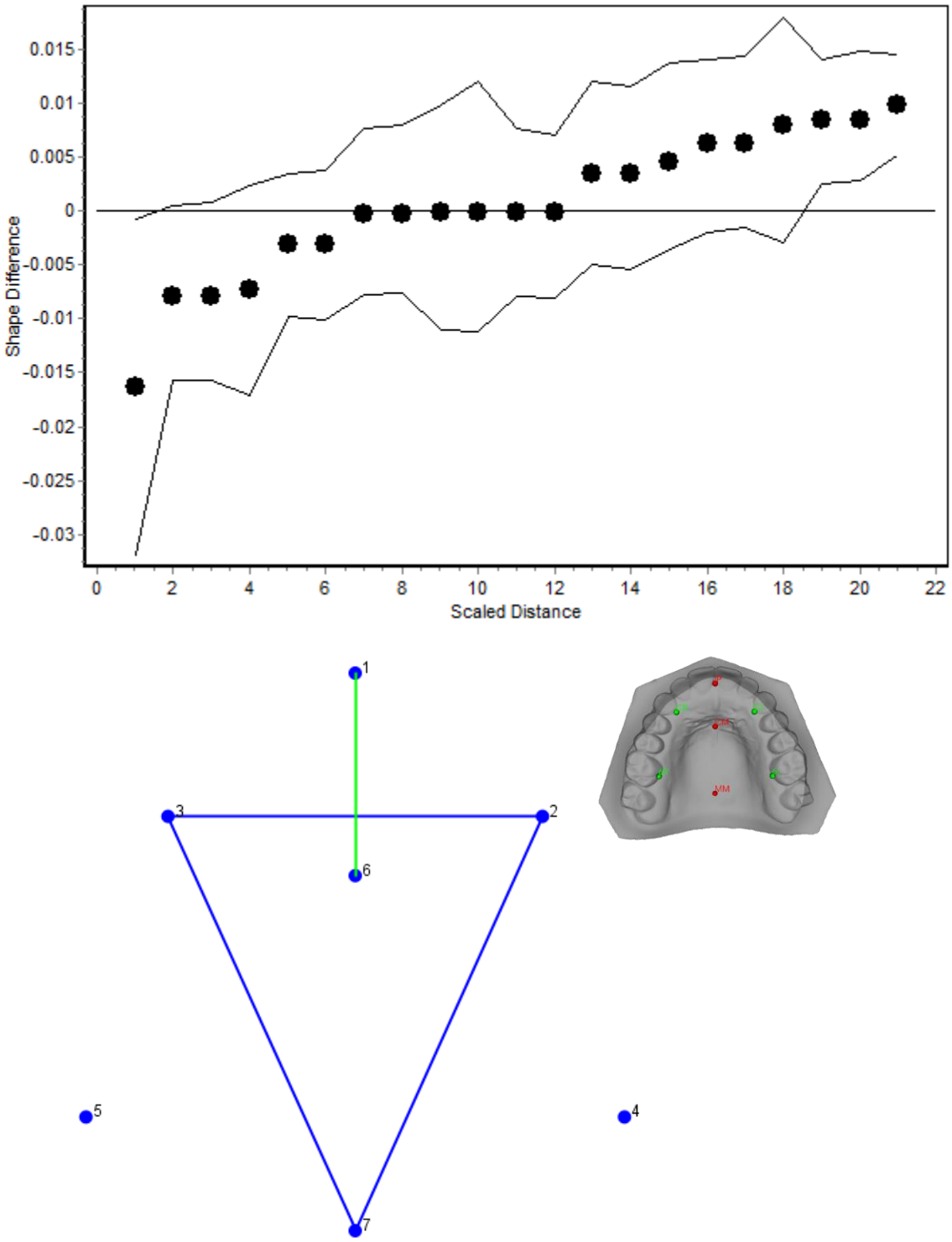

Figure 70 EDMA: Parent vs. control (sexes and ancestries combined).

Distances = Green: Parent < Control. Blue: Parent > Control.

3.2.3.3 Stratified Contrast 1: Comparison of males by parent/control status (ancestries combined)

No differences were found when comparing all fathers to all male controls.

- Canonical Variate Analysis: (Figure 71)

Eigenvalue	% Variance	Cumulative %
0.004479	100	100

Procrustes distance (p-value) = 0.0081 (0.8915)

Mahalanobis distance (p-value) = 0.2047 (0.9862)

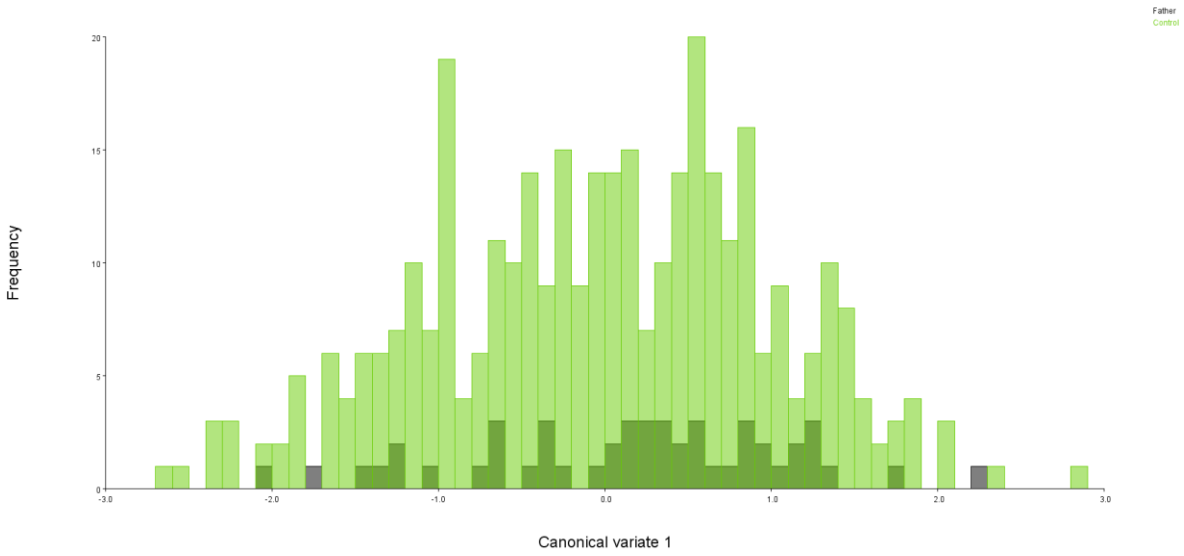

Figure 71 CVA of individual status in males (ancestries combined).

3.2.3.4 Stratified Contrast 2: Comparison of females by parent/control status (ancestries combined)

When comparing all mothers to all female controls, mothers had wider ML dimensions with more retruded anterior palates.

- Canonical Variate Analysis: (Figures 72 & 73)

Eigenvalues	% Variance	Cumulative %
0.059697	100	100

Procrustes distance (p-value) = 0.0157 (0.0352)[b]

Mahalanobis distance (p-value) = 0.6439 (0.0001)*

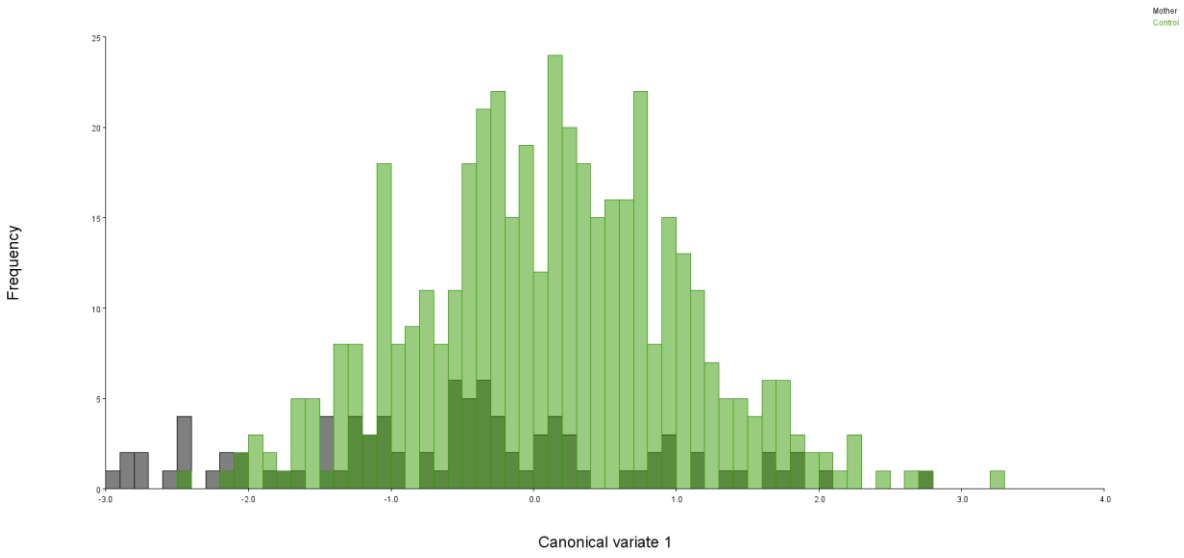

Figure 72 CVA of individual status in females (ancestries combined).

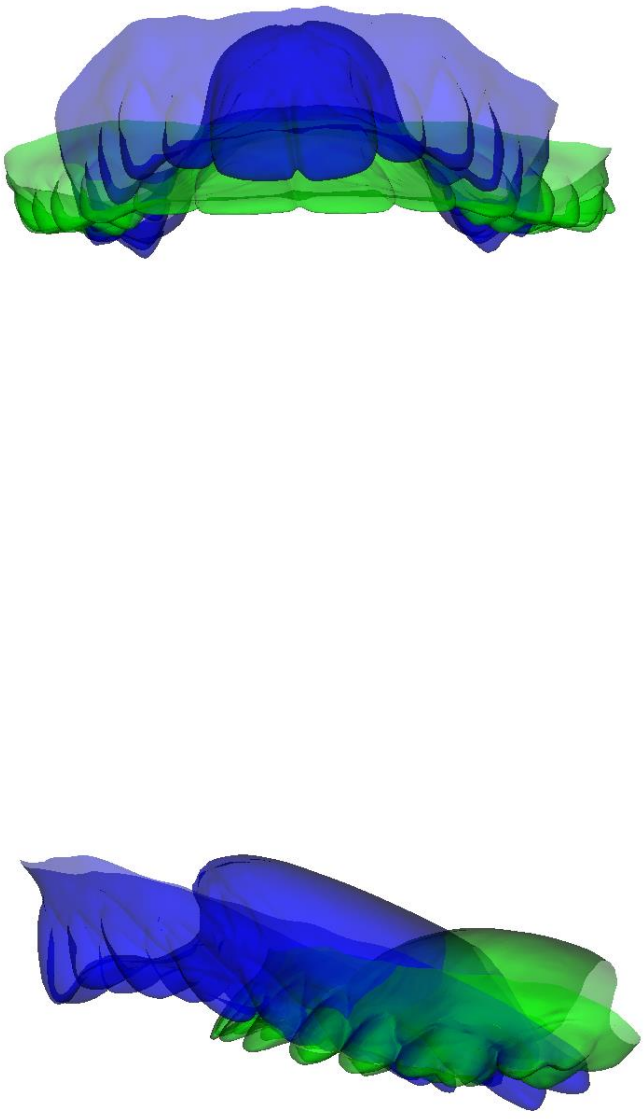

Figure 73 Canonical variate effect of individual status in females (ancestries combined).

Green = Negative (Mother). Blue = Positive (Control). Scale factor = 10

Table 33 Euclidean Distance Matrix Analysis: Parent vs. control female (ancestries combined). (Figure 74)

	Distance		Difference	90% Confidence Interval	
1	Lmk1	Lmk6	-0.02	-0.032	-0.008
2	Lmk1	Lmk4	-0.017	-0.026	-0.009
3	Lmk1	Lmk5	-0.017	-0.024	-0.01
4	Lmk1	Lmk2	-0.008	-0.015	-0.002
5	Lmk1	Lmk3	-0.008	-0.014	-0.002
6	Lmk1	Lmk7	-0.008	-0.017	0.001
7	Lmk4	Lmk6	-0.006	-0.015	0.003
8	Lmk5	Lmk6	-0.006	-0.016	0.004
9	Lmk3	Lmk5	-0.002	-0.009	0.004
10	Lmk2	Lmk4	-0.002	-0.008	0.004
11	Lmk3	Lmk6	0.004	-0.004	0.012
12	Lmk2	Lmk6	0.004	-0.005	0.012
13	Lmk6	Lmk7	0.009	-0.001	0.019
14	Lmk3	Lmk4	0.009	0.002	0.017
15	Lmk2	Lmk5	0.009	0.002	0.017
16	Lmk4	Lmk7	0.01	0.001	0.017
17	Lmk5	Lmk7	0.01	0.001	0.019
18	Lmk2	Lmk3	0.012	0.008	0.017
19	Lmk4	Lmk5	0.014	0.005	0.024
20	Lmk3	Lmk7	0.018	0.011	0.025
21	Lmk2	Lmk7	0.018	0.011	0.024

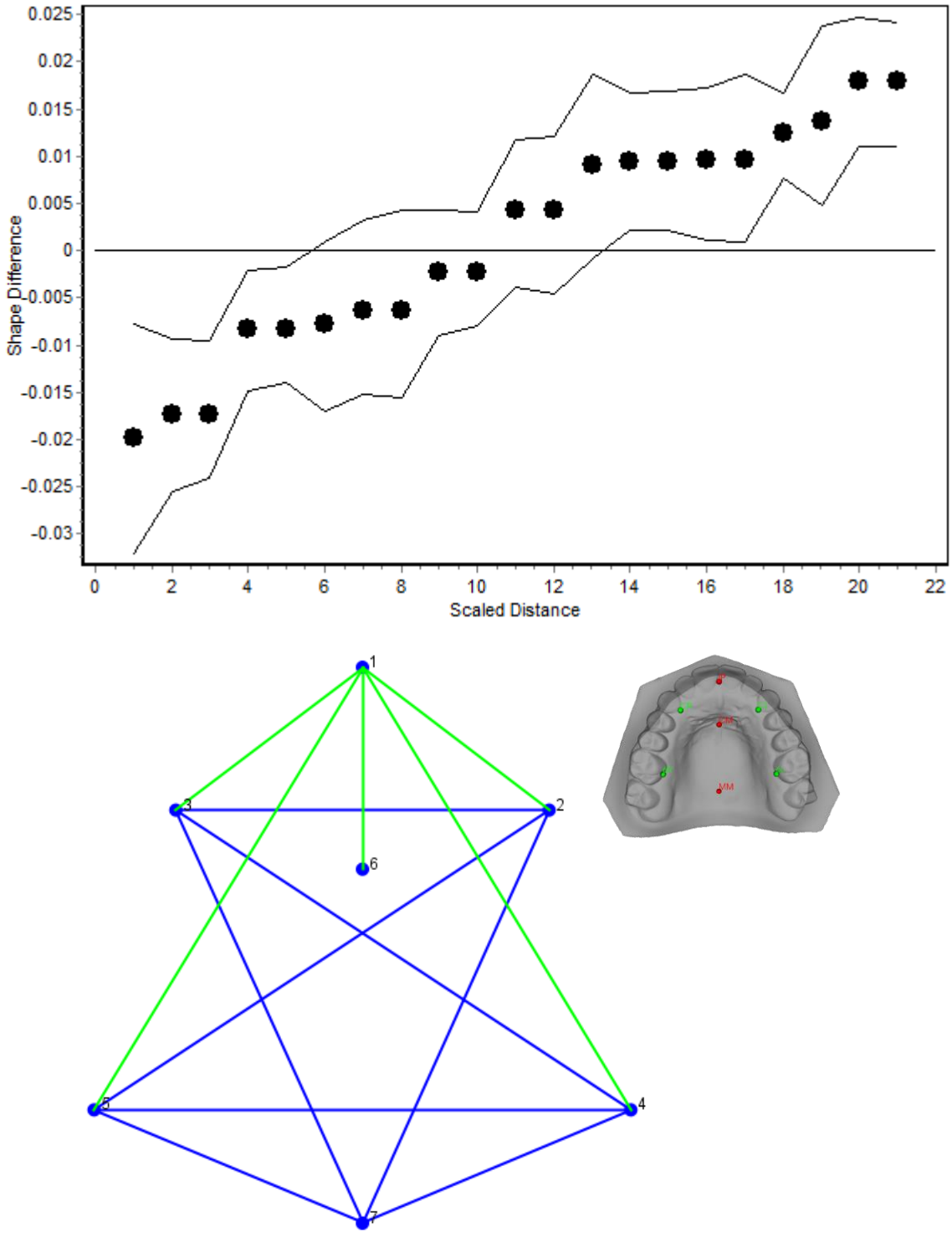

Figure 74 EDMA: Parent vs. control female (ancestries combined).

Distances = Green: Parent < Control, Blue: Parent > Control.

3.2.3.5 Stratified Contrast 3: Comparison by parent/control status within ancestries (sexes combined)

When comparing all parents to all controls within ancestries, no differences were detected among Africans. In Asians, parents were found to have shorter AP dimensions and wider ML dimensions than controls. In Europeans, parents were found to have narrower palates with higher anterior palatal vaults.

- Canonical Variates Analysis: (Figures 75 & 76)

Race	Eigenvalue	% Variance	Cumulative %
Asian	0.157549	100	100
African	0.017001	100	100
Euro	0.049814	100	100

Race	Procrustes distance (p-value)	Mahalanobis distance (p-value)
Asian	0.016 (0.4304)	0.7941 (0.0120)[b]
African	0.0104 (0.6753)	0.3901 (0.6874)
Euro	0.0153 (0.3089)	0.7668 (0.0025)*

Asian

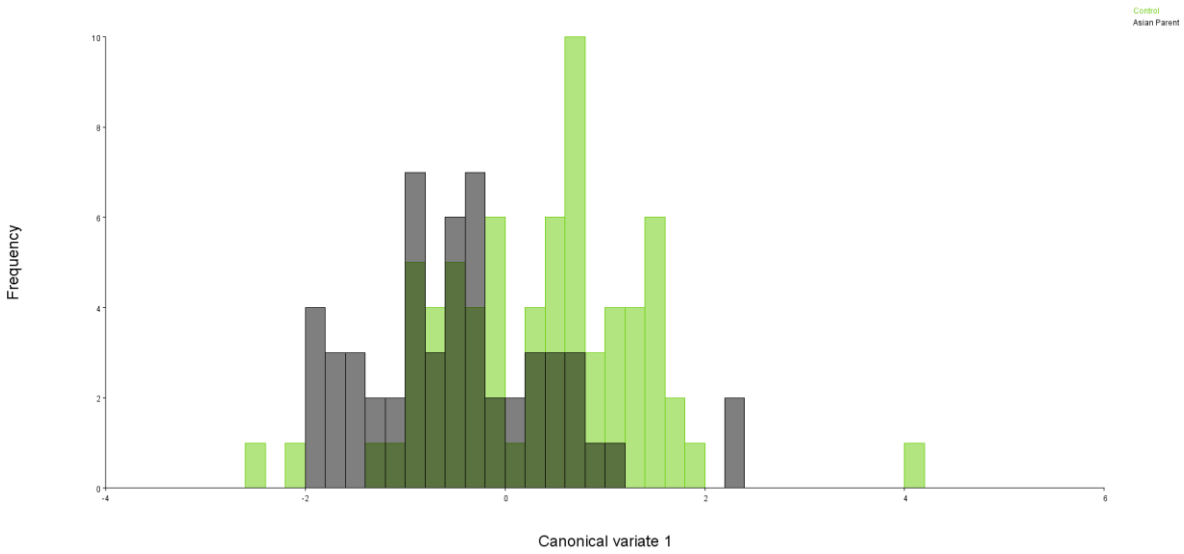

African

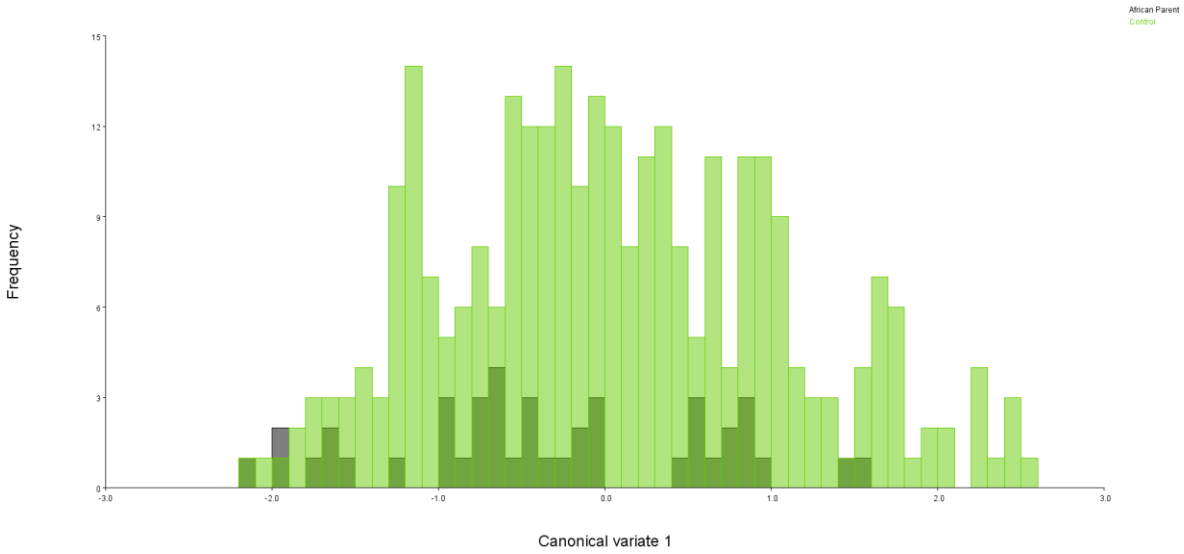

Euro

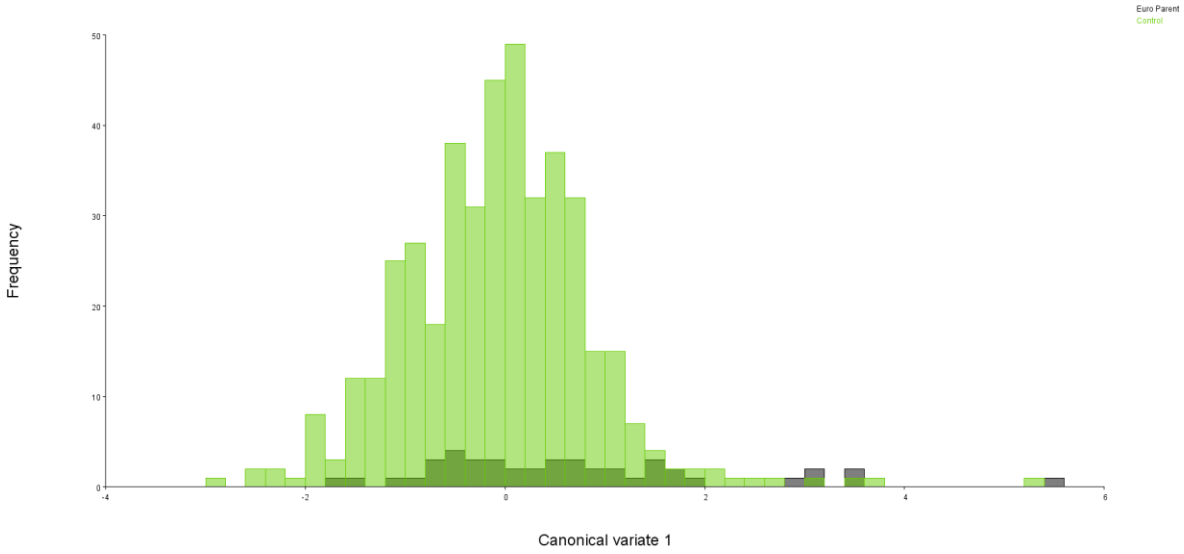

Figure 75 CVA of individual status within ancestries (sexes combined).

Asian

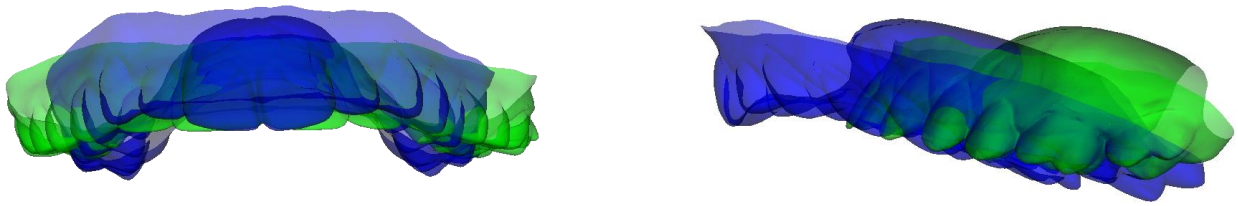

Euro

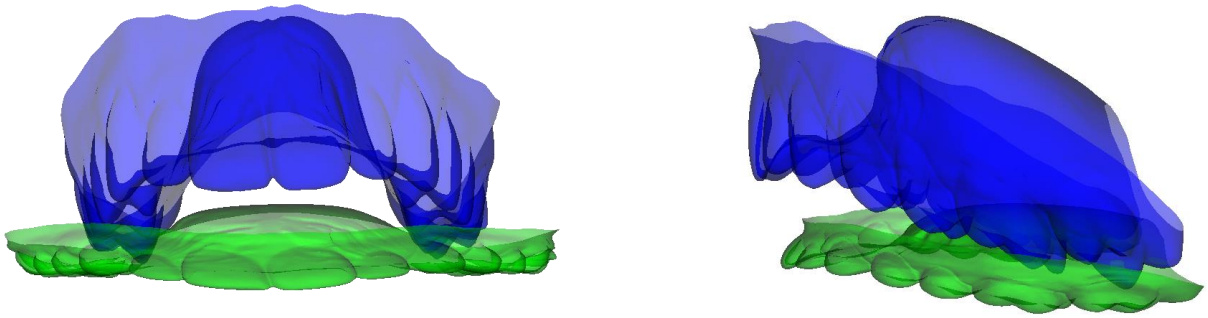

Figure 76 Canonical variate effects of individual status within ancestries (sexes combined).

Green = Negative. Blue = Positive. Scale factor = 10.

Asian: Green = Parent, Blue = Control.

Euro: Blue = Parent, Green = Control.

Table 34 Euclidean Distance Matrix Analysis: Asian parent vs. control (sexes combined). (Figure 77)

	Distance		Difference	90% Confidence Interval	
1	Lmk1	Lmk6	-0.03	-0.049	-0.01
2	Lmk1	Lmk5	-0.016	-0.031	-0.006
3	Lmk1	Lmk4	-0.016	-0.027	-0.004
4	Lmk3	Lmk5	-0.013	-0.024	-0.002
5	Lmk2	Lmk4	-0.013	-0.023	-0.004
6	Lmk1	Lmk7	-0.009	-0.022	0.003
7	Lmk5	Lmk6	-0.001	-0.015	0.013
8	Lmk4	Lmk6	-0.001	-0.016	0.012
9	Lmk1	Lmk3	-0.001	-0.011	0.008
10	Lmk1	Lmk2	-0.001	-0.011	0.01
11	Lmk3	Lmk4	0.004	-0.008	0.015
12	Lmk2	Lmk5	0.004	-0.009	0.014
13	Lmk3	Lmk6	0.007	-0.007	0.023
14	Lmk2	Lmk6	0.007	-0.008	0.019
15	Lmk5	Lmk7	0.012	-0.003	0.028
16	Lmk4	Lmk7	0.012	-0.003	0.027
17	Lmk2	Lmk3	0.012	0.005	0.019
18	Lmk3	Lmk7	0.016	0.007	0.026
19	Lmk2	Lmk7	0.016	0.006	0.024
20	Lmk4	Lmk5	0.016	0.002	0.027
21	Lmk6	Lmk7	0.018	0.005	0.032

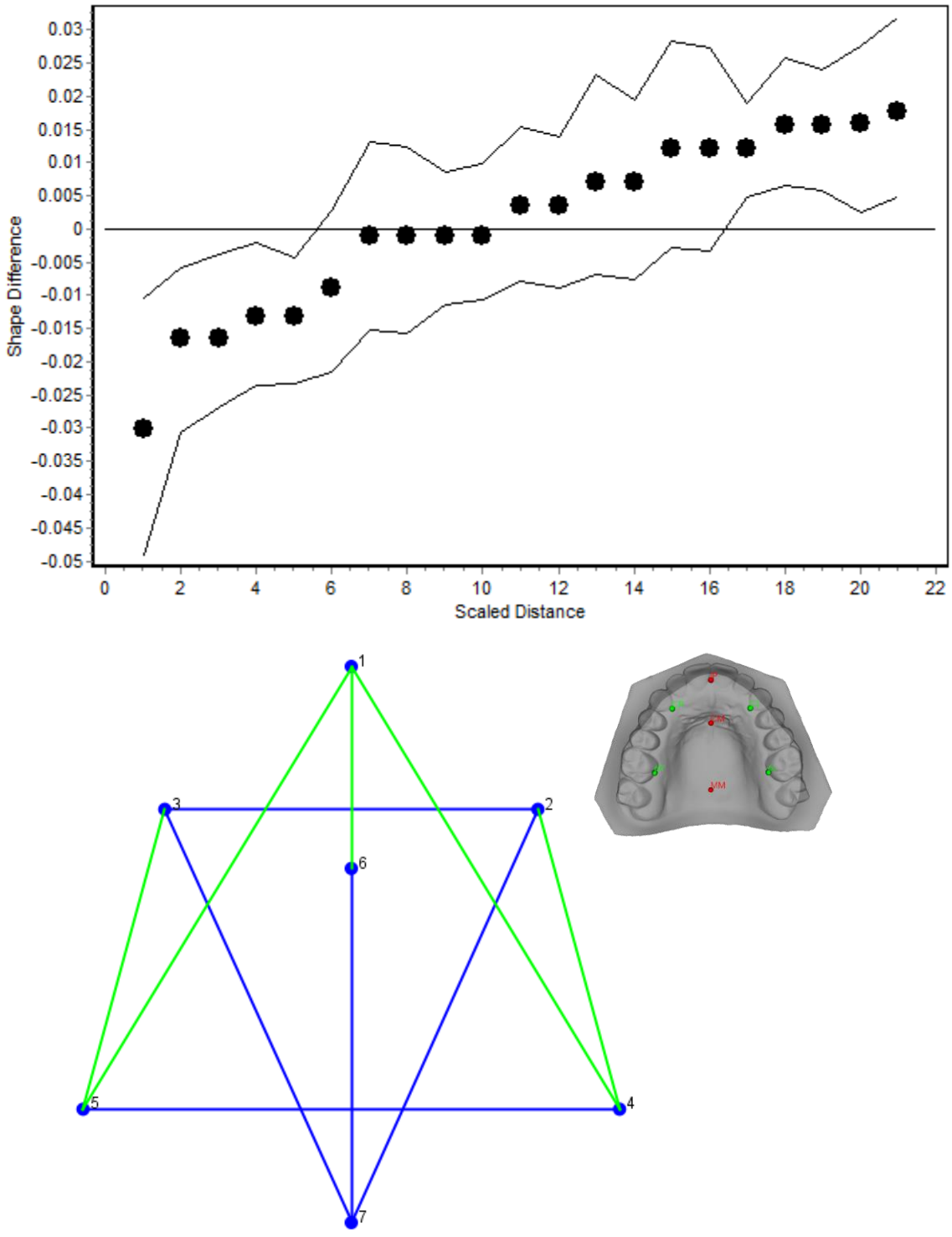

Figure 77 EDMA: Asian parent vs. control (sexes combined).

Distances = Green: Parent < Control, Blue: Parent > Control.

Table 35 Euclidean Distance Matrix Analysis: Euro parent vs. control (sexes combined). (Figure 78)

	Distance		Difference	90% Confidence Interval	
1	Lmk4	Lmk5	-0.028	-0.043	-0.012
2	Lmk6	Lmk7	-0.014	-0.029	0.001
3	Lmk4	Lmk7	-0.008	-0.021	0.007
4	Lmk5	Lmk7	-0.008	-0.021	0.008
5	Lmk1	Lmk7	-0.007	-0.022	0.008
6	Lmk2	Lmk5	-0.007	-0.019	0.004
7	Lmk3	Lmk4	-0.007	-0.019	0.003
8	Lmk2	Lmk7	-0.002	-0.011	0.007
9	Lmk3	Lmk7	-0.002	-0.011	0.008
10	Lmk1	Lmk3	-0.001	-0.01	0.007
11	Lmk1	Lmk2	-0.001	-0.009	0.008
12	Lmk1	Lmk4	-0.001	-0.012	0.01
13	Lmk1	Lmk5	-0.001	-0.011	0.009
14	Lmk2	Lmk3	0	-0.007	0.006
15	Lmk5	Lmk6	0.001	-0.014	0.014
16	Lmk4	Lmk6	0.001	-0.014	0.015
17	Lmk2	Lmk4	0.004	-0.007	0.012
18	Lmk3	Lmk5	0.004	-0.007	0.013
19	Lmk1	Lmk6	0.011	-0.005	0.03
20	Lmk3	Lmk6	0.012	0.002	0.024
21	Lmk2	Lmk6	0.012	0.001	0.025

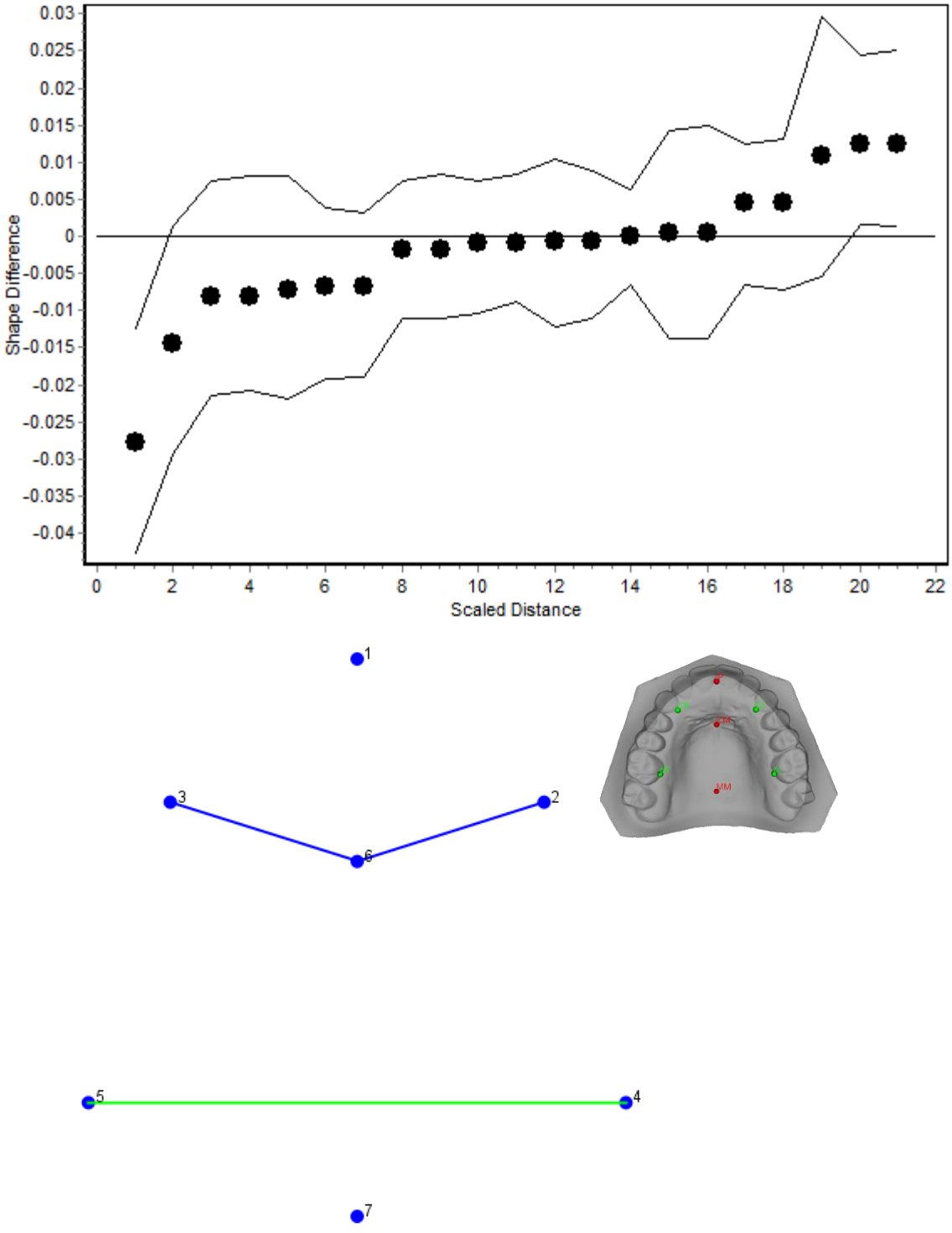

Figure 78 EDMA: Euro parent vs control (sexes combined).

Distance = Green: Parent < Control, Blue: Parent > Control.

3.2.3.6 Stratified Contrast 4: Comparison of males by parent/control status within ancestries

Within ancestries, no differences were detected among fathers and male controls.

- Canonical Variates Analysis: (Figure 79)

Race	Eigenvalue	% Variance	Cumulative %
Asian	0.058749	100	100
African	0.031803	100	100
Euro	0.06073	100	100

Race	Procrustes distance (p-value)	Mahalanobis distance (p-value)
Asian	0.0163 (0.8958)	0.52 (0.9198)
African	0.0188 (0.6825)	0.6671 (0.7115)
Euro	0.0159 (0.7183)	0.8066 (0.2399)

Asian

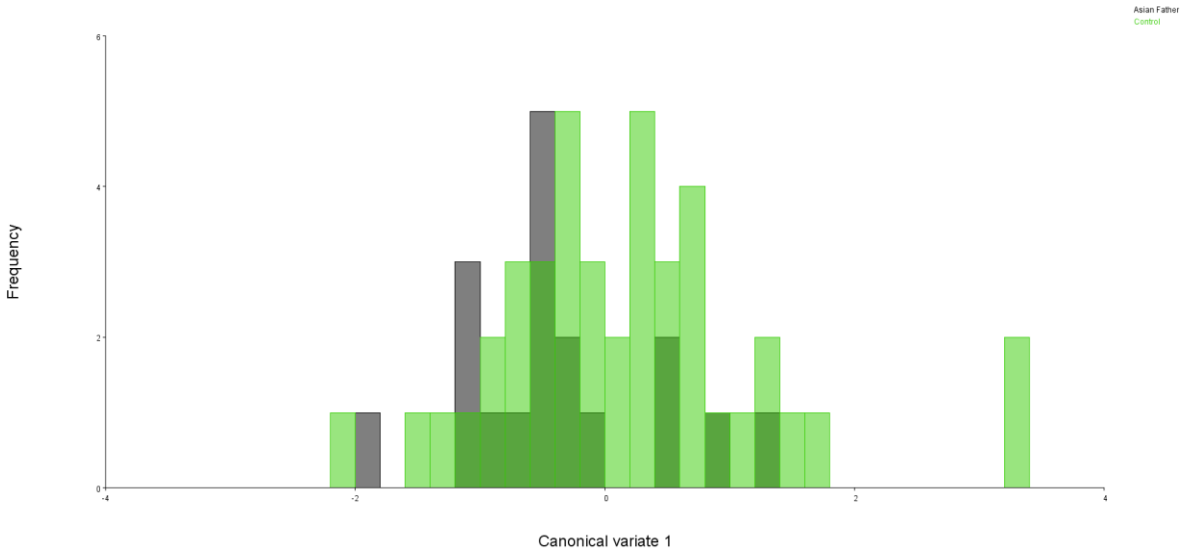

African

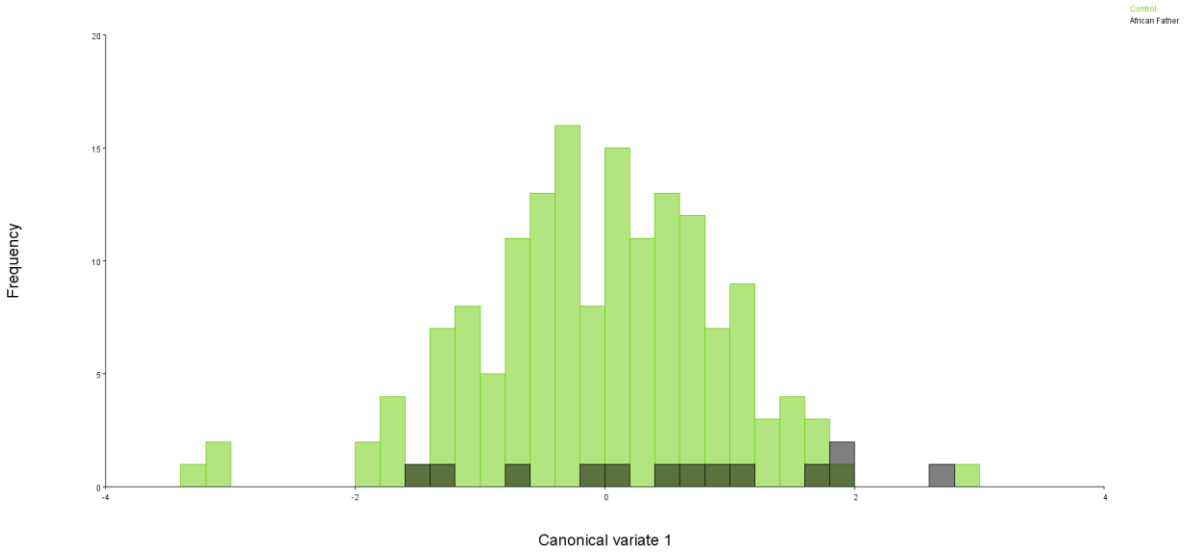

Euro

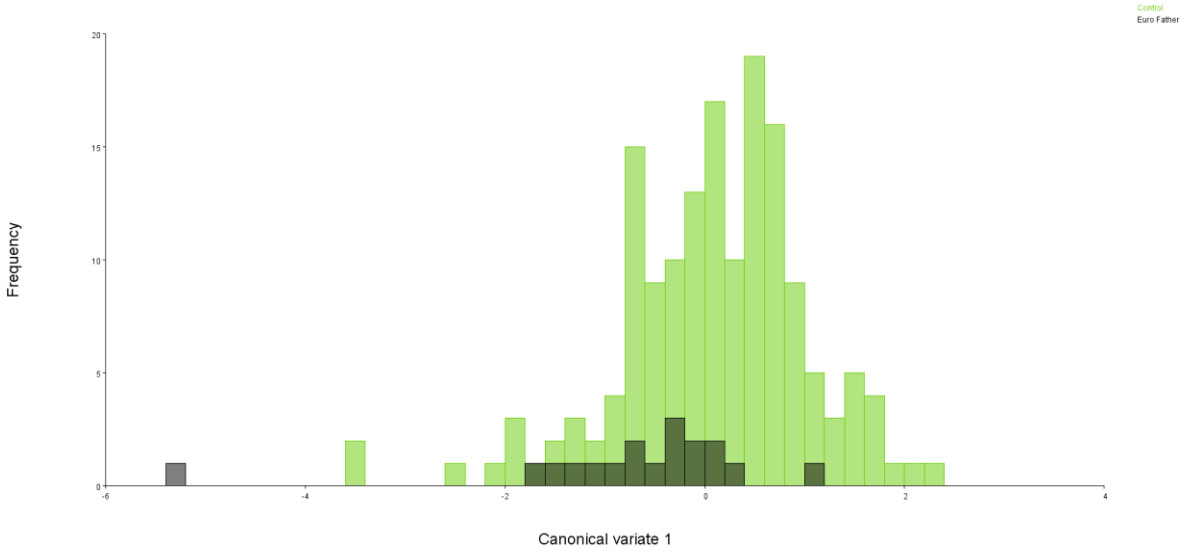

Figure 79 CVA of individual status in males within ancestries.

3.2.3.7 Stratified Contrast 5: Comparison of females by parent/control status within ethnicities

Within ancestries, Asians and Africans had similar patterns of mother-control differences, apart from Europeans. In Asians and Africans, mothers had wider ML dimensions, more retruded anterior palates and higher posterior palatal vaults than female controls. In Europeans, mothers had narrower palates and higher anterior palatal vaults than female controls.

- Canonical Variates Analysis: (Figures 80 & 81)

Race	Eigenvalue	% Variance	Cumulative %
Asian	0.546115	100	100
African	0.119099	100	100
Euro	0.091291	100	100

Race	Procrustes distance (p-value)	Mahalanobis distance (p-value)
Asian	0.0346 (0.0186)[b]	1.4662 (<.0001)*
African	0.0254 (0.0287)[b]	0.8957 (0.0093)[b]
Euro	0.025 (0.1062)	1.0671 (0.0005)*

Asian

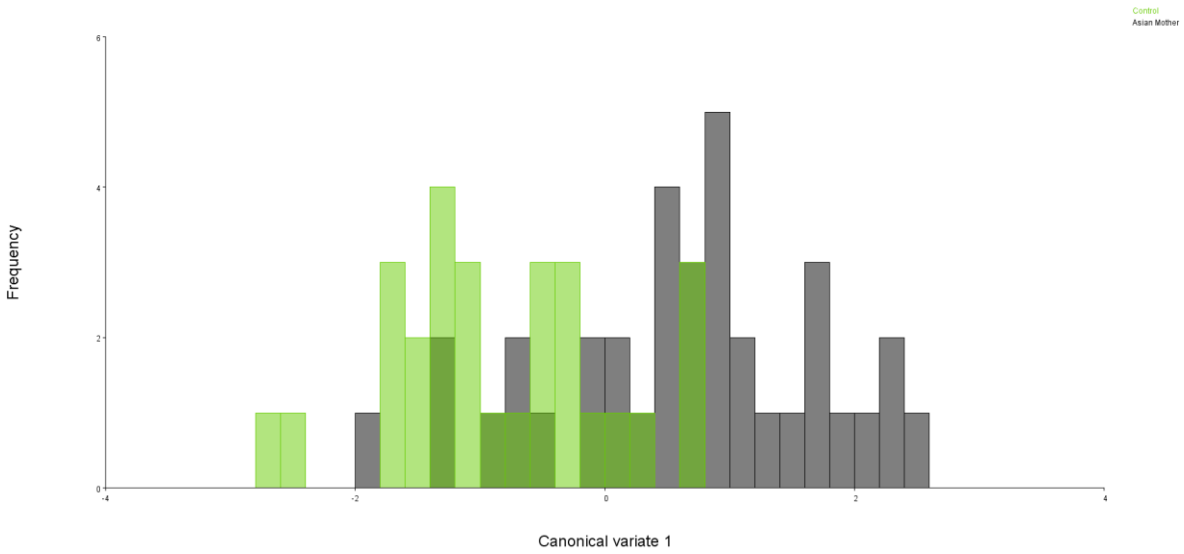

African

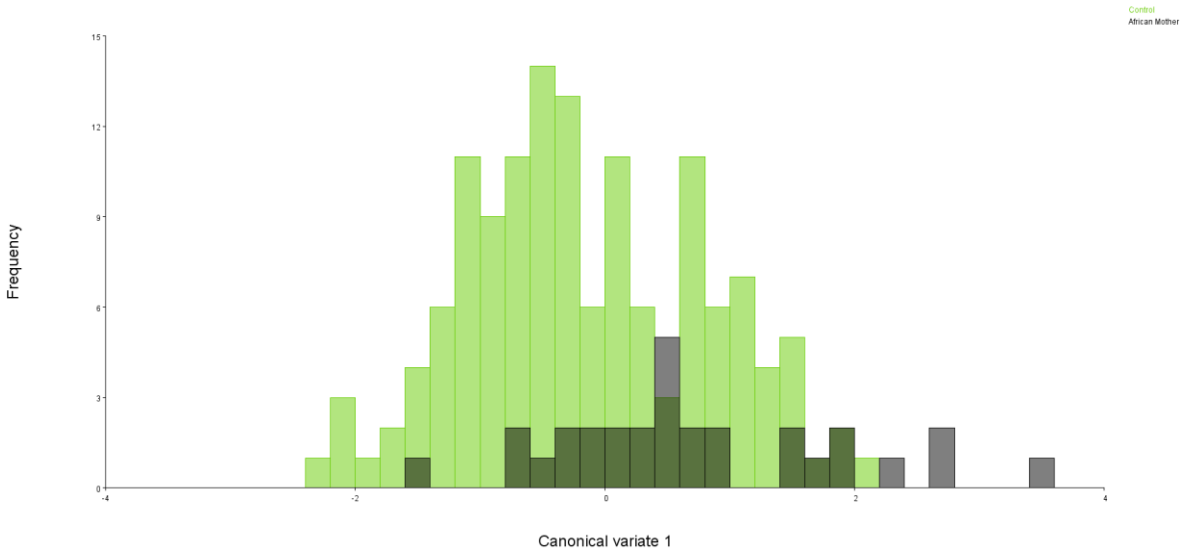

Euro

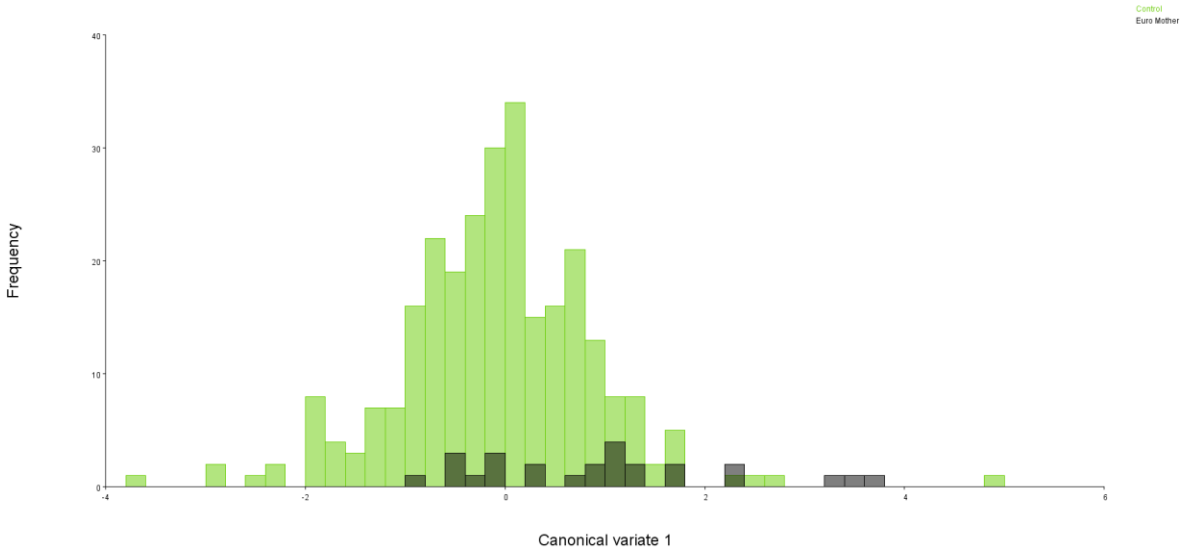

Figure 80 CVA of individual status in females within ethnicities.

Asian

African

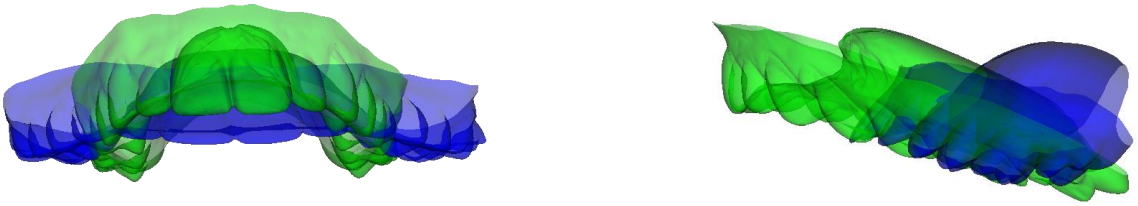

Euro

Figure 81 Canonical variate effects of individual status in females within ancestries.

Green = Negative (Control). Blue = Positive (Parent). Scale factor = 10.

Table 36 Euclidean Distance Matrix Analysis: Asian mother vs. control. (Figure 82)

	Distance		Difference	90% Confidence Interval	
1	Lmk1	Lmk6	-0.066	-0.078	-0.054
2	Lmk1	Lmk4	-0.031	-0.037	-0.024
3	Lmk1	Lmk5	-0.031	-0.036	-0.022
4	Lmk1	Lmk7	-0.019	-0.03	-0.01
5	Lmk1	Lmk3	-0.016	-0.022	-0.009
6	Lmk1	Lmk2	-0.016	-0.024	-0.009
7	Lmk2	Lmk4	-0.005	-0.013	0
8	Lmk3	Lmk5	-0.005	-0.011	0.001
9	Lmk2	Lmk6	-0.005	-0.015	0.004
10	Lmk3	Lmk6	-0.005	-0.013	0.003
11	Lmk5	Lmk6	0.005	-0.004	0.013
12	Lmk4	Lmk6	0.005	-0.004	0.015
13	Lmk2	Lmk3	0.019	0.014	0.025
14	Lmk2	Lmk5	0.021	0.014	0.029
15	Lmk3	Lmk4	0.021	0.015	0.028
16	Lmk2	Lmk7	0.031	0.02	0.039
17	Lmk3	Lmk7	0.031	0.022	0.039
18	Lmk5	Lmk7	0.035	0.024	0.044
19	Lmk4	Lmk7	0.035	0.024	0.046
20	Lmk6	Lmk7	0.037	0.026	0.048
21	Lmk4	Lmk5	0.043	0.035	0.053

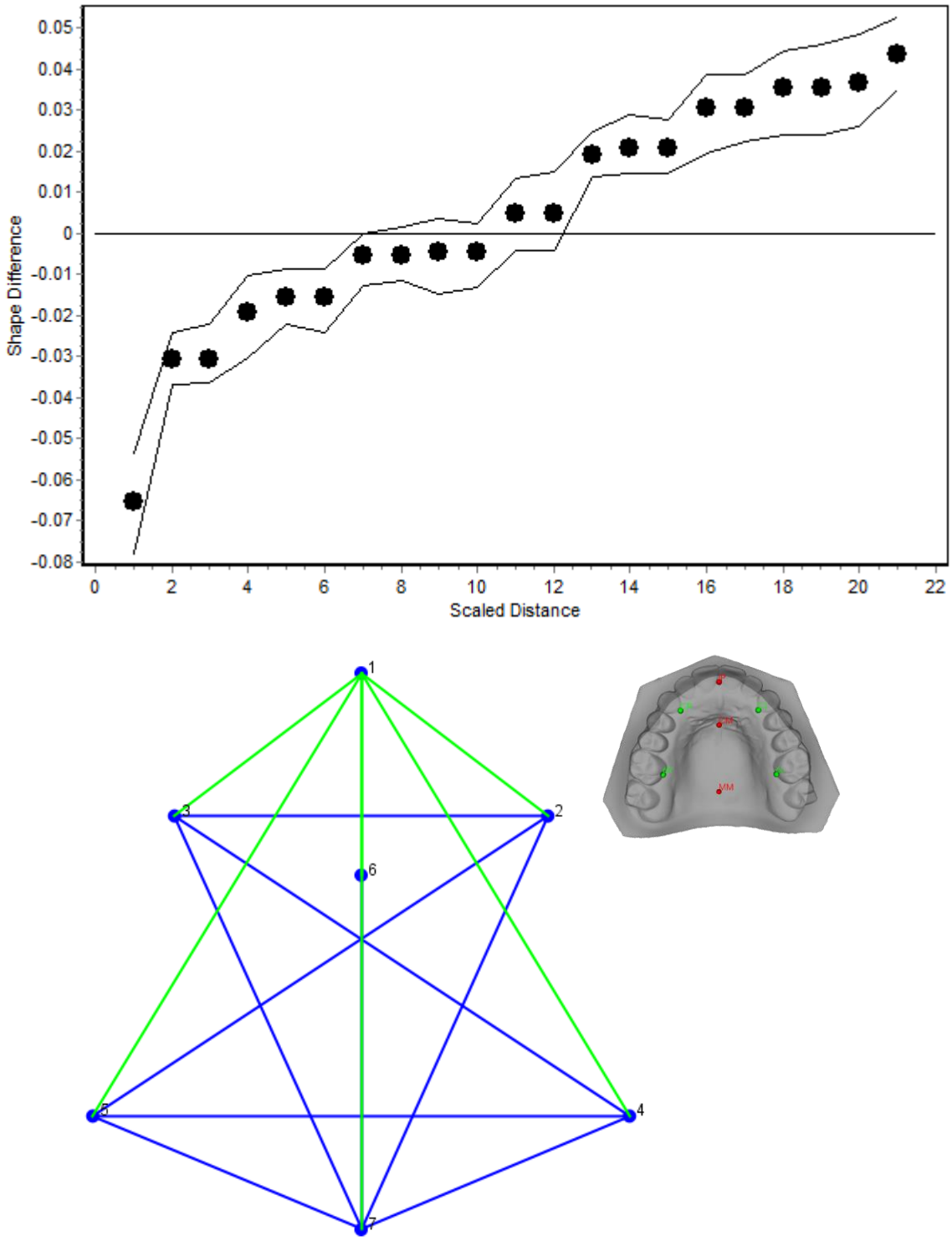

Figure 82 EDMA: Asian mother vs. control.

Distance = Green: Mother < Control, Blue: Mother > Control.

Table 37 Euclidean Distance Matrix Analysis: African mother vs. control. (Figure 83)

	Distance		Difference	90% Confidence Interval	
1	Lmk1	Lmk6	-0.022	-0.047	0
2	Lmk1	Lmk5	-0.02	-0.035	-0.006
3	Lmk1	Lmk4	-0.02	-0.034	-0.004
4	Lmk3	Lmk5	-0.01	-0.024	0.007
5	Lmk2	Lmk4	-0.01	-0.024	0.004
6	Lmk1	Lmk3	-0.009	-0.022	0
7	Lmk1	Lmk2	-0.009	-0.021	0.001
8	Lmk3	Lmk6	-0.007	-0.023	0.006
9	Lmk2	Lmk6	-0.007	-0.025	0.007
10	Lmk1	Lmk7	-0.006	-0.024	0.01
11	Lmk5	Lmk6	-0.005	-0.027	0.013
12	Lmk4	Lmk6	-0.005	-0.028	0.018
13	Lmk2	Lmk3	0.009	0.001	0.02
14	Lmk6	Lmk7	0.01	-0.006	0.031
15	Lmk3	Lmk4	0.012	-0.003	0.028
16	Lmk2	Lmk5	0.012	-0.003	0.027
17	Lmk3	Lmk7	0.014	0.003	0.026
18	Lmk2	Lmk7	0.014	0.001	0.027
19	Lmk5	Lmk7	0.033	0.018	0.049
20	Lmk4	Lmk7	0.033	0.015	0.054
21	Lmk4	Lmk5	0.04	0.025	0.056

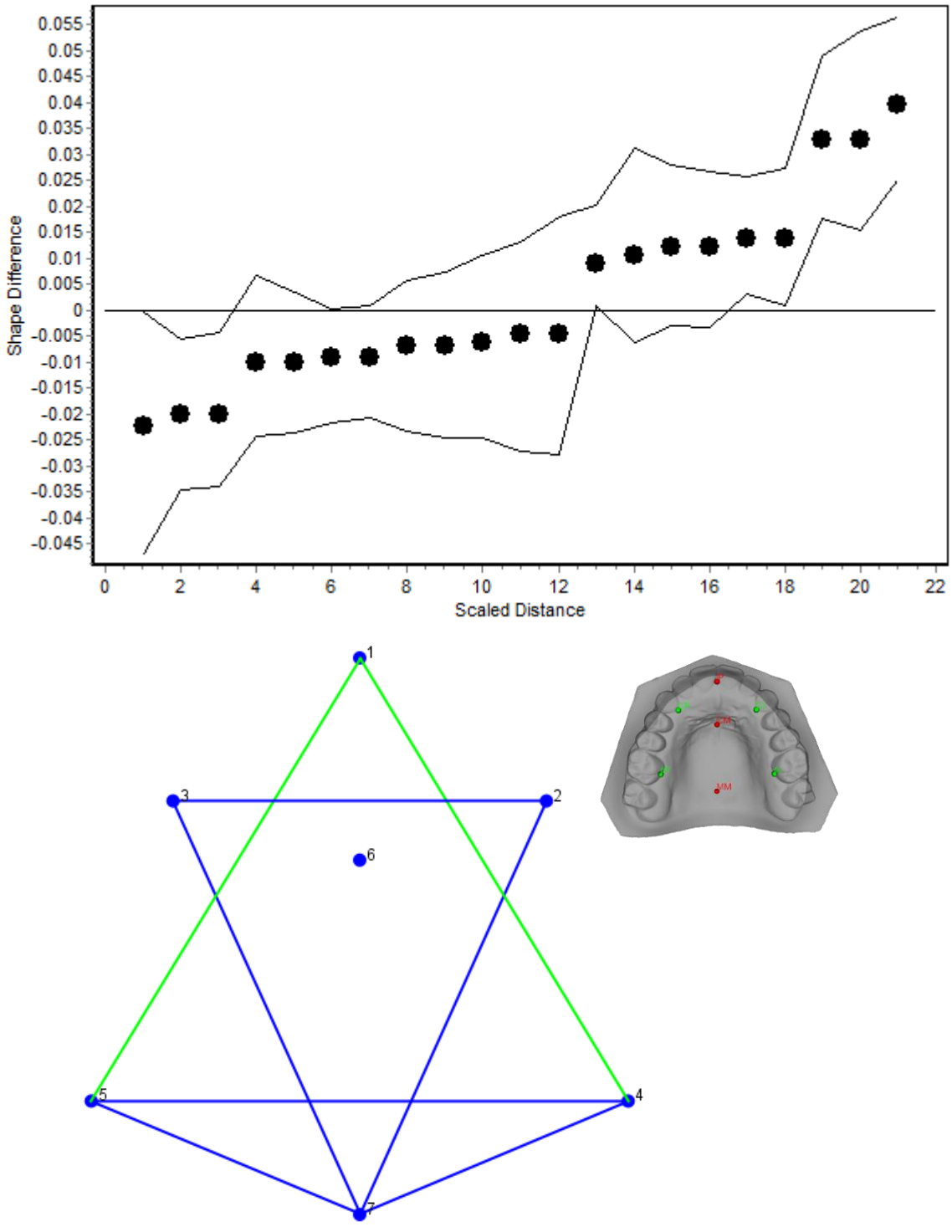

Figure 83 EDMA: African mother vs. control.

Distance = Green: Mother < Control, Blue: Mother > Control.

Table 38 Euclidean Distance Matrix Analysis: Euro mother vs. control. (Figure 84)

	Distance		Difference	90% Confidence Interval	
1	Lmk6	Lmk7	-0.035	-0.052	-0.02
2	Lmk4	Lmk5	-0.03	-0.049	-0.011
3	Lmk2	Lmk7	-0.017	-0.028	-0.007
4	Lmk3	Lmk7	-0.017	-0.026	-0.006
5	Lmk1	Lmk7	-0.017	-0.033	-0.003
6	Lmk4	Lmk7	-0.014	-0.028	0
7	Lmk5	Lmk7	-0.014	-0.027	0.001
8	Lmk2	Lmk5	-0.01	-0.025	0.005
9	Lmk3	Lmk4	-0.01	-0.022	0.006
10	Lmk2	Lmk3	-0.003	-0.01	0.005
11	Lmk1	Lmk3	0.002	-0.011	0.014
12	Lmk1	Lmk2	0.002	-0.01	0.015
13	Lmk1	Lmk5	0.002	-0.011	0.016
14	Lmk1	Lmk4	0.002	-0.012	0.018
15	Lmk2	Lmk4	0.003	-0.009	0.016
16	Lmk3	Lmk5	0.003	-0.009	0.015
17	Lmk5	Lmk6	0.004	-0.012	0.027
18	Lmk4	Lmk6	0.004	-0.013	0.021
19	Lmk3	Lmk6	0.022	0.007	0.038
20	Lmk2	Lmk6	0.022	0.006	0.038
21	Lmk1	Lmk6	0.029	0.005	0.052

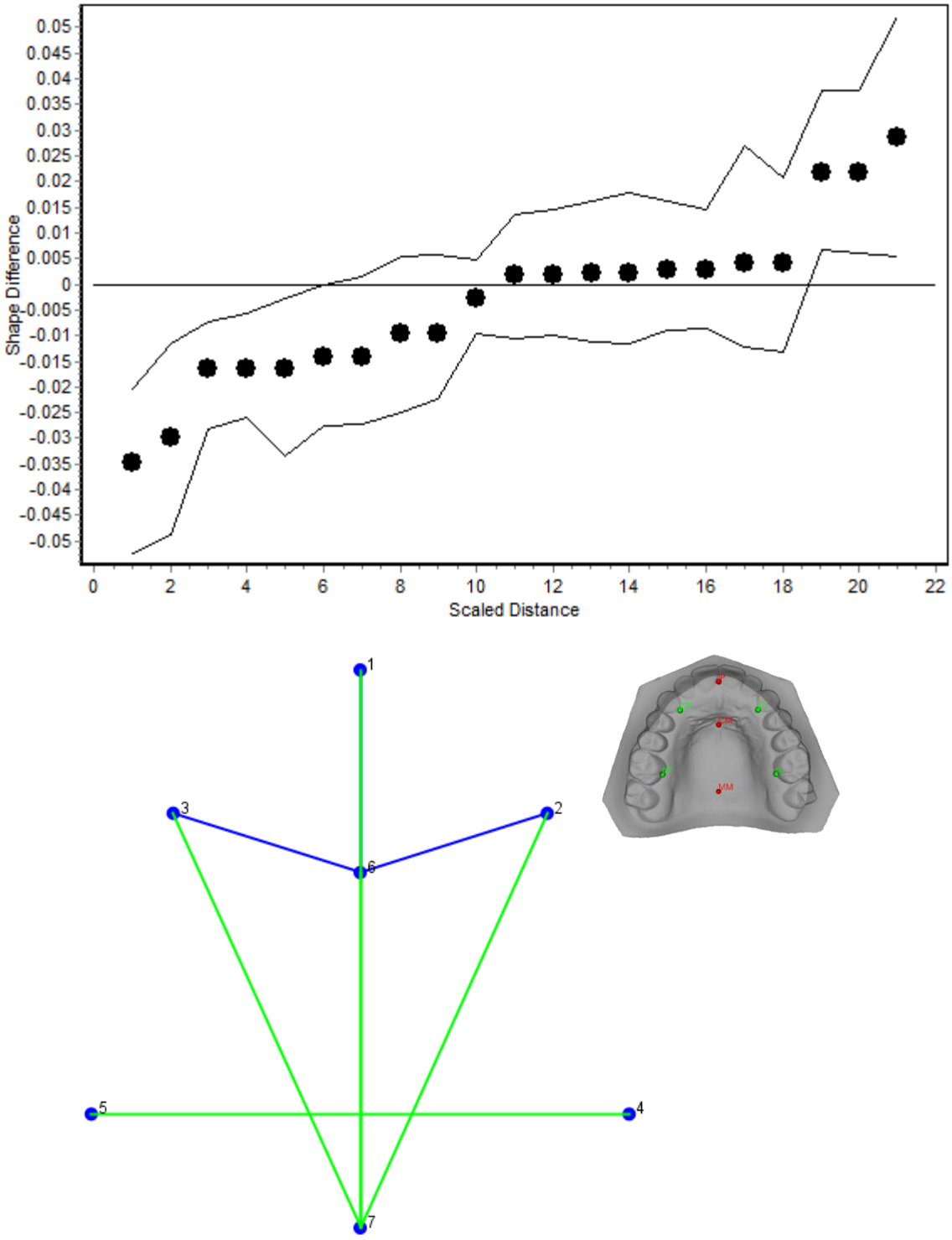

Figure 84 EDMA: Euro mother vs. control.

Distances = Green: Mother < Control, Blue: Mother > Control.

3.3 Summary of Results

Table 39 Summary of findings from all group contrasts.

p-value is from 10000 permutation test for Mahalanobis distance among groups.

[b] = Significant at the baseline alpha level. * = Significant at the corrected alpha level.

Aim	Contrast	Testing method	p-value	Description of shape difference
I	Comparison by sex in controls (ancestries combined)	PCA, CVA, EDMA	<.0001*	Males had wider ML and shorter AP dimensions. The point of maximum vault height is located more anteriorly in females.
	Comparison by ancestry in controls (sexes combined)	PCA, CVA, EDMA	≤.0001*	Africans had overall highest while Asians have overall shallowest vaults. Africans also had wider ML while Europeans had longer AP dimensions. The point of maximum vault height is located more anteriorly in Europeans.
	Comparison of male controls by ancestry	CVA, EDMA	≤.0148[b]	Africans had overall highest while Asians have overall shallowest vaults. Africans also had wider ML while Europeans had longer AP dimensions.
	Comparison of female controls by ancestry	CVA, EDMA	≤.0003*	Africans had overall highest while Asians have overall shallowest vaults. Europeans had longer AP dimensions. The point of maximum vault height is located more anteriorly in Europeans.

	Comparison of control sexes within ancestries	CVA, EDMA	≤.0006*	Males had wider ML and shorter AP dimensions. The point of maximum vault height is located more anteriorly in females.
II	Comparison by sex in parents (ancestries combined)	PCA, CVA, EDMA	≤.0001*	Males had wider ML dimension. The point of maximum vault height is located more anteriorly in females.
	Comparison by ancestry in parents (sexes combined)	PCA, CVA, EDMA	≤.0001*	Africans had overall highest while Asians have overall shallowest vaults. Africans also had wider ML while Europeans had longer AP dimensions. The point of maximum vault height is located more anteriorly in Europeans. The point of maximum vault height is located more anteriorly in Europeans.
	Comparison of fathers by ancestry	CVA, EDMA	See Description	Europeans had narrower ML dimension and more slender palates than other ancestries ($p \leq .017$)[b]. No difference was detected between Africans and Asians ($p \geq .602$)
	Comparison of mothers by ancestry	CVA, EDMA	≤.0004*	Europeans had narrower ML dimension and more slender palates than other ancestries with the point of maximum vault located more

				anteriorly. African had higher overall palatal vaults and wider ML dimension.
	Comparison of parent sexes within ancestries	CVA, EDMA	See Description	European females had higher anterior palatal vaults than males ($p \leq .0001$)*. Asian females had shallower vaults and wider AP dimension than males ($p \leq .0017$)*. No differences were detected among Africans.
III	Comparison by parent/control status (sexes and ancestries combined)	CVA, EDMA	.0322[b]	Parents had wider ML dimension and shorter anterior AP dimension.
	Comparison of males by parent/control status (ancestries combined)	CVA	.986	No shape difference detected.
	Comparison of females by parent/control status	CVA, EDMA	0.0001*	Mothers had a shorter anterior AP dimension and wider ML dimension with higher posterior palatal vault.

(ancestries combined)			
Comparison of parent/control status within ancestries (sexes combined)	CVA, EDMA	See Description	Asian parents had wider ML dimension with higher posterior palatal vault (p=.012)[b]. European parents had a constricted ML dimension and a higher anterior palatal vault (p=.0025)*. No difference was detected between African parents and controls (p=.687).
Comparison of males by parent/control status within ancestries	CVA	≥.24	No shape difference detected.
Comparison of females by parent/control status within ancestries	CVA, EDMA	≤.0093[b]	Asian mothers had wider ML dimension, shorter anterior AP dimension and a higher posterior palatal vault (p≤.0001)*. European mothers had narrower ML dimension with a higher anterior palatal vault (p=.0005)*. African mothers showed a pattern of shape difference similar to Asians (p=.0093)[b].

4.0 Discussion

4.1 Summary of Major Morphological Findings

4.1.1 Patterns of Variation in Normal Palatal Morphology

Based on our findings, up to 76.52% of normal palatal variation was cumulatively explained by the first three principal components whereby a higher palatal vault was associated with either a shortened anteroposterior dimension and/or a narrower mediolateral dimension. On the other hand, a shallower palatal vault was associated with either a longer anteroposterior or wider mediolateral dimensions.

4.1.2 Morphological Effects of Sex

In the present study, patterns of sexual dimorphism in palatal shape were detected. Those patterns were evident regardless of ancestry and were replicated within every ancestral group. Males had a relatively wider mediolateral palatal dimension than females, while females had a relatively more constricted palates than males. In addition, females also had a relatively longer anteroposterior dimension and more slender palates than males. Regarding palatal vault height, females had relatively higher anterior palatal vaults while males had relatively higher posterior palatal vaults.

4.1.3 Morphological Effects of Ancestry

The palatal shape differed across ancestries. Africans had the highest overall palatal vaults while Asians had the shallowest. Africans also had a relatively wider mediolateral dimension than the other ancestries while Europeans had relatively the narrowest mediolateral dimension with more slender palatal shapes than the other ancestries. The point of maximum vault height was located more anteriorly in Europeans while in Africans it was located more posteriorly.

4.1.4 Morphological Effects of Parent/Control Status

Patterns of shape difference were detected among females when mothers were compared to female controls but not among males. No difference in shape was detected between fathers and male controls. In addition, there was an ancestry-specific pattern to those sex-specific differences. For instance, Asian mothers were found to have a shorter anteroposterior dimension, a wider mediolateral dimension, and a higher posterior palatal vault in comparison to their demographically matched female controls. Interestingly, their shortened anteroposterior dimension was due to a localized retrusion of the anterior palate. On the other hand, European mothers were found to have a more constricted mediolateral dimension and a slenderer palate with a higher anterior palatal vault in comparison to demographically matched female controls. While achieving only baseline statistical significance, African mothers showed similar patterns of morphological difference to those of Asians when compared to their demographically matched female controls.

4.2 Comparison of the Results to Previous Findings

4.2.1 Normal Variation in Palatal Morphology

Normal palatal morphology can be thought about within two contexts. The first context is that of craniofacial growth and development, while the second is anthropological variation by sex and ancestry. Regarding craniofacial growth and development, growth at the cranial base has a major influence on maxillary growth, resulting in downward and forward displacement of the maxilla (Manlove, Romeo, & Venugopalan, 2020). Through a compensatory mechanism to this downward and forward displacement, bone is deposited at the intermaxillary and circumaxillary sutures and resorbed from the anterior surface of the maxilla, in addition to the dependency on early nasal septal growth (Manlove et al., 2020). Therefore, a superiorly posteriorly located cranial base might lead to a deficiency in the sagittal and transverse dimensions of the maxilla and might indicate a higher palatal vault. A systematic review investigated the relationship between cranial base flexion and types of malocclusion and concluded that those with Class III malocclusion tended to have more acute cranial base flexion angles (N-S-Ba, N-S-Ar) than those with Class I or Class II while those with Class II malocclusion had more obtuse angles than those with Class I or Class III (Almeida, Raveli, Vieira, Santos-Pinto, & Raveli, 2017). Tinano et al. studied cranial base flexion angles in individuals with CLP with Class III malocclusion and reported that those individuals had more acute cranial base flexion angles (Tinano, Martins, Bendo, & Mazzieiro, 2015). In addition, a three-dimensional study of palatal morphology reported that those with Class II malocclusion had shallower palates (Huang, Hu, Zhao, Wang, & Gu, 2020). A cross-sectional study on a large cohort of children (N = 1065) reported an association between a higher palatal vault with anterior and/or posterior cross-bites, which are an indication of deficient anteroposterior

or mediolateral maxillary dimensions (Galvez & Methenitou, 1989). Our findings agree with the association between a higher palatal vault and decreased anteroposterior and/or mediolateral dimensions.

Sexual dimorphism in craniofacial morphology has been studied through multiple methodological approaches and is well reported in the literature (Perri, Kairaitis, Wheatley, & Amis, 2015). Males have been consistently reported to have larger size dimensions than females (Perri et al., 2015). Ursi et al. investigated sexual dimorphism during craniofacial growth and reported that males have longer anterior cranial base and effective sagittal length of the maxilla than females, due to the fact that males continue to grow beyond a set timepoint while females do not. In addition, females tended to have more horizontal craniofacial growth trajectories than males (Ursi, Trotman, McNamara, & Behrents, 1993). Albeit scaling for unit centroid size in our data to analyze shape variables only, males have been found to have larger centroid sizes than females in the present study, which was no surprise. Daraze et al. investigated the sagittal dimension in a cohort of young Lebanese adults of both sexes using cephalometry, and reported that females had larger A-N-B angles with no significant differences in S-N-A values, indicating that females have more convex facial profiles (Daraze, Delatte, Bou Saba, & Majzoub, 2017). Geometric morphometric analysis comparing face shape in Caucasians reported that in adults, females had narrower nasolabial complexes and again, more convex facial profiles (Kesterke et al., 2016). A limited number of studies investigated sexual dimorphism in palatal vault height (depth). Mankapure et al. studied palatal depth in an equal cohort of males and females (N = 250 in each group) and found that although mean palatal depth was higher in males, it did not achieve statistical significance (Mankapure, Barpande, & Bhavthankar, 2017). Huang et al. reported that males had overall higher and wider palatal vault than females regardless of sagittal or transverse patterns

(Huang et al., 2020). Our findings have shown that, after scaling to unit centroid size, the area of maximum palatal height was located more anteriorly in females and more posteriorly in males, which might methodologically explain the findings by Mankapure et al.; as they measured the palatal depth from a fixed point corresponding to that in between the central fossae of the maxillary first molars. It is also worthy to note, however, that the findings of sexual dimorphism in our data were replicated across all three ancestral groups, thereby increasing robustness of the current study.

Variation in facial morphology by ancestry has been well studied and reported in the literature (Wen, Wong, Lin, Yin, & McGrath, 2015). Limited information is available on three-dimensional variability of palatal morphology across ancestries. However, cephalometric studies comparing Asians to Europeans have reported that Asians had more obtuse cranial base flexure angle (Almeida et al., 2017). This finding on cephalometry can be translated to a shallower palatal vault. Our findings are again in agreement with that Asians show the shallowest palatal vaults among all three ancestral groups. In addition, our ancestry-specific findings were replicated in both sexes in our control population, thus adding to the robustness of the present study.

4.2.2 The Cleft-related Morphological Phenotype

Cephalometric differences in biological parents of unaffected individuals with NSCL/P were addressed in multiple studies both radiographically as well as through stereophotogrammetry yielded significant differences between parents and demographically matched controls (McIntyre & Mossey, 2002, 2004; S. M. Weinberg et al., 2009; S. M. Weinberg et al., 2008). Studies on lateral and postero-anterior (PA) cephalometric radiographs have addressed the bony skeletal structure of those parents and have reported significant findings within the limitations of those studies. Despite the heterogeneity among those studies, they have all agreed that there are

distinctive characteristics that discriminate those parents from controls (McIntyre & Mossey, 2002, 2003). These two-dimensional analyses reported increased upper incisor proclination as well as decreased upper anterior facial height in comparison to lower facial height and other combinations indicating a more concave facial profile which may be suggestive of a deficient palate. A combination of an increased S-N-ANS angle in the presence of decreased upper anterior facial height, decreased facial height ratio and a concave facial profile may indicate a more superiorly situated cranial base. The limitations of those studies, however, included great variation in methodology and failure to account for sexual dimorphism, ethnic differences in craniofacial morphology and differing rates of orofacial clefting across populations (McIntyre & Mossey, 2002; S. M. Weinberg, Maher, & Marazita, 2006). However, morphological findings in our study agree with those reported in the previous studies, specifically those pointing towards some degree of retruded anterior palatal dimension and higher palatal vault.

Three-dimensional analyses of facial morphology through geometric morphometrics and Euclidean distance matrix analysis have been facilitated through 3D stereophotogrammetry. Again, the findings in general pointed towards morphological differences located at the nasomaxillary complex region in discordant twins for non-syndromic orofacial clefting and biological parents, in addition to a sex-specific pattern when compared to demographically matched controls (Roosenboom et al., 2017; S. M. Weinberg et al., 2009; S. M. Weinberg et al., 2008). The sex-specific pattern of morphological differences in the face remains unclear, with multiple studies reporting differing directionality to this sex-specific pattern with regards to nature and magnitude (S. M. Weinberg et al., 2009). With regards to our findings on palatal morphology in the present study, sex-specific findings were present only in mothers when compared to demographically matched female controls, but not among males. It is still unclear, however,

whether there was no true difference, or the difference is having an effect size smaller than to be detected given the current methodology or sample sizes of the father groups in our study. These findings will collectively benefit from further replication on a larger study cohort. A limitation of the aforementioned three-dimensional analyses of the face is that they were limited to only one ancestral group, thereby providing minimal information regarding possible ancestry-specific patterns of morphological differences affecting parents.

To the best of our knowledge, no prior study has addressed three-dimensional palatal morphology in the context of analyzing parent-control differences in craniofacial morphology. However, it has been addressed in the context of comparing affected individuals to controls or in assessing surgical outcome in operated individuals. Prior studies looking at mediolateral palatal dimensions in unoperated adult individuals with complete cleft lip and palate or unilateral cleft lip and alveolus pointed towards a more constricted anterior palatal transverse dimension at the canine region (Latief, Lekkas, & Kuijpers Jagtman, 2009; Latief, Lekkas, & Kuijpers, 2010; Latief, Lekkas, Schols, Fudalej, & Kuijpers, 2012). Ye et al. also studied craniofacial morphology in a cohort of unoperated adult individuals with cleft palate only using a series of cephalometric radiographs. They concluded that unoperated individuals with isolated cleft palate only were characterized by maxillary retrusion (Ye, Xu, Ahmatjian, & Bing, 2013).

4.3 The Biological Basis of the Observed Findings

In 1962, Dr. Melvin Moss introduced the “Functional Matrix Hypothesis” as a theory in the textbook, “Vistas in Orthodontics” (Pearce, 2006). This theory stressed the ontogenetic primacy of function over form and proposed that the structural makeup and morphology of skeletal

units are secondary, compensatory and mechanically obligatory responses to temporally and operationally prior demands of the related functional matrices, or in other words, that bones do not grow but are rather grown (Moss, 1997). At the time, this theory provided a reasonable explanation for the ability of orthodontists to perform dentofacial orthopedic procedures that would manipulate skeletal structures. In addition, the "buccinator mechanism" has been introduced whereby an external sphincter of muscle formed by the intercussation of the buccinator muscle with the orbicularis oris muscle anteriorly and attachment to the pterygomandibular raphe posteriorly, which in turn provides attachment to the superior constrictor muscle of the pharynx (Perkins, Blanton, & Biggs, 1977). As the superior constrictor muscle meets its contralateral counterpart, these three muscles form a ring-like structure encircling the dental arch from the external surface, while the tongue provides internal tonal counteraction from the inside, thereby positioning teeth in a "neutral zone" in between (Perkins et al., 1977). Interestingly, chronic mouth-breathers have been shown to have a higher arched palate with a more constricted mediolateral but normal anteroposterior dimensions (Lione, Buongiorno, Franchi, & Cozza, 2014). While one might explain this finding as an unopposed action of the external muscular sphincter of the buccinator mechanism, a question arises whether this observed palatal morphology is caused by this functional biomechanical mechanism or that the chronic mouth-breather is, in fact, genetically predisposed to having a smaller and underdeveloped nasomaxillary complex, and thus, a nasal cavity that is prone to obstruction, thereby causing them to breathe through their mouth.

Similarly, affected individuals with CL/P present with a similar phenotype indicative of maxillary hypoplasia. Again, this might be explained solely on the basis of loss of structural integrity of the craniofacial skeleton, making it prone to deformity through biomechanical means alone. Conflicting reports of causality have been published in the surgical literature whereby some

studies report that maxillary hypoplasia is indeed due to the scarring resulting from primary surgery while others report that primary surgery had no effect (Hoffmannova et al., 2016; Sakoda et al., 2017). However, unoperated individuals with unilateral cleft lip and alveolus have better mediolateral structural continuity and still present with a degree of mediolateral deficiency. In addition, unoperated individuals with CPO have better anteroposterior structural continuity and still present with some form of anteroposterior maxillary retrusion. Interestingly, Meazzini et al. investigated factors that lead to the highly variable degree of maxillary hypoplasia in individuals operated by the same surgeon using the same surgical protocol. They found a strong correlation between an increased degree of maxillary hypoplasia and agenesis of the maxillary lateral incisor (Meazzini, Tortora, Morabito, Garattini, & Brusati, 2011). While maxillary tooth agenesis has been reported to be genetically associated with the cleft phenotype, a higher rate of lateral incisor agenesis was significantly associated with the need for Le Forte I maxillary advancement surgery in individuals with CLP after completion of growth (Howe et al., 2015; Oberoi, Chigurupati, & Vargervik, 2008). Other studies also reported an association between hypodontia due to tooth agenesis and a shortened maxillary length in normal populations (Endo, Ozoe, Yoshino, & Shimooka, 2006; Tavajohi-Kermani, Kapur, & Sciote, 2002). Meazzini et al. also showed a correlation between the extent of maxillary hypoplasia and altered cranial base angles, and concluded that missing lateral incisors, as a sign of inherent tissue hypoplasia seemed to be strongly associated with maxillary growth potential and that initial cleft severity did not seem to correlate with maxillary growth (Meazzini et al., 2011).

In 1997, Dr. Moss revised the “Functional Matrix Hypothesis” based on decades of research findings following the first introduction of this theory to acknowledge the presence of a significant genomic component and to assert that there is a complex interplay of both genetic and

epigenetic factors (function) rather than function alone (Moss, 1997). The fact that the present study showed distinct morphological patterns differing by ancestral groups, each having their own distinct genetic makeup further adds to the genomic role in the morphology of the human palate.

Considering the morphological findings in the present study, it was shown that, while functional matrices may play a role, the morphological patterns of the palate comprised a strong genetic component regulating those patterns. In addition, the findings pointing towards some form of a relatively hypoplastic shape in the unaffected mothers of individuals with NSCL/P despite presence of normal structural integrity and functional matrices may further suggest that there are genetic risk factors being passed down in families that have a role in the cleft-related morphological phenotype of the palate.

Perhaps the most intriguing aspect of our findings is the connection to epidemiological patterns of orofacial clefting. By ancestry, orofacial clefting in general and NSCL/P in particular has been reported to be most common in those of Asian ancestry (Leslie & Marazita, 2013). Burg et al. reported the prevalence of CPO being highest among two subpopulations of European ancestry (Burg, Chai, Yao, Magee, & Figueiredo, 2016). To this extent, our findings in mothers showed an ancestry-specific pattern when compared to demographically matched control females. Asian mothers were found to have a more retruded anteroposterior palatal dimension, a wider mediolateral dimension and a shallower anterior palatal vault, while European mothers have been shown to have a more constricted mediolateral dimension, longer anteroposterior dimension and a higher anterior palatal vault. Beyond mother-control morphological differences, the same patterns have been found in an ancestry-specific manner in Asians and Europeans regarding normal variation in palatal morphology.

On another front, CL/P has been reported to be twice as common in males while CPO has been shown to be twice as common in females (Leslie & Marazita, 2013). The pattern of normal variation by sex in our data point towards males having wider mediolateral dimension, shorter anteroposterior dimension and shallower anterior palatal vaults while females had narrower and longer more slender palates and higher anterior palatal vaults. In addition, the distinction by sex in the parent population was absent in Africans, less distinct in Asians and most distinct in Europeans, with European females having a completely different pattern of variation as mentioned above. Therefore, our data show that there might be an association between CL/P risk and a morphological phenotype that has a shorter anteroposterior dimension, wider mediolateral dimension and a shallow anterior palatal vault.

It is of interest to note, however, that the biological parents included in the current study were from families with CL/P only. Despite this fact, a phenotypic heterogeneity has been noticed between Asian and European mothers when compared to demographically matched controls. This observed phenotypic heterogeneity maybe the result of population-specific cleft genetic risk factors and/or background loci constituting the genetic architecture of the palatal morphology (Leslie et al., 2016). In addition, Carlson et al. conducted a systematic genetic analysis of phenotypic heterogeneity in orofacial clefting and showed that a given genetic locus can be associated with more than one subtype of orofacial clefting as part of the genetic etiology of this complex trait (Carlson et al., 2019). Therefore, it comes as no surprise to us that our findings show some pattern of phenotypic heterogeneity among mothers even though we included those from families with CL/P only.

4.4 Strengths and Limitations of the Present Study

There are numerous strengths to this study, the first of which is the presence of a large multi-ethnic cohort of participants. Also, we are the first to characterize palatal morphology utilizing the current morphometric approach. Moreover, our data collection protocol is cost-effective and non-invasive, allowing for safe and rapid data collection on a large sample of participants. Three-dimensional landmark coordinate data allow for statistical analysis of the whole shape as a covariance matrix, which better illustrates morphological patterns of biological structures in comparison to direct anthropometric measurements. Those landmark coordinates will also pave the way towards more advanced morphometric analyses such as dense surface-mapping approaches.

On the other hand, there are multiple limitations. First, there are groups with limited sample sizes, in particular the sample of unaffected fathers. This might have hindered the possibility to detect a small difference in shape by the current methodology. In addition, there are limitations that are inherent to the methodology used. The use of sparse landmarks provides only limited morphological information about palate shape. The fact that some landmarks were dependent on the presence of the teeth further hindered the sample sizes due to the exclusion of individuals with missing teeth, and thus, missing landmarks. There were also artifacts present in a subset of plaster casts that have hindered the ability to place landmarks on those casts, further hindering the sample sizes. Furthermore, we were only limited to including families with CL/P only due to the limited number of families with CPO in our cohort for a statistically meaningful analysis.

4.5 Future Directions

There are many directions in which to venture further with this work. The first is to replicate our findings both in larger independent samples and by utilizing different morphometric approaches with our cohort. Further sophisticated morphometric methods include the use of semi-landmarks and dense surface-mapping that would allow the capturing of fine details regarding the palatal dome and its morphological patterns as well as analysis of modularity. In addition, we are planning to investigate the relationship between palatal shape and external facial shape by carrying out two-block partial least-squares analyses.

Regarding normal palatal morphology, we are interested in analyzing morphological patterns associated with growth through characterizing shape change patterns at different ages and timepoints during the growth and development phase. In addition, we are planning to carry out genetic association studies with our findings of morphological variation in order to better understand the genetic architecture implicated in shaping the human palate. On the other hand, with regards to relative-control differences, we are planning to carry out future analyses on different degrees of relatives and different family types, including different subtypes of orofacial clefting. In addition to genetic analyses, this will provide more insight and aid discovery of possible risk factors implicated in the genetic etiology of orofacial clefting.

Bibliography

Abbott, B. D. (2010). The etiology of cleft palate: a 50-year search for mechanistic and molecular understanding. *Birth Defects Res B Dev Reprod Toxicol, 89*(4), 266-274. doi:10.1002/bdrb.20252

Adameyko, I., & Fried, K. (2016). The Nervous System Orchestrates and Integrates Craniofacial Development: A Review. *Front Physiol, 7*, 49. doi:10.3389/fphys.2016.00049

Agbenorku, P. (2013). Orofacial Clefts: A Worldwide Review of the Problem. *ISRN Plastic Surgery, 2013*. Retrieved from http://dx.doi.org/10.5402/2013/348465

Almeida, K. C. M., Raveli, T. B., Vieira, C. I. V., Santos-Pinto, A. D., & Raveli, D. B. (2017). Influence of the cranial base flexion on Class I, II and III malocclusions: a systematic review. *Dental Press J Orthod, 22*(5), 56-66. doi:10.1590/2177-6709.22.5.056-066.oar

Austin, S. L., Mattick, C. R., & Waterhouse, P. J. (2015). Distraction osteogenesis versus orthognathic surgery for the treatment of maxillary hypoplasia in cleft lip and palate patients: a systematic review. *Orthod Craniofac Res, 18*(2), 96-108. doi:10.1111/ocr.12063

Bamforth, J. S., Hughes, I. A., Lazarus, J. H., Weaver, C. M., & Harper, P. S. (1989). Congenital hypothyroidism, spiky hair, and cleft palate. *J Med Genet, 26*(1), 49-51. doi:10.1136/jmg.26.1.49

Beaty, T. H., Marazita, M. L., & Leslie, E. J. (2016). Genetic factors influencing risk to orofacial clefts: today's challenges and tomorrow's opportunities. *F1000Res, 5*, 2800. doi:10.12688/f1000research.9503.1

Benko, S., Fantes, J. A., Amiel, J., Kleinjan, D. J., Thomas, S., Ramsay, J., . . . Lyonnet, S. (2009). Highly conserved non-coding elements on either side of SOX9 associated with Pierre Robin sequence. *Nat Genet, 41*(3), 359-364. doi:10.1038/ng.329

Bille, C., Winther, J. F., Bautz, A., Murray, J. C., Olsen, J., & Christensen, K. (2005). Cancer risk in persons with oral cleft--a population-based study of 8,093 cases. *Am J Epidemiol, 161*(11), 1047-1055. doi:10.1093/aje/kwi132

Bookstein, F. L. (1991). *Morphometric tools for landmark data : geometry and biology*. Cambridge England ; New York: Cambridge University Press.

Boyles, A. L., DeRoo, L. A., Lie, R. T., Taylor, J. A., Jugessur, A., Murray, J. C., & Wilcox, A. J. (2010). Maternal alcohol consumption, alcohol metabolism genes, and the risk of oral clefts: a population-based case-control study in Norway, 1996-2001. *Am J Epidemiol, 172*(8), 924-931. doi:10.1093/aje/kwq226

Braybrook, C., Doudney, K., Marçano, A. C., Arnason, A., Bjornsson, A., Patton, M. A., . . . Stanier, P. (2001). The T-box transcription factor gene TBX22 is mutated in X-linked cleft palate and ankyloglossia. *Nat Genet, 29*(2), 179-183. doi:10.1038/ng730

Buchanan, E. P., Xue, A. S., & Hollier, L. H. (2014). Craniofacial syndromes. *Plast Reconstr Surg, 134*(1), 128e-153e. doi:10.1097/PRS.0000000000000308

Burg, M. L., Chai, Y., Yao, C. A., Magee, W., & Figueiredo, J. C. (2016). Epidemiology, Etiology, and Treatment of Isolated Cleft Palate. *Front Physiol, 7*, 67. doi:10.3389/fphys.2016.00067

Carlson, J. C., Anand, D., Butali, A., Buxo, C. J., Christensen, K., Deleyiannis, F., . . . Leslie, E. J. (2019). A systematic genetic analysis and visualization of phenotypic heterogeneity

among orofacial cleft GWAS signals. *Genet Epidemiol, 43*(6), 704-716. doi:10.1002/gepi.22214

Celli, J., Duijf, P., Hamel, B. C., Bamshad, M., Kramer, B., Smits, A. P., . . . van Bokhoven, H. (1999). Heterozygous germline mutations in the p53 homolog p63 are the cause of EEC syndrome. *Cell, 99*(2), 143-153. doi:10.1016/s0092-8674(00)81646-3

Center for Disease Control and Prevention: Facts about Cleft Lip and Cleft Palate. In.

Chai, Y., & Maxson, R. E. (2006). Recent advances in craniofacial morphogenesis. *Dev Dyn, 235*(9), 2353-2375. doi:10.1002/dvdy.20833

Claes, P., Roosenboom, J., White, J. D., Swigut, T., Sero, D., Li, J., . . . Weinberg, S. M. (2018). Genome-wide mapping of global-to-local genetic effects on human facial shape. *Nat Genet, 50*(3), 414-423. doi:10.1038/s41588-018-0057-4

Daraze, A., Delatte, M., Bou Saba, S., & Majzoub, Z. (2017). Craniofacial characteristics in the sagittal dimension: A cephalometric study in Lebanese young adults. *Int Orthod, 15*(1), 114-130. doi:10.1016/j.ortho.2016.12.001

Deferm, J. T., Schreurs, R., Baan, F., Bruggink, R., Merkx, M. A. W., Xi, T., . . . Maal, T. J. J. (2018). Validation of 3D documentation of palatal soft tissue shape, color, and irregularity with intraoral scanning. *Clin Oral Investig, 22*(3), 1303-1309. doi:10.1007/s00784-017-2198-8

Dixon, M. J., Marazita, M. L., Beaty, T. H., & Murray, J. C. (2011). Cleft lip and palate: understanding genetic and environmental influences. *Nat Rev Genet, 12*(3), 167-178. doi:10.1038/nrg2933

Dodé, C., Levilliers, J., Dupont, J. M., De Paepe, A., Le Dû, N., Soussi-Yanicostas, N., . . . Hardelin, J. P. (2003). Loss-of-function mutations in FGFR1 cause autosomal dominant Kallmann syndrome. *Nat Genet, 33*(4), 463-465. doi:10.1038/ng1122

el Ghouzzi, V., Le Merrer, M., Perrin-Schmitt, F., Lajeunie, E., Benit, P., Renier, D., . . . Bonaventure, J. (1997). Mutations of the TWIST gene in the Saethre-Chotzen syndrome. *Nat Genet, 15*(1), 42-46. doi:10.1038/ng0197-42

Endo, T., Ozoe, R., Yoshino, S., & Shimooka, S. (2006). Hypodontia patterns and variations in craniofacial morphology in Japanese orthodontic patients. *Angle Orthod, 76*(6), 996-1003. doi:10.2319/082905-303

Ferrante, M. I., Giorgio, G., Feather, S. A., Bulfone, A., Wright, V., Ghiani, M., . . . Franco, B. (2001). Identification of the gene for oral-facial-digital type I syndrome. *Am J Hum Genet, 68*(3), 569-576. doi:10.1086/318802

FitzPatrick, D. R., Carr, I. M., McLaren, L., Leek, J. P., Wightman, P., Williamson, K., . . . Bonthron, D. T. (2003). Identification of SATB2 as the cleft palate gene on 2q32-q33. *Hum Mol Genet, 12*(19), 2491-2501. doi:10.1093/hmg/ddg248

Foster, J. W., Dominguez-Steglich, M. A., Guioli, S., Kwok, C., Weller, P. A., Stevanović, M., . . . Goodfellow, P. N. (1994). Campomelic dysplasia and autosomal sex reversal caused by mutations in an SRY-related gene. *Nature, 372*(6506), 525-530. doi:10.1038/372525a0

Frebourg, T., Oliveira, C., Hochain, P., Karam, R., Manouvrier, S., Graziadio, C., . . . Seruca, R. (2006). Cleft lip/palate and CDH1/E-cadherin mutations in families with hereditary diffuse gastric cancer. *J Med Genet, 43*(2), 138-142. doi:10.1136/jmg.2005.031385

Fukuhara, T., & Saito, S. (1962). Genetic consideration on the dysplasia of the nasopalatal segments as

a "Formes Frustes" radiologically found in parents of cleft children: a preliminary report. *Jpn J Hum Genet.*(7), 3.

Fukuhara, T., & Saito, S. (1963). Possible carrier status of hereditary cleft palate with cleft lip: report
of cases. *Bull Tokyo Med Dent Univ*.(10), 12.

Galvez, J., & Methenitou, S. (1989). Airway obstruction, palatal vault formation and malocclusion: a cross-sectional study. *J Pedod, 13*(2), 133-140. Retrieved from https://www.ncbi.nlm.nih.gov/pubmed/2600739

Ganoo, T., & Sjöström, M. (2019). Outcomes of Maxillary Orthognathic Surgery in Patients with Cleft Lip and Palate: A Literature Review. *J Maxillofac Oral Surg, 18*(4), 500-508. doi:10.1007/s12663-019-01217-w

Gripp, K. W., Wotton, D., Edwards, M. C., Roessler, E., Ades, L., Meinecke, P., . . . Elledge, S. J. (2000). Mutations in TGIF cause holoprosencephaly and link NODAL signalling to human neural axis determination. *Nat Genet, 25*(2), 205-208. doi:10.1038/76074

Group, T. T. C. S. C. (1996). Positional cloning of a gene involved in the pathogenesis of Treacher Collins syndrome. The Treacher Collins Syndrome Collaborative Group. *Nat Genet, 12*(2), 130-136. doi:10.1038/ng0296-130

Hahn, H., Wicking, C., Zaphiropoulous, P. G., Gailani, M. R., Shanley, S., Chidambaram, A., . . . Bale, A. E. (1996). Mutations of the human homolog of Drosophila patched in the nevoid basal cell carcinoma syndrome. *Cell, 85*(6), 841-851. doi:10.1016/s0092-8674(00)81268-4

Hallgrímsson, B., Donnabháin, B. O., Blom, D. E., Lozada, M. C., & Willmore, K. T. (2005). Why are rare traits unilaterally expressed?: trait frequency and unilateral expression for cranial nonmetric traits in humans. *Am J Phys Anthropol, 128*(1), 14-25. doi:10.1002/ajpa.20187

Hoffmannova, E., Bejdová, Š., Borský, J., Dupej, J., Cagáňová, V., & Velemínská, J. (2016). Palatal growth in complete unilateral cleft lip and palate patients following neonatal cheiloplasty: Classic and geometric morphometric assessment. *Int J Pediatr Otorhinolaryngol, 90*, 71-76. doi:10.1016/j.ijporl.2016.08.028

Hooper, J. E., Feng, W., Li, H., Leach, S. M., Phang, T., Siska, C., . . . Williams, T. (2017). Systems biology of facial development: contributions of ectoderm and mesenchyme. *Dev Biol, 426*(1), 97-114. doi:10.1016/j.ydbio.2017.03.025

Howard, T. D., Paznekas, W. A., Green, E. D., Chiang, L. C., Ma, N., Ortiz de Luna, R. I., . . . Jabs, E. W. (1997). Mutations in TWIST, a basic helix-loop-helix transcription factor, in Saethre-Chotzen syndrome. *Nat Genet, 15*(1), 36-41. doi:10.1038/ng0197-36

Howe, B. J., Cooper, M. E., Vieira, A. R., Weinberg, S. M., Resick, J. M., Nidey, N. L., . . . Moreno Uribe, L. M. (2015). Spectrum of Dental Phenotypes in Nonsyndromic Orofacial Clefting. *J Dent Res, 94*(7), 905-912. doi:10.1177/0022034515588281

Huang, X., Hu, X., Zhao, Y., Wang, Y., & Gu, Y. (2020). Preliminary comparison of three-dimensional reconstructed palatal morphology in subjects with different sagittal and vertical patterns. *BMC Oral Health, 20*(1), 55. doi:10.1186/s12903-020-1041-9

Indencleef, K., Roosenboom, J., Hoskens, H., White, J. D., Shriver, M. D., Richmond, S., . . . Claes, P. (2018). Six NSCL/P Loci Show Associations With Normal-Range Craniofacial Variation. *Front Genet, 9*, 502. doi:10.3389/fgene.2018.00502

Jensen, B. L., Kreiborg, S., Dahl, E., & Fogh-Andersen, P. (1988). Cleft lip and palate in Denmark, 1976-1981: epidemiology, variability, and early somatic development. *Cleft Palate J, 25*(3), 258-269. Retrieved from https://www.ncbi.nlm.nih.gov/pubmed/3262457

Johnson, R. L., Rothman, A. L., Xie, J., Goodrich, L. V., Bare, J. W., Bonifas, J. M., . . . Scott, M. P. (1996). Human homolog of patched, a candidate gene for the basal cell nevus syndrome. *Science, 272*(5268), 1668-1671. doi:10.1126/science.272.5268.1668

Johnston, J. J., Sapp, J. C., Turner, J. T., Amor, D., Aftimos, S., Aleck, K. A., . . . Biesecker, L. G. (2010). Molecular analysis expands the spectrum of phenotypes associated with GLI3 mutations. *Hum Mutat, 31*(10), 1142-1154. doi:10.1002/humu.21328

Jugessur, A., Shi, M., Gjessing, H. K., Lie, R. T., Wilcox, A. J., Weinberg, C. R., . . . Murray, J. C. (2009). Genetic determinants of facial clefting: analysis of 357 candidate genes using two national cleft studies from Scandinavia. *PLoS One, 4*(4), e5385. doi:10.1371/journal.pone.0005385

Juriloff, D. M., & Harris, M. J. (2008). Mouse genetic models of cleft lip with or without cleft palate. *Birth Defects Res A Clin Mol Teratol, 82*(2), 63-77. doi:10.1002/bdra.20430

Kalay, E., Sezgin, O., Chellappa, V., Mutlu, M., Morsy, H., Kayserili, H., . . . Akarsu, N. A. (2012). Mutations in RIPK4 cause the autosomal-recessive form of popliteal pterygium syndrome. *Am J Hum Genet, 90*(1), 76-85. doi:10.1016/j.ajhg.2011.11.014

Kernahan, D. A., & Stark, R. B. (1958). A new classification for cleft lip and cleft palate. *Plast Reconstr Surg Transplant Bull, 22*(5), 435-441. doi:10.1097/00006534-195811000-00001

Kesterke, M. J., Raffensperger, Z. D., Heike, C. L., Cunningham, M. L., Hecht, J. T., Kau, C. H., . . . Weinberg, S. M. (2016). Using the 3D Facial Norms Database to investigate craniofacial sexual dimorphism in healthy children, adolescents, and adults. *Biol Sex Differ, 7*, 23. doi:10.1186/s13293-016-0076-8

Klingenberg, C. P. (2016). Size, shape, and form: concepts of allometry in geometric morphometrics. *Dev Genes Evol, 226*(3), 113-137. doi:10.1007/s00427-016-0539-2

Kondo, S., Schutte, B. C., Richardson, R. J., Bjork, B. C., Knight, A. S., Watanabe, Y., . . . Murray, J. C. (2002). Mutations in IRF6 cause Van der Woude and popliteal pterygium syndromes. *Nat Genet, 32*(2), 285-289. doi:10.1038/ng985

Krantz, I. D., McCallum, J., DeScipio, C., Kaur, M., Gillis, L. A., Yaeger, D., . . . Jackson, L. G. (2004). Cornelia de Lange syndrome is caused by mutations in NIPBL, the human homolog of Drosophila melanogaster Nipped-B. *Nat Genet, 36*(6), 631-635. doi:10.1038/ng1364

Latief, B. S., Lekkas, C., & Kuijpers Jagtman, A. M. (2009). Maxillary arch width in unoperated adult of the unilateral cleft lip and alveolus patients. *J Maxillofac Oral Surg, 8*(3), 218-220. doi:10.1007/s12663-009-0053-4

Latief, B. S., Lekkas, C., & Kuijpers, M. A. (2010). Maxillary arch width in unoperated adult bilateral cleft lip and alveolus and complete bilateral cleft lip and palate. *Orthod Craniofac Res, 13*(2), 82-88. doi:10.1111/j.1601-6343.2009.01479.x

Latief, B. S., Lekkas, K. C., Schols, J. G., Fudalej, P. S., & Kuijpers, M. A. (2012). Width and elevation of the palatal shelves in unoperated unilateral and bilateral cleft lip and palate patients in the permanent dentition. *J Anat, 220*(3), 263-270. doi:10.1111/j.1469-7580.2011.01468.x

Laumonnier, F., Holbert, S., Ronce, N., Faravelli, F., Lenzner, S., Schwartz, C. E., . . . Briault, S. (2005). Mutations in PHF8 are associated with X linked mental retardation and cleft lip/cleft palate. *J Med Genet, 42*(10), 780-786. doi:10.1136/jmg.2004.029439

Lederer, D., Grisart, B., Digilio, M. C., Benoit, V., Crespin, M., Ghariani, S. C., . . . Verellen-Dumoulin, C. (2012). Deletion of KDM6A, a histone demethylase interacting with MLL2, in three patients with Kabuki syndrome. *Am J Hum Genet, 90*(1), 119-124. doi:10.1016/j.ajhg.2011.11.021

Lele, S., & Richtsmeier, J. T. (2001). *An invariant approach to statistical analysis of shapes : interdisciplinary statistics*. Boca Raton, Fla.: Chapman & Hall/CRC.

Leslie, E. J., Carlson, J. C., Shaffer, J. R., Feingold, E., Wehby, G., Laurie, C. A., . . . Marazita, M. L. (2016). A multi-ethnic genome-wide association study identifies novel loci for non-syndromic cleft lip with or without cleft palate on 2p24.2, 17q23 and 19q13. *Hum Mol Genet, 25*(13), 2862-2872. doi:10.1093/hmg/ddw104

Leslie, E. J., & Marazita, M. L. (2013). Genetics of cleft lip and cleft palate. *Am J Med Genet C Semin Med Genet, 163C*(4), 246-258. doi:10.1002/ajmg.c.31381

Lione, R., Buongiorno, M., Franchi, L., & Cozza, P. (2014). Evaluation of maxillary arch dimensions and palatal morphology in mouth-breathing children by using digital dental casts. *Int J Pediatr Otorhinolaryngol, 78*(1), 91-95. doi:10.1016/j.ijporl.2013.09.028

Little, J., Cardy, A., & Munger, R. G. (2004). Tobacco smoking and oral clefts: a meta-analysis. *Bull World Health Organ, 82*(3), 213-218. Retrieved from https://www.ncbi.nlm.nih.gov/pubmed/15112010

Loeys, B. L., Chen, J., Neptune, E. R., Judge, D. P., Podowski, M., Holm, T., . . . Dietz, H. C. (2005). A syndrome of altered cardiovascular, craniofacial, neurocognitive and skeletal development caused by mutations in TGFBR1 or TGFBR2. *Nat Genet, 37*(3), 275-281. doi:10.1038/ng1511

Mankapure, P. K., Barpande, S. R., & Bhavthankar, J. D. (2017). Evaluation of sexual dimorphism in arch depth and palatal depth in 500 young adults of Marathwada region, India. *J Forensic Dent Sci, 9*(3), 153-156. doi:10.4103/jfo.jfds_13_16

Manlove, A. E., Romeo, G., & Venugopalan, S. R. (2020). Craniofacial Growth: Current Theories and Influence on Management. *Oral Maxillofac Surg Clin North Am*. doi:10.1016/j.coms.2020.01.007

Mason, C. A., Kirby, R. S., Sever, L. E., & Langlois, P. H. (2005). Prevalence is the preferred measure of frequency of birth defects. *Birth Defects Res A Clin Mol Teratol, 73*(10), 690-692. doi:10.1002/bdra.20211

May, M. A., Sanchez, C. A., Deleyiannis, F. W., Marazita, M. L., & Weinberg, S. M. (2015). Evidence of olfactory deficits as part of the phenotypic spectrum of nonsyndromic orofacial clefting. *J Craniofac Surg, 26*(1), 84-86. doi:10.1097/SCS.0000000000001242

McGrath, J. A., Duijf, P. H., Doetsch, V., Irvine, A. D., de Waal , R., Vanmolkot, K. R., . . . van Bokhoven, H. (2001). Hay-Wells syndrome is caused by heterozygous missense mutations in the SAM domain of p63. *Hum Mol Genet, 10*(3), 221-229. doi:10.1093/hmg/10.3.221

McIntyre, G. T., & Mossey, P. A. (2002). The craniofacial morphology of the parents of children with orofacial clefting: a systematic review of cephalometric studies. *J Orthod, 29*(1), 23-29. doi:10.1093/ortho/29.1.23

McIntyre, G. T., & Mossey, P. A. (2003). Posteroanterior cephalometric analysis of the parental craniofacial morphology in orofacial clefting. *Cleft Palate Craniofac J, 40*(4), 416-425. doi:10.1597/1545-1569_2003_040_0416_pcaotp_2.0.co_2

McIntyre, G. T., & Mossey, P. A. (2004). Parental craniofacial morphology in orofacial clefting. *Eur J Orthod, 26*(4), 375-384. doi:10.1093/ejo/26.4.375

Meazzini, M. C., Tortora, C., Morabito, A., Garattini, G., & Brusati, R. (2011). Factors that affect variability in impairment of maxillary growth in patients with cleft lip and palate treated using the same surgical protocol. *J Plast Surg Hand Surg, 45*(4-5), 188-193. doi:10.3109/2000656X.2011.583493

Mills, L. F., Niswander, J. D., Mazaheri, M., & Brunelle, J. A. (1968). Minor oral and facial defects in relatives of oral cleft patients. *Angle Orthod, 38*(3), 199-204. doi:10.1043/0003-3219(1968)0382.0.CO;2

Milunsky, J. M., Maher, T. A., Zhao, G., Roberts, A. E., Stalker, H. J., Zori, R. T., . . . Lin, A. E. (2008). TFAP2A mutations result in branchio-oculo-facial syndrome. *Am J Hum Genet, 82*(5), 1171-1177. doi:10.1016/j.ajhg.2008.03.005

Mitchell, K., O'Sullivan, J., Missero, C., Blair, E., Richardson, R., Anderson, B., . . . Dixon, M. J. (2012). Exome sequence identifies RIPK4 as the Bartsocas-Papas syndrome locus. *Am J Hum Genet, 90*(1), 69-75. doi:10.1016/j.ajhg.2011.11.013

Morgan, N. V., Brueton, L. A., Cox, P., Greally, M. T., Tolmie, J., Pasha, S., . . . Maher, E. R. (2006). Mutations in the embryonal subunit of the acetylcholine receptor (CHRNG) cause lethal and Escobar variants of multiple pterygium syndrome. *Am J Hum Genet, 79*(2), 390-395. doi:10.1086/506256

Moss, M. L. (1997). The functional matrix hypothesis revisited. 3. The genomic thesis. *Am J Orthod Dentofacial Orthop, 112*(3), 338-342. doi:10.1016/S0889-5406(97)70265-8

Mossey, P. A., Little, J., Munger, R. G., Dixon, M. J., & Shaw, W. C. (2009). Cleft lip and palate. *Lancet, 374*(9703), 1773-1785. doi:10.1016/S0140-6736(09)60695-4

Murray, J. C. (2002). Gene/environment causes of cleft lip and/or palate. *Clin Genet, 61*(4), 248-256. Retrieved from https://www.ncbi.nlm.nih.gov/pubmed/12030886

Murray, J. C., Daack-Hirsch, S., Buetow, K. H., Munger, R., Espina, L., Paglinawan, N., . . . Magee, W. (1997). Clinical and epidemiologic studies of cleft lip and palate in the Philippines. *Cleft Palate Craniofac J, 34*(1), 7-10. doi:10.1597/1545-1569_1997_034_0007_caesoc_2.3.co_2

Neiswanger, K., Walker, K., Chirigos, K. W., Klotz, C. M., Cooper, M. E., Bardi, K. M., . . . Marazita, M. L. (2009). Whorl patterns on the lower lip are associated with nonsyndromic cleft lip with or without cleft palate. *Am J Med Genet A, 149A*(12), 2673-2679. doi:10.1002/ajmg.a.33089

Neiswanger, K., Weinberg, S. M., Rogers, C. R., Brandon, C. A., Cooper, M. E., Bardi, K. M., . . . Marazita, M. L. (2007). Orbicularis oris muscle defects as an expanded phenotypic feature in nonsyndromic cleft lip with or without cleft palate. *Am J Med Genet A, 143A*(11), 1143-1149. doi:10.1002/ajmg.a.31760

Ng, D., Thakker, N., Corcoran, C. M., Donnai, D., Perveen, R., Schneider, A., . . . Biesecker, L. G. (2004). Oculofaciocardiodental and Lenz microphthalmia syndromes result from distinct classes of mutations in BCOR. *Nat Genet, 36*(4), 411-416. doi:10.1038/ng1321

Ng, S. B., Bigham, A. W., Buckingham, K. J., Hannibal, M. C., McMillin, M. J., Gildersleeve, H. I., . . . Shendure, J. (2010). Exome sequencing identifies MLL2 mutations as a cause of Kabuki syndrome. *Nat Genet, 42*(9), 790-793. doi:10.1038/ng.646

Ng, S. B., Buckingham, K. J., Lee, C., Bigham, A. W., Tabor, H. K., Dent, K. M., . . . Bamshad, M. J. (2010). Exome sequencing identifies the cause of a mendelian disorder. *Nat Genet, 42*(1), 30-35. doi:10.1038/ng.499

Niemann, S., Zhao, C., Pascu, F., Stahl, U., Aulepp, U., Niswander, L., . . . Müller, U. (2004). Homozygous WNT3 mutation causes tetra-amelia in a large consanguineous family. *Am J Hum Genet, 74*(3), 558-563. doi:10.1086/382196

Niswander, J. D. (1968). Laminographic x-ray studies in families with cleft lip and cleft palate. *Arch Oral Biol, 13*(8), 1019-1022. doi:10.1016/0003-9969(68)90017-4

Nopoulos, P., Richman, L., Murray, J., & Canady, J. (2002). Cleft palate and craniofacial conditions. *Cleft Palate Craniofac J, 39*(1), 123-124. doi:10.1597/1545-1569_2002_039_0123_ltte_2.0.co_2

Oberoi, S., Chigurupati, R., & Vargervik, K. (2008). Morphologic and management characteristics of individuals with unilateral cleft lip and palate who required maxillary advancement. *Cleft Palate Craniofac J, 45*(1), 42-49. doi:10.1597/06-053.1

Packham, E. A., & Brook, J. D. (2003). T-box genes in human disorders. *Hum Mol Genet, 12 Spec No 1*, R37-44. doi:10.1093/hmg/ddg077

Palci, A., & Lee, M. S. Y. (2019). Geometric morphometrics, homology and cladistics: review and recommendations. *Cladistics, 35*(2). doi:10.1111/cla.12340

Paulozzi, L. J., & Lary, J. M. (1999). Laterality patterns in infants with external birth defects. *Teratology, 60*(5), 265-271. doi:10.1002/(SICI)1096-9926(199911)60:5<265::AID-TERA7>3.0.CO;2-H

Pearce, J. (2006). Dr. Melvin Moss, 83, Theorist on How Bones of Face Grow, Is Dead. *The New York Times*.

Perkins, R. E., Blanton, P. L., & Biggs, N. L. (1977). Electromyographic analysis of the "buccinator mechanism" in human beings. *J Dent Res, 56*(7), 783-794. doi:10.1177/00220345770560071301

Perri, R. A., Kairaitis, K., Wheatley, J. R., & Amis, T. C. (2015). Anthropometric and craniofacial sexual dimorphism in obstructive sleep apnea patients: is there male-female phenotypical convergence? *J Sleep Res, 24*(1), 82-91. doi:10.1111/jsr.12205

Quaderi, N. A., Schweiger, S., Gaudenz, K., Franco, B., Rugarli, E. I., Berger, W., . . . Ballabio, A. (1997). Opitz G/BBB syndrome, a defect of midline development, is due to mutations in a new RING finger gene on Xp22. *Nat Genet, 17*(3), 285-291. doi:10.1038/ng1197-285

Rahimov, F., Jugessur, A., & Murray, J. C. (2012). Genetics of nonsyndromic orofacial clefts. *Cleft Palate Craniofac J, 49*(1), 73-91. doi:10.1597/10-178

Reardon, W., Winter, R. M., Rutland, P., Pulleyn, L. J., Jones, B. M., & Malcolm, S. (1994). Mutations in the fibroblast growth factor receptor 2 gene cause Crouzon syndrome. *Nat Genet, 8*(1), 98-103. doi:10.1038/ng0994-98

Richtsmeier, J. T., DeLeon, V. B., & Lele, S. R. (2002). The promise of geometric morphometrics. *Am J Phys Anthropol, Suppl 35*, 63-91. Retrieved from https://www.ncbi.nlm.nih.gov/pubmed/12653309

Robertson, S. P., Twigg, S. R., Sutherland-Smith, A. J., Biancalana, V., Gorlin, R. J., Horn, D., . . . Group, O.-s. D. C. C. (2003). Localized mutations in the gene encoding the cytoskeletal protein filamin A cause diverse malformations in humans. *Nat Genet, 33*(4), 487-491. doi:10.1038/ng1119

Roessler, E., Belloni, E., Gaudenz, K., Jay, P., Berta, P., Scherer, S. W., . . . Muenke, M. (1996). Mutations in the human Sonic Hedgehog gene cause holoprosencephaly. *Nat Genet, 14*(3), 357-360. doi:10.1038/ng1196-357

Roessler, E., Du, Y. Z., Mullor, J. L., Casas, E., Allen, W. P., Gillessen-Kaesbach, G., . . . Muenke, M. (2003). Loss-of-function mutations in the human GLI2 gene are associated with pituitary anomalies and holoprosencephaly-like features. *Proc Natl Acad Sci U S A, 100*(23), 13424-13429. doi:10.1073/pnas.2235734100

Rogers, C. R., Weinberg, S. M., Smith, T. D., Deleyiannis, F. W., Mooney, M. P., & Marazita, M. L. (2008). Anatomical basis for apparent subepithelial cleft lip: a histological and

ultrasonographic survey of the orbicularis oris muscle. *Cleft Palate Craniofac J, 45*(5), 518-524. doi:10.1597/07-115.1

Roosenboom, J., Indencleef, K., Hens, G., Peeters, H., Christensen, K., Marazita, M. L., . . . Weinberg, S. M. (2017). Testing the face shape hypothesis in twins discordant for nonsyndromic orofacial clefting. *Am J Med Genet A, 173*(11), 2886-2892. doi:10.1002/ajmg.a.38471

Roosenboom, J., Saey, I., Peeters, H., Devriendt, K., Claes, P., & Hens, G. (2015). Facial Characteristics and Olfactory Dysfunction: Two Endophenotypes Related to Nonsyndromic Cleft Lip and/or Palate. *Biomed Res Int, 2015*, 863429. doi:10.1155/2015/863429

Rose, W. (1891). *On Hare Lip and Cleft Palate*. London: H. K. Lewis.

Sakoda, K. L., Jorge, P. K., Carrara, C. F. C., Machado, M. A. A. M., Valarelli, F. P., Pinzan, A., & Oliveira, T. M. (2017). 3D analysis of effects of primary surgeries in cleft lip/palate children during the first two years of life. *Braz Oral Res, 31*, e46. doi:10.1590/1807-3107BOR-2017.vol31.0046

Sant'Anna, E. F., Cury-Saramago, A. e. A., Lau, G. W., Polley, J. W., & Figueroa, Á. (2013). Treatment of midfacial hypoplasia in syndromic and cleft lip and palate patients by means of a rigid external distractor (RED). *Dental Press J Orthod, 18*(4), 134-143. doi:10.1590/s2176-94512013000400005

Shapira, Y., Lubit, E., Kuftinec, M. M., & Borell, G. (1999). The distribution of clefts of the primary and secondary palates by sex, type, and location. *Angle Orthod, 69*(6), 523-528. doi:10.1043/0003-3219(1999)0692.3.CO;2

Shi, M., Wehby, G. L., & Murray, J. C. (2008). Review on genetic variants and maternal smoking in the etiology of oral clefts and other birth defects. *Birth Defects Res C Embryo Today, 84*(1), 16-29. doi:10.1002/bdrc.20117

Singh, S., & Groves, A. K. (2016). The molecular basis of craniofacial placode development. *Wiley Interdiscip Rev Dev Biol, 5*(3), 363-376. doi:10.1002/wdev.226

Snead, M. P., & Yates, J. R. (1999). Clinical and Molecular genetics of Stickler syndrome. *J Med Genet, 36*(5), 353-359. Retrieved from https://www.ncbi.nlm.nih.gov/pubmed/10353778

Stanier, P., & Moore, G. E. (2004). Genetics of cleft lip and palate: syndromic genes contribute to the incidence of non-syndromic clefts. *Hum Mol Genet, 13 Spec No 1*, R73-81. doi:10.1093/hmg/ddh052

Suzuki, K., Hu, D., Bustos, T., Zlotogora, J., Richieri-Costa, A., Helms, J. A., & Spritz, R. A. (2000). Mutations of PVRL1, encoding a cell-cell adhesion molecule/herpesvirus receptor, in cleft lip/palate-ectodermal dysplasia. *Nat Genet, 25*(4), 427-430. doi:10.1038/78119

Tavajohi-Kermani, H., Kapur, R., & Sciote, J. J. (2002). Tooth agenesis and craniofacial morphology in an orthodontic population. *Am J Orthod Dentofacial Orthop, 122*(1), 39-47. doi:10.1067/mod.2002.123948

Tessier, P. (1976). Anatomical classification facial, cranio-facial and latero-facial clefts. *J Maxillofac Surg, 4*(2), 69-92. doi:10.1016/s0301-0503(76)80013-6

Tinano, M. M., Martins, M. A., Bendo, C. B., & Mazzieiro, Ê. (2015). Base of the skull morphology and Class III malocclusion in patients with unilateral cleft lip and palate. *Dental Press J Orthod, 20*(1), 79-84. doi:10.1590/2176-9451.20.1.079-084.oar

Tolarová, M. (1987). A study of the incidence, sex-ratio, laterality and clinical severity in 3,660 probands with facial clefts in Czechoslovakia. *Acta Chir Plast, 29*(2), 77-87. Retrieved from https://www.ncbi.nlm.nih.gov/pubmed/2444052

Tolarová, M. M., & Cervenka, J. (1998). Classification and birth prevalence of orofacial clefts. *Am J Med Genet, 75*(2), 126-137. Retrieved from https://www.ncbi.nlm.nih.gov/pubmed/9450872

Tonkin, E. T., Wang, T. J., Lisgo, S., Bamshad, M. J., & Strachan, T. (2004). NIPBL, encoding a homolog of fungal Scc2-type sister chromatid cohesion proteins and fly Nipped-B, is mutated in Cornelia de Lange syndrome. *Nat Genet, 36*(6), 636-641. doi:10.1038/ng1363

Ursi, W. J., Trotman, C. A., McNamara, J. A., & Behrents, R. G. (1993). Sexual dimorphism in normal craniofacial growth. *Angle Orthod, 63*(1), 47-56. doi:10.1043/0003-3219(1993)0632.0.CO;2

van den Boogaard, M. J., Dorland, M., Beemer, F. A., & van Amstel, H. K. (2000). MSX1 mutation is associated with orofacial clefting and tooth agenesis in humans. *Nat Genet, 24*(4), 342-343. doi:10.1038/74155

Vieira, A. R., McHenry, T. G., Daack-Hirsch, S., Murray, J. C., & Marazita, M. L. (2008). A genome wide linkage scan for cleft lip and palate and dental anomalies. *Am J Med Genet A, 146A*(11), 1406-1413. doi:10.1002/ajmg.a.32295

Vissers, L. E., van Ravenswaaij, C. M., Admiraal, R., Hurst, J. A., de Vries, B. B., Janssen, I. M., . . . van Kessel, A. G. (2004). Mutations in a new member of the chromodomain gene family cause CHARGE syndrome. *Nat Genet, 36*(9), 955-957. doi:10.1038/ng1407

Wagner, T., Wirth, J., Meyer, J., Zabel, B., Held, M., Zimmer, J., . . . Scherer, G. (1994). Autosomal sex reversal and campomelic dysplasia are caused by mutations in and around the SRY-related gene SOX9. *Cell, 79*(6), 1111-1120. doi:10.1016/0092-8674(94)90041-8

Waitzman, N. J., Romano, P. S., & Scheffler, R. M. (1994). Estimates of the economic costs of birth defects. *Inquiry, 31*(2), 188-205. Retrieved from https://www.ncbi.nlm.nih.gov/pubmed/8021024

Wallis, D. E., Roessler, E., Hehr, U., Nanni, L., Wiltshire, T., Richieri-Costa, A., . . . Muenke, M. (1999). Mutations in the homeodomain of the human SIX3 gene cause holoprosencephaly. *Nat Genet, 22*(2), 196-198. doi:10.1038/9718

Watkins, S. E., Meyer, R. E., Strauss, R. P., & Aylsworth, A. S. (2014). Classification, epidemiology, and genetics of orofacial clefts. *Clin Plast Surg, 41*(2), 149-163. doi:10.1016/j.cps.2013.12.003

Wehby, G. L., & Cassell, C. H. (2010). The impact of orofacial clefts on quality of life and healthcare use and costs. *Oral Dis, 16*(1), 3-10. doi:10.1111/j.1601-0825.2009.01588.x

Wehby, G. L., & Murray, J. C. (2010). Folic acid and orofacial clefts: a review of the evidence. *Oral Dis, 16*(1), 11-19. doi:10.1111/j.1601-0825.2009.01587.x

Weinberg, S. (2007). *Three-dimensional morphometric analysis of the craniofacial complex in the Unaffected relatives of individuals with nonsydnromic orofacial clefts.* (Doctor of Philosophy). University of Pittsburgh,

Weinberg, S. M., Maher, B. S., & Marazita, M. L. (2006). Parental craniofacial morphology in cleft lip with or without cleft palate as determined by cephalometry: a meta-analysis. *Orthod Craniofac Res, 9*(1), 18-30. doi:10.1111/j.1601-6343.2006.00339.x

Weinberg, S. M., Naidoo, S. D., Bardi, K. M., Brandon, C. A., Neiswanger, K., Resick, J. M., . . . Marazita, M. L. (2009). Face shape of unaffected parents with cleft affected offspring: combining three-dimensional surface imaging and geometric morphometrics. *Orthod Craniofac Res, 12*(4), 271-281. doi:10.1111/j.1601-6343.2009.01462.x

Weinberg, S. M., Neiswanger, K., Richtsmeier, J. T., Maher, B. S., Mooney, M. P., Siegel, M. I., & Marazita, M. L. (2008). Three-dimensional morphometric analysis of craniofacial shape

in the unaffected relatives of individuals with nonsyndromic orofacial clefts: a possible marker for genetic susceptibility. *Am J Med Genet A, 146A*(4), 409-420. doi:10.1002/ajmg.a.32177

Weinberg, S. M., Parsons, T. E., Fogel, M. R., Walter, C. P., Conrad, A. L., & Nopoulos, P. (2013). Corpus callosum shape is altered in individuals with nonsyndromic cleft lip and palate. *Am J Med Genet A, 161A*(5), 1002-1007. doi:10.1002/ajmg.a.35835

Wen, Y. F., Wong, H. M., Lin, R., Yin, G., & McGrath, C. (2015). Inter-Ethnic/Racial Facial Variations: A Systematic Review and Bayesian Meta-Analysis of Photogrammetric Studies. *PLoS One, 10*(8), e0134525. doi:10.1371/journal.pone.0134525

West, J. R., & Blake, C. A. (2005). Fetal alcohol syndrome: an assessment of the field. *Exp Biol Med (Maywood), 230*(6), 354-356. doi:10.1177/15353702-0323006-02

Wilcox, A. J., Lie, R. T., Solvoll, K., Taylor, J., McConnaughey, D. R., Abyholm, F., . . . Drevon, C. A. (2007). Folic acid supplements and risk of facial clefts: national population based case-control study. *BMJ, 334*(7591), 464. doi:10.1136/bmj.39079.618287.0B

Wilderman, A., VanOudenhove, J., Kron, J., Noonan, J. P., & Cotney, J. (2018). High-Resolution Epigenomic Atlas of Human Embryonic Craniofacial Development. *Cell Rep, 23*(5), 1581-1597. doi:10.1016/j.celrep.2018.03.129

Wilkie, A. O., Slaney, S. F., Oldridge, M., Poole, M. D., Ashworth, G. J., Hockley, A. D., . . . Rutland, P. (1995). Apert syndrome results from localized mutations of FGFR2 and is allelic with Crouzon syndrome. *Nat Genet, 9*(2), 165-172. doi:10.1038/ng0295-165

Ye, Z., Xu, X., Ahmatjian, A., & Bing, S. (2013). The Craniofacial Morphology in Adult Patients with Unoperated Isolated Cleft Palate. *Bone Res, 1*(2), 195-200. doi:10.4248/BR201302008

Zelditch, M., Swiderski, D. L., & Sheets, H. D. (2012). *Geometric morphometrics for biologists a primer*(2nd ed., pp. 1 online resource). Retrieved from http://pitt.idm.oclc.org/login?url=http://site.ebrary.com/lib/pitt/docDetail.action?docID=10582130 Pitt users please click through to access via ebrary.